

## INFORMATION TO USERS

This material was produced from a microfilm copy of the original document. While the most advanced technological means to photograph and reproduce this document have been used, the quality is heavily dependent upon the quality of the original submitted.

The following explanation of techniques is provided to help you understand markings or patterns which may appear on this reproduction.

1. The sign or "target" for pages apparently lacking from the document photographed is "Missing Page(s)". If it was possible to obtain the missing page(s) or section, they are spliced into the film along with adjacent pages. This may have necessitated cutting thru an image and duplicating adjacent pages to insure you complete continuity.
2. When an image on the film is obliterated with a large round black mark, it is an indication that the photographer suspected that the copy may have moved during exposure and thus cause a blurred image. You will find a good image of the page in the adjacent frame.
3. When a map, drawing or chart, etc., was part of the material being photographed the photographer followed a definite method in "sectioning" the material. It is customary to begin photoing at the upper left hand corner of a large sheet and to continue photoing from left to right in equal sections with a small overlap. If necessary, sectioning is continued again – beginning below the first row and continuing on until complete.
4. The majority of users indicate that the textual content is of greatest value, however, a somewhat higher quality reproduction could be made from "photographs" if essential to the understanding of the dissertation. Silver prints of "photographs" may be ordered at additional charge by writing the Order Department, giving the catalog number, title, author and specific pages you wish reproduced.
5. PLEASE NOTE: Some pages may have indistinct print. Filmed as received.

**Xerox University Microfilms**

300 North Zeeb Road  
Ann Arbor, Michigan 48106

76-30,269

LEFFAK, Ira Michael, 1947-  
PHYSICAL STUDIES OF HISTONE - DNA INTERACTIONS.

City University of New York, Ph.D., 1976  
Chemistry, biological

**Xerox University Microfilms**, Ann Arbor, Michigan 48106

© COPYRIGHT BY

IRA MICHAEL LEFFAK

1976

PHYSICAL STUDIES OF  
HISTONE - DNA INTERACTIONS

by

IRA MICHAEL LEFFAK

A dissertation submitted to the  
Graduate Faculty in Biochemistry  
in partial fulfillment of the  
requirements for the degree of  
Doctor of Philosophy, The City  
University of New York.

1976

This manuscript has been read and accepted for the Graduate Faculty in Biochemistry in satisfaction of the dissertation requirement for the degree of Doctor of Philosophy.

22 July, 1976  
date

Hsueh-jei Li  
Professor Hsueh-jei Li  
Chairman of Examining Committee

22 July 1976  
date

Aaron Lukton  
Professor Aaron Lukton  
Executive Officer

Robert Bittman  
Professor Robert Bittman

Marion Himes  
Professor Marion Himes

Horst Schulz  
Professor Horst Schulz

## ABSTRACT

### PHYSICAL STUDIES OF HISTONE - DNA INTERACTIONS

by

Ira Michael Leffak

Adviser: Professor Hsueh - jei Li

Circular dichroism and thermal denaturation have been used to investigate the properties of the histone - DNA interaction. The similarity of the thermal denaturation profiles of nucleohistones reconstituted from various histones with different DNAs suggests common features in the binding of the assorted histone species to homologous mammalian or heterologous bacterial DNAs. It is found in particular that the slightly lysine - rich histone pair H2 and whole histone, when reannealed to calf thymus DNA, yield nucleohistones in which the thermal stabilities of the DNA and the number of amino acid residues per bound nucleotide are similar to those of calf thymus chromatin.

The ability of the positively charged histone residues to stabilize the DNA against melting has been shown to be related to the secondary structure of the hydrophobic amino acid residues. It is proposed that the hydrophobic forces of attraction within the histone - DNA unit antagonize the electrostatic repulsive forces between phosphates or between like - charged amino acids and that the balance of these forces is affected

by the pH and ionic strength of the medium, covalent modifications of the histones and other physiological agents which modulate the dynamic state of the nucleohistone.

Circular dichroism reveals that the extent of the distortion of the B form of DNA towards that seen in chromatin, C form, is also related to the degree of ordered secondary structure within the histones. It is seen that the protein conformation in histone H2 - DNA complexes is qualitatively and quantitatively similar to the protein conformation in chromatin while both the histone and DNA conformations approach those of chromatin when whole histone is reannealed to DNA by salt - urea - tris gradient reconstitution.

The formation of a stable aggregate of histone H2A, H2B, H3 and H4 was shown to occur in 2 M NaCl after the proteins were dissociated from one another by 5 M urea. The reformed histone unit maintained its conformation upon binding to DNA and had the same conformation after its dissociation from the DNA by 2 M NaCl.

When DNAs of different G+C content were allowed to compete for various histones during salt - urea - tris reconstitution it was found that each histone tested preferentially annealed to A+T - rich DNA. In addition, the extent of the selectivity decreased when mixtures of the histone fractions were used in the competition. The selectivity was greatest for histone H2B and decreased in the order: H2B > H2A > H2 > whole - H1 > whole histone. The effect of omitting urea from the reconstitution medium was to decrease the selectivity of histone binding, suggesting that enhanced hydrophobic forces counteract the A+T selectivity. This leads to the conclusion that under conditions of reversible and ionic histone - DNA binding, the histones selectively bind the more hydrophilic A · T base

pairs. Under conditions promoting hydrophobic interaction (high salt, no urea) the preference for A · T pairs decreases while that for the more hydrophobic G · C pairs increases.

DEDICATION

To Ella

Whose unselfishness and understanding made this dissertation possible.

## ACKNOWLEDGEMENTS

I wish to thank Professor Hsueh-jei Li for the help and guidance which he gave me and for his contributions to my training as a scientist. Also, my sincere thanks to Cathy Chang, Regina Santella and Robert Hwan whose friendship helped ease some of the more trying times, and especially to Peggy Pinkston whose constant good humor and good example taught me a great deal.

## TABLE OF CONTENTS

	<u>Page</u>
Chapter I, Introduction	1
Chapter II, Materials and Methods	6
Chapter III, Thermal Denaturation	21
Chapter IV, Circular Dichroism	91
Chapter V, Selectivity of Histone Binding	174
Chapter VI, Discussion	200

## LIST OF TABLES

1. Characteristics of the Histones	Page 2
2. Amino Acid Composition of Histone H2A	Page 15
3. Features of Thermal Denaturation Profiles	Page 28
4. Characteristics of Circular Dichroism Spectra	Page 167
5. Physical Parameters of DNA in A, B, C Forms	Page 93
6. Properties of Cations	Page 94
7. Characteristics of DNA in Various Conformations	Page 95

## LIST OF FIGURES

	<u>Page</u>
1. Gel electrophoresis of histones	8a
2. Amberlite chromatography of whole histone	9
3. Bio-Gel chromatography of histone H2 + H3	11
4. Sephadex chromatography of whole histone	11
5. Bio-Gel chromatography of histone H2B + H3	12
6. Bio-Gel chromatography of CNBr-treated whole - H1 histone	14
7. Thermal denaturation of histone H2B nucleohistones	31-33
8. Thermal denaturation of histone H2B nucleohistones (minus - urea reconstitution)	37,38
9. Beta value determination. Histone H2B nucleohistones	39
10. Thermal denaturation of histone H2A nucleohistones	41-43
11. Beta value determination. Histone H2A nucleohistones	44
12. Thermal denaturation of histone H2A nucleohistones (minus - urea reconstitution)	47
13. Thermal denaturation of histone H2 nucleohistones	48-50
14. Thermal denaturation of purified nucleohistone	52,53
15. Beta value determination. Histone H2 nucleohistones	54
16. Thermal denaturation of histone H2 nucleohistones (minus - urea reconstitution)	55-57
17. Thermal denaturation of histone H2 nucleohistones (phosphate reconstitution)	59
18. Thermal denaturation of histone H2 nucleohistones (direct - mixed in EDTA)	61
19. Thermal denaturation of histone H2 nucleohistones (direct - mixed in salt / EDTA)	62
20. Beta value determination. Direct - mixed histone H2 nucleohistones	63
21. Effect of urea on thermal denaturation of histone H2 nucleohistones	64

	<u>Page</u>
22. Thermal denaturation of histone H2 B nucleohistone in urea	66
23. Thermal denaturation of whole histone - H 1 nucleohistones	68-70
24. Beta value determination. Whole - H 1 histone nucleohistones	71
25. Thermal denaturation of whole - H 1 nucleohistones (minus - urea reconstitution)	72-74
26. Thermal denaturation of whole - H 1 histone nucleohistones (phosphate reconstitution)	76
27. Thermal denaturation of whole histone nucleohistones	78-80
28. Beta value determination. Whole histone nucleohistones	81
29. Thermal denaturation of whole histone nucleohistones (minus - urea reconstitution)	82-84
30. Thermal denaturation of whole histone nucleohistones (phosphate reconstitution)	86
31. Thermal denaturation of whole histone and whole - H 1 histone nucleohistones in urea	88
32. CD spectra of histone H 2 A nucleohistones	101-103
33. CD spectra poly - L - lysine	104
34. Deformability of histone H 2 A nucleohistones	106
35. CD spectra of histone H 2 A nucleohistones (minus - urea reconstitution)	108
36. CD spectra of histone H 2 B nucleohistones	109-111
37. Deformability of histone H 2 B nucleohistones	112
38. CD spectra of histone H 2 B nucleohistone (supernatant and pellet)	114
39. CD spectra of histone H 2 B nucleohistones (minus-urea reconstitution)	115,116
40. CD spectra of histone H 2 nucleohistones	118-120

	<u>Page</u>
41. Deformability of histone H2 nucleohistones	121
42. CD spectra of histone H2 nucleohistones (minus - urea reconstitution)	122-124
43. CD spectra of histone H2 nucleohistones (phosphate reconstitution)	125
44. CD spectra of histone H2 nucleohistones (direct - mixed in EDTA)	127
45. CD spectra of histones in solution	128,128a
46. CD difference spectra of histone H2 nucleohistones (direct - mixed complexes)	129
47. Deformability of histone H2 nucleohistones (direct - mixed and phosphate reconstitution complexes)	130
48. CD spectra of histone H2 nucleohistones (direct-mixed salt / EDTA, predialysis)	132
49. CD spectra of histone H2 nucleohistones (direct-mixed salt / EDTA, postdialysis)	133
50. CD spectra of whole - H1 histone nucleohistones	134-136
51. Deformability of whole - H1 histone nucleohistones	137
52. CD spectra of whole - H1 histone nucleohistones (minus - urea reconstitution)	139-141
53. Deformability of whole - H1 histone nucleohistones	142
54. CD spectra of whole - H1 histone nucleohistones (supernatant and pellet, minus - urea reconstitution)	144
55. CD spectra of whole - H1 histone nucleohistones (urea - out - first reconstitution)	145
56. CD difference spectra of whole - H1 histone nucleohistones (minus - urea reconstitution)	147
57. CD spectra of whole - H1 histone nucleohistones (phosphate reconstitution)	148
58. CD difference spectra of whole - H1 histone nucleohistones (phosphate reconstitution)	149

	<u>Page</u>
59. CD spectra of whole histone nucleohistones	151-153
60. Deformability of whole histone nucleohistones	154
61. CD spectra of whole histone nucleohistones (minus - urea reconstitution)	155-157
62. CD spectra of whole histone nucleohistones (direct - mixed in EDTA)	159
63. Deformability of whole histone nucleohistones (direct - mixed complexes)	160
64. CD spectra of whole histone nucleohistones (direct - mixed in salt / EDTA predialysis)	161
65. CD spectra of whole histone nucleohistones (direct - mixed in salt / EDTA postdialysis)	162
66. CD spectra of whole histone nucleohistones (direct - mixed, salt / phosphate, predialysis)	164
67. CD spectra of whole histone nucleohistones (direct - mixed, salt / phosphate, postdialysis)	165
68,69. Selectivity of histone H 2 B binding to <u>Cl. perfringens</u> and <u>M. luteus</u> DNAs	176,179
70. Selectivity of histone H 2 B binding to calf thymus and <u>M. luteus</u> DNAs	181
71. Selectivity of histone H 2 B binding to calf thymus and <u>M. luteus</u> DNAs (minus - urea reconstitution)	182
72,73. Selectivity of histone H 2 A binding to <u>Cl. perfringens</u> and <u>M. luteus</u> DNAs	184,185
74,75. Selectivity of histone H 2 binding to <u>Cl. perfringens</u> and <u>M. luteus</u> DNAs	186,187
76. Selectivity of histone H 2 binding to poly dAT · poly dAT and calf thymus DNA	188
77. Selectivity of histone H 2 binding to <u>Cl. perfringens</u> and calf thymus DNAs	189
78. Relation between selectivity of histone H 2 binding and difference in G+C content	189
79. Selectivity of histone H 2 binding to <u>Cl. perfringens</u> and <u>M. luteus</u> DNAs (minus - urea reconstitution)	191

	<u>Page</u>
80,81. Selectivity of whole -H 1 histone binding to <u>C1. perfringens</u> and <u>M. luteus</u> DNAs	192,193
82. Selectivity of whole -H 1 histone binding to <u>C1. perfringens</u> and <u>M. luteus</u> DNAs (minus - urea reconstitution)	194
83,84. Selectivity of whole histone binding to <u>C1. perfringens</u> and <u>M. luteus</u> DNAs	195,196
85. Selectivity of whole histone binding to <u>C1. perfringens</u> and calf thymus DNAs	197
86. Selectivity of whole histone binding to <u>C1. perfringens</u> and <u>E. coli</u> DNAs	197
87. Selectivity of whole histone binding to <u>C1. perfringens</u> and <u>M. luteus</u> DNAs (minus - urea reconstitution)	198

## CHAPTER I

### INTRODUCTION

Repression of the transcriptional capacity of DNA in chromatin is due primarily to the binding of the histones (1-3). Although chromatin contains both histones and non-histone proteins, the histones were the first chromosomal proteins isolated (4), and in the early 1950s the importance of the histones in the restriction of DNA template activity was realized (5). At that time Stedman and Stedman (5) proposed that a large number of tissue-specific histones would be found. It is now known that aside from a handful of tissue or cell-cycle specific histones such as the H5 erythrocyte histone (6), the histones in general comprise a limited class of proteins rich in the basic residues Lys, Arg, His, which carry a net positive charge at physiological pH (6). Histones H2A, H2B, H3 and H4 in chromatin were found to be approximately in equimolar quantities while H1, which is nearly twice as large, is present in half-molar quantity (6). Some of the features of the histones are shown in Table 1.

Selective transcription of the eucaryotic genome could conceivably be controlled by soluble repressors or activators interacting with the genetic material as in procaryotes (7,8). However, in eucaryotes structural modification of the DNA conformation has been related to alterations in genetic activity (9-11). The strongly conserved amino acid sequence of the histones (6) implies that mutations which result in change in the primary structure of these proteins would adversely alter strictly defined histone-histone, histone-non-histone or histone-DNA interactions. Because of the great homology between histones of different

tissues or organisms, the tissue- and species - specificity of chromatin transcription appears to be determined by the non - histone proteins (12 - 14).

TABLE 1  
 PROPERTIES OF THE CALF THYMUS HISTONES

<u>CLASS</u>	<u>FRACTION</u>	<u>LYS / ARG</u>	<u>TOTAL RESIDUES</u>	<u>MOLECULAR WEIGHT</u>
Lys - Rich	H 1	22.0	~215	~22,000
Slightly Lys - Rich	H 2 A	1.17	129	~14,000
	H 2 B	2.50	125	~14,000
Arg - Rich	H 3	.72	135	~15,000
	H 4	.79	102	~11,000

The non - histone proteins are a diverse set of nearly one hundred proteins (depending on the tissue of origin and the method of analysis) with average molecular weight ca. 100,000 (15, 16). This class of proteins includes the RNA and DNA polymerases, DNA ligases, endonucleases, histone acetyltransferases, methylases, kinases and proteases, non - histone kinases and poly ADP - ribose polymerases to name a few (6). It has been observed that some of these proteins bind strongly to DNA in a species - specific manner (17 - 19). Due to their great heterogeneity the majority of the non - histone proteins is only beginning to receive detailed study.

While the non - histones have come to be thought of as dynamic effectors within chromatin, attention has also turned to the non - static aspects of the function of histones as well. It is known that the

histones are bound to both transcribed and nontranscribed regions of the genome (20) and subject to a wide variety of site- and cell-cycle-specific post-synthetic covalent modifications such as the methylation of lysine, arginine and histidine residues, the acetylation of lysine and serines, and the phosphorylation of serine, threonine, lysine and histidine amino acids (21). It is known that the phosphorylation of specific residues in the H1 histone occurs during S phase, when both histones and DNA are synthesized (22) while other sites are phosphorylated during metaphase (23) and dephosphorylated as the cells enter G1 phase (24-26). In contrast to the rapid turnover of many of the covalent histone modifications, these proteins have long half-lives, comparable to that of the DNA itself (27-28).

In solution, the histones tend to associate strongly to form dimers or tetramers, depending on ionic strength, pH and concentration (29-36). The strongest associations are formed between the pairs H2A-H2B, H2B-H4 and H3-H4 (29-33). Skandriani et al. (37) have reported that histone H2A and H2B interact during guanidine hydrochloride gradient chromatography on Amberlite. By using protein cross-linking reagents it has been found that these dimers may also be isolated from chromatin (38-40).

The pattern of histone-histone associations led Kornberg (41) and Kornberg and Thomas (42) to propose that the histones in chromatin were organized into an octamer protein core, containing two each of histones H2A, H2B, H3 and H4, around which the DNA was wound. Support for this theory has come from the work of Weintraub et al. (34) and Weintraub and Van Lente (43) who isolated a tetramer of histones H2A, H2B, H3 and H4 from chromatin and demonstrated specific attachments of the

amino- and carboxyl - termini portions of the histones to defined DNA segments. Using endogenous and exogenous nucleases as probes of the in situ structure of chromatin a number of laboratories have observed a reproducible pattern of discrete DNA fragments representing multiples of a basic 150 - 200 base pair unit (42 - 47).

Olins and Olins (48) and Woodcock (49) have observed regularly repeating 80A particles in electron micrographs of chromatin while Oudet et al. (50) have succeeded in reconstructing the nodular appearance of chromatin by salt gradient reconstitution of DNAs to homologous or heterologous whole histone depleted of histone H1. These results relate the histone tetramer isolated by Weintraub et al. (34) to the appearance of the nodular nu bodies (48) or nucleosomes (50) visualized by the electron microscope.

Results provided by X - ray diffraction studies of chromatin reveal regular repeats at intervals of 22A, 27A, 37A, 55A and 110A (51, 52). It was also found that all four histones H2A, H2B, H3 and H4 were required to achieve the X - ray pattern of chromatin (52, 53). Oudet et al. also observed that all four histones were required to reproduce the nucleosome appearance of chromatin (51). Using the technique of neutron diffraction Bradbury et al. (53) have concluded that the 27A and 55A repeats are due to DNA while the 37A and 110A repeats are due to the protein configuration. Senior et al. (54) and Finch and Klug (55) believe the 110A repeat to be due to the packing together of the nu bodies. The latter authors have found that isolated monomer nucleosomes may aggregate in solution in a side - by - side fashion to form patterns of association similar to those seen in electron micrographs of chromatin.

Recent models of chromatin structure (41, 55 - 57) have been based on the existence of a core of histones interacting with each other through hydrophobic regions of secondary structure and binding the DNA through ionic and hydrophobic forces which cause it to conform to a distorted path defined by binding sites or grooves along the protein core. The most dynamic model of chromatin structure (57) envisions the nucleosomal particle in equilibrium with a more extended chromatin supercoil, the direction of the equilibrium being dictated by the environmental pH, ionic strength and presumably covalent histone modifications or protein effectors. The picture which emerges is that of interacting side-by-side particles each analogous to a subunit of an allosteric enzyme where the balance of ionic and hydrophobic forces determines the physical and chemical properties of the DNA substrate. The purpose of the experiments to be described is to investigate the nature of the forces between histones and between histones and DNA.

CHAPTER II  
MATERIALS AND METHODS

MATERIALS

DNA: Calf thymus DNA was purchased from the Sigma Chemical Company and was further purified by phenol extraction or the chloroform : isoamyl alcohol procedure of Marmur (58) with minor modification. In some instances the calf thymus DNA (2 mg/ml in 2 M NaCl, 0.01 M tris, pH 8.0) was mixed with an equal volume of previously autodigested pronase (Sigma Chemical Company, 100 $\mu$ g/ml in 2 M NaCl, 0.01 M tris, pH 8.0) and stirred overnight at 4°C prior to the chloroform : isoamyl alcohol purification. The pronase treatment reduced the number of extractions necessary to isolate DNA which showed no visible protein contaminant during the extractions and which exhibited the melting profile and CD spectrum of pure DNA. This DNA was assumed protein-free. The DNA was stored in 0.15 M NaCl, 0.01 M tris, pH 8.0 at 4°C with no detectable change in its physical parameters over a period of weeks.

Micrococcus luteus DNA and Clostridium perfringens DNA were purchased from Miles Laboratories or Worthington Biochemicals and used without further purification.

HISTONES: Calf thymus tissue was frozen on dry ice immediately after slaughter and broken into smaller pieces to be stored at -70°C until used. Calf thymus chromatin was prepared by the method of Shih and Bonner (1). All procedures were carried out at 4°C. Twenty-five grams of tissue were homogenized in a Waring blender in 100 ml grinding medium (0.25 M sucrose, 1 mM MgCl<sub>2</sub>, 0.01 M tris, pH 8.0) at 50 V for 2 minutes, followed by the addition of aliquots of grinding medium to a

total of 400 ml and further homogenization. The homogenate was filtered through cheesecloth, then Miracloth and centrifuged (4000 rpm, 20 minutes, Sorvall SS-34 rotor). The nuclear pellet was washed with grinding medium until the supernatant was clear. The nuclei were lysed in 0.01 M tris (pH 8.0), spun and washed twice with .01 M tris (pH 8.0). The pellet was re-suspended in 0.01 M tris (pH 8.0) and homogenized with a teflon-glass homogenizer. This crude chromatin was further purified by sedimentation through 1.7 M sucrose, 0.01 M tris, pH 8.0 in a Beckman Spinco Model L SW25.1 rotor (22,000 rpm, 2 hours). The pellet was homogenized in 0.01 M tris, pH 8.0, the sucrose removed by dialysis and the histones extracted using acid. The chromatin was treated with  $H_2SO_4$  to a final concentration of 0.4 N (pH  $\approx$  0.8) on ice and stirred for 30 minutes at 4°C. The DNA was pelleted at 12,000 g for 20 minutes and the supernatant combined with 10 volumes of cold, absolute ethanol and stored at -20°C for 24 hours. The precipitated whole histone (Figure 1) was isolated by centrifugation at 2000 g, 20 minutes, washed with cold absolute ethanol and dried under vacuum.

Whole histone minus histone H 1 (whole-H 1) was prepared by dissolving whole histone in 1 mM HCl (4°C), adding concentrated (5.5 N) perchloric acid (PCA) to 0.5 N (5%) and incubating on ice for 15 minutes. The sample was spun (10,000 g, 30 minutes) the supernatant extracted and dialysed against 0.5 N  $H_2SO_4$  and then against ethanol (-20°C, 24 hours) followed by centrifugation to collect the histone H 1-sulphate precipitate (Figure 1). The original PCA precipitate was washed with 5% PCA, dissolved in 1 mM HCl, dialysed vs. dilute (0.1N) HCl or  $H_2SO_4$  and then vs. ethanol and the precipitate collected. This

is whole-H 1 histone (Figure 1).

Histone H 2 (H 2 A and H 2 B) was purified by chromatography of whole or whole-H 1 histone on Amberlite CG-50 by the method of Bonner et. al.(59). Approximately 400 mg of crude histone was dissolved in 10 ml of 14% guanidinium hydrochloride (GuCl), 0.1 M sodium phosphate, pH 6.8, and applied to a 5 x 55 cm column of Amberlite CG-50 (type I, Rohm and Haas Chemicals) previously equilibrated with 8% GuCl, 0.1 M sodium phosphate, pH 6.8. When the GuCl was Sigma practical grade it was purified by elution through a column of activated charcoal and Celite. GuCl concentration was determined by monitoring the refractive index of the stock solution, and using the equation:

$$\frac{n_{(\text{GuCl})}^{25^{\circ}} - n_{(\text{H}_2\text{O})}^{25^{\circ}}}{\text{weight \% GuCl in H}_2\text{O}} = 0.00166 \quad (1)$$

where  $n$  = refractive index, which holds for solutions up to 60% in GuCl. Ultrapure GuCl, purchased from Schwarz-Mann, was used directly. A stepwise GuCl gradient of 8%, 10%, 13% and 40% was employed to elute the histones from the Amberlite, at a flow rate of 40 - 45 ml/hr. Fractions of 10 ml were collected and histone-containing fractions identified by turbidity at 400 nm in 1.32 M trichloroacetic acid (TCA) (Figure 2). The histone H 2 collected after dialysis vs. 0.1 N acetic acid (HAc) and lyophilization was frequently contaminated with small amounts of histone H 3 which could be removed by oxidizing the entire sample in 6 M GuCl, 0.3 M tris HCl, pH 8.3 with stirring at room

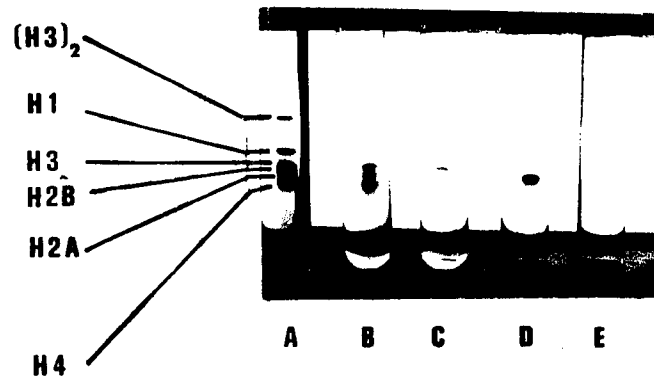


Figure 1. Gel electrophoresis of the calf thymus histones.

Gel A : whole histone.

Gel B : whole histone minus H 1 .

Gel C : histone H 2 B.

Gel D : histone H 2 A.

Gel E : histone H 2 ( H 2 B + H 2 A ) .

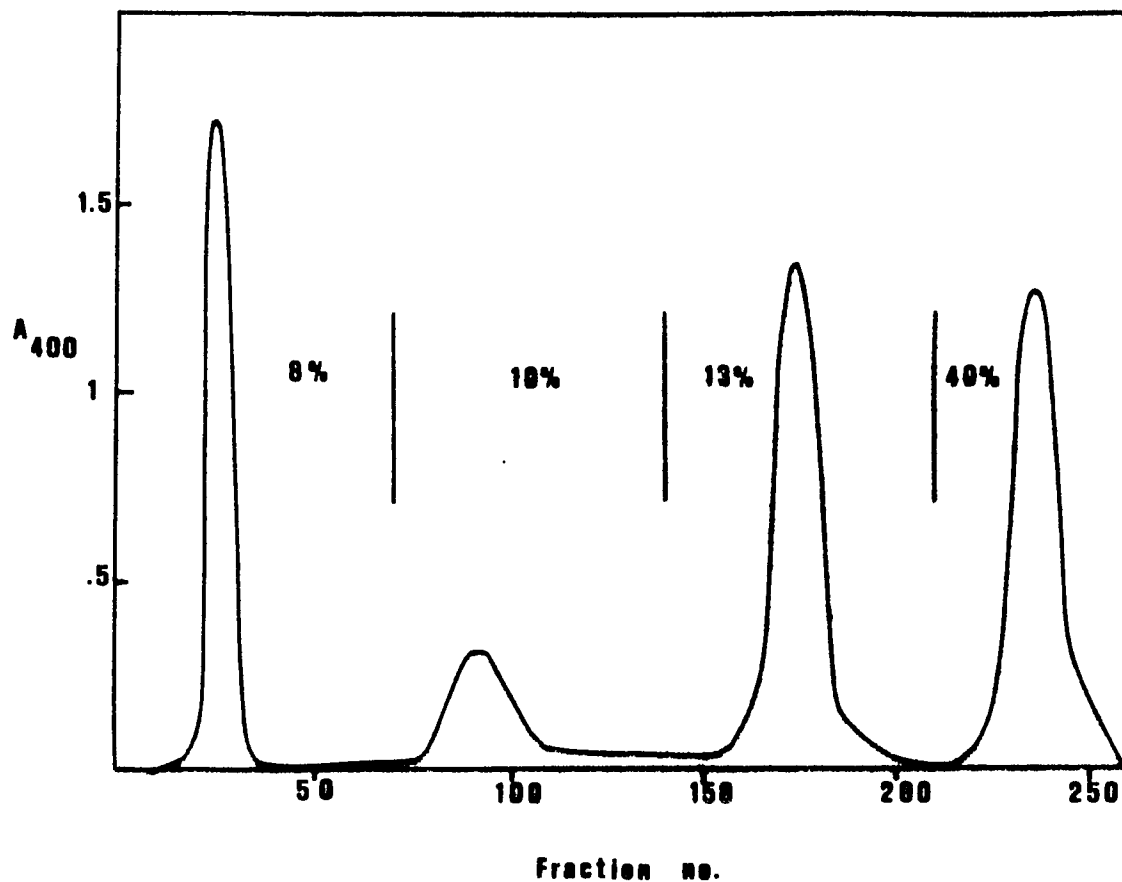


Figure 2. Amberlite column chromatography of whole histone.  
 Amberlite column, 5 x 55 cm.  
 Applied 400 mg whole histone.  
 10 ml / fraction, 40 ml / hr.  
 Elution: GuCl in 0.1M phosphate  
 buffer, pH 6.80.  
 % of GuCl indicated.

temperature for 24 hours (60), dialysing against 0.01N HCl, and eluting from a 1.6 x 200 cm Bio-Gel P-60 column with 0.01N HCl (Figure 3). The eluted histone H2 was electrophoretically homogeneous (61).

Alternatively, histone H2 was purified by eluting whole histone or whole histone-H1 from a 1.6 x 300 cm Sephadex G-50 column with 0.02N HCl (Figure 4). This histone H2 was also contaminated with H3, necessitating oxidation and further gel filtration.

Histone H2B was isolated from partially pure histone H2 by the procedure of Oliver et al. (62), originally devised for the purification of *Drosophila* histones. Histone H2 was extracted with ethanol-HCl (EtOH-HCl) (400 ml absolute EtOH, 10 ml conc. HCl, 90 ml H<sub>2</sub>O) at 4°C using a glass homogenizer, and incubated for 10 minutes. After centrifugation the supernatant containing H2A and some of the contaminating H3 was removed. The H2B pellet was redissolved in 1 mM HCl, precipitated with PCA and re-extracted with EtOH-HCl. After six such cycles the H2B was washed with acetone and dried under vacuum. The H2B obtained was further purified from residual H3 contamination by oxidation and Bio-Gel P-100 gel filtration (Figure 5). The histone H2B sample was electrophoretically pure, did not show any dimerizing contaminant upon oxidation and was completely cleaved by cyanogen bromide (CNBr) to give amino- and carboxyl-terminal fragments with electrophoretic mobilities equivalent to those previously reported for H2B half-molecules (63).

Histone H2A was purified by adding solid cyanogen bromide (CNBr, Eastman Chemicals) to whole-H1 histone (20 mg/ml in 0.1N HCl) to a final CNBr concentration in excess of 25 mg/ml. The mixture stirred

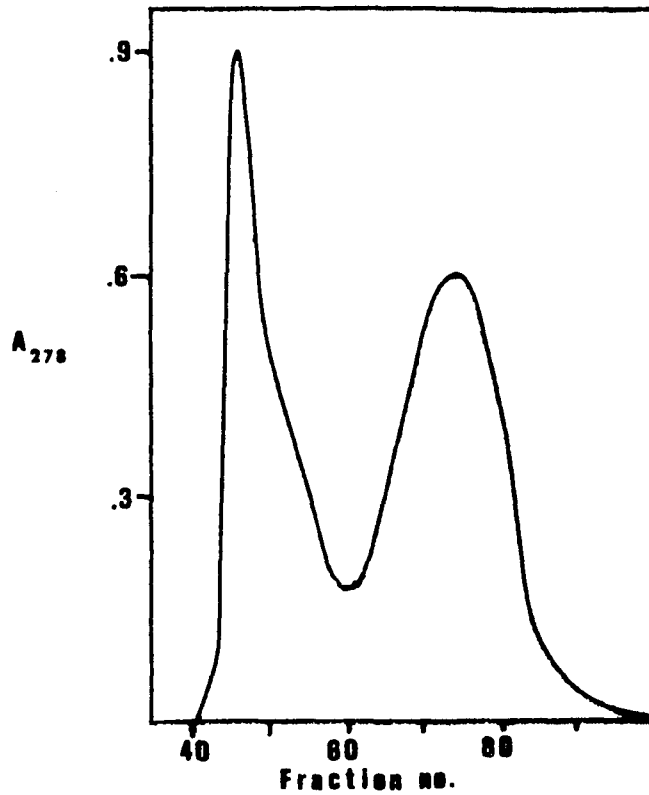


Figure 3. Gel filtration chromatography of H2 + H3. Bio-Gel P-60 column, 1.6 x 200 cm. Applied 50 mg oxidized H2 + H3. 2 ml / fraction, 20 ml / hr. Elution: .01N HCl.

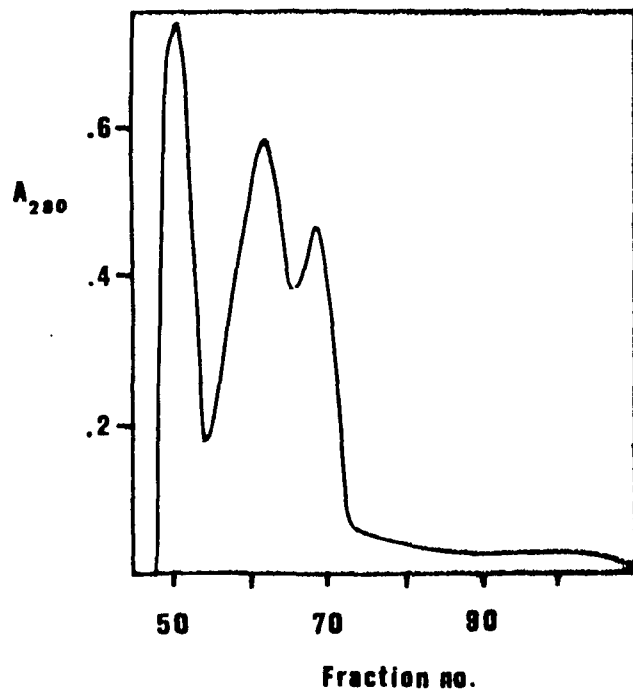
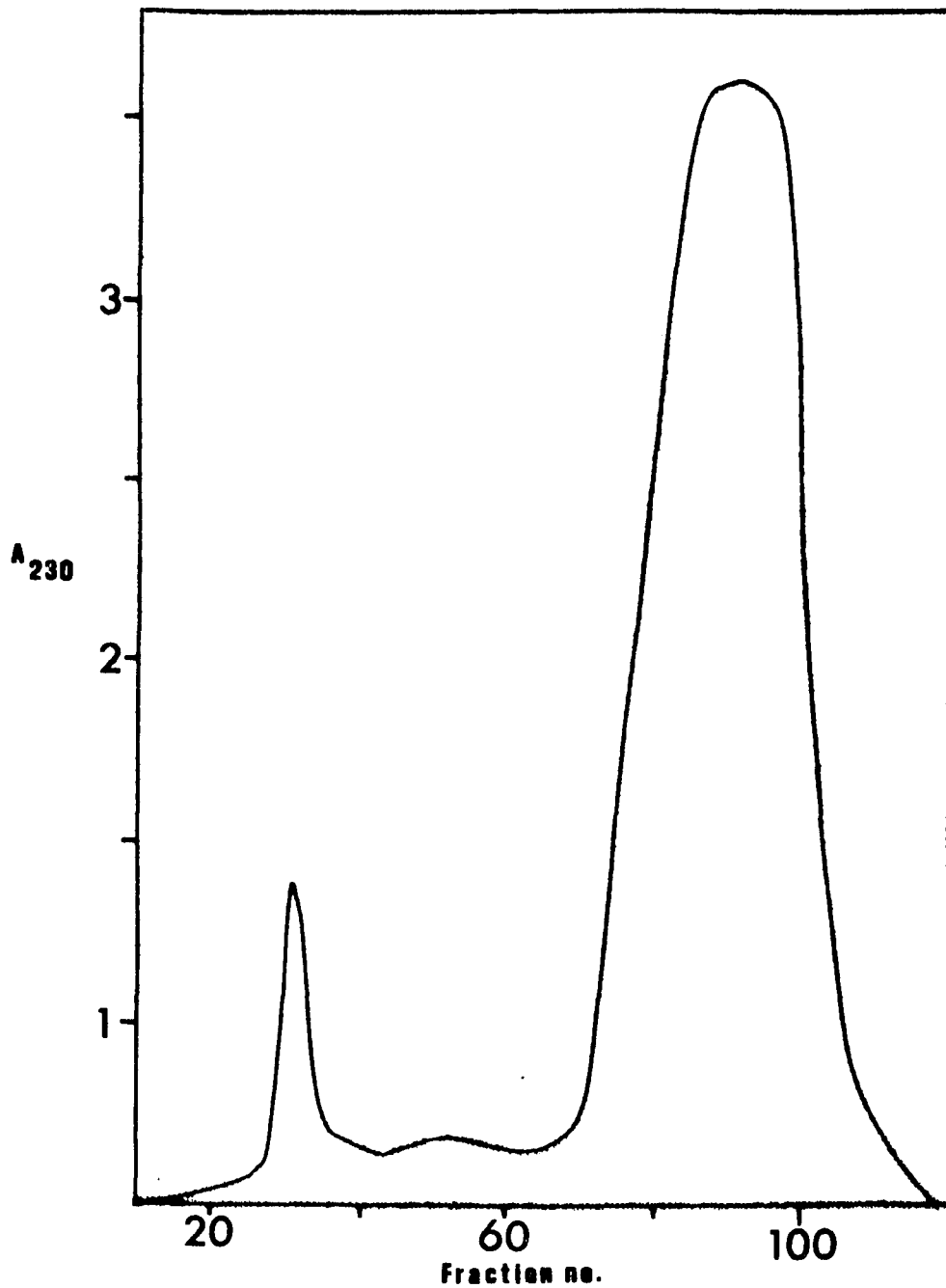


Figure 4. Gel filtration chromatography of whole histone. Sephadex G-50 column, 1.6 x 300 cm. Applied 40 mg whole histone. 2 ml / fraction, 20 ml / hr. Elution: .02N HCl.



**Figure 5 . Gel filtration chromatography of histones H 2 B + H 3 .**

Bio - Gel P - 100 column,  
1.6 x 300 cm.  
Applied 30 mg H 2 B + H 3 (oxidized).  
2 ml / fraction, 10 ml / hr.  
Elution: .02 N HCl.

for at least 24 hours at room temperature in a sealed vial, was lyophilized and re-dissolved in 0.2 N HCl and applied to a 1.6 x 300 cm Bio-Gel P-60 column (Figure 6). The H2A was eluted, dialysed vs. 0.2 N H<sub>2</sub>SO<sub>4</sub> and EtOH and the precipitate re-dissolved in 0.9 N HAc - 25% sucrose for electrophoresis. The histone H2A was electrophoretically pure; however, the purified H2A band migrated slightly faster than the analogous H2A band on whole histone gels. For this reason the amino acid content of the histone was analysed and found to agree with published values (Table 2).

## METHODS

GEL ELECTROPHORESIS: The procedure followed was basically that of Panyim and Chalkley (61). Three stock solutions were prepared and refrigerated:

Solution A: 60% acrylamide (w:w), 0.4% bis - acrylamide (w:w) in H<sub>2</sub>O (Bio-Rad Laboratories, Electrophoretic grade).

Solution B: 43.2% HAc (w:w), 5% N,N,N',N' - tetramethylethylenediamine (v:w) in H<sub>2</sub>O (Bio-Rad Laboratories, Electrophoretic grade).

Solution C: 10 M urea (Ultra Pure, Schwarz-Mann Biochemicals), 0.118 M HCl.

One volume of B and two of A were mixed and spun at high speed in an IEC Clinical Centrifuge for ca. 10 minutes. Ammonium persulfate (Eastman Chemicals) was dissolved (2 mg/ml) in three volumes of water and dessicated under vacuum for ca. 10 minutes. Two volumes of solution C were added and mixed with the three volumes of A+B. The

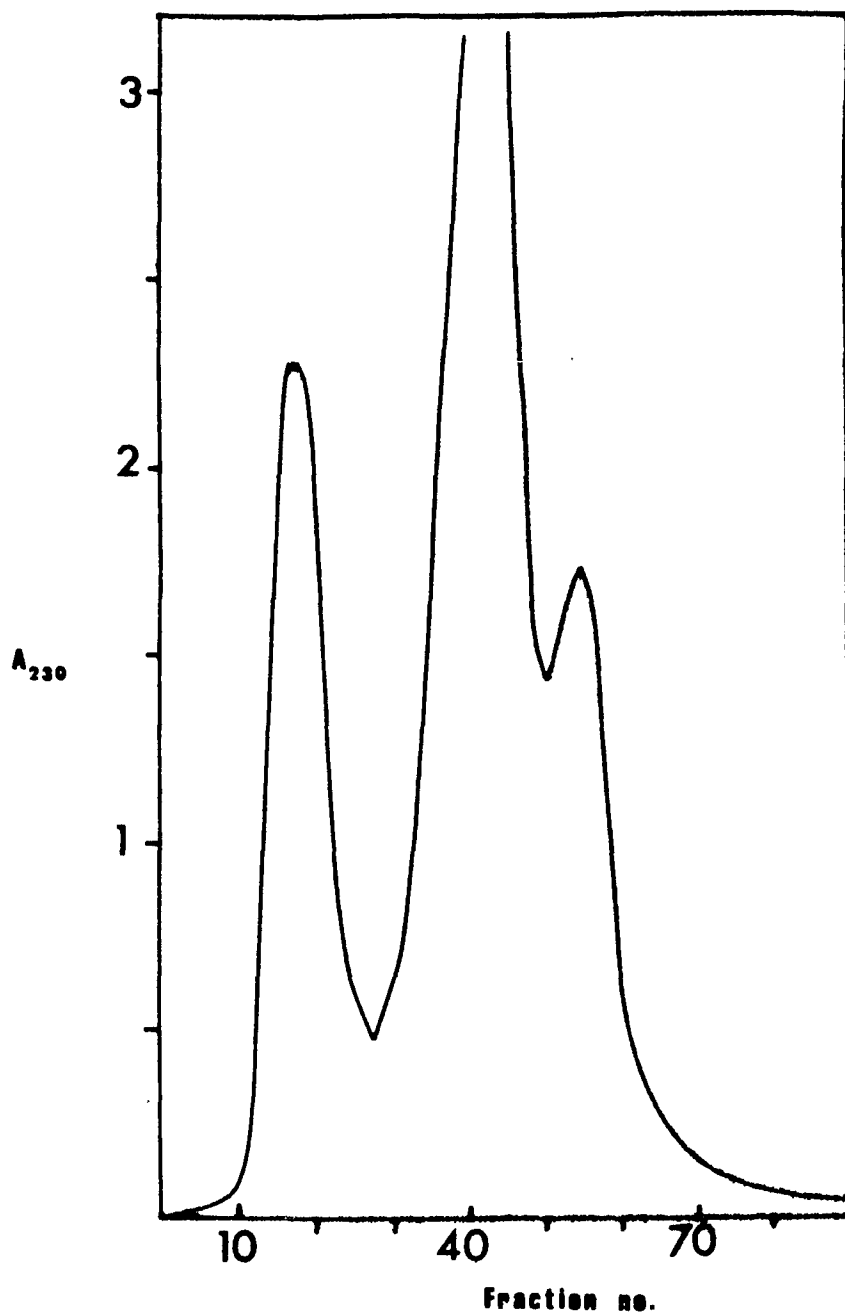


Figure 6 . Gel filtration chromatography of CNBr-treated histones.

Bio - Gel P - 60 column, 1.6 x 300 cm.  
 Applied 25 mg CNBr - treated whole - H1 histone.  
 2 ml / fraction, 10 ml / hr.  
 Elution: .02 N HCl.

TABLE 2

<u>AMINO ACID</u>	<u>OBSERVED</u>	<u>PUBLISHED (64)</u>
lysine	15	15
histidine	4	4
arginine	13	12
aspartic acid/ asparagine	8	9
glutamic acid/ glutamine	13	13
threonine	5	6
serine	4	5
proline	5	5
glycine	14	14
alanine	17	17
cysteine	0	0
valine	8	9
methionine	0	0
isoleucine	6	6
leucine	16	17
tyrosine	3	3
phenylalanine	1	1

mixture was poured into 6 mm x 8 cm glass tubes which had been stored in acid-dichromate cleaning solution, rinsed with water, boiled in a solution of 1% sodium dodecyl sulfate, rinsed with distilled water to remove visible traces of detergent and oven-dried.

The tubes were filled to a height of 7 cm, the gel solution overlaid with 3M urea (diluted from solution C) and incubated in a 31°C water bath for 30 minutes to 1 hour. The polymerized gels were prerun at room temperature, at 2 mA / 7 cm gel until the voltage reached 110 v which normally took 5 to 6 hours. Histone samples (5 - 20  $\mu$ l, 2 - 4 mg/ml) were applied to the gels and run for 4 hours at 2 mA / 7 cm gel. The gels were removed by cracking the tubes or injecting a stream of cold water between the tube and the gel. The gels were stained in 0.1% Amido black in 7% acetic acid, 20% EtOH or in 0.1% Amido black 7% acetic acid, 45% MeOH. The latter solution gave sharper bands. The gels were destained either electrophoretically or by diffusion in the staining solution solvent minus Amido black.

NUCLEOHISTONE RECONSTITUTION: The following extinction coefficients at 260 nm were used to determine DNA concentration: Calf thymus 6500  $M^{-1}cm^{-1}$ ; C. perfringens 7400  $M^{-1}cm^{-1}$ ; M. luteus 7000  $M^{-1}cm^{-1}$  (65). An extinction coefficient of 470  $M^{-1}cm^{-1}$  at 230 nm was used to determine histone concentration (66). DNA was dissolved in water or 0.01M tris, pH 8.0 or was dialysed from purification solvents into water, 0.01M tris pH 8.0, or 0.15M NaCl, 0.01M tris pH 8.0 and adjusted to  $2 \times 10^{-4}$  M by adding 2M NaCl, 5M urea, 0.01M tris, pH 8.0. In the case of salt-tris complexes, the urea was omitted. Histone was dissolved in water and adjusted to  $8 \times 10^{-4}$  M by dilution with the same

solvent as the DNA. The samples were equilibrated by dialysis vs. 2 M NaCl, 0.01 M tris, pH 8.0 ( $\pm$  5 M urea) for ca. 2 hours after which a gradient, continuously decreasing to 0.01 M tris, pH 8.0 ( $\pm$  5 M urea) was applied. For those nucleohistone complexes made in urea, the salt gradient was followed by a gradient to 0.01 M tris, pH 8.0. The complexes, now in 0.01 M tris, pH 8.0, were dialysed directly with 4 - 5 changes vs. .25 mM NaEDTA, pH 8.0 for thermal denaturation or circular dichroism studies.

PHOSPHATE RECONSTITUTION: Histone and DNA, each in 2 M NaCl, 5 M urea, 5 mM Na - phosphate buffer (pH 7.0), were mixed and dialysed (4<sup>0</sup>C) by gradient (18 hours) to 0.3 M NaCl, 5 M urea, 5 mM phosphate (pH 7.0) followed by gradient dialysis to 0.3 M NaCl, 5 mM phosphate (pH 7.0) (18 hours). The samples were then dialysed directly with four changes against 0.1 M NaCl, NaEDTA (pH 8.0), and again with four or five changes directly against 0.25 mM EDTA, pH 8.0 for thermal denaturation and circular dichroism studies.

DIRECT-MIXED COMPLEXES: Histones ( $8 \times 10^{-4}$  M) were dissolved in the appropriate buffer and were added dropwise from a pipette fitted with a hypodermic needle to a vigorously stirring solution of DNA in the same buffer. The samples were dialysed into .25 mM EDTA, pH 8.0 for experimentation.

THERMAL DENATURATION: The melting of nucleohistone complexes ( $A_{260}$  ca. 0.5) was monitored at 260 nm using a Gilford Model 2400 - S spectrophotometer. The temperature of the Haake circulating water bath was programmed to rise at a rate of ca. 0.6 - 0.7<sup>0</sup>C / min. The recorder

displayed the temperature at ca. 0.4°C intervals. At each 1°C interval the hyperchromicity (h) or derivative of the hyperchromicity with respect to temperature, dh/dT, were calculated using the equations of Li and Bonner (63):

$$h_T = \frac{(A_{260, T} - A_{260, T_i})}{A_{260, T_i}} \times 100\% \quad (2)$$

$$\frac{dh(260, T)}{dT} = \frac{h(260, T+1) - h(260, T-1)}{2} \quad (3)$$

where  $A_{260, T}$  = absorbance at 260 nm, temperature = T.

$A_{260, T_i}$  = absorbance at 260 nm, temperature = initial temperature.

$\frac{dh(260, T)}{dT}$  = rate of change of the 260 nm hyperchromicity with temperature at temperature T.

$h(260, T \pm 1)$  = hyperchromicity at 260 nm, at 1°C above / below temperature T.

The accuracy of the dh/dT values, considering the accuracy of the Gilford spectrophotometer and errors introduced during data transfer and calculations amount to an estimated error range of  $\pm 0.1$  unit dh/dt.

Errors in the determination of the beta (Equation 9) value of each series of complexes arising from (a) inaccuracy in  $\frac{dh}{dT}$ ; (b) estimation of protein or DNA concentration; (c) choice of boundaries representing end of free DNA thermal transition are estimated to contribute a maximum of uncertainty of  $\pm 10\%$ . For each DNA-histone complex a series of samples with increasing amino acid per nucleotide ratio (aa/n) from 0 to 3 (or 4) was prepared. To allow comparison of the peak heights of the various samples upon denaturation, and reduce the effect of light scattering on the apparent hyperchromicity, the total hyperchromicity of each sample in a series was normalized to the total hyperchromicity of the free DNA sample which had been used to prepare the histone-bound complexes of that series.

CIRCULAR DICHROISM: The circular dichroism (CD) spectra of the samples were taken on a Durrum-Jasco Model J-20 spectropolarimeter at room temperature. The CD results are reported as

$$\Delta \mathcal{E} = \mathcal{E}_l - \mathcal{E}_r \quad (4)$$

where  $\mathcal{E}_l$  and  $\mathcal{E}_r$  are the molar extinction coefficients for the left- and right-handed circularly polarized light. The units of  $\Delta \mathcal{E}$  are  $M^{-1} \text{ cm}^{-1}$  in nucleotide residues:

$$\Delta \mathcal{E} = \frac{\Theta}{33.05 \cdot C \cdot l} \quad (5)$$

where:

$\Theta$  = measured ellipticity in degrees

c = concentration in moles / liter

l = pathlength in cm

The error in CD measurements varies with the change in noise to signal ratio, which normally increased with decreasing wavelength.

The maximum error due to this effect as well as to inaccuracies introduced during the analysis of the raw data amounts to a maximum error range of  $\pm 5\%$ .

DNA concentration in nucleoprotein solutions cannot be evaluated directly by  $A_{260}$  measurements due to the effects of light scattering. Dissociation of the complexes in 0.1% sodium dodecyl sulfate did not yield satisfactory results, nor was the sensitivity of the diphenylamine procedure (67) found to be sufficiently reproducible in the DNA concentration range employed. The method finally adopted was the hydrolysis of the complex in 0.5 N  $\text{HClO}_4$  followed by UV spectroscopy (68) or the procedure of Leach and Scheraga (69). In this method the log of the absorbance at wavelengths far from the absorption maximum (normally 360 nm - 320 nm) is plotted vs. log wavelength and extrapolated to the wavelength of interest (here, 260 nm). On complexes tested by both methods the discrepancy was no greater than 5% - 7% in the  $A_{260}$  determination.

CHAPTER III  
THERMAL DENATURATION

INTRODUCTION

The physical properties and template activity of chromatin are determined largely by the interactions between its constituents - DNA, histones, non-histone chromosomal proteins and RNA.

Thermal denaturation of a DNA-protein complex, monitored by the change in optical absorbance, is an extremely sensitive probe of such interactions, since both qualitative and quantitative aspects of the binding can be revealed.

In 1967 Ohlenbusch et al. (70) observed that calf thymus nucleohistone and salt-dissociated partially dehistonized nucleohistone could be melted in a low ionic strength buffer ( $2.5 \times 10^{-4}$  M EDTA, pH 8.0) to give multiphasic melting profiles. The progressive removal of histone sharpened the transitions and finally decreased the number of melts until only the melting of free DNA was observed ( $T_m = 45^{\circ} - 50^{\circ}\text{C}$ ).

Ansevin et al. (71) thermally denatured rat liver chromatin in the presence of urea and concluded that autolysis or tryptic digestion of histones preferentially decreased the highest melting band. This indicated that the prime targets for tryptic digestion and proteolysis, the most basic portions of the histone molecules, were responsible for the high temperature stabilization of DNA.

In order to more specifically characterize the histone stabilization of DNA, polylysine was used as a polypeptide model protein for

the polycationic histones. Tsuboi et. al. (72) observed that polylysine complexes with poly I · poly C exhibited two melting bands, at 57°C and 89°C. Increasing ratios of lysine / nucleotide (+/-) caused enhancement of the 89°C band at the expense of the 57°C band. At a +/- ratio of 1.0 the 57°C band was entirely eradicated. The addition of free DNA to a solution of pre-formed complex at low ionic strength resulted in no transfer of the polypeptide to the free DNA, demonstrating the irreversibility of polylysine binding at low ionic strength. The presence of a biphasic melting profile was also taken as evidence of binding irreversibility since complexes of DNA and reversibly bound ligands (salt, tetralysine, tetraarginine) showed elevated, but monophasic thermal profiles.

Olins, Olins and Von Hippel (73) observed that during salt gradient reconstitution of polylysine - DNA or polyarginine - DNA complexes two thermally distinguishable forms of DNA were present: essentially free DNA and complexed, electrostatically neutralized DNA. The biphasic melting of the complexes indicated the cooperative nature of the polypeptide binding to DNA. In oligolysine (degree of polymerization [d.p.] 8)-DNA complexes no biphasic melting was seen merely an elevation of the free DNA melting band. They concluded that a minimum length polypeptide was needed to establish the complex exhibiting the biphasic type of thermal denaturation pattern. Decreasing the length of the DNA by sonication did not change the thermal characteristics of the complexes. The same authors extended their studies to include DNA complexes with polyhomoarginine and polyornithine. In all cases biphasic melting was observed at +/- ratios less than 1.0. The low

temperature  $T_m$  was characteristic of the DNA while the second transition,  $T_m'$ , was dependent on the specific polypeptide which was bound.

In 1973 Li (74) proposed a theory of helix-coil transitions in DNA and nucleoprotein which assumed the irreversibility of complex formation at low ionic strength and a characteristic  $T_m'$  of the melting of any polypeptide-bound DNA region. The input ratio of amino acid to nucleotide,  $r$ , of a particular polypeptide,  $k$ , was proportional to the fraction of DNA bound by  $k$  ( $F_k$ ) ; the constant of proportionality being  $\beta_k$ , the amino acid to nucleotide ratio (aa/n) in the polypeptide-bound region:

$$r_k = \beta_k F_k \quad (6)$$

$F_k$  is determinable from analysis of the thermal melting profile of the complex:

$$F_k = \frac{A_k}{\sum_{i=0}^n A_i} \quad (7)$$

Then:

$$r_k = \beta_k (A_k / A_T) \quad (8)$$

For nucleoproteins with biphasic melting:

$$r_k = \beta_k (1 - A_{Tm} / A_T) \quad (9)$$

Where  $A_k$  is the area under melting band  $k$ ,  $A_{T_m}$  is the area beneath the free DNA peak, and  $A_T$  is the total area beneath the melting curve.

In direct-mixed or salt gradient reconstituted DNA-polylysine complexes  $\beta = 1.0$  aa/n. Direct-mixed polyarginine complexes precipitate as fibrous aggregates (73) while polyarginine-DNA complexes made in the presence of urea have  $\beta = 1.0$ , and polyarginine-DNA complexes reconstituted without urea show  $\beta = 1.4$ . (It is known that the arginine-rich histones are most susceptible to aggregation in a high salt environment (75); the absence of urea from the reconstitution medium may allow the aggregation of polyarginine and an increase in the apparent  $\beta$ . In pea bud nucleohistone  $\beta = 3.2$ , while in calf thymus nucleohistone  $\beta = 3.7$  (76).

From the melting profile the percent of free DNA in a complex can be determined by:

(10)

$$F_{DNA} = A_{T_m} / A_T$$

where  $A_{T_m}$  is the area under the melting band of free DNA. By this method the fraction of bound DNA in calf thymus chromatin was estimated to be  $75\% \pm 8\%$  (74), a value exceeding the 50% bound DNA proposed by Clark and Felsenfeld (77) based on polylysine titration.

In 1974 Li et al. (76) showed that polylysine could bind to histone-bound DNA sequences, leading to over-estimates of the fraction of free DNA and hence under-estimates of bound DNA. It was shown that polylysine would bind calf thymus nucleohistone with the following order of preference: A+T-rich free DNA > G+C-rich free

DNA > DNA bound by less - basic half of histones > DNA bound by more - basic half of histones.

It was also demonstrated that the removal of histones by salt did not eliminate the two highest melting bands of nucleohistone until practically all the histone was lost - indicating that higher order structures, such as supercoiling, did not make a major contribution to the thermal denaturation profile. This coincided with the results of Shih and Lake (1972) (78) who found that interphase chromatin and metaphase chromosomes have identical melting profiles.

In 1970 Shih and Bonner (1) found that complexes of purified individual histones with DNA were formed cooperatively during salt gradient dialysis with urea, exhibited biphasic melting at sub-equivalent aa/n ratios, and were inactive in supporting RNA synthesis in an in vitro transcription system. Since their complexes of mixtures of histones with DNA did not melt as sharply as the pure - histone complexes with DNA, they concluded that the mixed histones were binding randomly and heterogeneously to the DNA with no extended regions occupied exclusively by a single histone class.

Because both high - temperature melting bands of nucleohistone decreased simultaneously as histones were removed by either NaCl, MgCl<sub>2</sub> or H<sub>2</sub>SO<sub>4</sub> (63) and each histone apparently contributed to each band, Li and Bonner (63) reconstructed complexes of DNA with each half of the histone H2B molecule separately. Each of these complexes showed a single characteristic high temperature band (although 4<sup>o</sup> - 10<sup>o</sup>C lower than in whole H2B - DNA complexes; the difference in Tm' was attributed to the shortened polypeptide length). It was therefore

concluded that the charge asymmetry occurring on histones is responsible for the splitting of the high temperature melting transition into at least two sub-bands.

In addition to complexes of DNA with histones or synthetic homopolymers, thermal denaturation has been applied to DNA complexes with the basic sperm proteins of salmonid fishes - the protamines. These small (ca. 30 amino acids) highly basic proteins (70% of their amino acids are arginine residues) exhibit a  $\beta$  value of 1.38 aa/n in complexes with DNA made by direct-mixing (79), corresponding to almost full charge neutralization of the DNA phosphates (arginine / nucleotide = 0.92). Protamine stabilized DNA to 91°C ( $T_m'$ ) in EDTA buffer. At higher ionic strengths the  $T_m$  of free DNA increases while the  $T_m'$  of protamine-bound DNA remains constant, indicating full electrostatic shielding of the phosphates in the protamine-bound regions. Similar results have been found in polylysine-DNA complexes formed by direct-mixing (76).

Inoue<sup>1</sup> and Ando (80) observed biphasic melting of DNA complexes with clupeine (a herring protamine), which stabilized DNA to 80° - 85°C. With short polyarginines (d.p. = 4), however, they reported monophasic melting, similar to oligolysine (d.p. = 8) and salt stabilization of DNA. Polyarginine (d.p. = 20) did exhibit biphasic melting, however. Biphasic melting has been used as a criterion for irreversible complex formation in polylysine, polyornithine, polyhomoarginine and histone to DNA complexes. Monophasic, elevated  $T_m$  melting is taken to indicate the reversibility of complex formation.

## EXPERIMENTAL

Thermal denaturation profiles of various DNAs complexed with individual or mixed histone fractions reveal certain properties of each nucleohistone which are characteristic of the DNA component and others which are determined by the histones. Some of the features of the thermal denaturation profiles to be discussed are shown in Table 3.

Figure 7 presents the derivative thermal denaturation (T.D.) profile ( $dh/dT$  vs. temperature) of a series of histone H2B complexes with various DNAs (nucleohistone H2B). The lowest melting band in each melting curve is due to the helix-random coil transition of the DNA free of protein binding (76). The temperature of this transition ( $T_m$ ) is proportional to the percentage of guanine and cytosine base pairs (% G+C) in the DNA (65). The temperature of the  $T_m$  for each DNA in the low ionic strength medium .25 mM NaEDTA, pH 8.0 (sodium salt, ethylene diaminetetraacetic acid) is given in Table 3.

As increasing amounts of H2B annealed to the DNA three higher temperature transitions appear in the T.D. profile,  $T_{mII}$ ,  $T_{mIII}$  ( $68^{\circ}\text{C}$  and  $91^{\circ}\text{C}$ , Figure 7a;  $70^{\circ}\text{C}$  and  $89^{\circ}\text{C}$ , Figure 7b; and  $87^{\circ}\text{C}$  and  $105 - 110^{\circ}\text{C}$ , Figure 7c) and a small shoulder at a temperature intermediate to the free DNA and bound DNA melting bands ( $56^{\circ}\text{C}$ , Figure 7a;  $60^{\circ}\text{C}$ , Figure 7b;  $73^{\circ}\text{C}$ , Figure 7c). The two highest peaks  $T_{mII}$ ,  $T_{mIII}$  can be interpreted as due to the melting of DNA complexed with the less basic ( $T_{mII}$ ) and more basic ( $T_{mIII}$ ) portions of the histone H2B molecule as previously done for the derivative thermal denaturation profile of chromatin (63), while the shift of  $T_m$  from  $47^{\circ}\text{C}$  to about

Table 3. (a) C1. perfringens DNA ( T<sub>m</sub> = 37°C )

[ All data refers to r = 3 complexes unless noted ]

	<u>T<sub>m</sub> III</u>	<u>A<sub>320</sub> / A<sub>260</sub> (b)</u>	<u>A<sub>320</sub> / A<sub>260</sub> (a)</u>	<u>h<sub>max</sub></u>	<u>β</u> <u>aa/n</u>
H2A (urea)	86°,103°	0.22		28%	---
H2B (urea)	84°,92°	0.16		26%	4.2
H2 (urea)	82°	0.06 (r=2)	0.04	34%	3.7
		0.12 (r=3)	0.13	42%	
H2 (-urea)	77°	0.04		32%	4.1
W-H1 (urea)	82°	0.09		37%	6.0
W-H1 (-urea)	76°	0.08		36%	4.5
Whole (urea)	83°	0.08 (r=2)	0.07	34%	3.7
		0.19 (r=3)	0.19	42%	
Whole (-urea)	79°	0.03	0.03	37%	3.2

Notes:

(a) = after denaturation

(b) = before denaturation

Table 3. (b) Calf thymus DNA (  $T_m = 47^\circ$  )

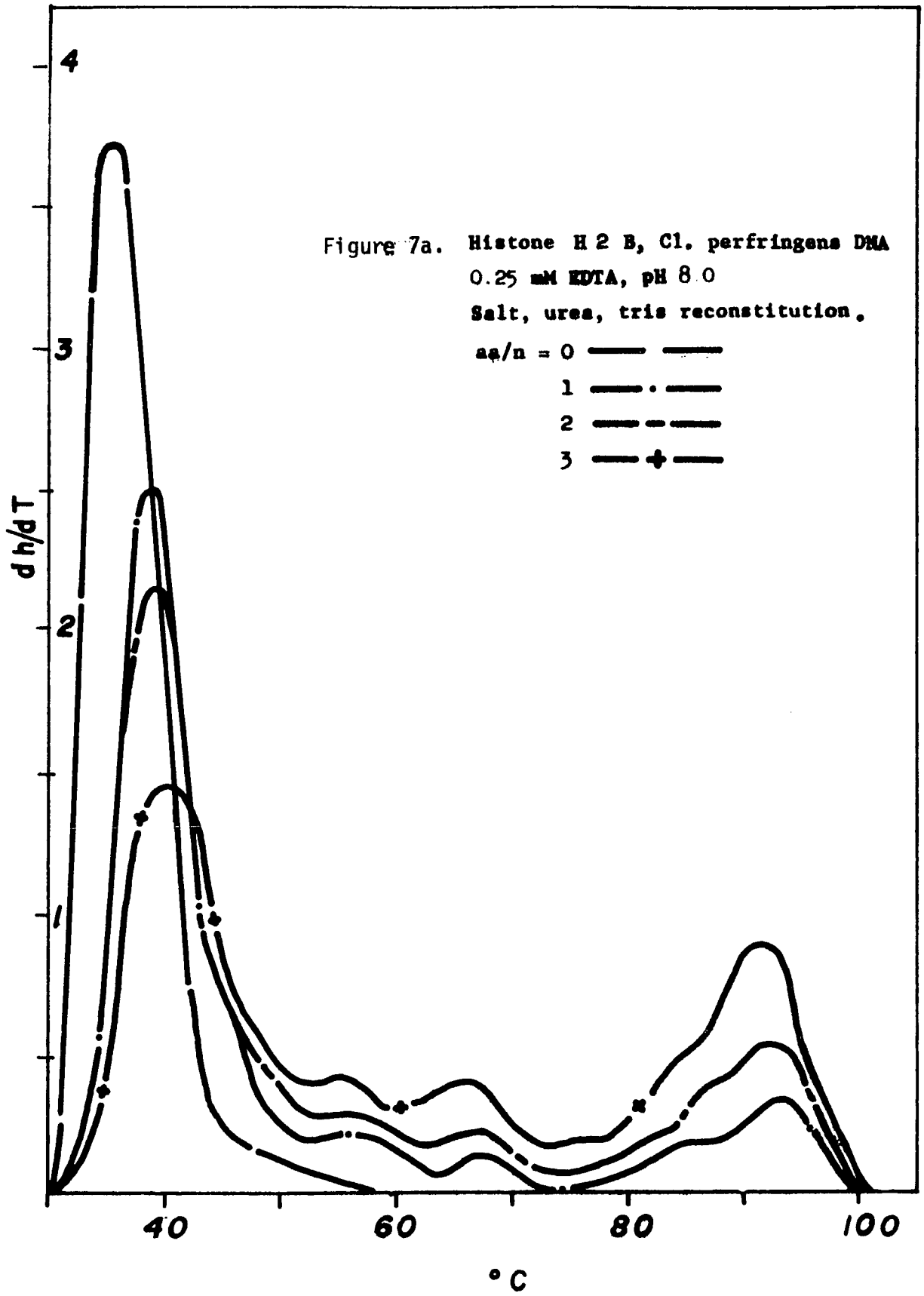
[ All data refers to  $r = 3$  complexes unless noted ]

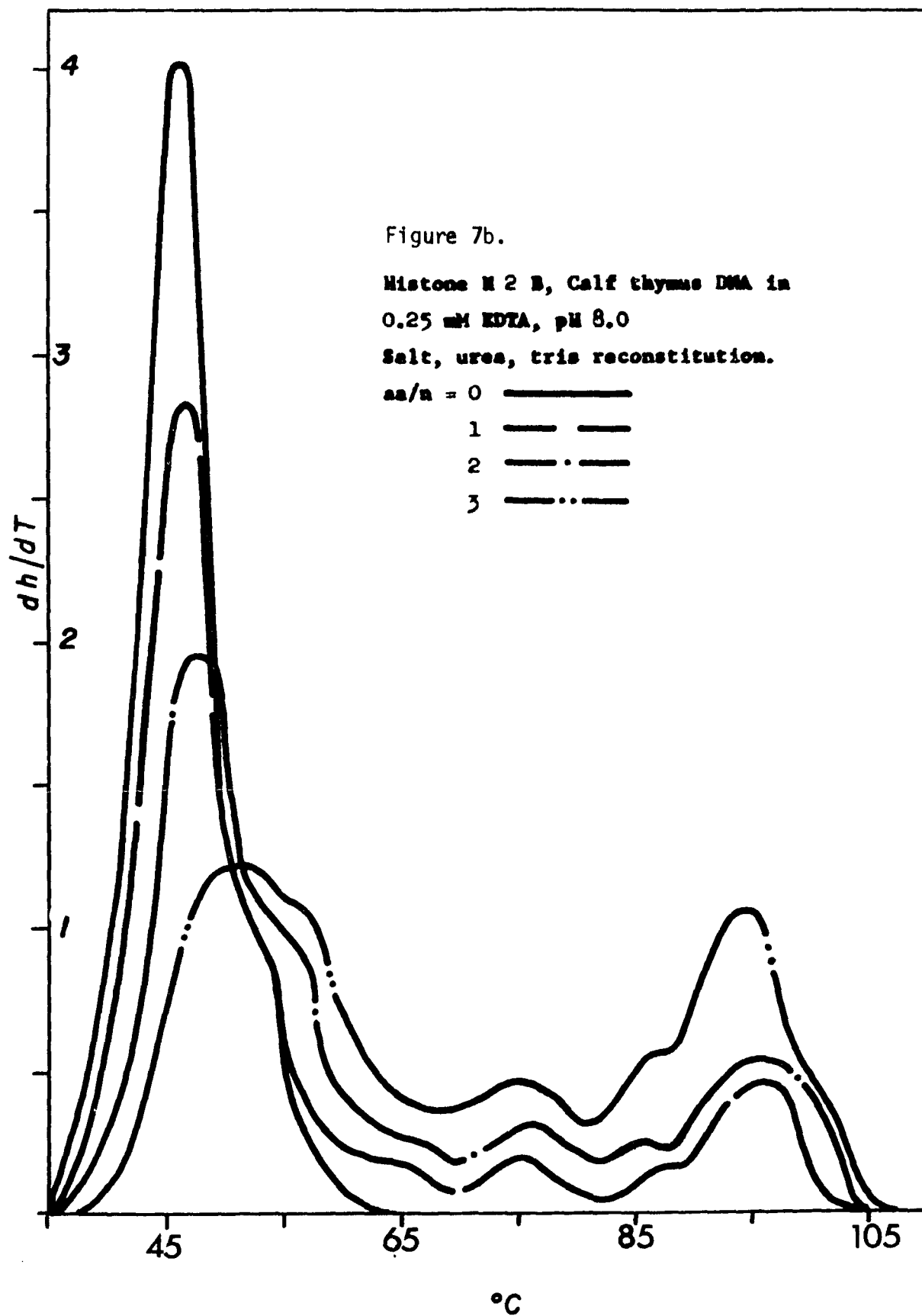
	$T_m$ III	$A_{320}/A_{260}$ (b)	$A_{320}/A_{260}$ (a)	$h_{max}$	$\frac{\beta}{aa/n}$
H2A (urea)	83°, 93°	0.32		31%	---
H2A (-urea)	86°-93°	0.38		18%	---
H2B (urea)	90°	0.20		21%	4.2
H2B (-urea)	83°	0.08		26%	5.2
H2B (melted in urea)	85°, 89°	0.21		19%	---
H2 (urea)	99°	0.06 (r=2) 0.13 (r=3)	0.07 0.20	36% 50%	3.7
H2 (-urea)	89°	0.12		30%	4.1
H2 (+ urea)	86°	0.14		18%	---
H2 (phos)	92°	0.15		38%	ca. 4.2
H2 (d.m. NaCl)	85°, 95°	0.12		31%	3.9
H2 (d.m. EDTA)	96°	0.05		34%	4.4
H2 (melted in urea)	83°	0.09		25%	---
W-H1 (urea)	98°	0.20		27%	6.0
W-H1 (-urea)	92°	0.24		24%	4.5
W-H1 (phos)	96°	0.21		29%	4.2
W-H1 (melted in urea)	89°	0.00		46%	---
Whole (urea)	93°	0.04 (r=3) 0.09 (r=4)	0.03 0.13	34% 40%	3.7
Whole (-urea)	87°	0.14		32%	3.2
Whole (phos)	90°-95°	0.12	0.10	40%	3.2
Whole (melted in urea)	81°	0.00		58%	---
Chromatin	83°	0.05		25%	3.7

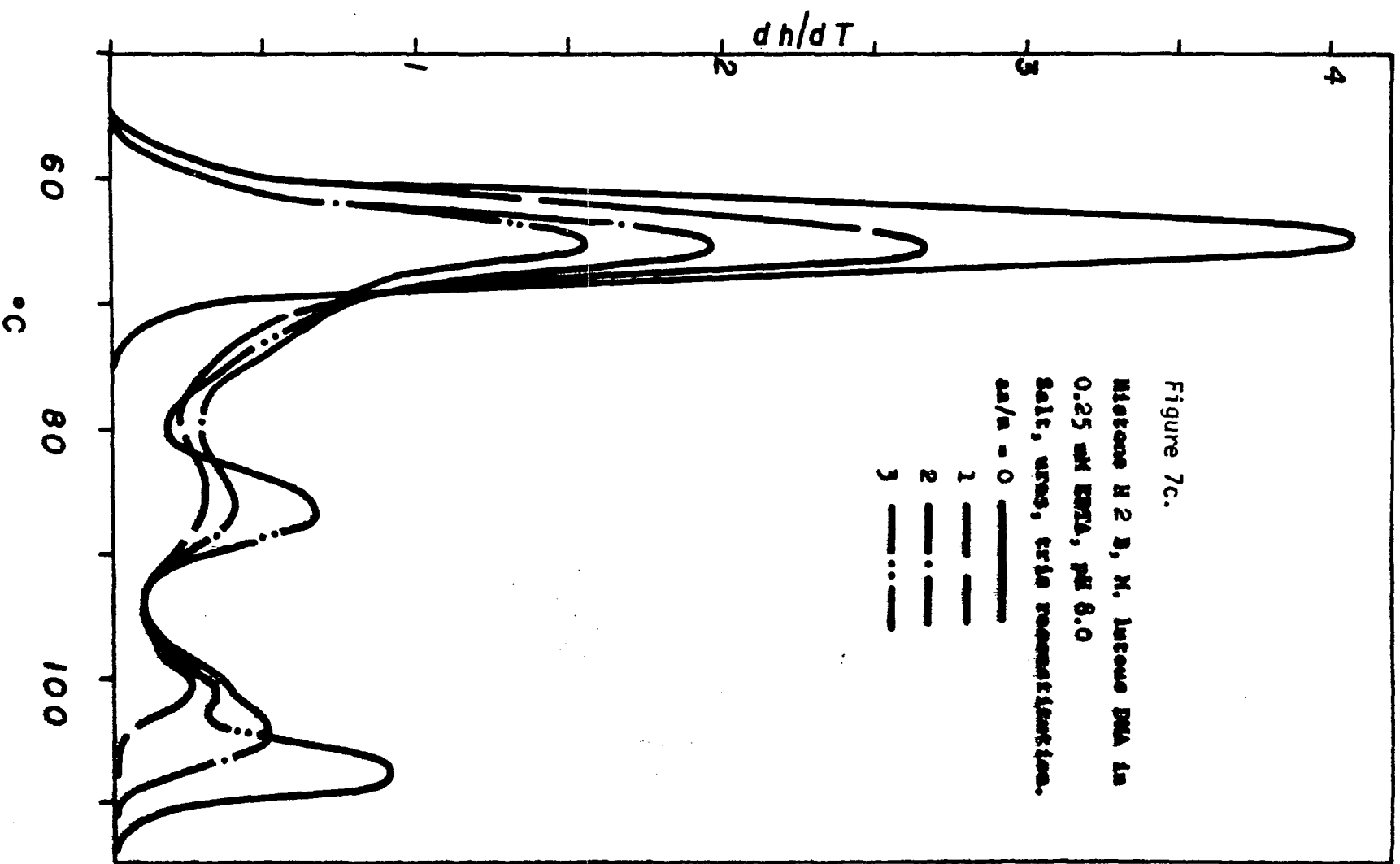
Table 3. (c) M. luteus DNA ( T<sub>m</sub> = 63°C )

[ All data refers to r = 3 complexes unless noted ]

	<u>T<sub>m</sub> III</u>	<u>A<sub>320</sub> / A<sub>260</sub></u> (b)	<u>A<sub>320</sub> / A<sub>260</sub></u> (a)	<u>h<sub>max</sub></u>	<u>β</u> <u>aa/n</u>
H2A (urea)	102°, 109°	0.27		22%	---
H2B (urea)	101°, 109°	0.22		13%	4.2
H2B (-urea)	93°	0.06		24%	5.2
H2 (urea)	103°	0.07 0.13	0.06 0.14	28% 30%	3.7
H2 (-urea)	96°	0.04 0.04	(r=2) (r=3) 0.05 0.08	30% 34%	4.1
W-HI (urea)	107°	0.17		31%	6.0
W-HI (-urea)	92°	0.11		31%	4.5
Whole (urea)	102°	0.17		30%	3.7
Whole (-urea)	93°	0.05		33%	3.2







50°C and the appearance of the intermediate melting ( $T_{mI}$ ) could be due to the melting of short gaps of free DNA between two histone-bound segments. An alternative explanation, which does not exclude this possibility, is that the  $T_{mI}$  transition(s) represents a conformational change in the protein-bound DNA regions from C form to B form. Evidence supporting this view comes from the results of Wilhelm et. al. (81) who have followed the thermal denaturation of chick nucleoprotein (chick DNA  $T_m = 47^\circ\text{C}$ ) by changes in its circular dichroism spectrum. These authors observed a decrease in the helical conformation of the histones at 60°C as a necessary prior condition to a C→B conformational change in the DNA which occurs near 65°C. Their data suggested that changes in the secondary structure of the hydrophobic, helical regions of the histones may influence the binding of the more basic protein regions and influence the conformational constraints imposed by these latter regions on the DNA.

Ivanov (82) has suggested that the C form of DNA represents a less hydrated state of the nucleic acid while the more expanded B form accommodates a larger amount of water of hydration. It is then possible that a change in the secondary structure of the hydrophobic protein segments could alter the balance of DNA hydration and induce conformational changes in the nucleic acid.

It may also be that the intermediate melting is related to the state of aggregation of these complexes and the associated light scattering. In complexes of DNA with histones H2B, H2A or H2 (Figures 7, 10, 13) omission of urea from the reconstitution medium decreases the amount of intermediate melting (Figures 8, 12, 16) as

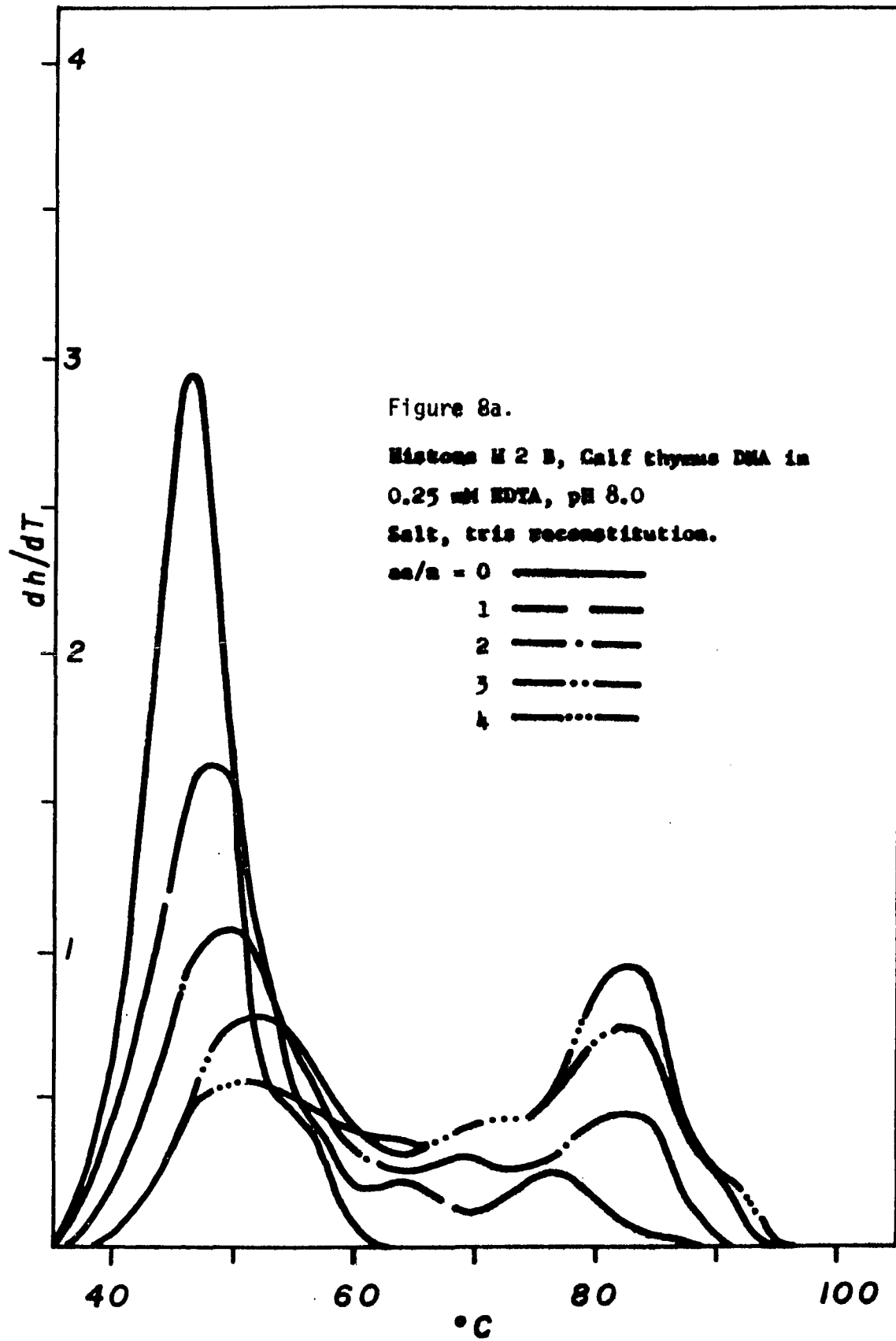
well as the value  $A_{320} / A_{260}$  (Table 3). Since the  $A_{320} / A_{260}$  ratio is an indicator of the extent of light scattering in the complex, it appears that the intermediate melting may be related to this phenomenon. In whole histone complexes with DNA, however, the minus - urea complexes (Figure 29) show enhanced intermediate melting over the plus - urea complexes (Figure (27) while the ratio  $A_{320} / A_{260}$  decreased significantly (Table 3). It is therefore impossible to definitely assign the intermediate melting transitions exclusively to DNA conformational changes, especially since the hyperchromicity associated with these changes is small. However, the effect of the hydrophobic residues on the conformation of the DNA may be one of the factors, along with light scattering, the melting of short DNA gaps and the heterogeneity of reconstituted complexes, which contributes to the melting between the free and bound DNA melting bands.

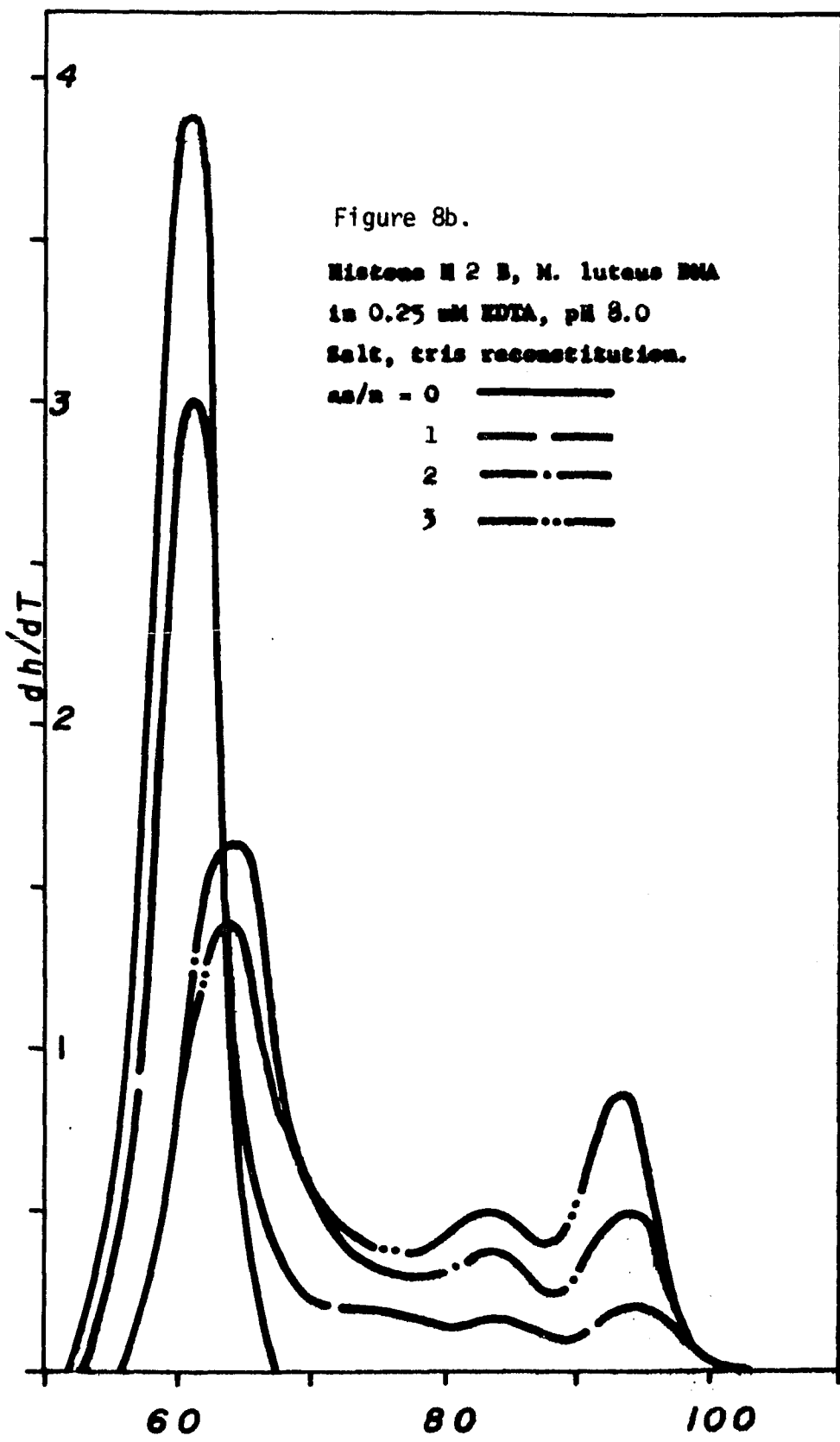
It may be noted that the  $T_{mIII}$  transition in each nucleohistone H2B (Figures 7a,b,c) is reproducibly split into two transitions. Examination of the amino acid sequence of H2B (6) reveals that the more basic "half" of the molecule may be considered as divided into two parts, with local accumulations of basic residues at each end of the H2B molecule, separated by a hydrophobic central core region prone to extensive ordered secondary structure and through which segment the histones are believed to interact (87, 88). This general arrangement has been observed for each of the main histone species H2A, H2B, H3 and H4 (89). It may be that  $T_{mIII}$  is split as a result of the physical separation of these regions of highly positively charged residues along the histone molecule itself. It is also possible that

the strength of binding of histone H2B to DNA in a reconstituted complex varies slightly between DNA segments of different G+C content, giving rise to sub-bands within each major band.

When nucleohistone H2B is reconstituted in the absence of urea (Figure 8) the highest temperature transitions now appear at 82°C (C-DNA) and 93°C (L-DNA), whereas previously they occurred at 90°C (C-DNA) and 108°C (L-DNA). These nucleohistones were annealed in a high salt medium containing no urea. The absence of urea in this environment would be expected to promote hydrophobic interactions and secondary structure among the histones. It is reasonable then to explain the decrease in temperature of the highest melting transition by postulating that the structure of the histone-DNA unit is condensed and more constrained because of the enhanced hydrophobic attractive forces within the central region of the histone. This leads to a decrease in the ability of the more basic regions to stabilize the DNA due to the emergence of electrostatic repulsive forces within the histone-DNA unit which had previously been neutralized by salt at the beginning of the reconstitution.

That the amino acid residues are in fact closer to one another can be demonstrated by calculating the number of amino acid residues per nucleotide in the protein bound regions of the nucleohistone, the beta value,  $\beta = aa/n$ . Figure 9 is a graph of Equation 9 whose slope represents  $\beta$ . It can be seen that complexes reconstituted in the presence of urea have 4.2 aa/n in the protein bound region while those reconstituted in the absence of urea have  $\beta = 5.2$  aa/n. It should also be noted that regardless of the DNA component of the nucleohistone, the r vs. F (fraction of DNA bound) values fall on the





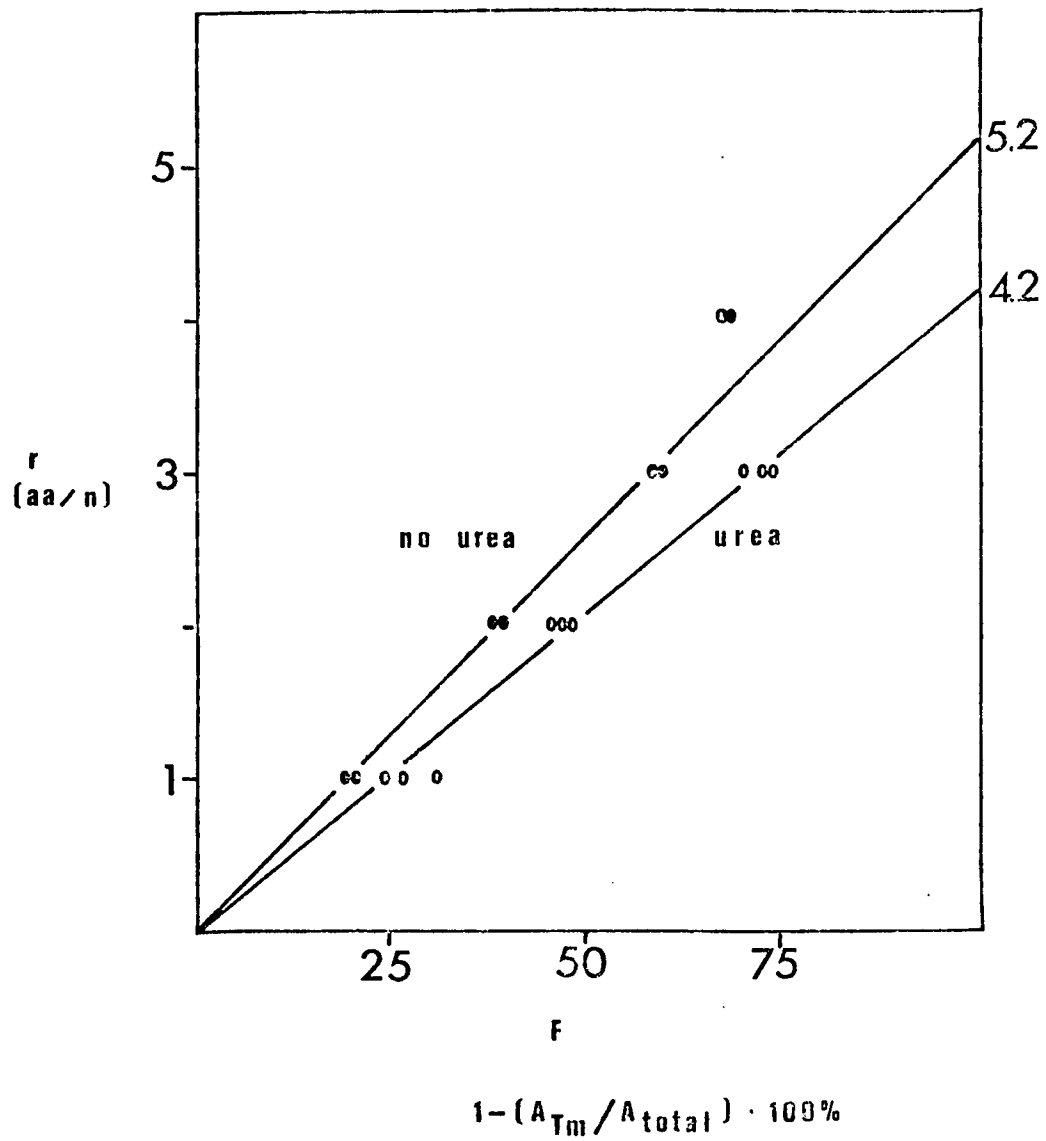
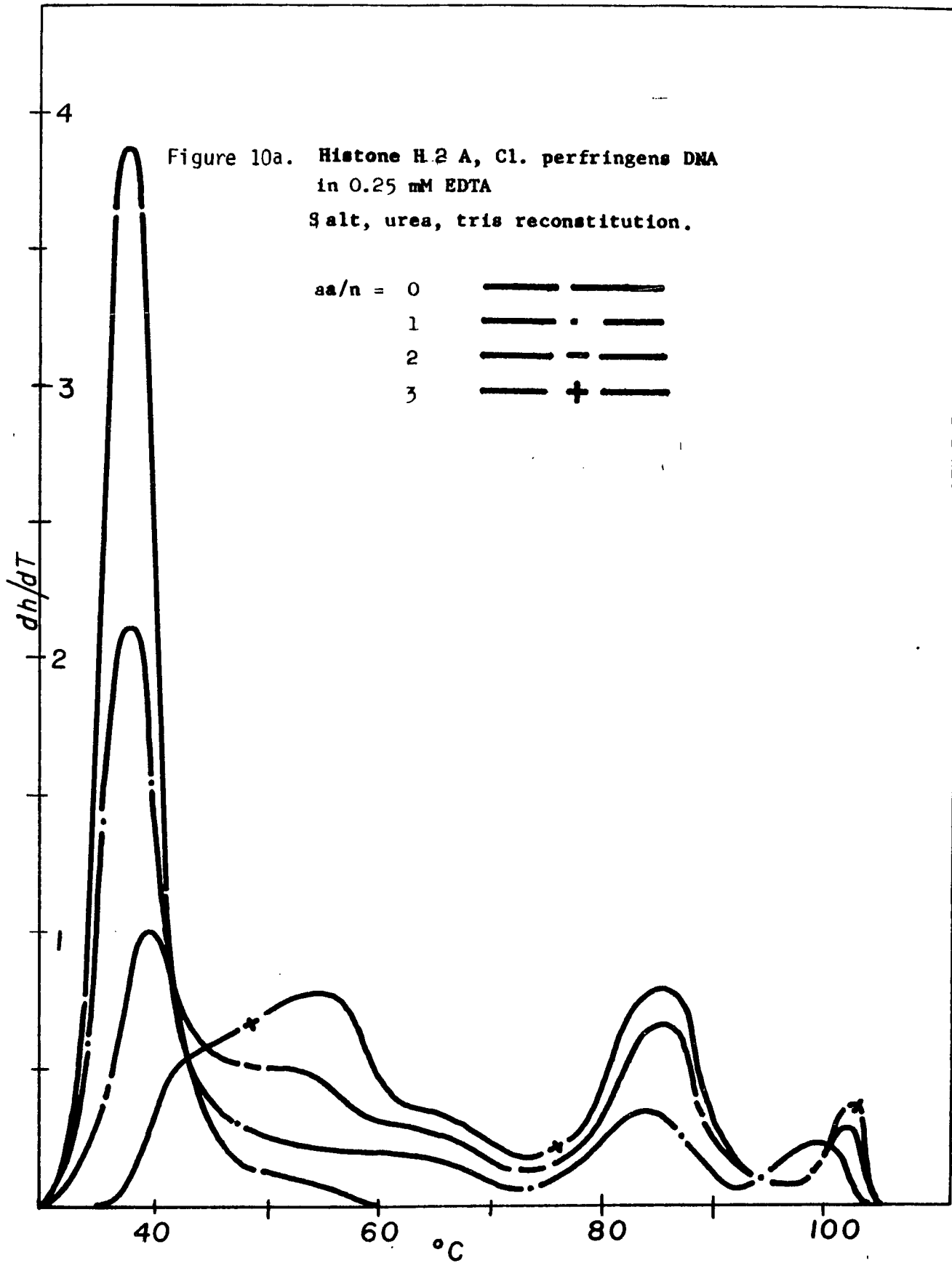


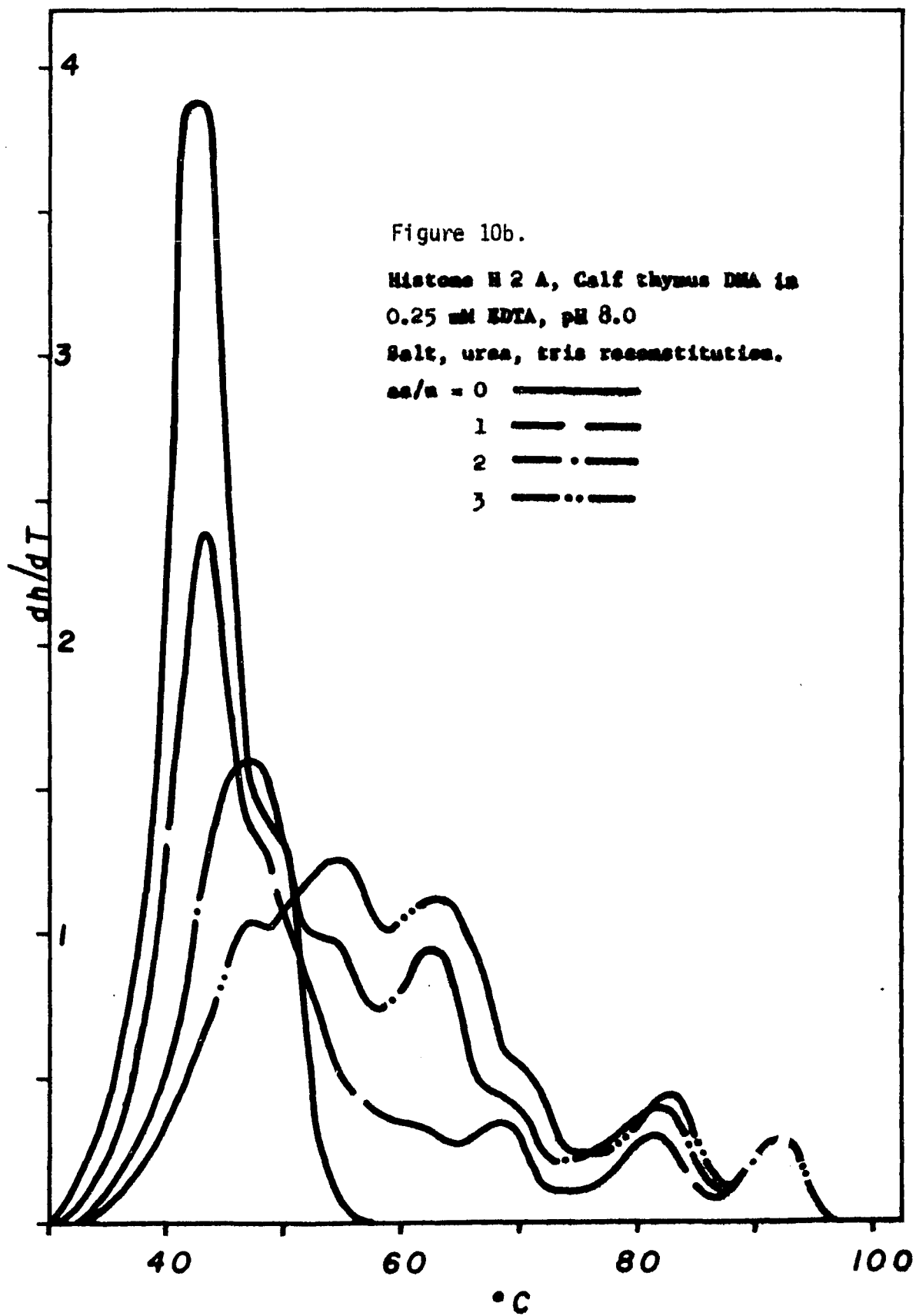
Figure 9.  $\beta$  value determination.  
 Histone H2B nucleohistones.

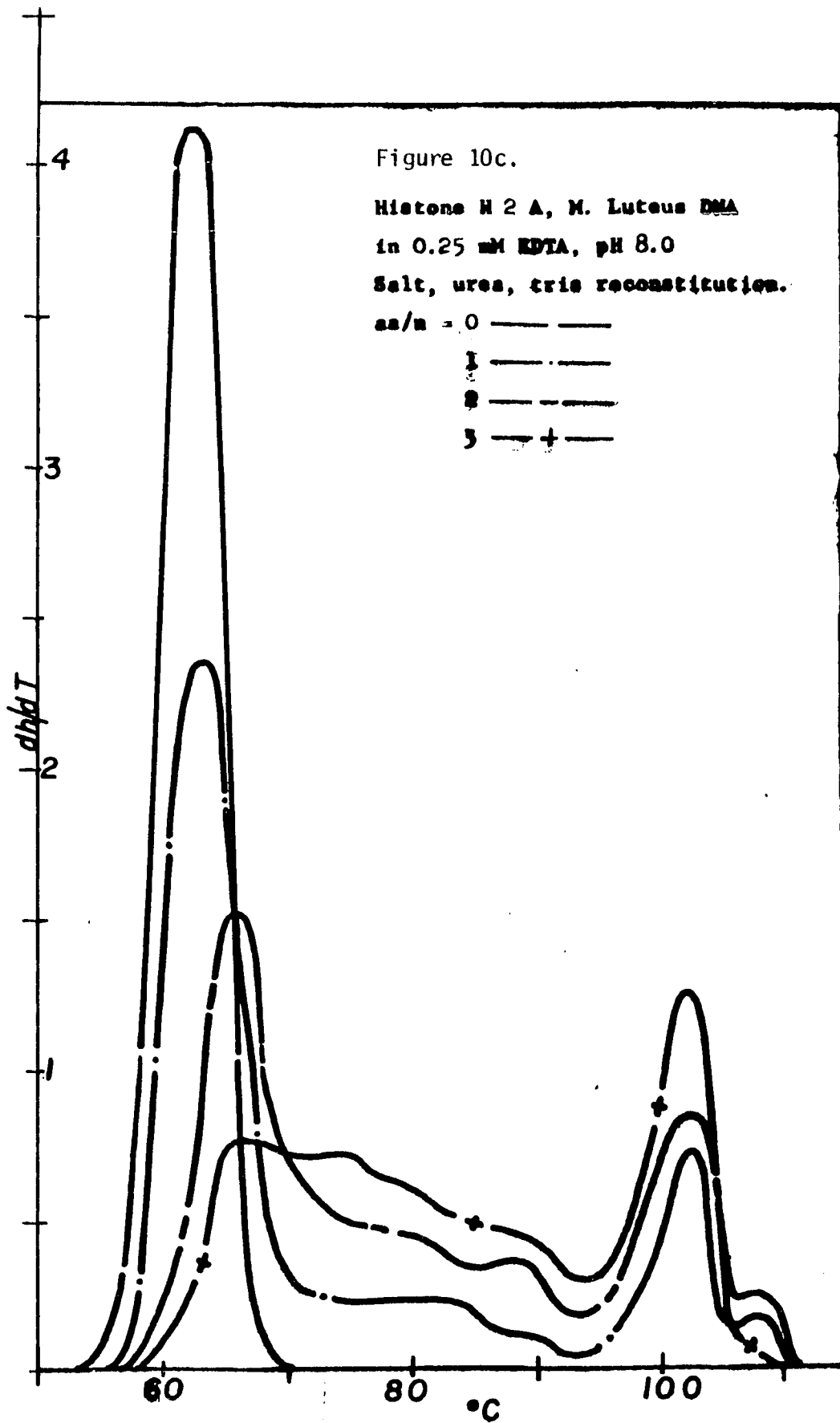
same line. This implies a similarity in the binding of the histones to both homologous mammalian calf DNA as well as to bacterial DNAs. This feature is also illustrated by the general resemblance of the melting profiles of the nucleohistones reconstituted with the widely different DNAs. These facts support the view that the histones are neither sequence - nor species - specific in their binding (84).

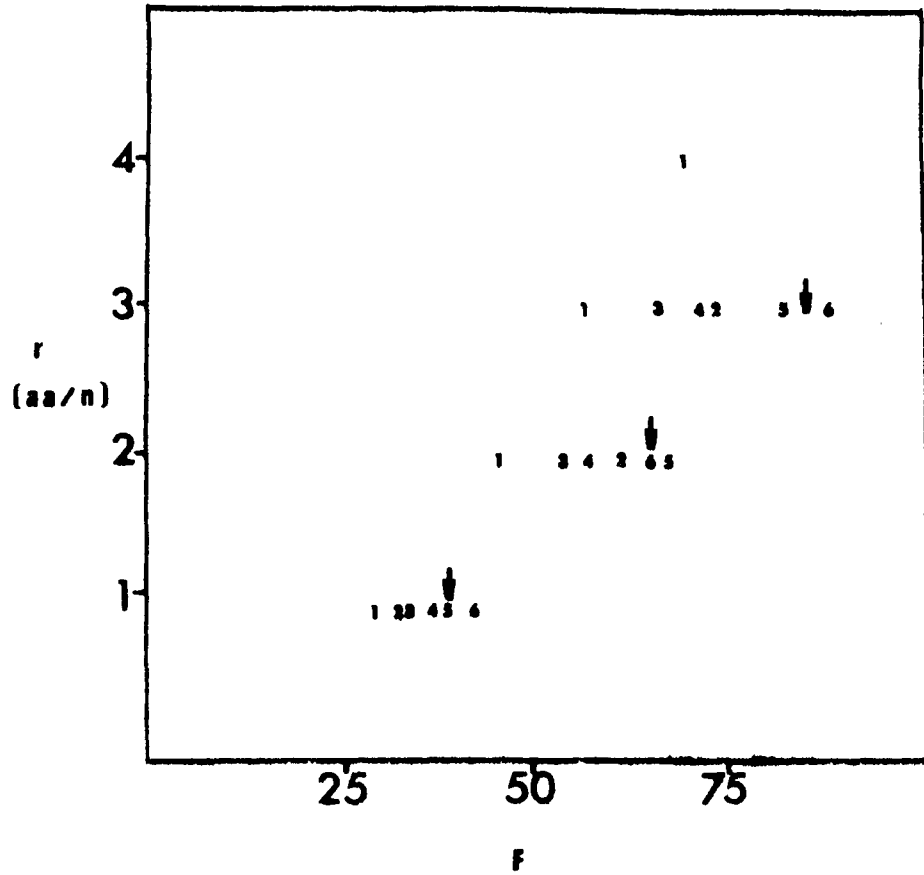
Another point which deserves mention is best illustrated by Figure 7b. As increasing amounts of protein are annealed to the DNA an upwards shift in  $T_m$  is noted. This may be due to two factors. First, calf DNA has been shown to contain a satellite fraction with G+C content higher than the average G+C content of the DNA (55% vs. 42%) (65). Although not sequence - specific, histone H2B preferentially binds A+T - rich DNA regions (Chapter V). As the A+T - rich DNA is bound the remaining free DNA has a progressively increased G+C content which shifts the  $T_m$  upwards. Secondly, in the high salt reconstitution medium histones bind with less apparent cooperativity than if mixed directly with DNA at low ionic strength. This results in free DNA regions between protein - bound regions. As the protein / DNA ratio increases these regions become shorter and their  $T_m$  increases (85).

The thermal denaturation profiles of nucleohistone H2A are shown in Figure 10. Again, the general  $T_m$ ,  $T_{mI}$ ,  $T_{mII}$ ,  $T_{mIII}$  pattern is discernible although the increased amount of melting in the  $T_{mI}$  -  $T_{mII}$  ( $45^{\circ}\text{C}$  -  $65^{\circ}\text{C}$ , Figure 10a;  $50^{\circ}\text{C}$  -  $70^{\circ}\text{C}$ , Figure 10b;  $70^{\circ}\text{C}$  -  $90^{\circ}\text{C}$ , Figure 10c) region considerably camouflages peak delineation. A possible explanation for these effects is suggested by the amino acid composition of









$$1 - (A_{Tm} / A_{total}) \cdot 100\%$$

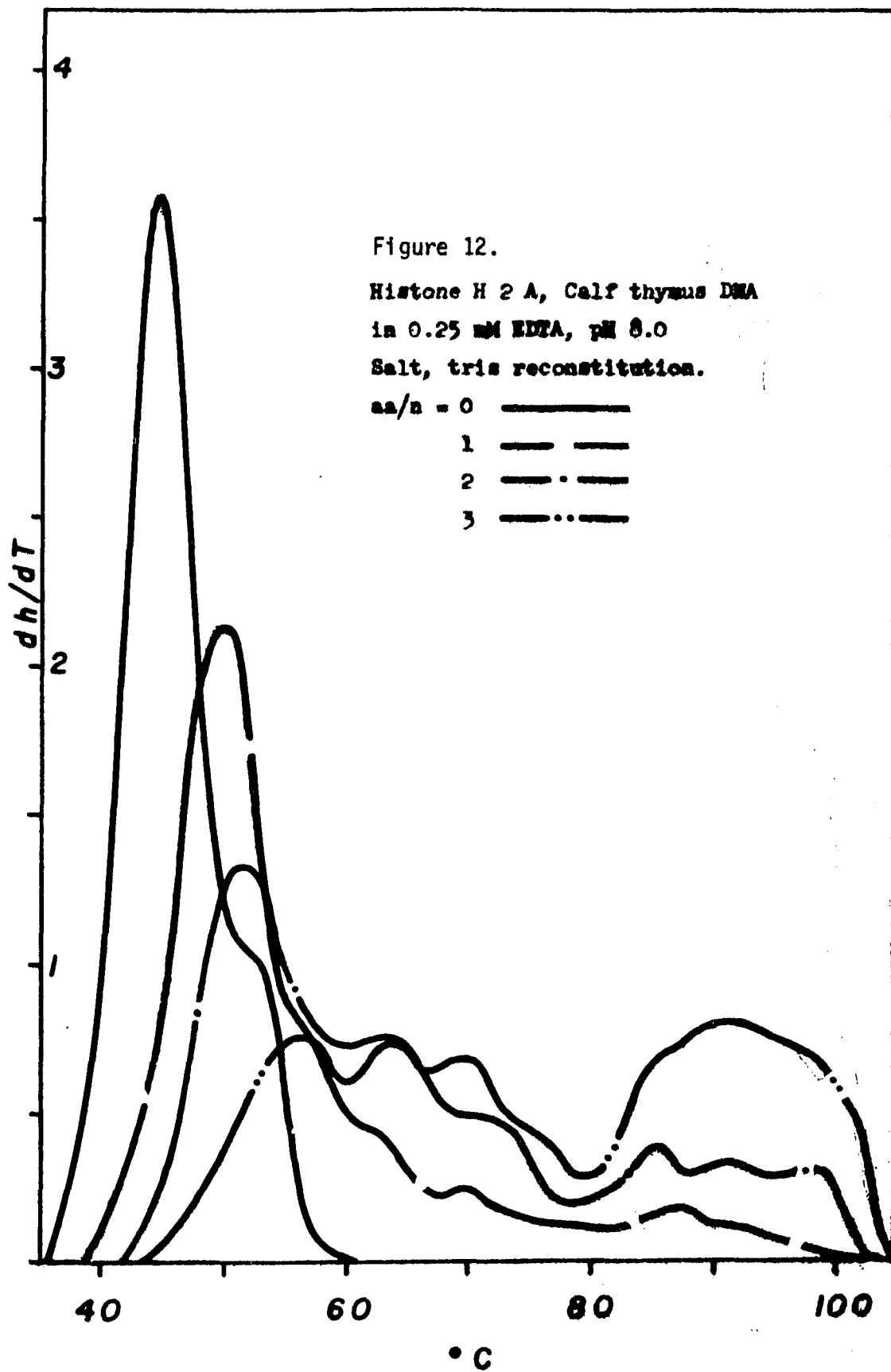
Figure 11.  $\beta$  value determination.  
 Histone H2A nucleohistones.  
 Numbers refer to individual  
 plus - urea complexes.  
 Arrows denote average values  
 of minus - urea complexes.

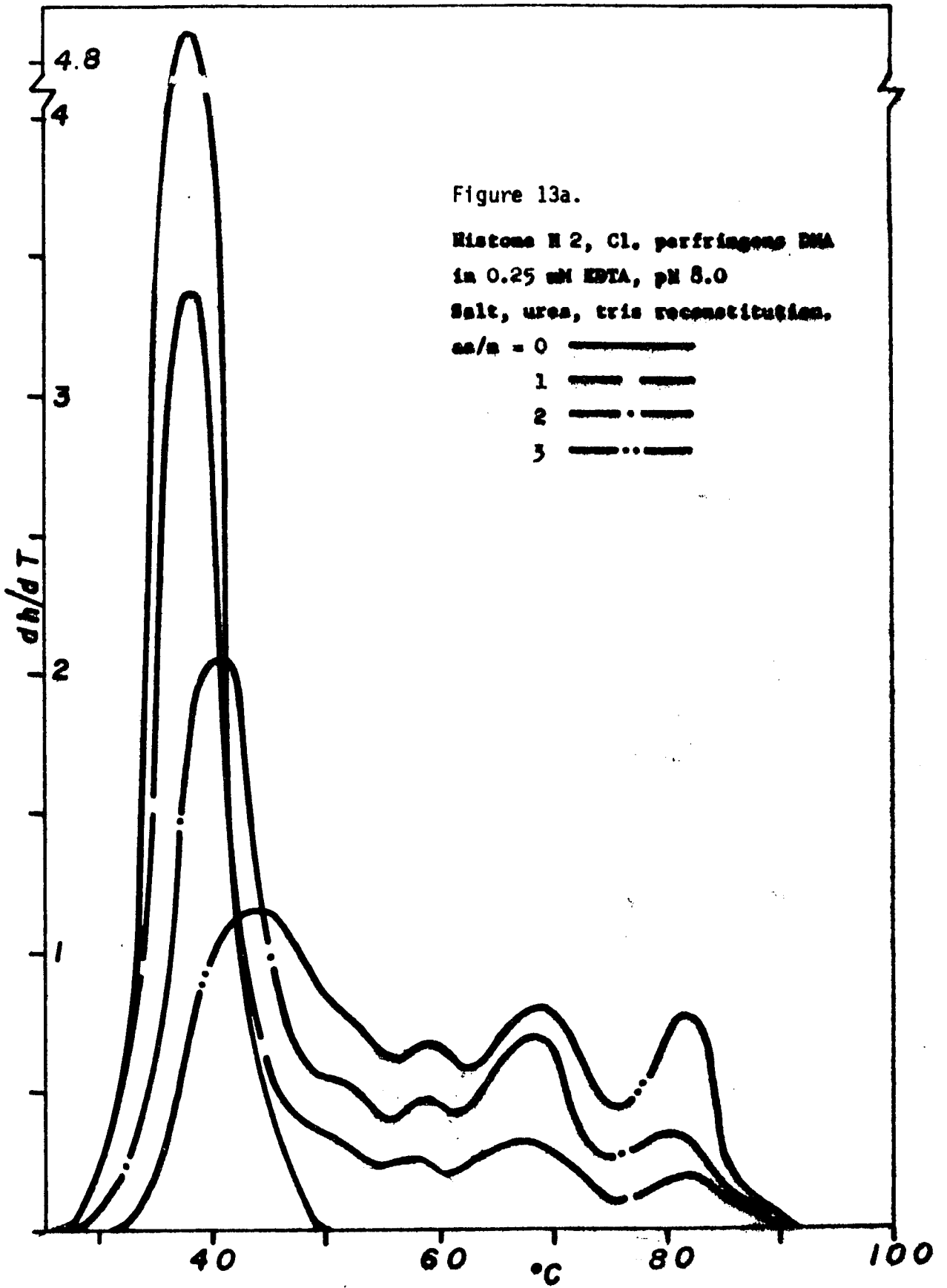
histone H 2 A. H 2 A contains ca. 50% more of those hydrophobic residues classified by Chou and Fasman (86) as strong alpha-helix formers (i.e. Glu, Ala, Leu) relative to H 2 B (H 2 B, 29 of 125 aa; H 2 A, 47 of 136 aa). In addition D'Anna and Isenberg (32) have reported that the secondary structure of histone H 2 A is significantly more sensitive to low concentrations of salt than that of H 2 B. In sodium chloride the amount of salt required to induce a change in secondary structure equal to 50% of the total possible change is 0.2 M for H 2 B and 0.06 M for H 2 A. Phosphate is still more efficient in inducing this change. The values in phosphate are 0.0045 M for H 2 B and 0.0019 M for H 2 A. The great enhancement of the intermediate temperature melting may well be due to the abundance of hydrophobic residues in H 2 A. That hydrophobic attractive forces play a large role in the binding of H 2 A to DNA is evidenced by Figure 11 which represents an attempt to evaluate  $\beta$  for nucleohistones H 2 A. Either with or without urea a strong dependence of  $\beta$  on the input ratio of histone to DNA is observed. Without urea however, the effect of increasing input ratio appears to be slightly less. A possible explanation for this effect is that in the high salt and urea reconstitution medium the histones contain minimal amounts of ordered secondary structure prior to binding the DNA. Once salt has been removed the histones have bound the nucleic acid and the subsequent removal of urea allows the intramolecular hydrophobic forces to form regions of alpha-helix or beta-sheet through which the histones react intermolecularly. The interaction of histones anchored to physically separate regions of the DNA would be expected to deform

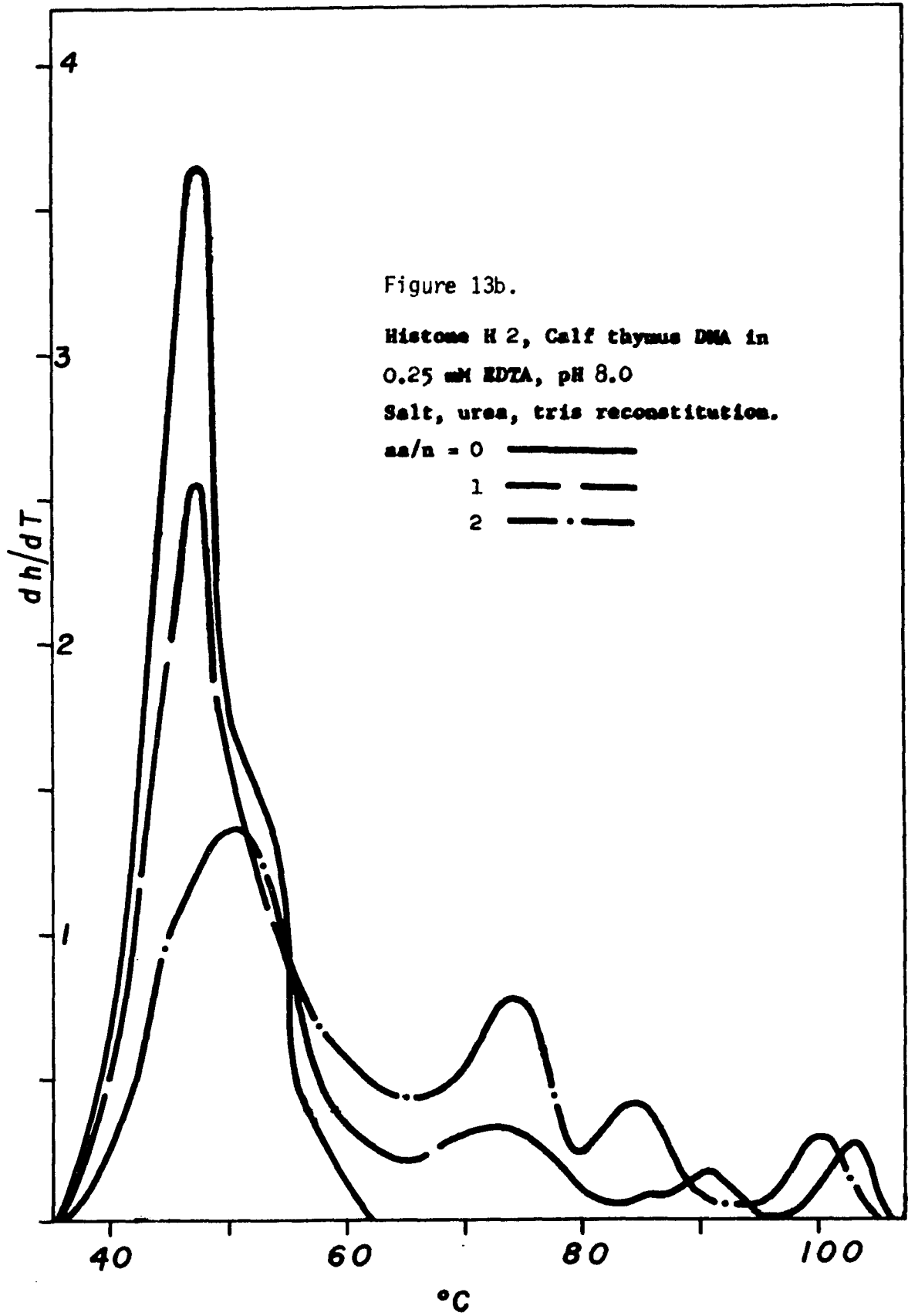
the conformation of the helix. As the hydrophobic regions become more ordered they may also contort the DNA either by strain imposed on the basic regions of the histone and transmitted to the DNA or by direct dehydration effects on the helix. When the histones are reannealed to DNA in the absence of urea, however, the hydrophobic histone-histone interactions have taken place prior to the act of binding and so may not have as great a structural effect on the DNA conformation in the final complex. Reconstitution of histone H2A to DNA in the absence of urea (Figure 12) reduces the amount of melting between  $T_m$  and  $T_{mII}$  (compare Figure 10b).

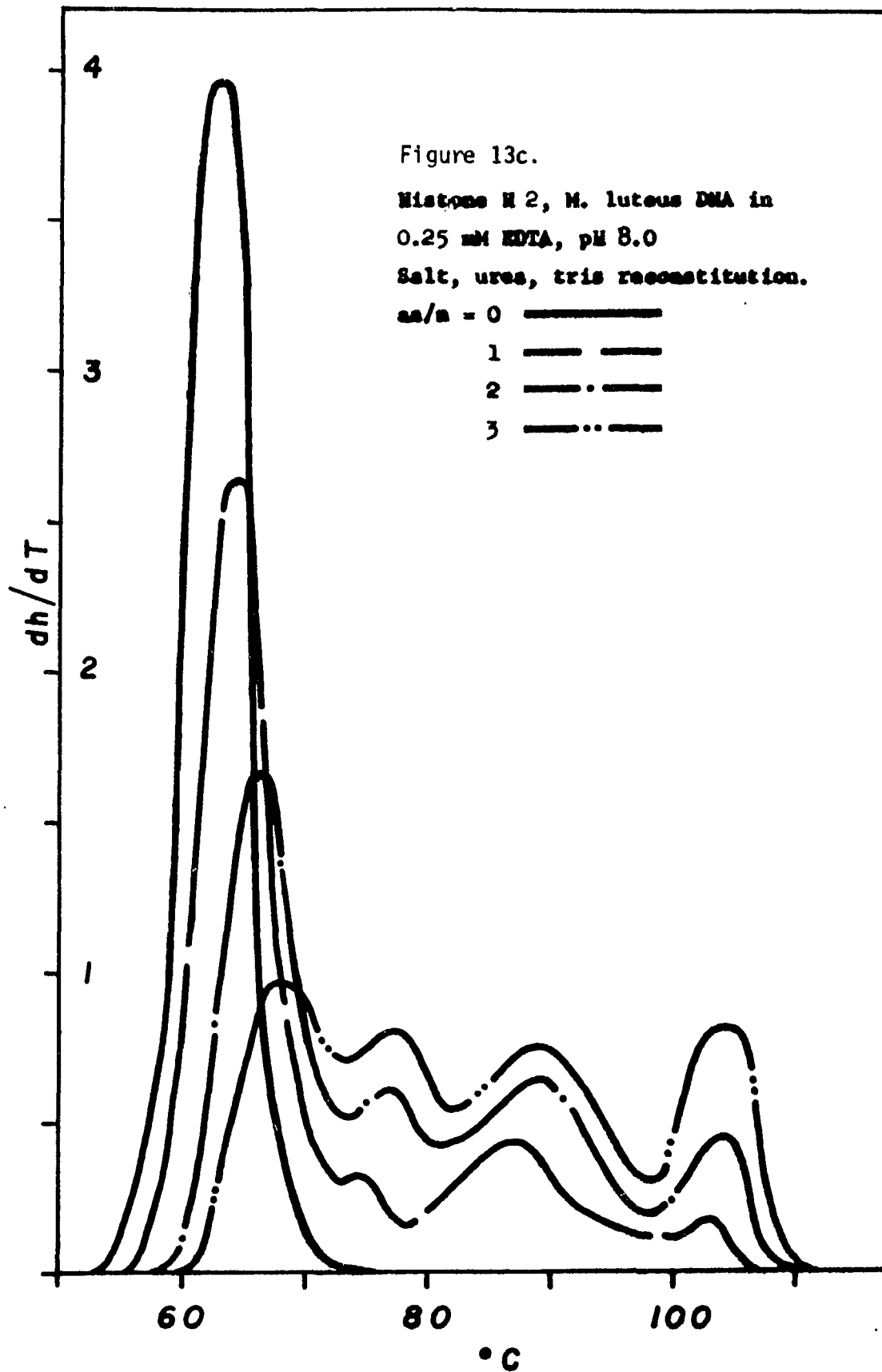
According to the above model, reconstitution without urea does not deform the DNA to as great an extent, decreasing the amount of strain which must be released during denaturation. At the start of the reconstitution the high ionic strength environment stabilizes hydrophobic interactions and neutralizes like-charge repulsion between cationic residues on the histones. As the salt concentration decreases the proteins bind the DNA. As the gradient proceeds to lower ionic strength an antagonism arises between the hydrophobic attractive forces and electrostatic repulsive forces within the histone subunit. For this reason the binding of the basic residues to DNA is not as stable as it would be if the histone-DNA binding had occurred in the presence of urea with the hydrophobic forces more effectively neutralized.

When histone H2, an equimolar combination of H2A and H2B, is annealed to DNA the four main melting peaks are again discernible (Figure 13). The  $T_{mIII}$  transition now appears as a single peak with each DNA, whereas it had previously been split. D'Anna and Isenberg









(32), and Hartinson and McCarthy (38) have shown strong interactions between H2A and H2B both in solution and in vivo respectively. Evidently, the interaction of these histones contributes to a modification of the binding of their more basic regions to the DNA molecule.

Examination of Figure 13b and comparison with the T.D. profile of calf thymus or rat liver chromatin (Figure 14) reveals similarities in the temperatures of the thermal transitions near 60°C, 75°C and 85°C. Above 85°C a band is observed which is apparently due to light scattering artifacts. In r=3 complexes (not shown) the denaturation curve resembles that of chromatin even more closely, however, there appears a strong transition (ca. 90°C-100°C) due to light scattering. The  $A_{320}/A_{260}$  value of the r=3 complex, 0.13, is considerably greater than the value for chromatin, 0.05, and increases further upon melting, to 0.20. The effect of light scattering is to increase the observed hyperchromicity and consequently the maximum hyperchromicity of the sample,  $h_{max}$ , equals ca. 50% which is larger than the ca. 35% hyperchromicity character- of calf thymus DNA. For this reason complexes exhibiting excessively high  $h_{max}$  values are not included in the  $\beta$  value determination.

As Figure 15 illustrates, the  $\beta$  value of nucleohistone H2 complexes prepared with urea,  $\beta = 3.7 \text{ aa/n}$ , is the same as the value obtained for calf thymus chromatin by Li et al. (75). Figure 16 shows that reconstitution of nucleohistone H2 without urea reduces the temperature of the  $T_m$  III transition of P-DNA from 82°C (Figure 13a) to 77°C (Figure 16a), of C-DNA from 98°C (Figure 13b) to 88°C (Figure 16b) and of L-DNA from 103°C (Figure 13c) to 96°C (Figure 16c). That the reduction of the temperature of the highest melting band is seen with each DNA suggests that the effect is due to the histone component of the complex. Exclusion of urea in the high salt medium increases

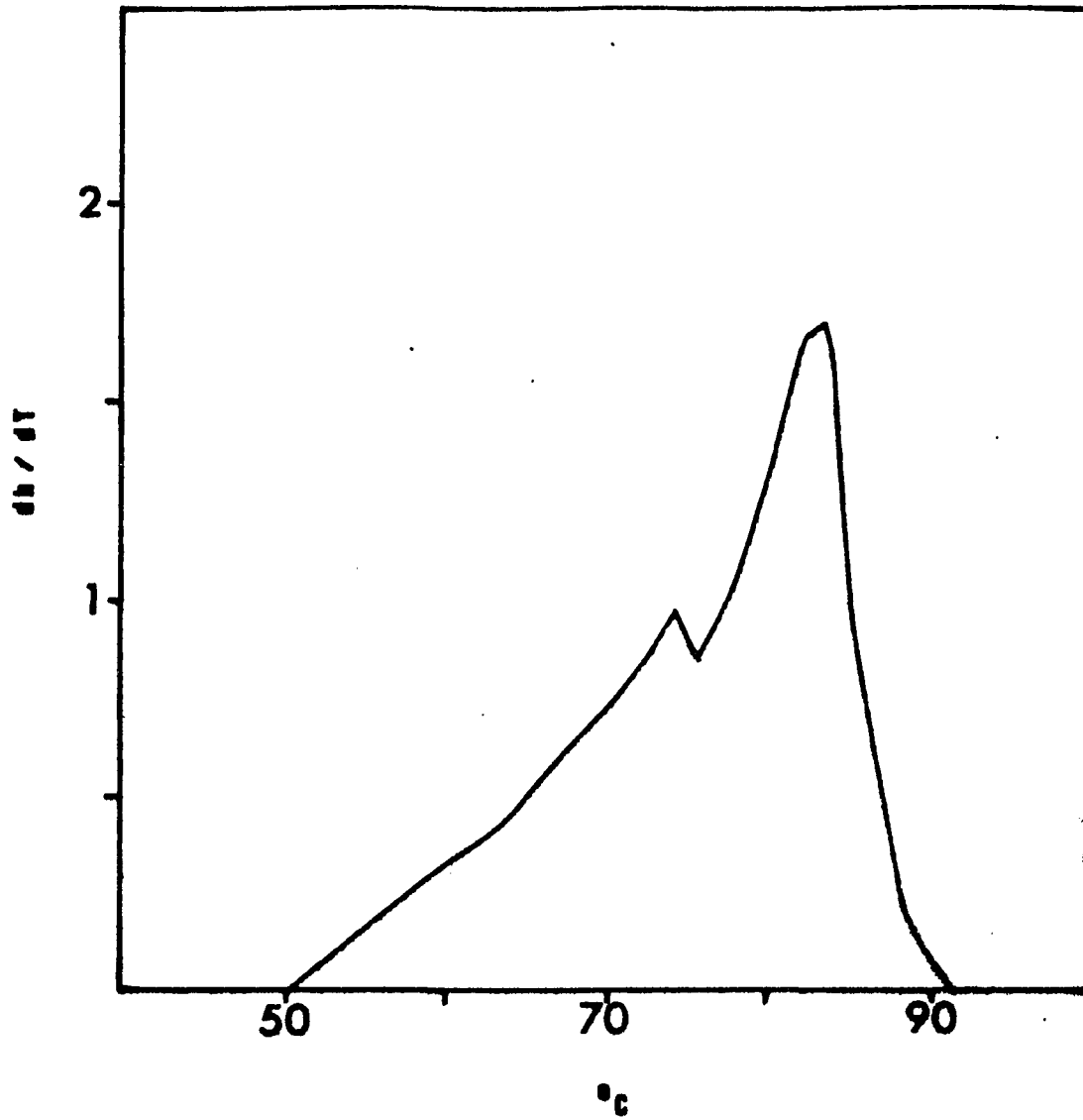
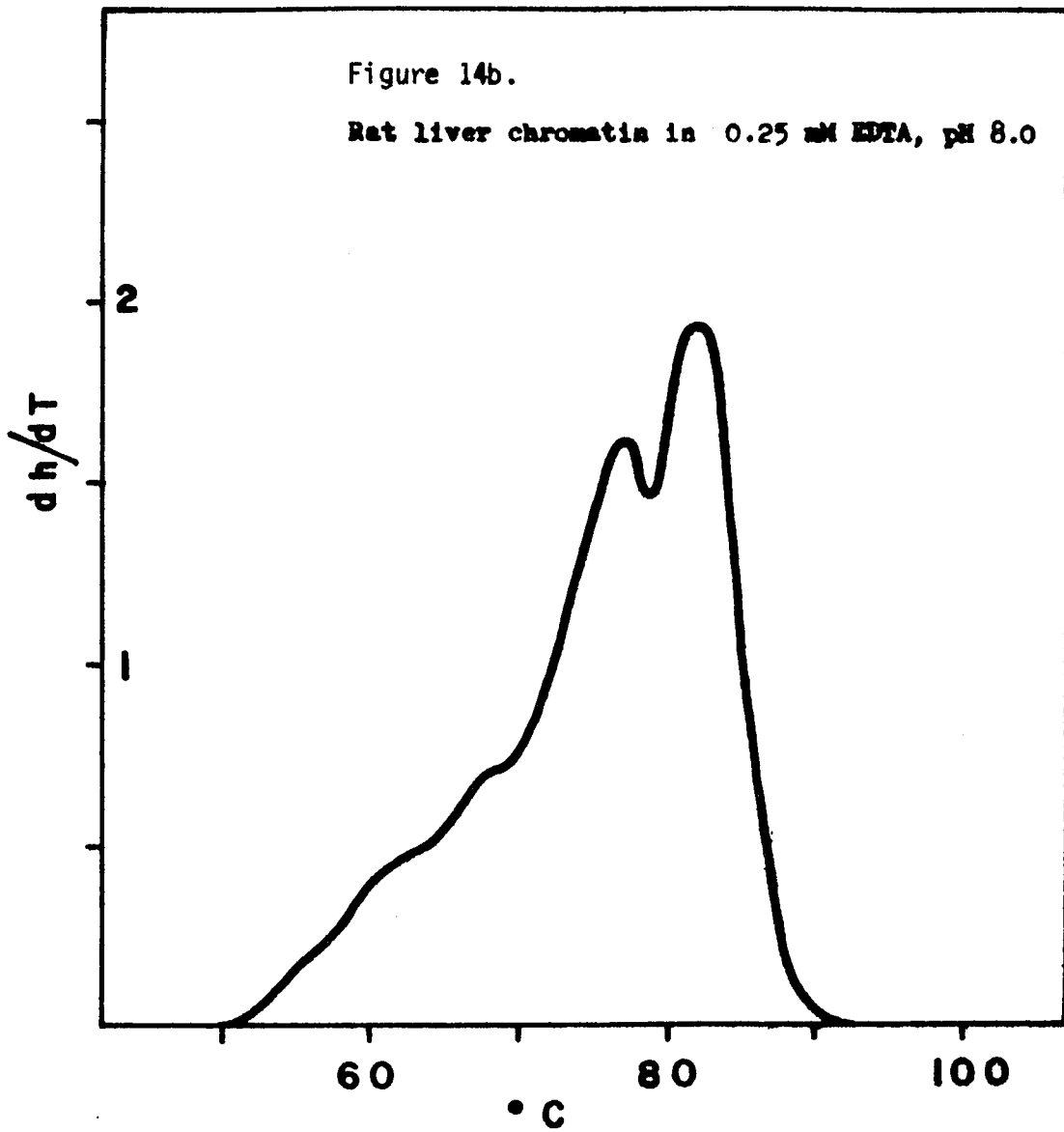


Figure 14a. Purified calf thymus nucleohistone  
in 0.25 mM EDTA, pH 8.0.

(From the Ph.D. dissertation of  
C. Chang, with permission)



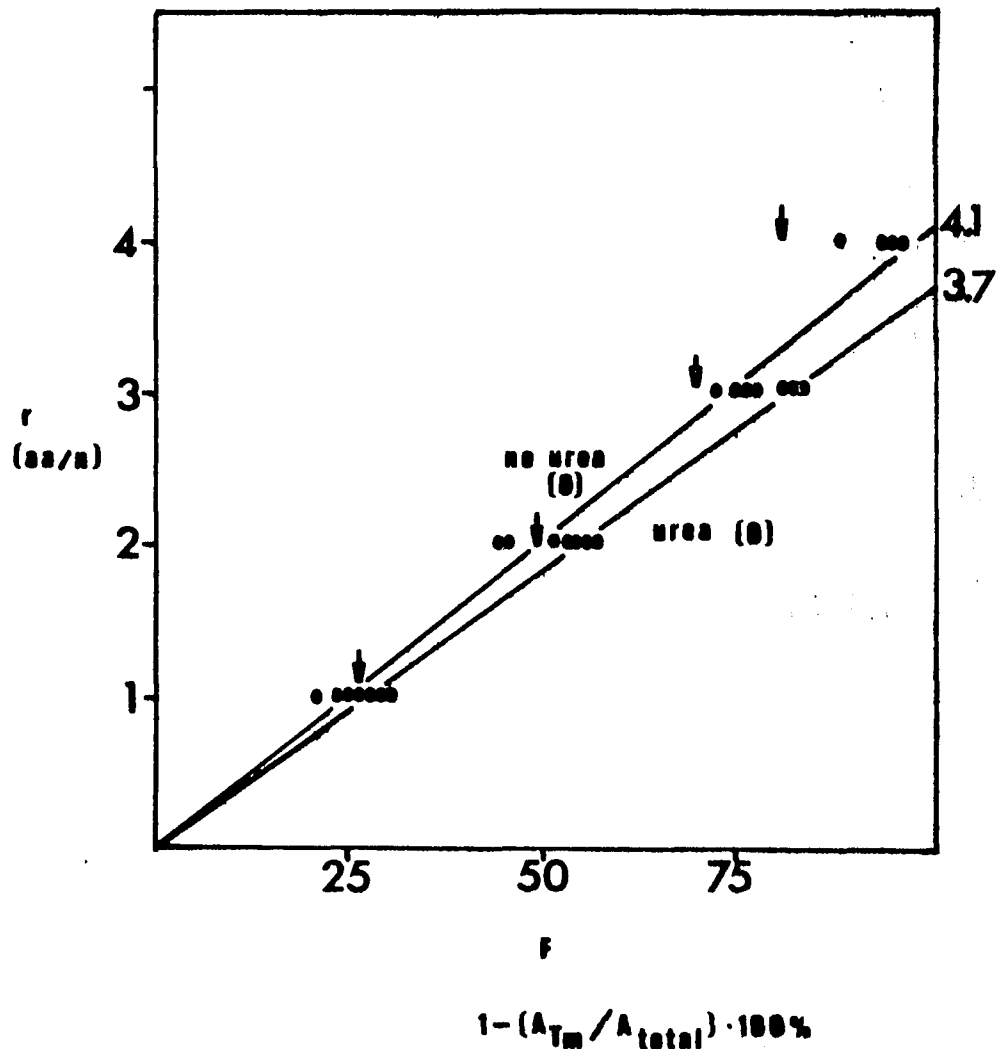
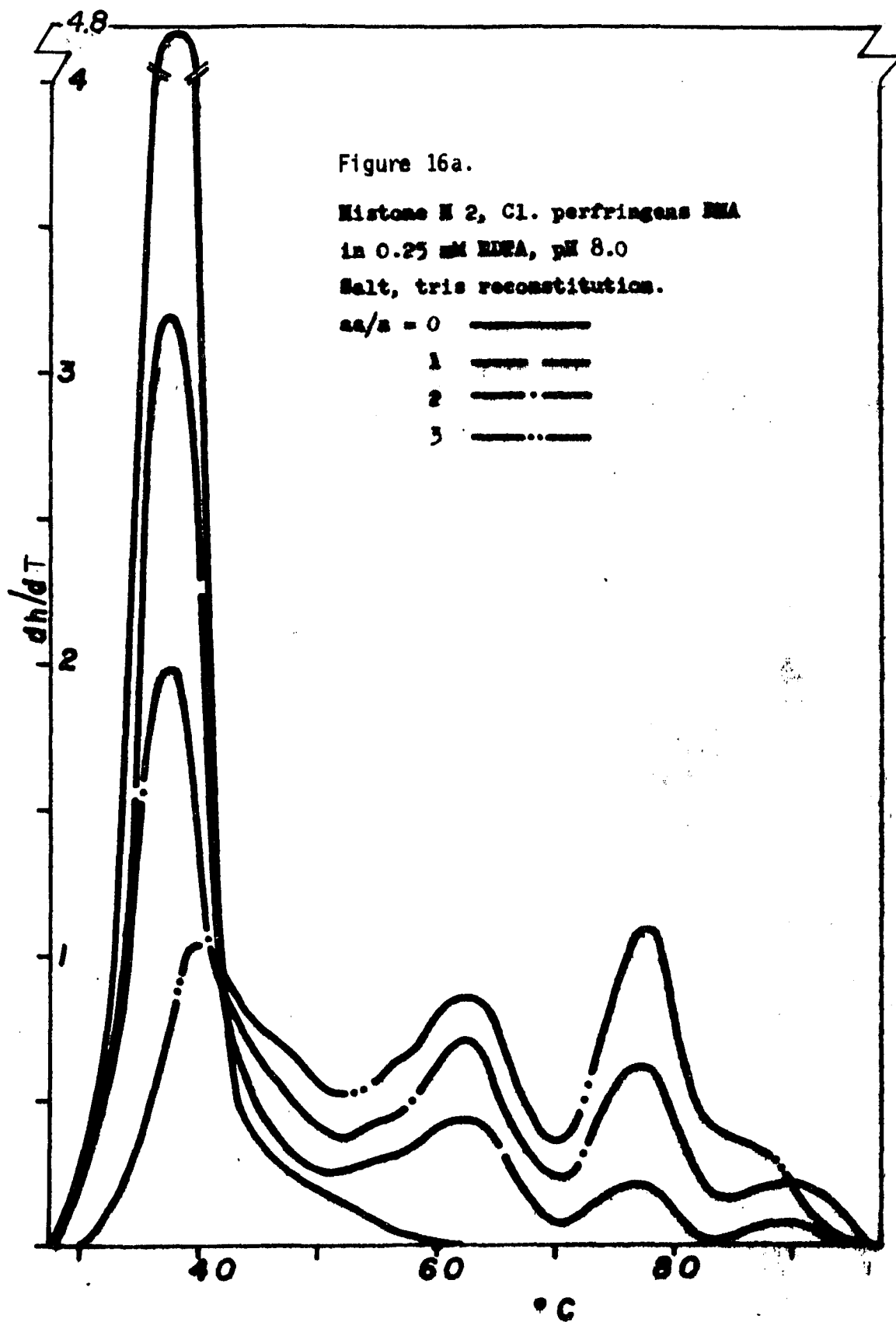
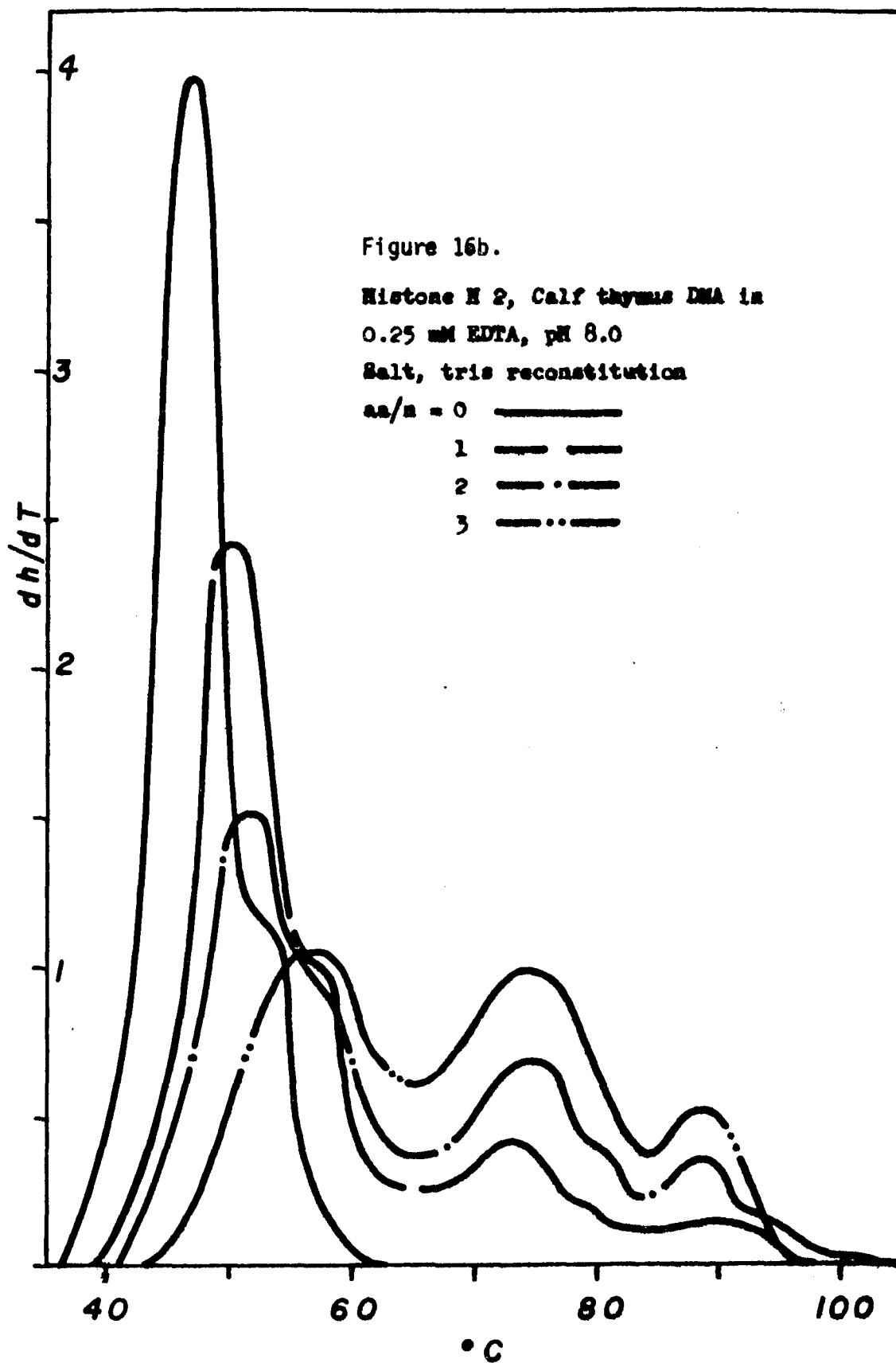
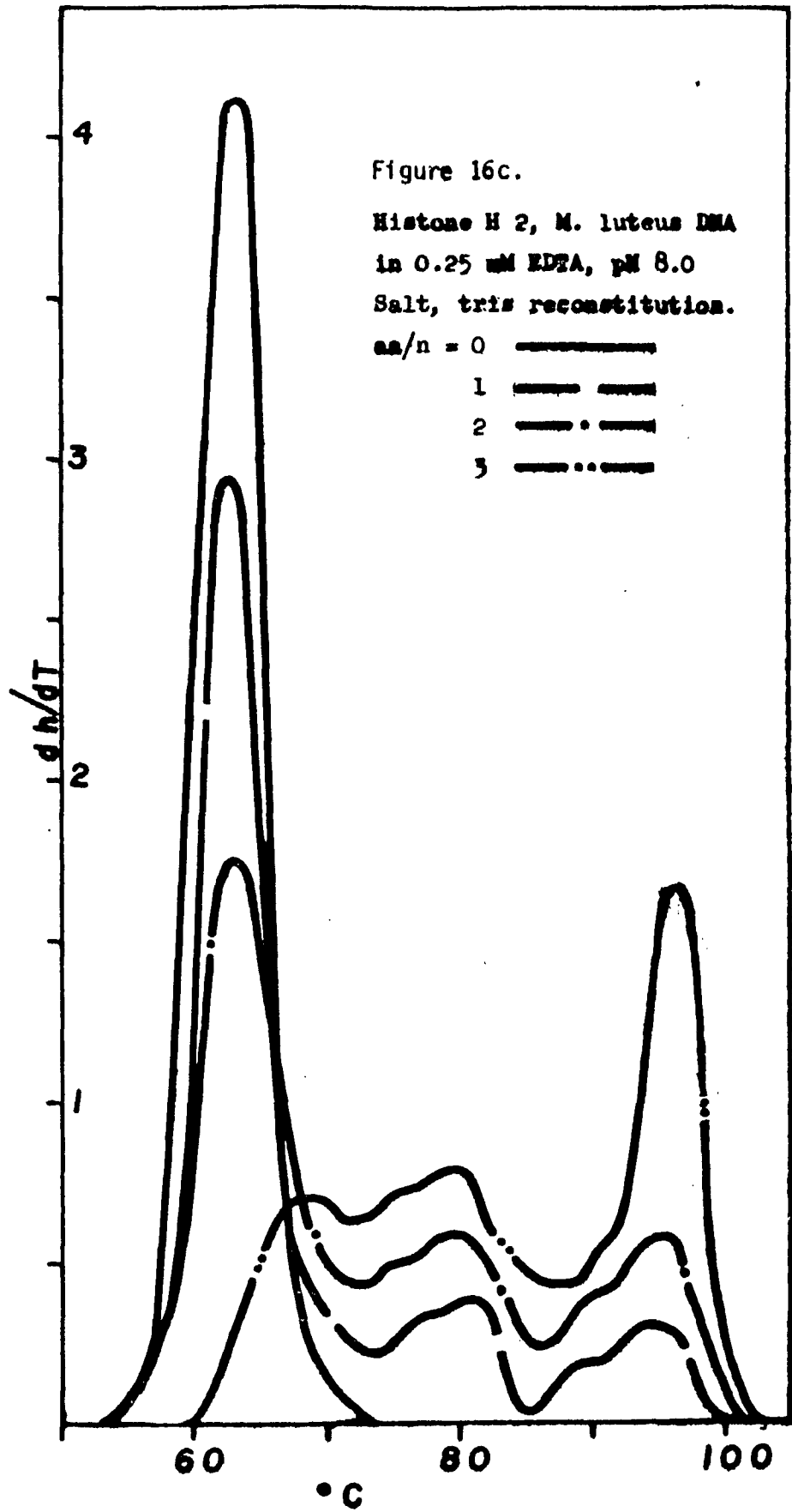


Figure 15.  $\beta$  value determination.  
Histone H2 nucleohistones.

Open circles = plus - urea complexes.  
 Filled circles = minus - urea complexes.  
 Arrows = average value for  
 salt - urea - phosphate complexes.



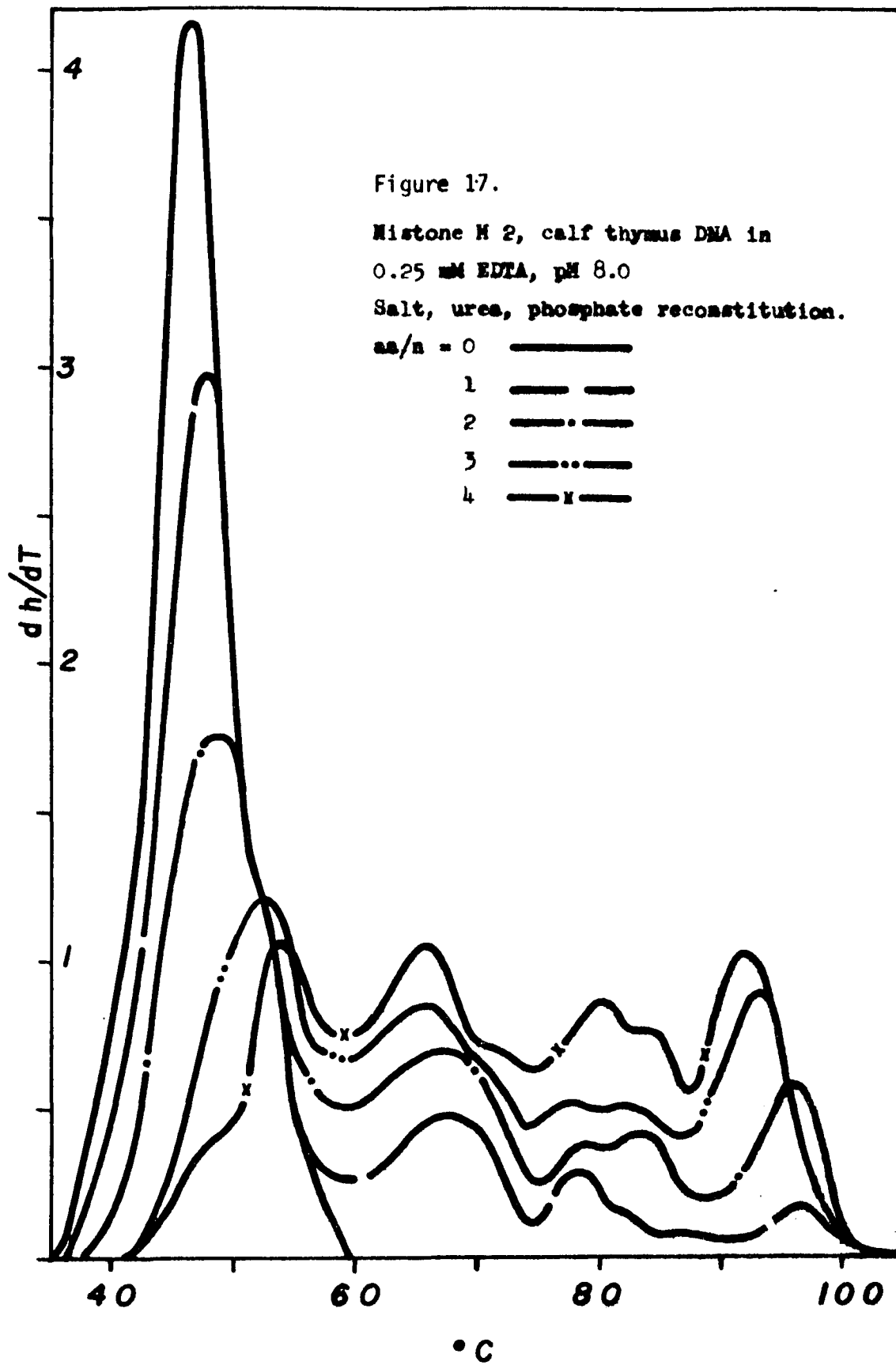




the ordered secondary structure of the histones and may cause them to bind while in a more condensed conformation. Once bound, the reduction in the ionic strength of the medium may increase the mutual repulsion between neighboring cationic residues which decreases their ability to stabilize the DNA. Histones reannealed to DNA in the presence of urea are then pictured as binding in a more extended configuration and the greater distance between like - charged residues increases their ability to stabilize the DNA.

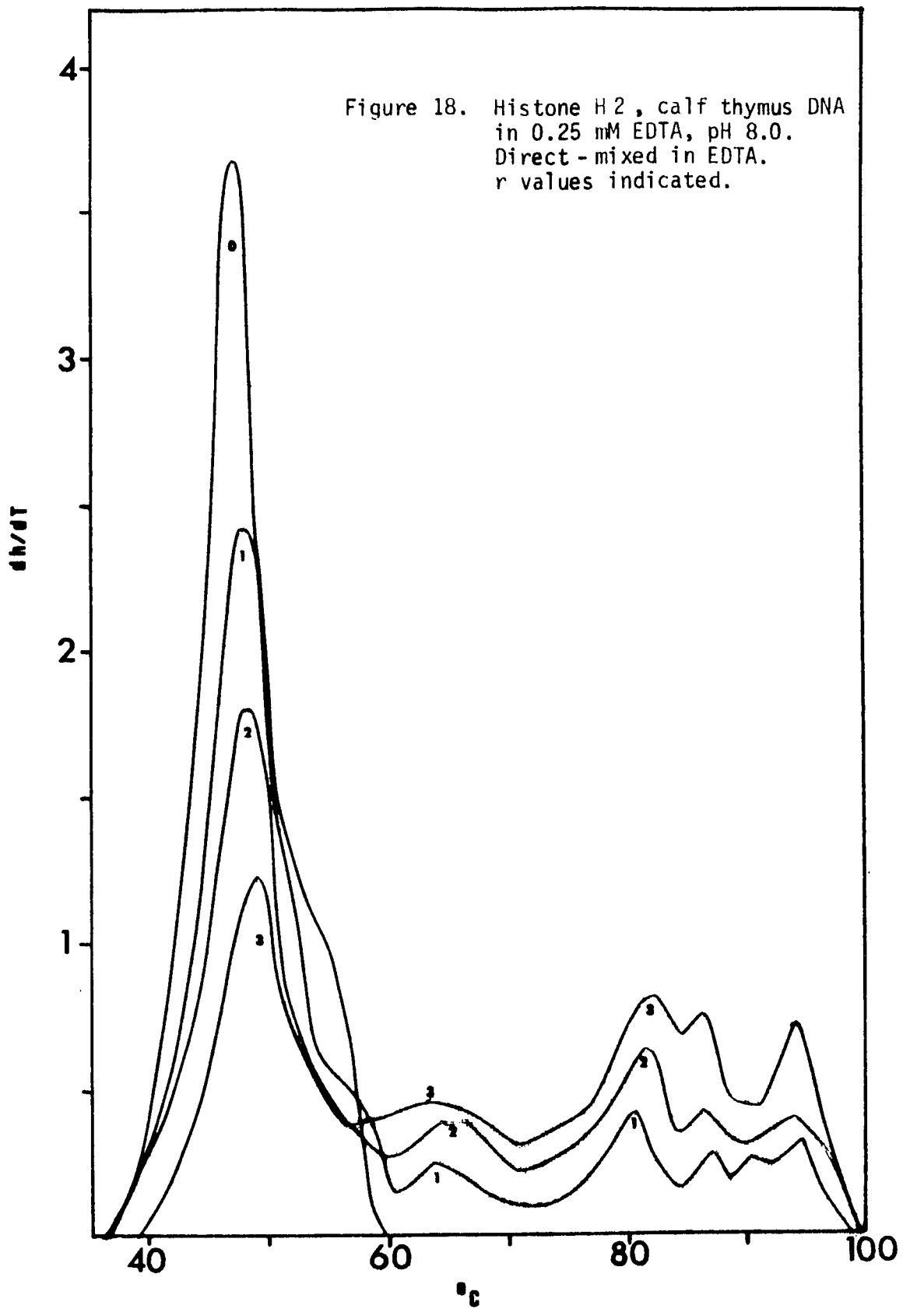
When nucleohistone H 2 is reconstituted in salt - urea - phosphate the T<sub>m</sub>III transition is also translocated to lower temperature (Figure 17) relative to the salt - urea - tris complexes and the transitions between 60<sup>o</sup>C - 80<sup>o</sup>C are enhanced. It is known that phosphate buffer maximizes the secondary structure of histones (32). In the salt - urea - phosphate reconstitution medium the histones bind as the ionic strength is gradually reduced. Once the urea is removed the phosphate is able to induce highly ordered secondary structure in the histones, which now interact. The situation is analogous to reconstitution in the absence of urea, however, the strong effect of phosphate in stabilizing hydrophobic interactions can be seen by comparing the beta values of the plus - urea, minus - urea and urea - phosphate reconstitutions. The  $\beta$  values of these complexes (Figure 15) increases when the nucleohistone is reconstituted without urea and increases further when the reconstitution is carried out in phosphate. Also, the increasing input ratio is seen to have a greater effect on the  $\beta$  value slope in the urea - phosphate nucleohistone than in the minus - urea nucleohistone.

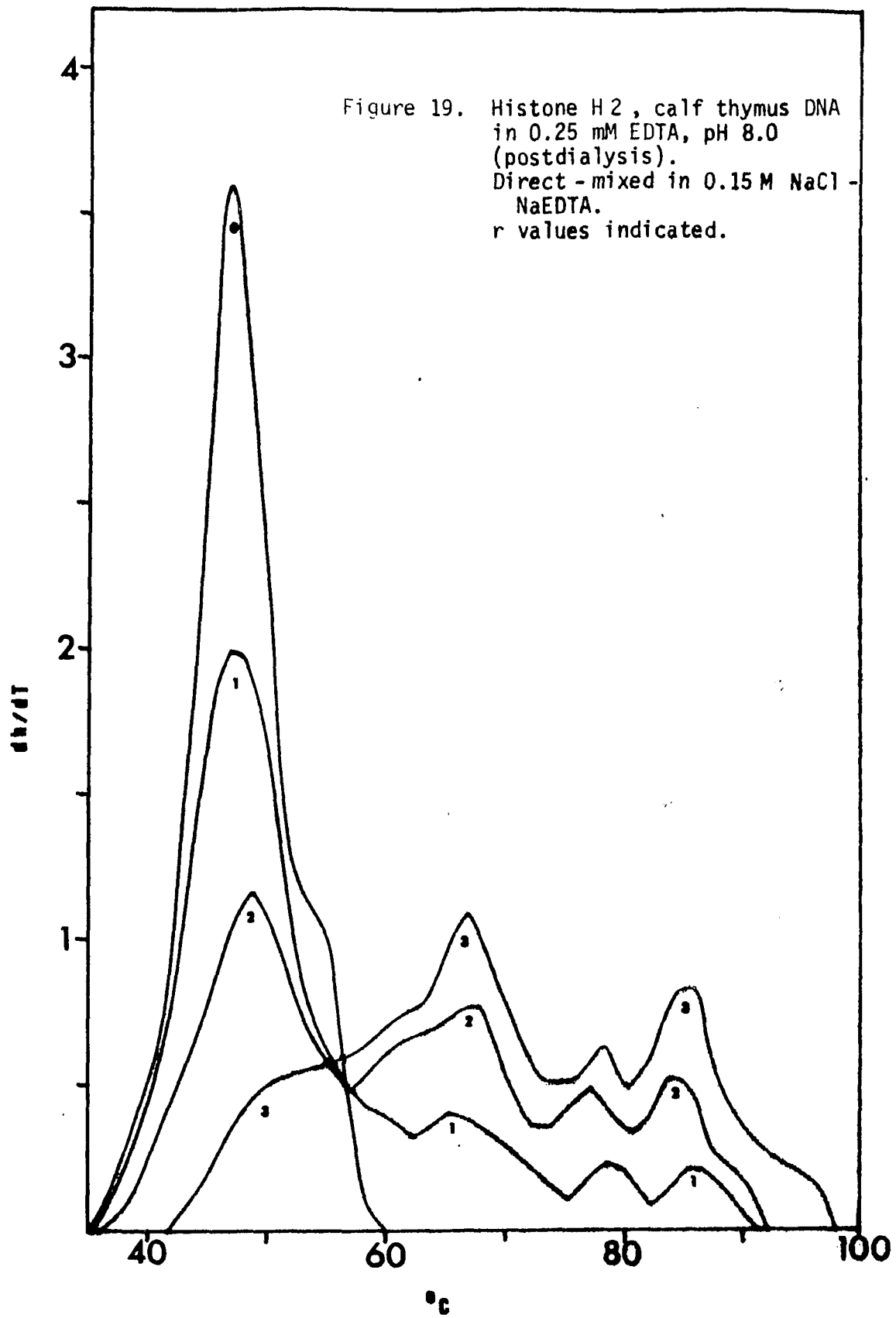
When histone H 2 is complexed to calf DNA by direct - mixing in



.25 mM EDTA, pH 8.0 or in .15 M NaCl, .25 mM EDTA, pH 8.0 and denatured, Figures 18 and 19 respectively result. The temperature of the highest transitions of the low ionic strength reconstitute (Figure 18), 87°C and 95°C, correspond to T<sub>m</sub>II and T<sub>m</sub>III of the salt-urea-tris nucleohistone H2 at 88°C and 97°C (Figure 13b). When direct-mixing is done in the presence of .15 M NaCl the corresponding peaks occur at 79°C and 86°C (Figure 19). In addition there is a large increase in the peak at 67°C. In .25 mM EDTA the histones exist as predominantly random coil (Chapter III) and bind in the most stable conformation possible. When the direct-mixing occurs in the presence of salt and salt-induced hydrophobic interactions, however, the most stable binding conformation is not the same as it is once the salt is dialysed away for the denaturation. Consequently the highest temperature transitions of these complexes occur at lower temperature and there also appears a large conformational change in the DNA in the 60°C - 70°C temperature region. The beta values of these complexes (Figure 20) are  $\beta = 4.4$  aa / n for direct-mixed in EDTA and 3.9 aa / n for direct-mixed in salt-EDTA. Both values are higher than the 3.7 aa / n derived for salt-urea-tris nucleohistone H2 presumably reflecting the irreversibility and apparent cooperativity of histone binding in direct-mixed complexes (72). The slightly lower beta value of the salt-EDTA complex may be due to the presence of salt decreasing this cooperativity.

Figure 21 is a composite melting profile of a nucleohistone H2 complex annealed in the absence of urea. A control aliquot was denatured immediately upon preparation. Another aliquot was mixed with





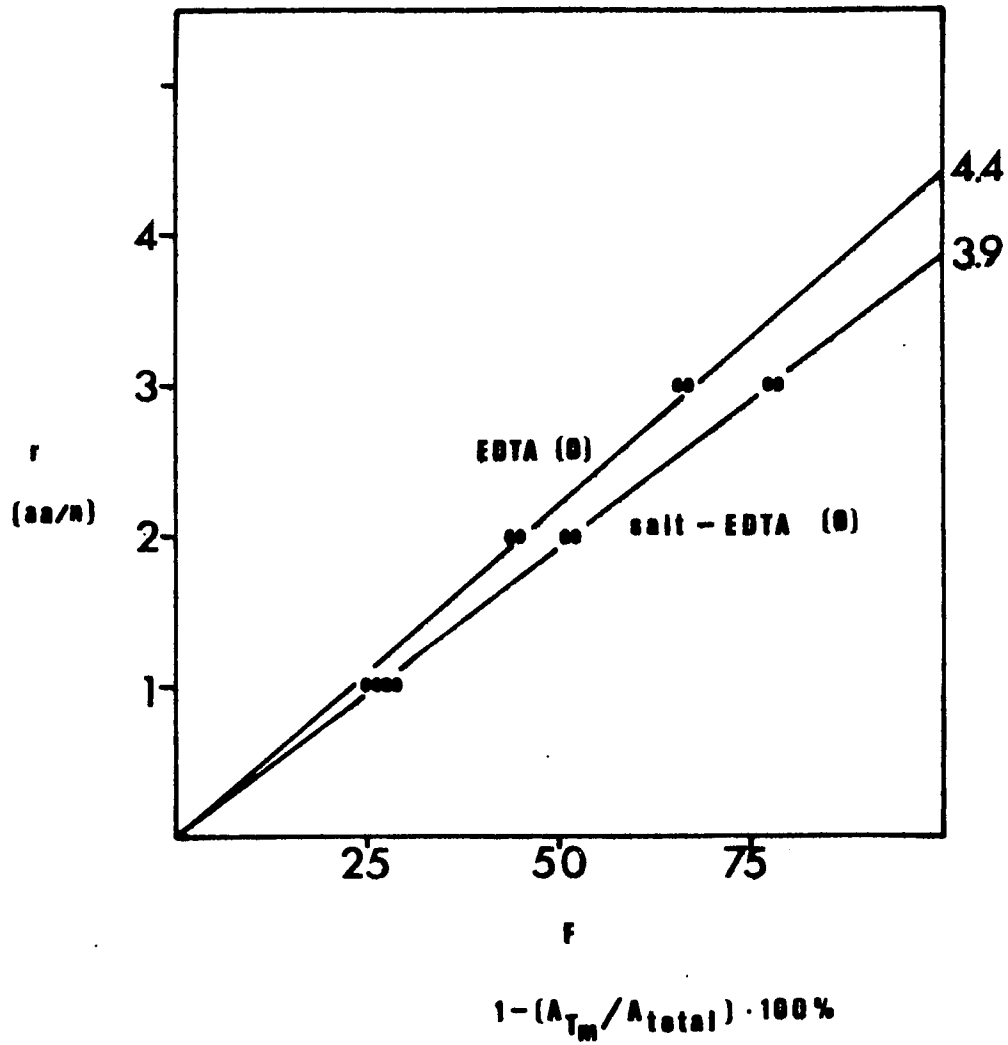


Figure 20.  $\beta$  value determination.  
Histone H2 nucleohistones prepared  
by direct-mixing.

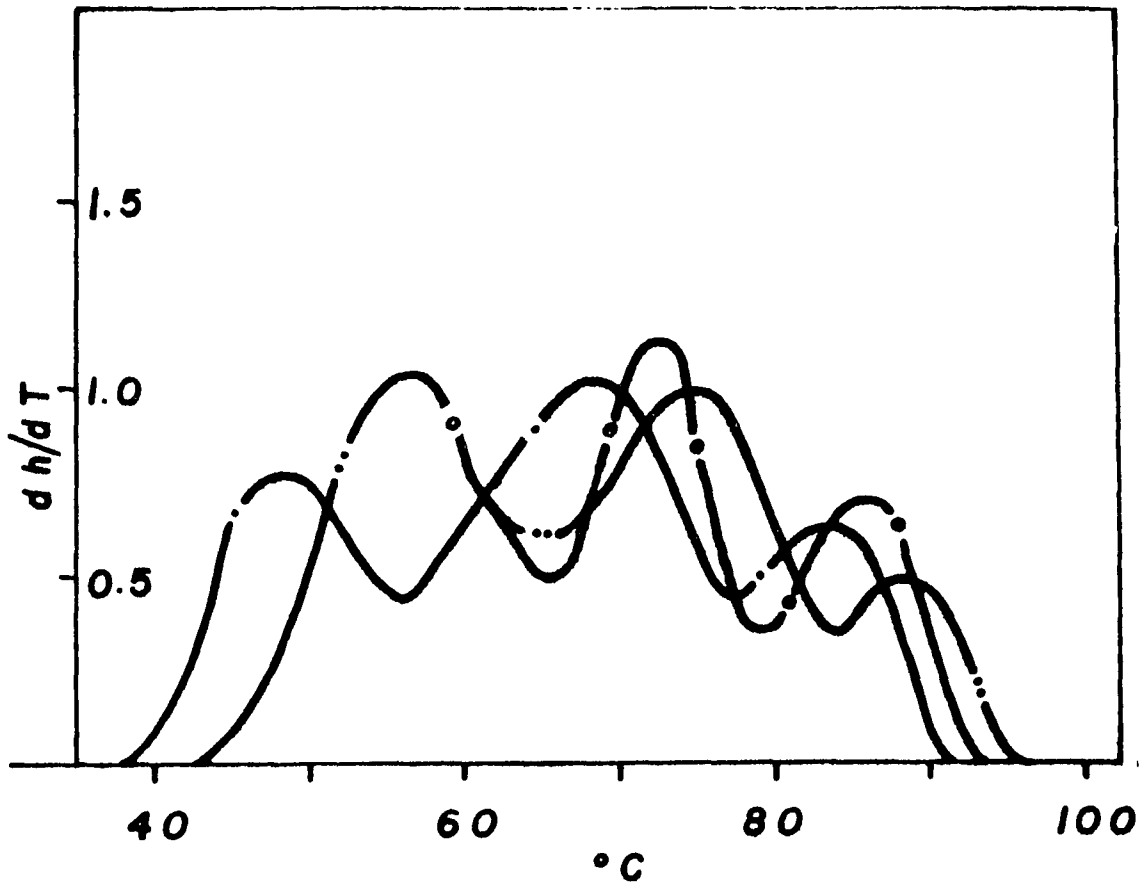


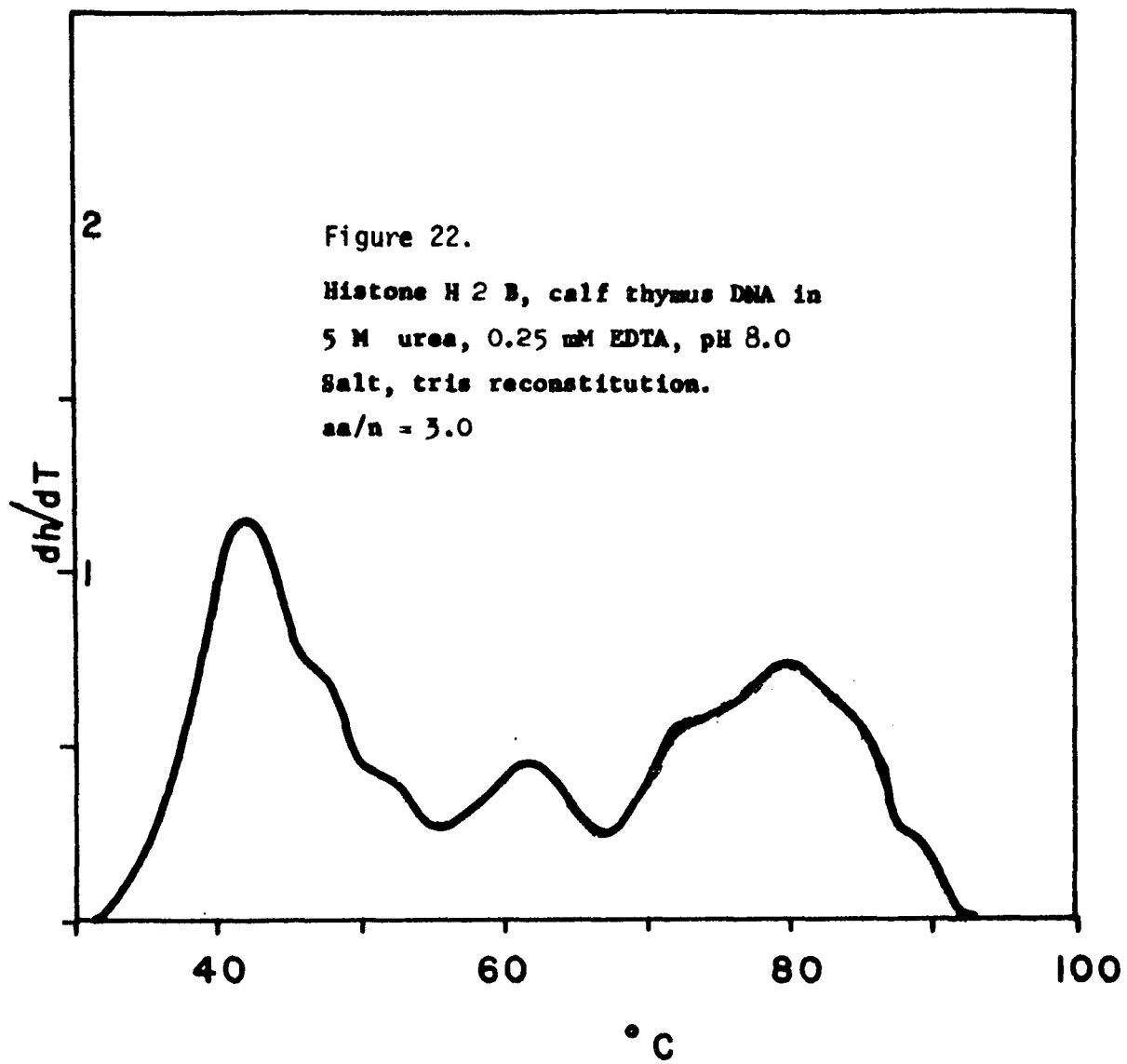
Figure 21. Histone H2, calf thymus DNA in  
0.25 mM EDTA, pH 8.0.

- · — denatured after salt - tris reconstitution  
without further treatment.
- · — mixed with equal volume of 10 M urea and  
denatured in 5 M urea - EDTA.
- · — mixed with equal volume of 10 M urea, dialysed  
vs. EDTA, denatured in EDTA.

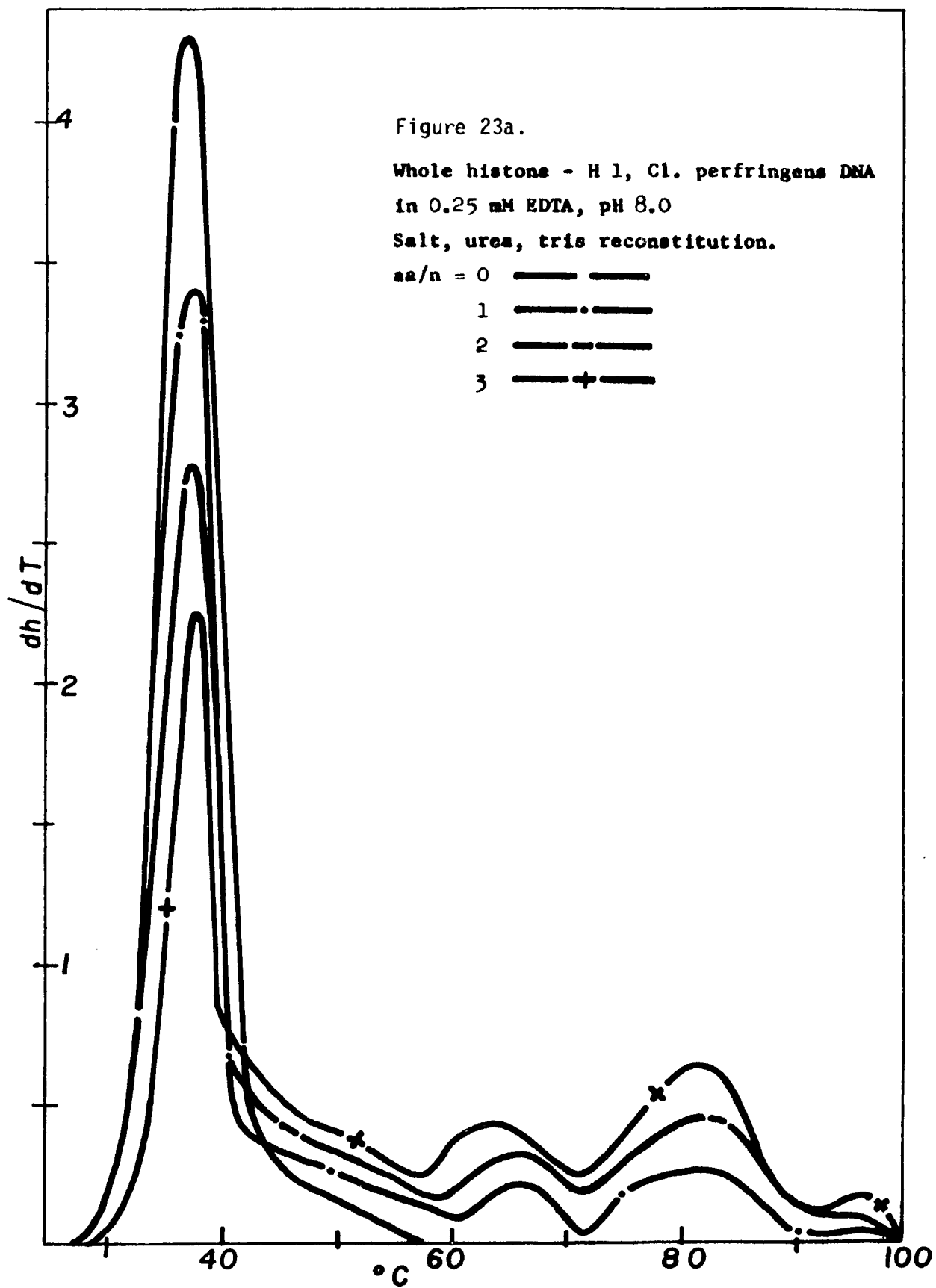
an equal volume of 10 M urea and denatured. It can be seen that every peak has been shifted to lower temperature in the latter profile. This is evidently a direct destabilization by urea of the hydrogen bonds between base pairs, as artifactual effects on the thermal denaturation profile of nucleoprotein complexes by urea in equilibrium with cyanate ion have been excluded after extensive study by Ansevin and Brown (87) and Ansevin et al. (71).

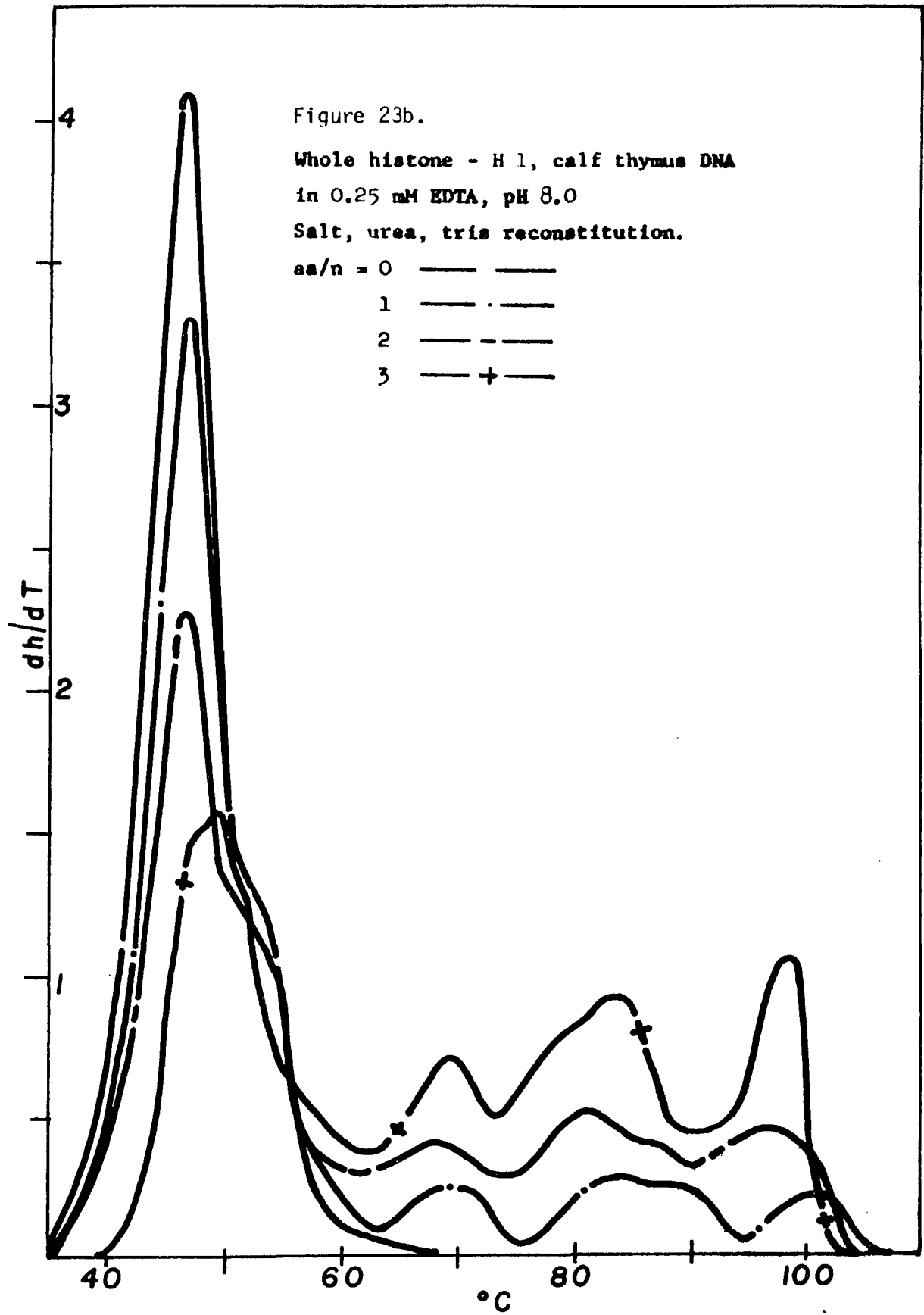
The addition of an equal volume of 10 M urea to a third aliquot of salt - tris nucleohistone, followed by direct dialysis vs. EDTA results in the remaining curve of Figure 21. Although the  $T_m$  transition of this profile coincides with that of the control, all other transitions are lowered. Since the total hyperchromicity and the % of free DNA are equivalent for these two samples, the % of bound DNA and their beta values must be equivalent, indicating no net shift of proteins from one bound region to another. The reduced temperature of the transitions must then be the result of the proteins changing to a second conformation in urea (due to the reduced hydrophobic interactions) and to a third conformation, less stable than the first, due to the antagonism of hydrophobic attractions and electrostatic repulsions upon removal of the urea. When a nucleohistone H 2 B complex prepared in the absence of urea is melted in 5 m urea (Figure 22) a minor shift to lower temperature of the highest melting transition is seen. The small effect of urea on this complex relative to the urea - T.D. of nucleohistone H 2 may be due to the absence of the H 2 A histone.

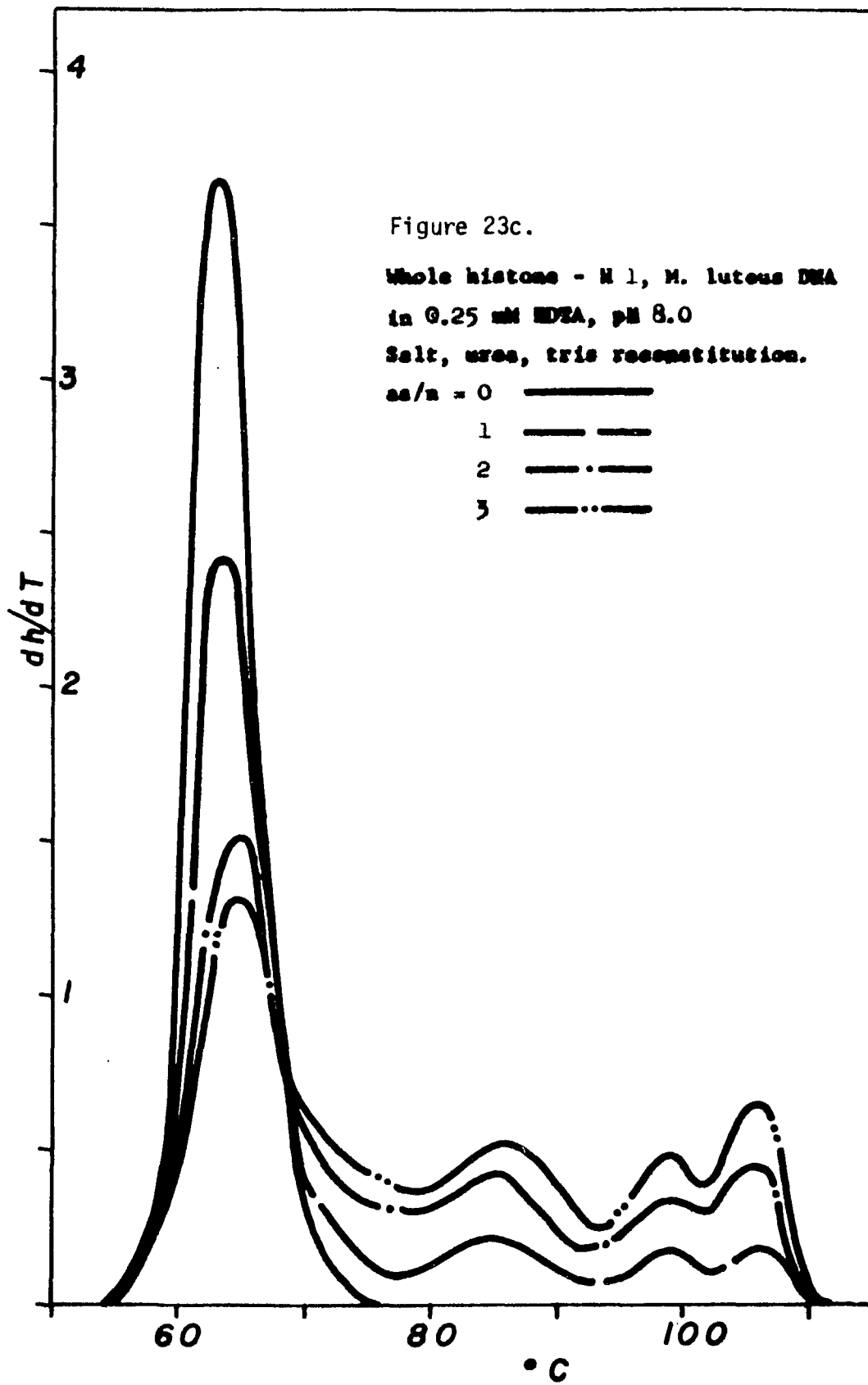
When whole histone minus histone H 1 (whole - H 1), a combination of H 2 A, H 2 B, H 3, H 4, is complexed with DNA and denatured by



heating, the profiles presented in Figure 23 are obtained. While these nucleohistones display the four characteristic melting transitions, the profiles of these complexes do not resemble the profile of chromatin (Figure 14). The inclusion of the arginine-rich histones apparently modifies the binding of the slightly lysine-rich histones possibly by altering the histone-histone interactions in the complex. The arginine-rich histones are known to have a strong tendency to aggregate (34). This may be responsible for the high beta value observed in whole-H1 nucleohistone:  $\beta = 6 \text{ aa} / n$  (Figure 24). When whole-H1 nucleohistone is reconstituted in the absence of urea the amount of material melting between  $T_m$  and the two highest transitions ( $T_{mII}$ ,  $T_{mIII}$ ) is greatly reduced. This effect is most clearly seen with calf DNA (compare Figures 23 and 25), and correlates well with the increased hydrophobic nature of the arginine-rich histones. The transitions  $T_{mII}$  and  $T_{mIII}$  although shifted to lower temperature are generally increased in amplitude. The decreased melting in the  $60^{\circ}\text{C} - 70^{\circ}\text{C}$  range and the shift of the  $T_{mII} - T_{mIII}$  region to lower temperature may be due to strong hydrophobic interactions between the arginine-rich histones in high salt which occur prior to their binding of the DNA, while the enhanced hydrophobic interactions between the arginine-rich histones and DNA may be responsible for the increased amplitude and complexity of the melting in the  $T_{mII} - T_{mIII}$  range. That these effects are due to the arginine-rich histones gains credence from the report of Yu (88) who observed that relative to plus-urea complexes, DNA-(H3 + H4) complexes reconstituted in the absence of urea showed enhanced  $T_{mIII}$







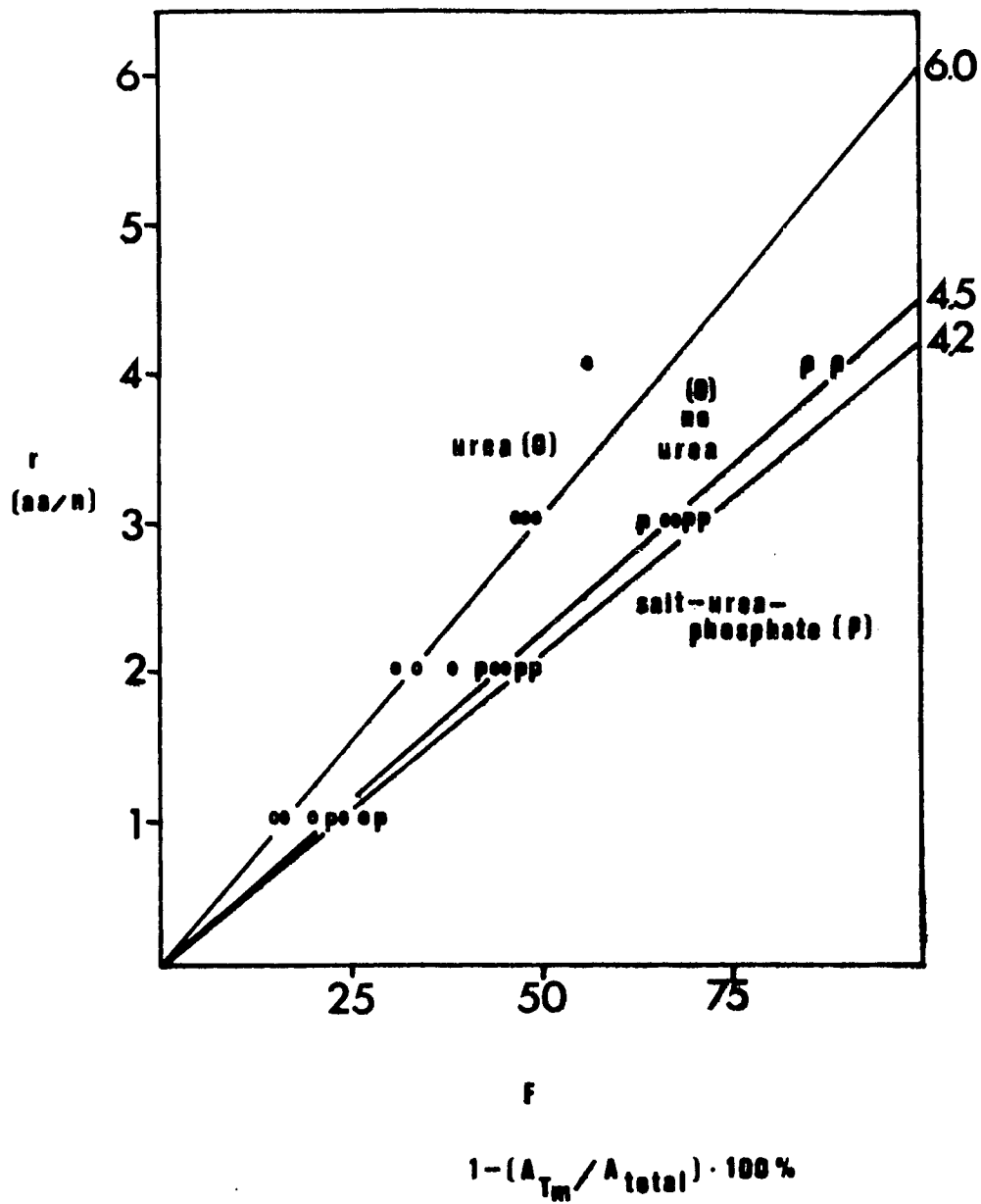
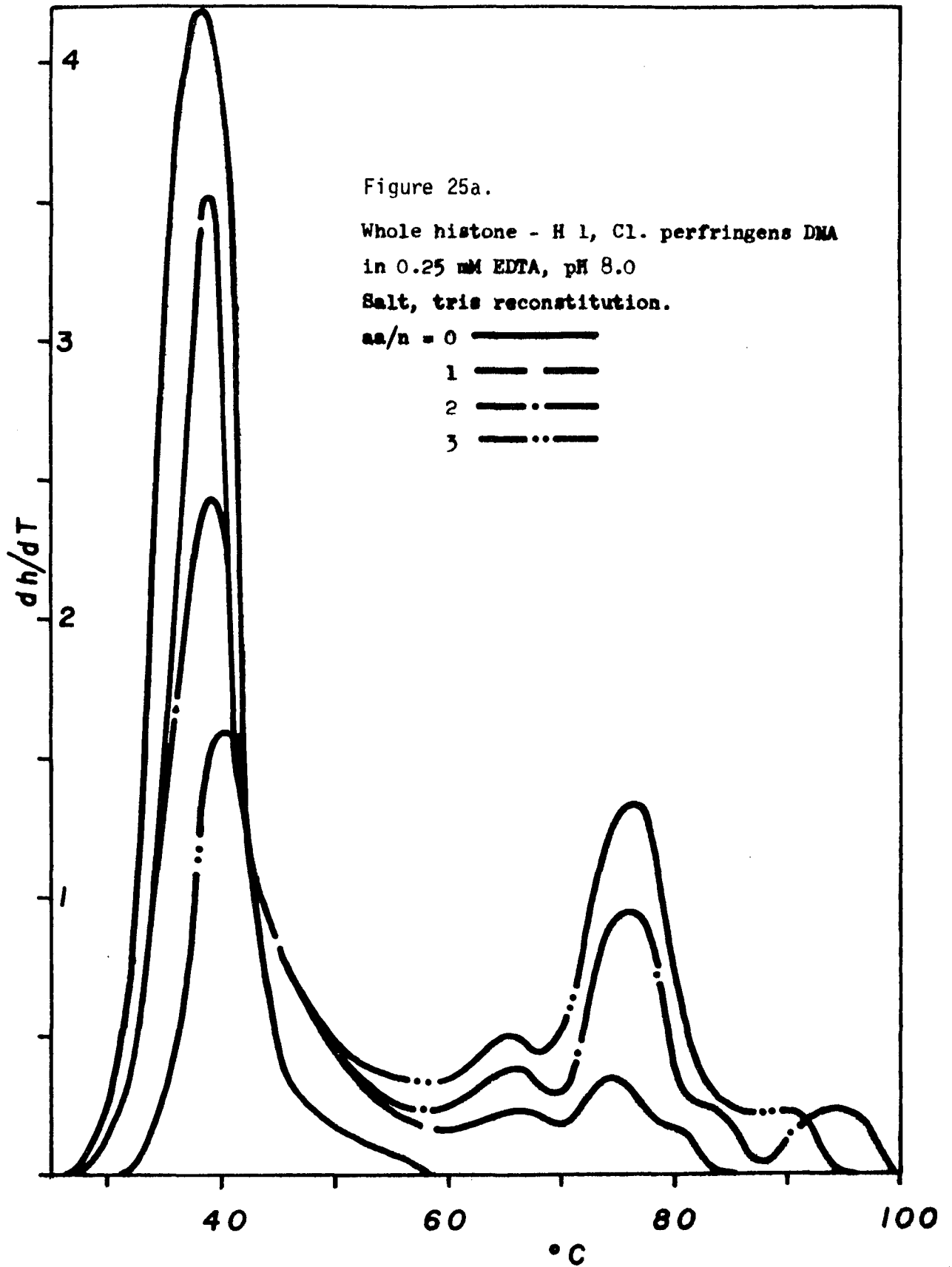
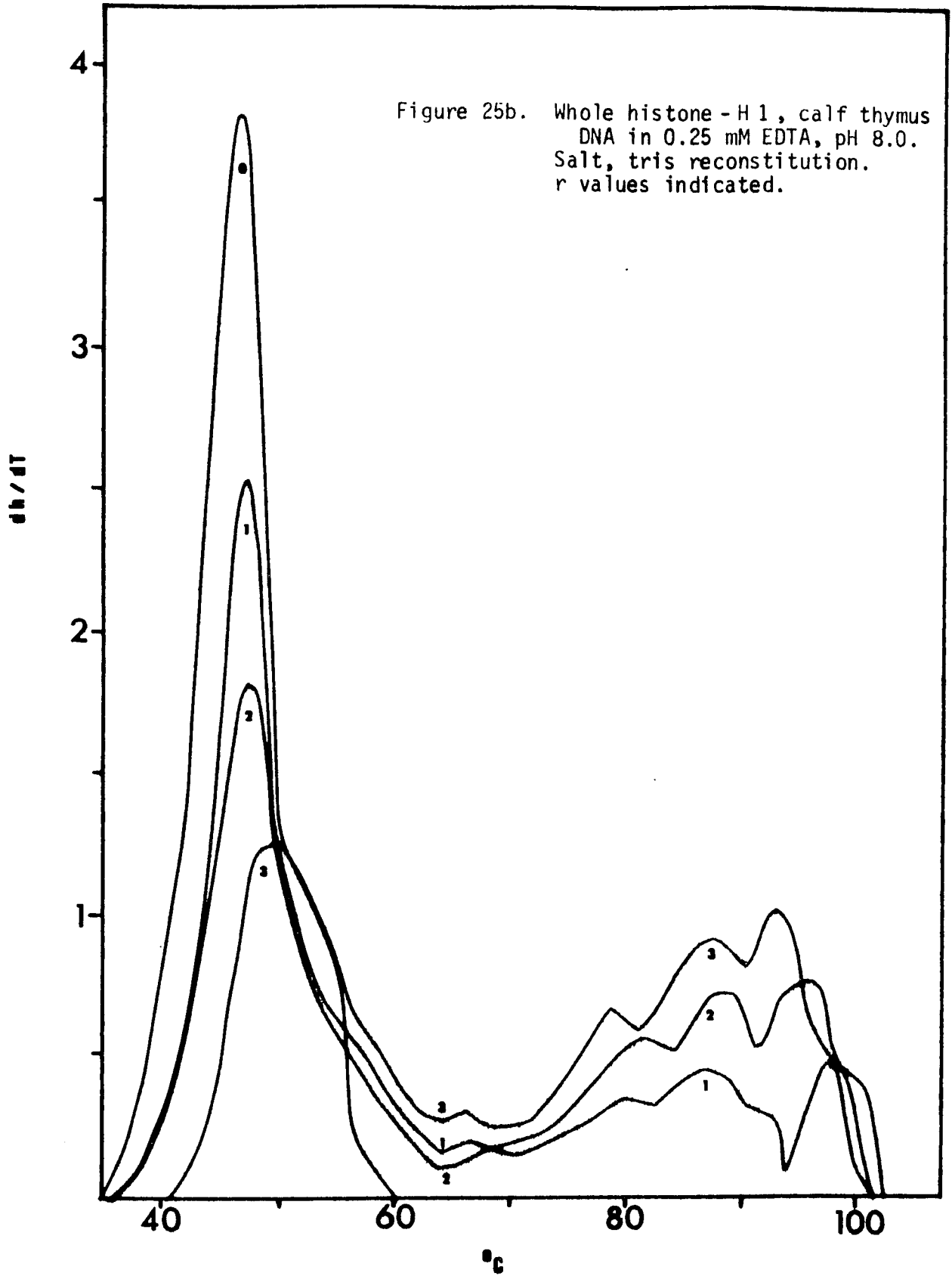
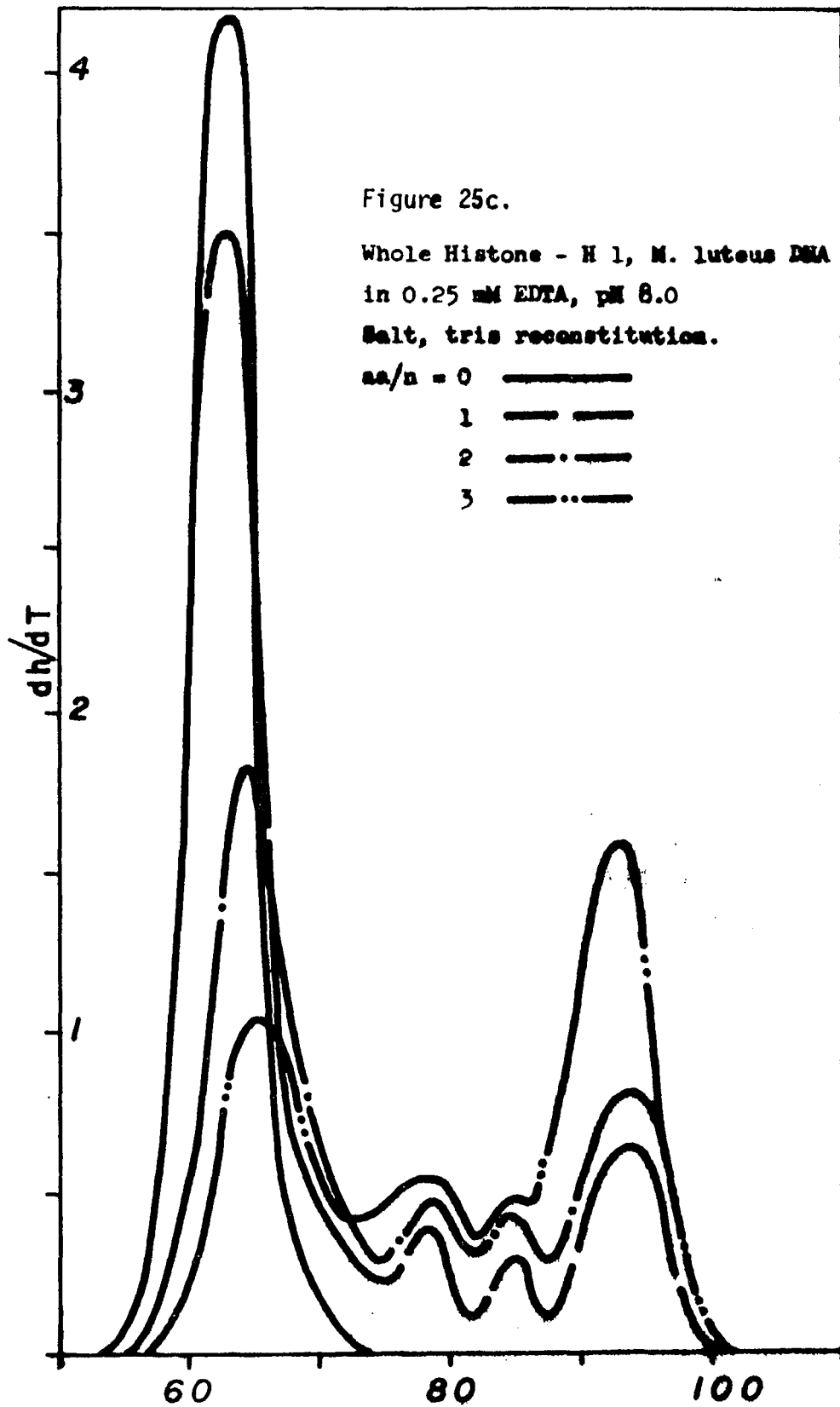


Figure 24.  $\beta$  value determination.  
Whole - H1 histone nucleohistones.



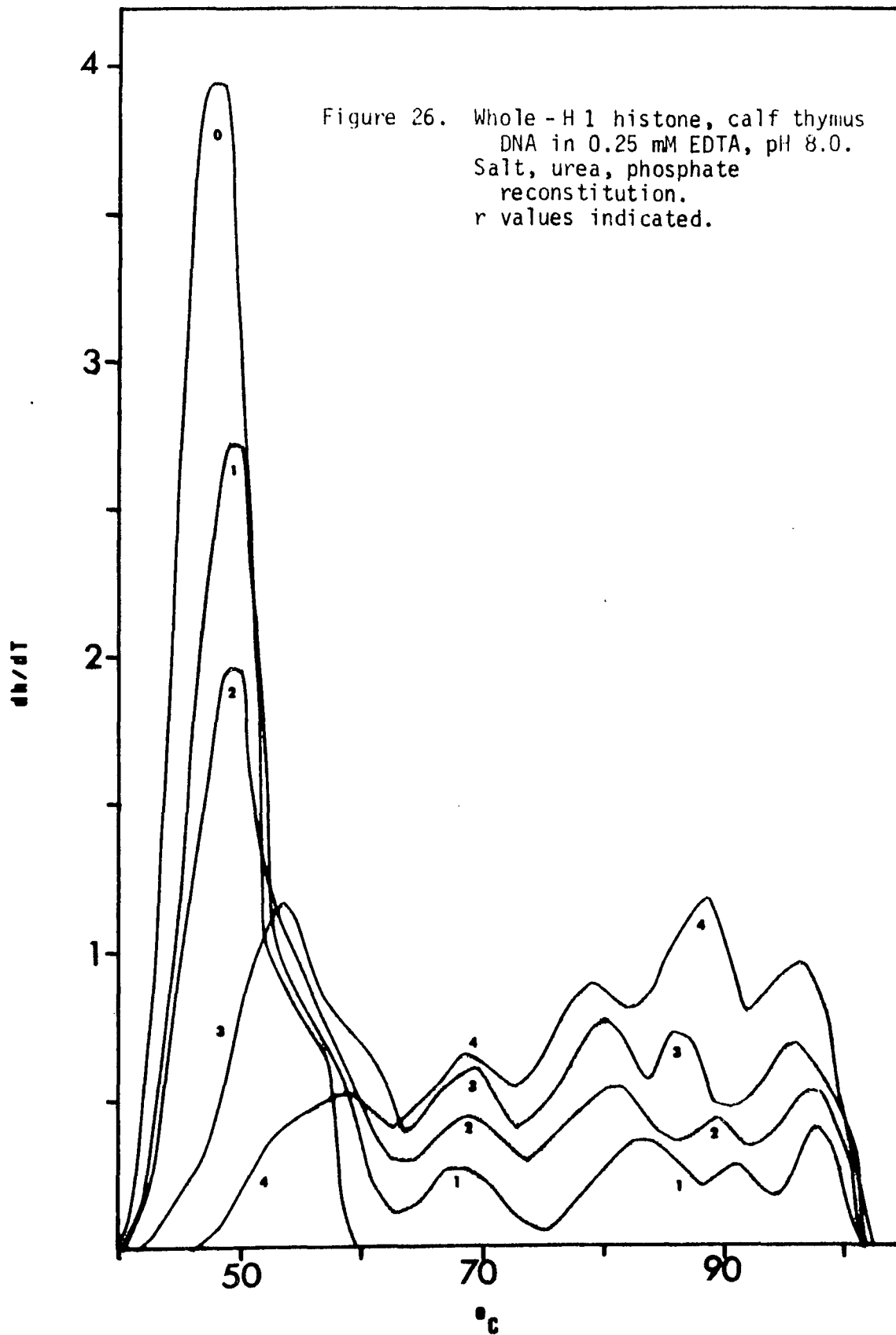




transitions. This suggests a significant contribution of hydrophobic forces to the binding of these histones to DNA. Bartley and Chalkley (89) have observed that high concentrations of urea (5 M - 6 M) are required before the arginine - rich histones can be extracted from heat - treated nucleoprotein by acid. Urea at lower concentration (1 M - 3 M) was sufficient to facilitate the removal of the slightly lysine - rich histones. (Urea had little effect on the extractability of histone H 1.) These authors also invoked a high degree of hydrophobicity in the binding of H 3 and H 4 to DNA.

The effect of omission of urea or inclusion of phosphate during the reconstitution of whole - H 1 nucleohistones on the beta value of the complex is opposite to the effect of these agents on H 2 A, H 2 B or H 2 nucleohistones (Figure 24). Without urea the beta value decreases to 4.5 aa / n while phosphate causes a further decrease, to 4.2 aa / n. Evidently, in an environment which enhances hydrophobic interactions the binding of the arginine - rich histones to the DNA is strengthened more than the attendant histone - histone interactions. It should be recognized, however, that these beta values are still higher than those of chromatin or reconstituted H 2 nucleohistone.

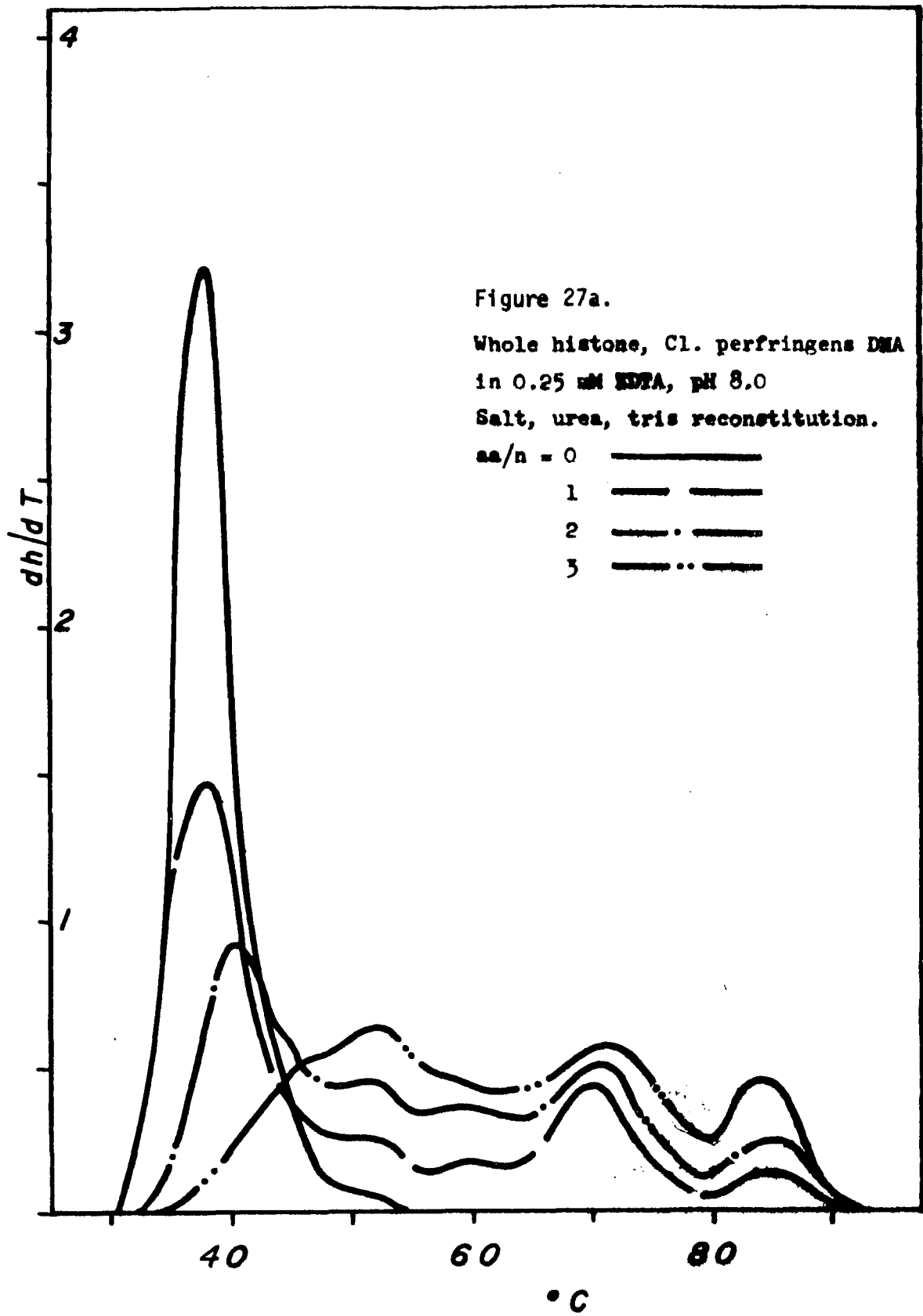
The T.D. profile of whole - H 1 nucleohistone reconstituted in salt - urea - phosphate buffer (Figure 26) is quite similar to the whole - H 1 reconstitute without urea. Relative to the plus - urea complex however, the 87<sup>0</sup>C (TmII) transition (Figure 26) is elevated from 83<sup>0</sup>C (Figure 23b) while the highest transition (TmIII) is destabilized by approximately 3<sup>0</sup>C. This further supports the hydrophobic nature of the binding associated with the TmII transition. As

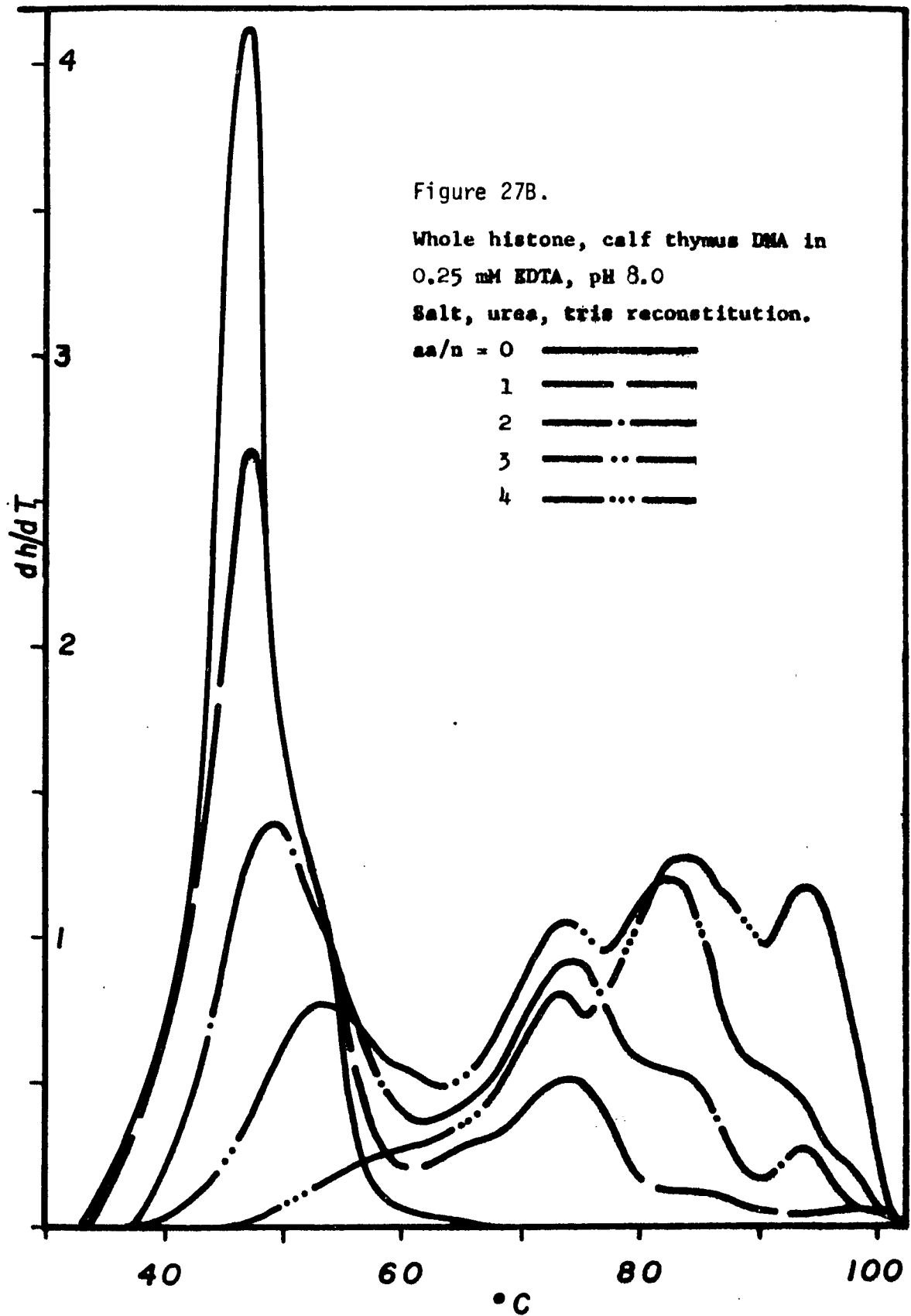


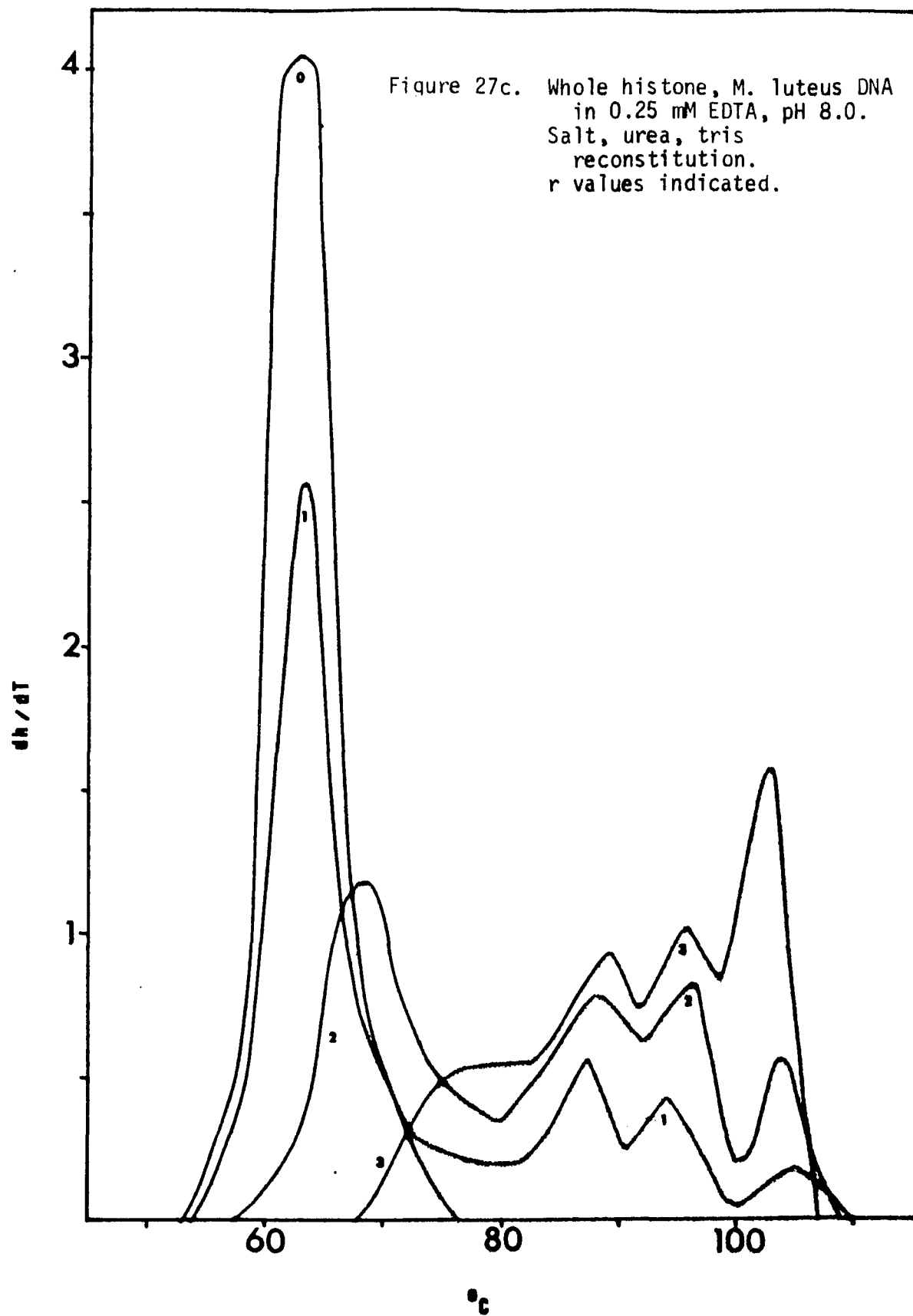
the hydrophobic attractions within the histone subunit are enhanced the stability of the second transition is increased while the binding of the more basic half-molecule is destabilized.

When whole histone is reconstituted to DNA in urea the shape of the melting profiles is changed drastically relative to urea-annealed whole-H1 complexes (Figure 27). This effect is seen most clearly in Figures 27b and c. The presence of histone H1 changes the interaction of the other four species of histones such that at an aa/n ratio of **three** the C-DNA nucleohistone profile (Figure 27b) resembles that of chromatin (Figure 14) quite closely. With the inclusion of H1 the beta value of the complex (Figure 28) becomes 3.7 aa/n, equal to the  $\beta$  value of chromatin, 3.7 aa/n (76). This role for H1 appears to be unique, however, many workers have observed striking differences between H1 and the other histones. It has been noted that the primary sequence of H1 is the largest and most variable of the histones (90), it is the most species-specific of this group of proteins (91), and is subject to the greatest number of covalent modifications (22, 23). H1 has been found to bind primarily to the internucleosome DNA regions (92), is most accessible to its homologous antibody of all the histones (93), is not found in histone-histone complexes either in solution (94) or in vivo (38, 39), and has essentially no effect on DNA conformation (95).

The presence of H1 also changes the effect of urea omission on the reconstituted nucleohistone. Whereas minus-urea whole-H1 nucleohistones exhibited some stabilization of the TmII and TmIII peaks the minus-urea whole histone complexes display enhancement of the low







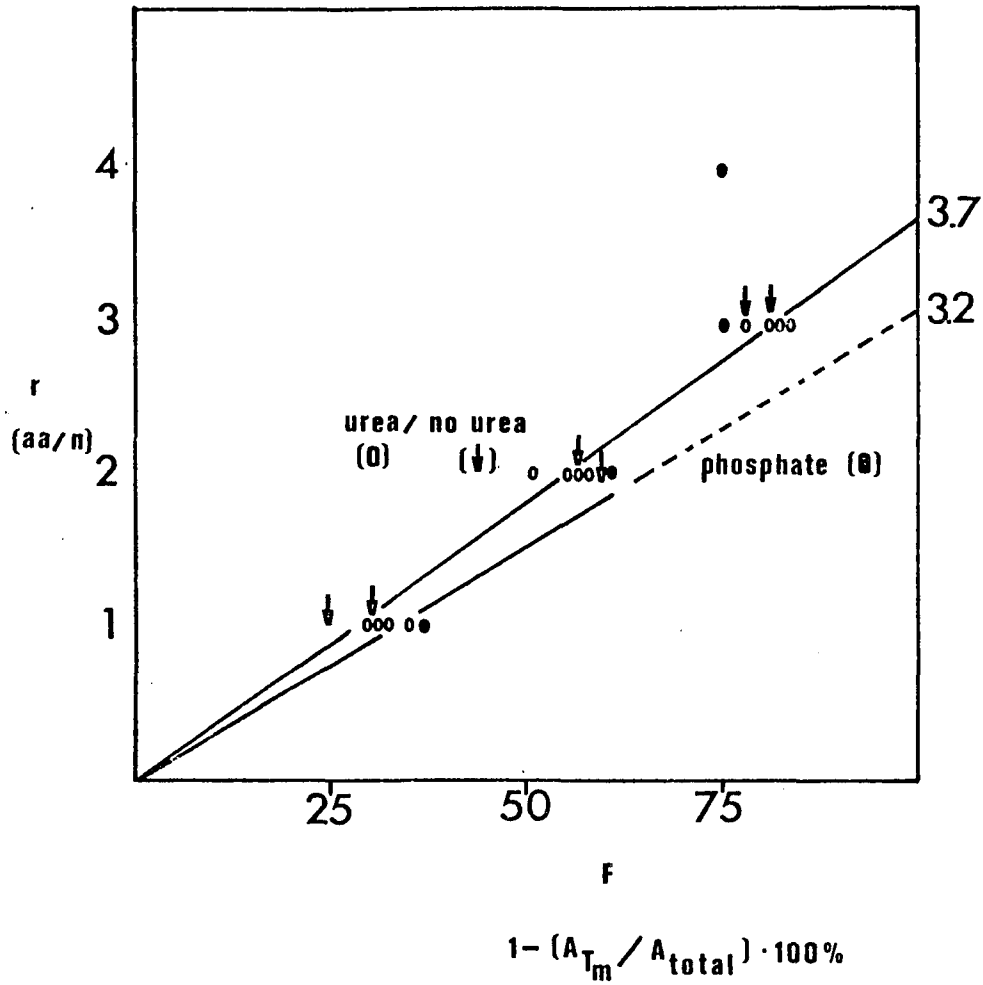
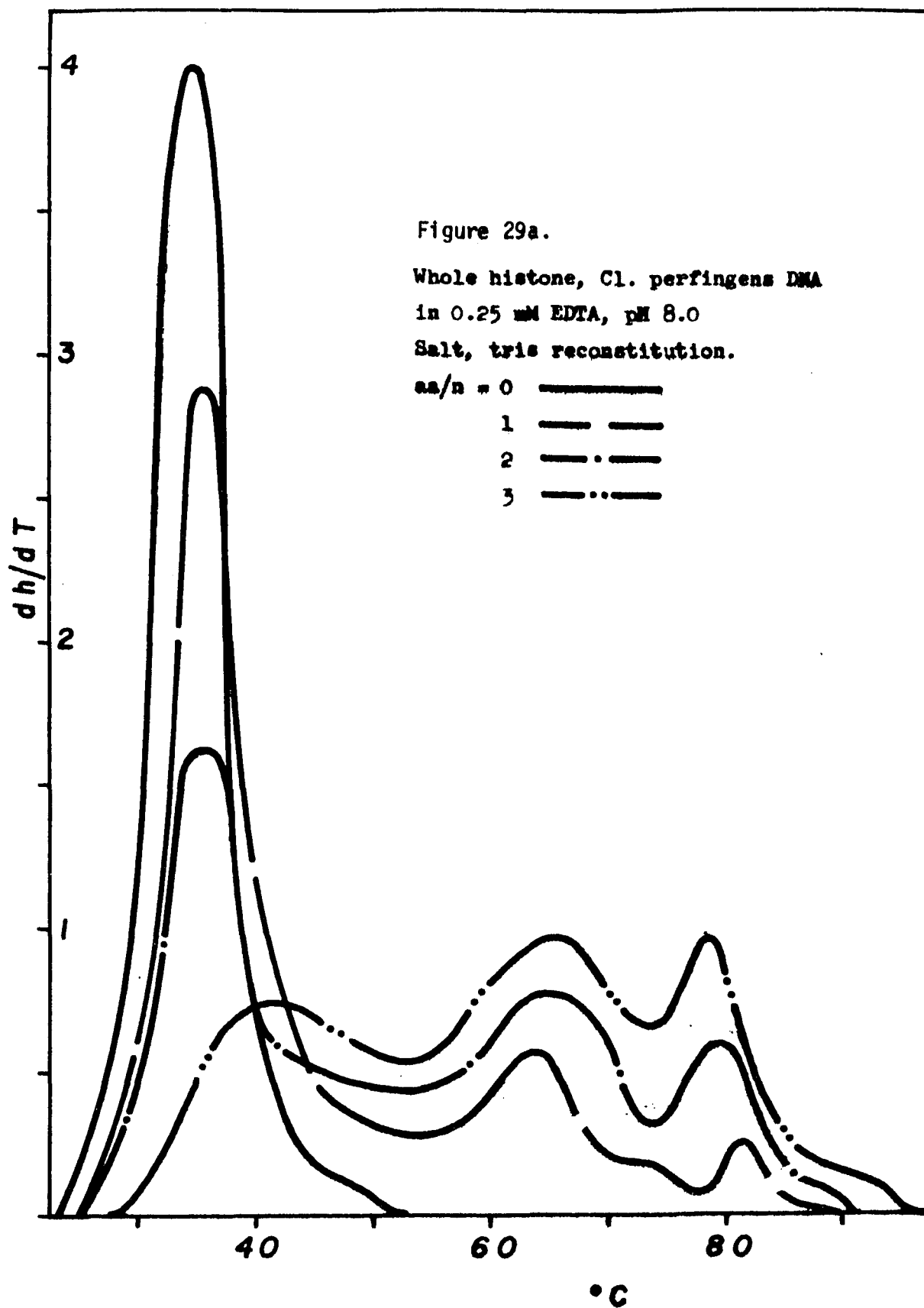
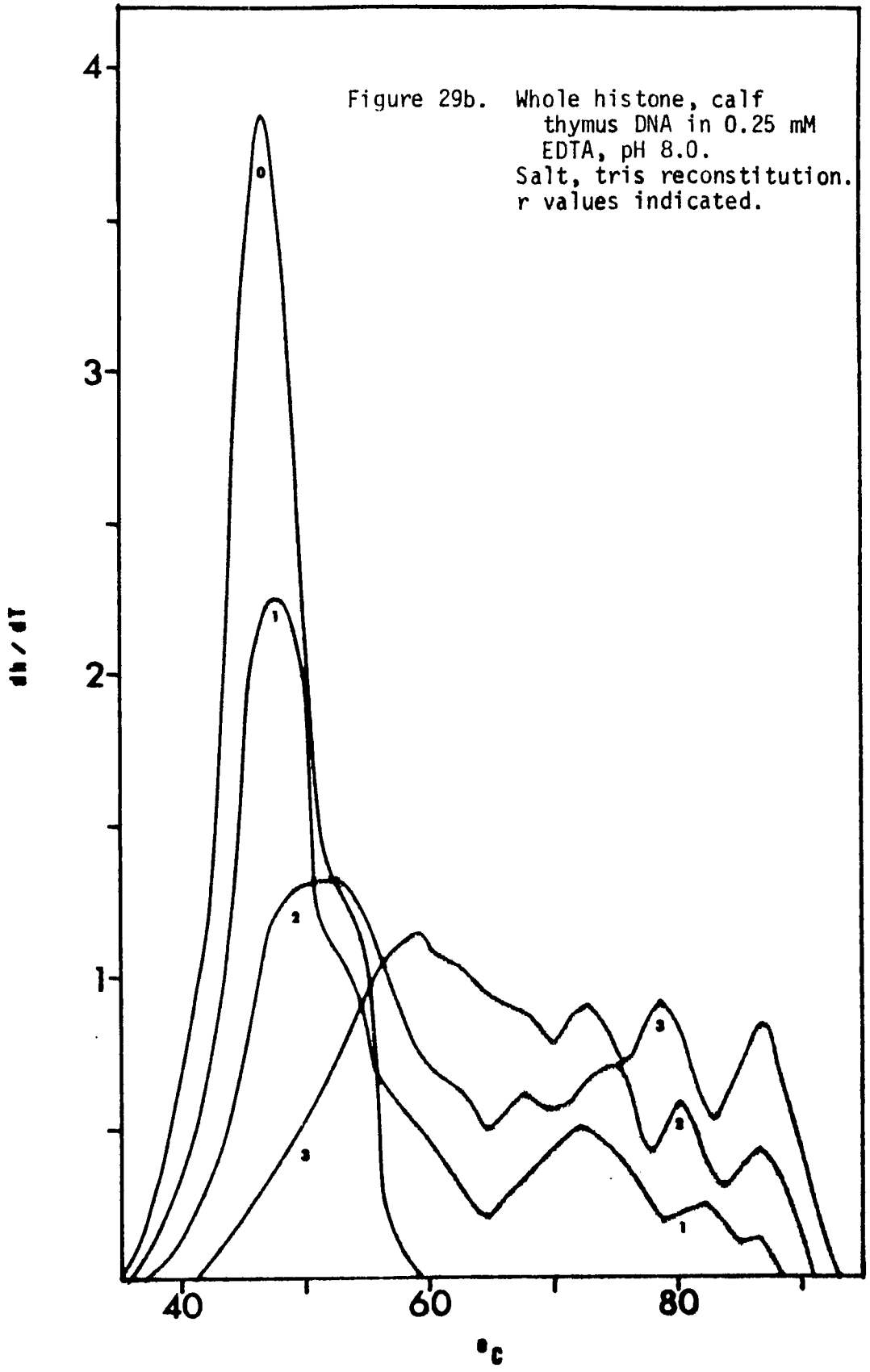
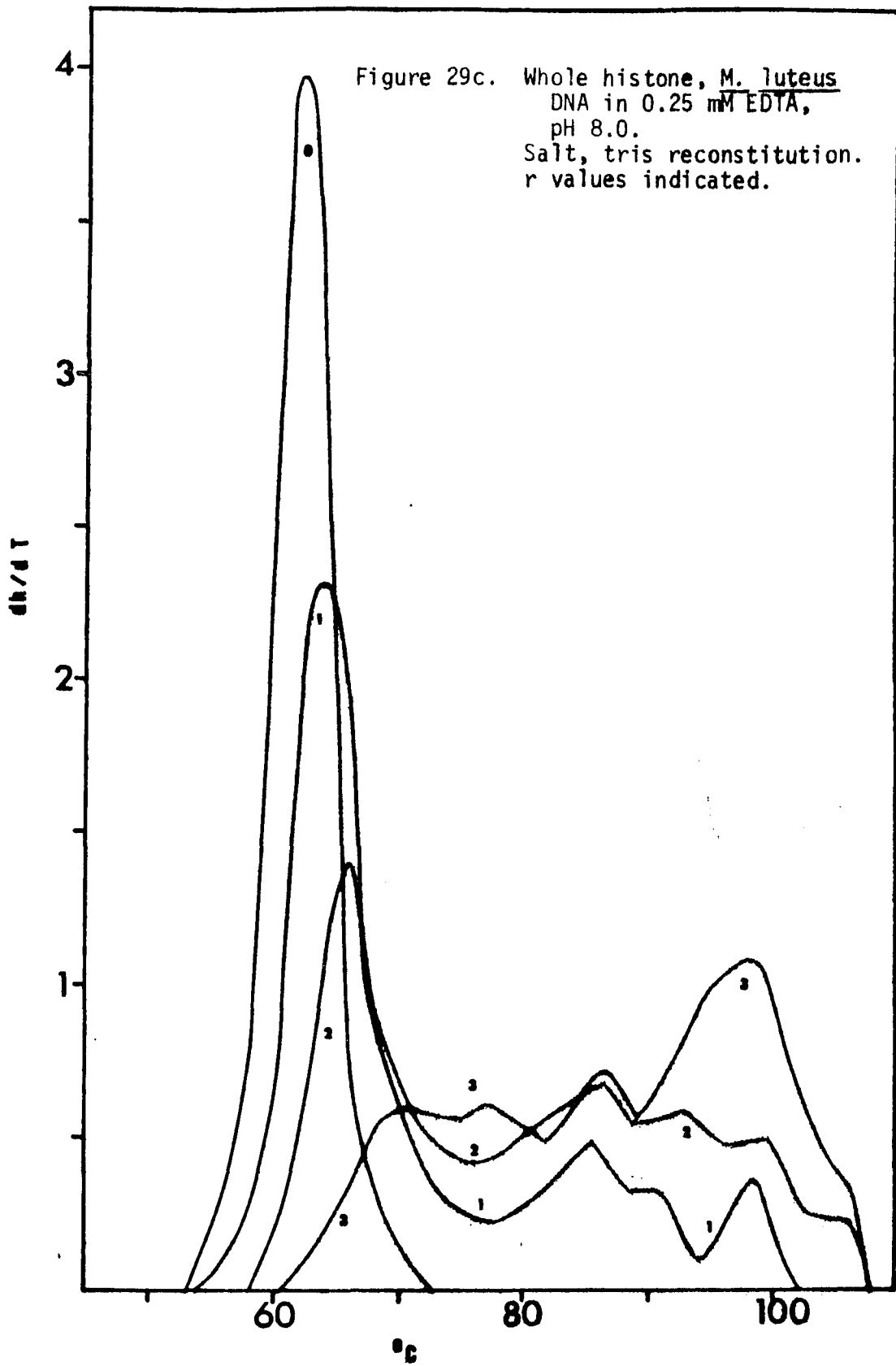


Figure 28.  $\beta$  value determination.  
Whole histone nucleohistones.

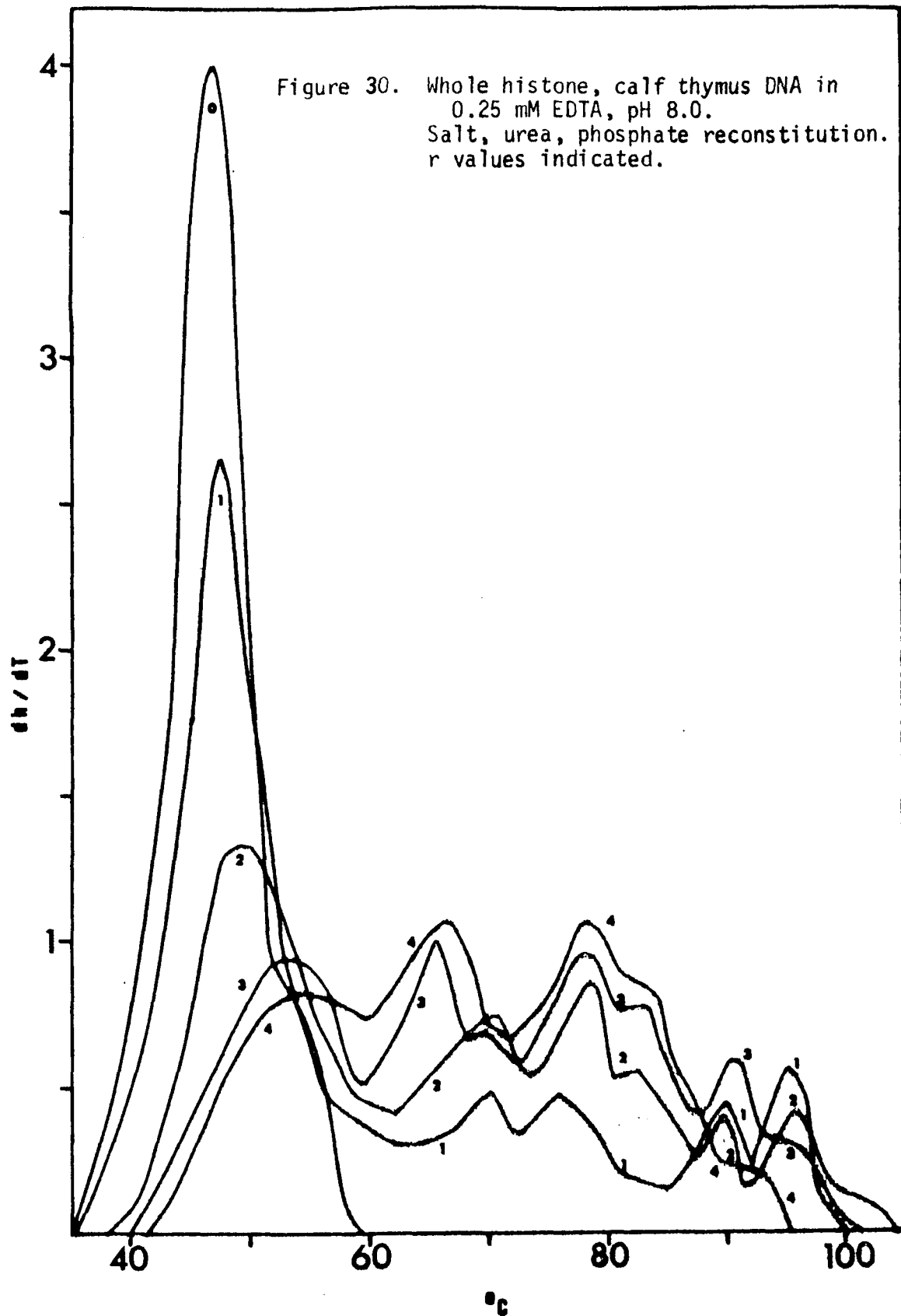




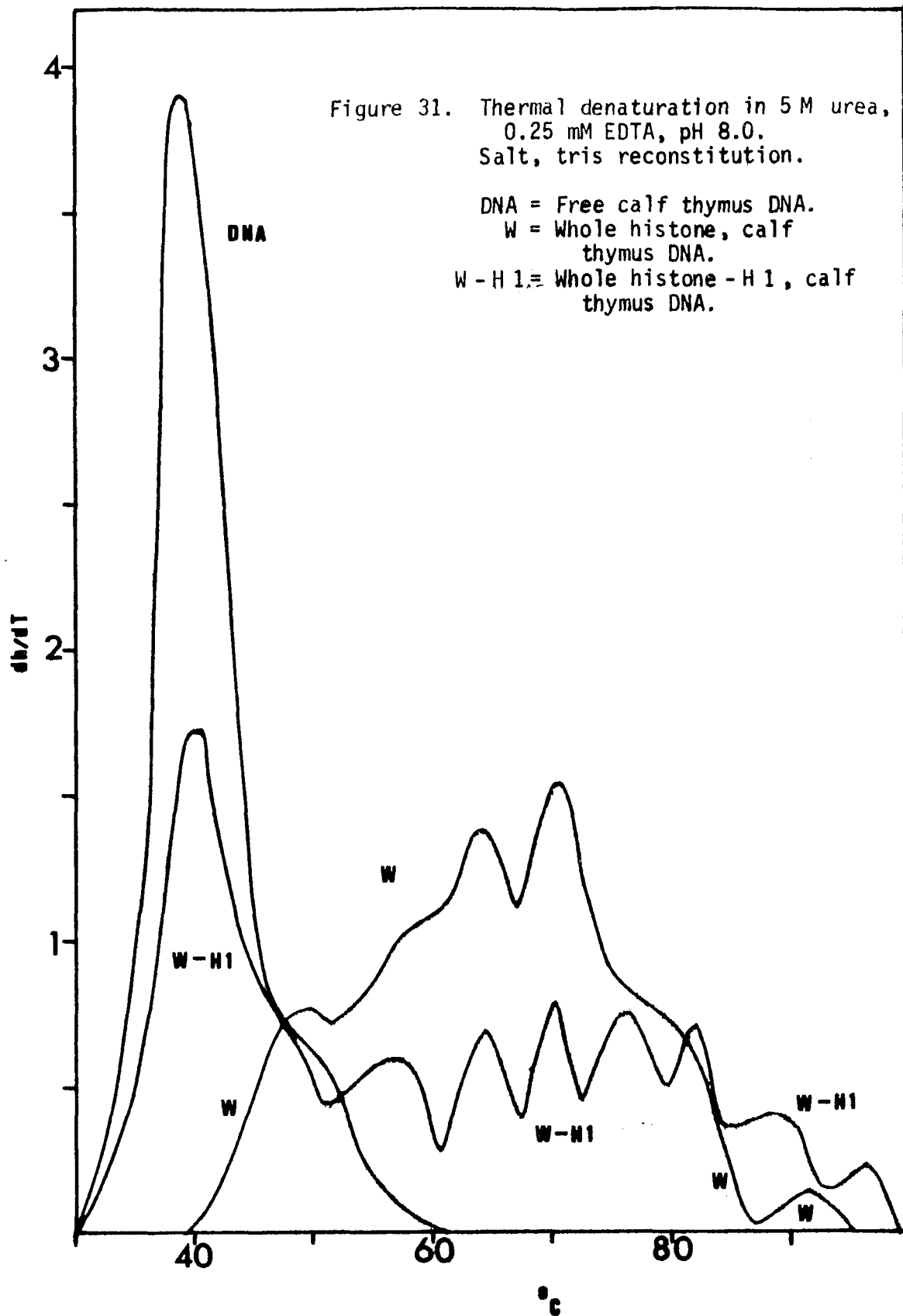


temperature transitions apparently at the expense of the TmII, TmIII peaks. This is seen most clearly in Figure 29b. Thus H1 has acted to somewhat reverse the effects of the arginine-rich histones. When whole nucleohistone is reconstituted in salt-urea-phosphate (Figure 30) a very large decrease in TmIII (90°C - 100°C) is observed but little change in TmII (82°C) is noticeable. The transitions near 65°C and 77°C have increased however, further supporting the hypothesis that these three transitions are related to conformational changes of the DNA due to the hydrophobic nature of the histone core. Although drastic modifications of the profiles are evident as a result of urea omission or phosphate inclusion the beta value of the nucleohistone is relatively constant (Figure 28). Without urea  $\beta = 3.6$  aa/n, with phosphate  $\beta = 3.1 - 3.3$  aa/n (initial slope). Again, phosphate reconstitution increases the effectiveness of histone-histone interaction so that at high input ratios of 3-4 aa/n the slope of the beta plot increases sharply. This drastic rise parallels the enhancement of the postulated low temperature conformational transitions. A comparison of the thermal denaturation profile of purified nucleohistone derived from calf thymus (97) with the profile of the salt-urea-phosphate whole histone nucleohistone (aa/n = 4) shows that these samples display nearly identical thermal transitions. This result strongly implicates histone-histone hydrophobic interactions as a central force in the maintenance of chromatin structure. As described below, the removal of these forces has the identical effect on both the salt-urea-phosphate reconstitute as on the purified nucleohistone.

In 1974 Chang and Li (97) observed that nucleohistone purified



from calf thymus chromatin and melted in urea displayed a general temperature decrease in all thermal transitions except one. There appeared at 96<sup>0</sup>C a new transition, higher than any in the control nucleohistone melted in the absence of urea. The appearance of this additional band was also noted in 0.6 M NaCl treated nucleohistone denatured in urea. (0.6 M NaCl removes histone H 1 and some non-histone proteins.) In Figure 31 the profiles of whole and whole - H 1 nucleohistones reconstituted without urea, but melted in urea, are presented. In the whole histone complex, there appears a new peak (T<sub>m</sub>IV) at 93<sup>0</sup>C (Figure 31) which is higher than any transition in the profile of the minus - urea complex (Figure 29). In the whole - H 1 complex there is a peak at 98<sup>0</sup>C which was present only as a shoulder in the minus - urea complex (Figure 25). In the H 2 B or H 2 nucleohistones reconstituted minus - urea but melted in urea (Figure 21, 22) no new peak is observed which is higher than the highest transition in the controls. It seems plausible then that the bulk of the histone - histone interactions are destroyed in 5 M urea and the histone subunit is opened allowing the high temperature stabilization of a small fraction of the DNA bound by the arginine - rich histones. In the original work by Chang and Li (96) when purified nucleohistone was extracted with 1.6 M NaCl (a salt concentration which removes some of the arginine - rich histones) and melted in urea the extra transition did not appear. Comparison of Figure 31 with the melting profile of purified calf thymus nucleohistone in urea presented by Chang and Li (96) shows that the shapes of the profiles, and more importantly, the temperatures of each transition are virtually identical. This strongly suggests that it is the difference in the strength of the hydrophobic forces which distinguishes in vivo nucleohistone from the minus - urea reconsti-



tuted whole histone nucleohistone. Once these differences have been eliminated by urea, both samples show identical thermal stabilities. Relative to whole histone nucleohistone reconstituted without urea, melted in EDTA (Figure 29), the transitions apparent at 78°C and 85°C are altered only slightly in the melted-in-urea complexes (78°C and 81°C) (Figure 31), but there has occurred a large increase in the amount of material melting between 55°C and 70°C. The appearance of this low melting material may correlate with the emergence of the TmIV band. Li (57) has proposed a dynamic model for chromatin structure. In it he proposes that although histones interact with each other through hydrophobic regions of secondary structure to form a protein octamer subunit, the subunit may open or close depending on the environmental pH, polarity, ionic strength or the disruptive force imposed on it by the DNA helix distorted by histone binding. The 55°C - 70°C transitions may represent conformational changes in the double helix specifically related to the release of constraint imposed either directly by the hydrophobic residues or secondarily via forces transmitted through the more basic regions. The conformational change in the secondary structure of the histones to a less ordered posture would release this strain allowing the electrostatic repulsive forces to dominate and extend the histone subunit. This in turn would allow the basic regions of the arginine-rich histones to stabilize the DNA to a temperature higher than that possible were the hydrophobic constraining forces not released. Support for this view derives from the observation by Weintraub et al. (34) that a tetrameric complex of histones H2A, H2B, H3 and H4 which is stable in 2 M NaCl but

dissociates in 0.2 M NaCl will remain intact in 0.2 M NaCl if the positively charged, more basic amino terminal arms (~20% of each histone) are first digested away by trypsin.

CHAPTER IV  
CIRCULAR DICHROISM

INTRODUCTION

In an attempt to relate the structure of biological macromolecules to their function, investigators have sought means of objectively ascertaining the three dimensional structure of proteins. Short of precise structural determination by X-ray diffraction crystallography, circular dichroism (CD) represents a most useful tool for the estimation of the secondary structure of biological macromolecules.

Plane polarized light may be dissected to its circularly polarized vector components by passing the light through a birefringent material which serves to retard one vector by  $90^{\circ}$  with respect to the other in the direction of wave propagation. The magnetic moments of the two circularly polarized vectors are non-identical. When light of the appropriate wavelength excites the electrons of a chromophore their elevation to an upper state and the dissipation of the energy as heat gives rise to an absorption band. If the excited electron is displaced in a nonlinear fashion from its initial position, the circular component of the motion will induce a magnetic moment. The interaction of the magnetic moment of the electron with the magnetic moments of the circularly polarized vectors causes the chromophore to preferentially absorb either the left- or right-handed component of the circularly polarized light and generates a CD response. The CD response of a chromophore ( $\Delta\epsilon$ ) is reported as the difference between the absorption of the left- ( $\epsilon_l$ ) and right-handed ( $\epsilon_r$ ) circular polarized components:

(11)

$$\Delta \mathcal{E} = \mathcal{E}_l - \mathcal{E}_r$$

Since the left-handed and right-handed vectors are absorbed to different extents their relative velocities through the optically active material (refractive indices) will also be unequal. The combination of differential absorption and nonequal propagation velocities changes the polarization of the light from circular to elliptical. It is the ellipticity ( $\Theta$ ) which is measured instrumentally and can be converted to the molar residue ellipticity ( $\Delta\mathcal{E}$ ) by the formula:

(12)

$$\Delta \mathcal{E} = \Theta / 3305$$

Therefore, while the intensity of absorption depends on the electric dipole transition moment, the circular dichroism response depends on both the electric and magnetic dipole transition moments. Thus, the CD signal, which appears only in regions of an absorption band, may be much more intense than the absorption band at the same wavelength.

To make CD measurements relevant to the conformations of biomolecules the CD spectrum of a sample must be compared to some reference spectrum which has been assigned a given structure by independent means, such as X-ray diffraction. For nucleic acids, the work of Tunis-Schneider and Maestre (97) on the CD of DNA under conditions generating the A, B and C forms of DNA (as determined by X-ray studies) have given the reference spectra to which are compared the CD spectra of DNA under a wide variety of conditions. Some of the physical parameters of DNA in A, B and C forms are given in Table 5.

TABLE 5 (98,99)

FORM	ANGLE OF ROTATION BETWEEN BASE PAIRS	INCLINATION OF BASES TO HELICAL AXIS	RESIDUES PER TURN	PITCH, A	TRANSLATION PER TURN
A	32.7 <sup>0</sup>	+20 <sup>0</sup>	11	28.15	2.55
B	36 <sup>0</sup>	0 <sup>0</sup>	10	34	3.4
C	38.6 <sup>0</sup>	- 6 <sup>0</sup>	9.3	31	3.3

The characteristics of the CD response to the various DNA conformations can be summarized as follows:

- A form: a large positive band centered near 270 nm, a small negative band near 235 nm and a crossover near 245 nm.
- B form: nearly equal positive band (275 nm) and negative band (245 nm) with crossover near 260 nm.
- C form: no positive response between 260 nm - 300 nm, negative trough near 245 nm. Spectrum between 210 nm - 250 nm is essentially the same as B form spectrum.

Ivanov et al. (98) have observed that the three prime forces determining DNA conformation are:

- a) hydrogen bonding between complementary bases,
- b) stacking interactions,
- c) electrostatic repulsion of the negatively charged phosphate groups.

With the addition of salt (NaCl, MgCl<sub>2</sub>, KCl, NH<sub>4</sub>Cl, LiCl, CsCl) to an aqueous solution of DNA, the B form of DNA is progressively distorted towards C form. Presumably, the salts neutralize the phosphate repulsion by forming a Debye shell around the anion and allow a more compact structure. In methanol-water solutions the effects of salt are enhanced. Salt concentrations one order of magnitude less are required under these less polar conditions. The repulsion of the phosphates is increased by the apolar environment but up to a finite limit determined by the dielectric constant of the medium. In water-methanol the cations form true complexes with the phosphates in the region of the highest charge density, the narrow groove. The largest [ion+hydrate shell], which is lithium (Table 6) (98), has the smallest effect on the DNA conformation. The cesium cation, which binds approximately 0.2 moles of associated water per mole, is ca. 50% smaller and is significantly more effective in causing the compaction of the narrow groove.

TABLE 6 (98)

	<u>Li<sup>+</sup></u>	<u>Na<sup>+</sup></u>	<u>Cs<sup>+</sup></u>
radius, A	7.4	5.6	3.6
H <sub>2</sub> O, moles	12.6	8.4	0.2

In apolar medium (dioxane-water, ethanol-water) at low ionic strength (10<sup>-4</sup> M) the B form of DNA is altered towards the A form. Increased phosphate repulsion overcomes the weakened vertical stacking interactions allowing a cooperative change in the DNA conformation.

These features are summarized in Table 7.

TABLE 7

	<u>A FORM</u>	<u>B FORM</u>	<u>C FORM</u>
medium	apolar	aqueous	more ionic
phosphate repulsion	greatest	intermediate	least
stacking interaction	least	intermediate	greatest
H - bonding	greatest	intermediate	least
narrow groove width	greatest	intermediate	least
transition	cooperative	non-cooperative	

Determination of the appropriate references for analysis of protein CD spectra has been less successful. In general, two approaches have been utilized. The spectra of synthetic polypeptides such as poly-L-lysine (100), poly- $\alpha$ -L-glutamic acid and copoly-L-glu<sup>42</sup>lys<sup>28</sup>, ala<sup>30</sup> (101, 102) (under conditions defined by X-ray diffraction or studies of oriented films) were taken and compared to the spectrum under analysis. Although the shapes of these reference spectra and the wavelengths of their extrema agree very well, the absolute amplitude of the response is quite variable. In addition, since the amount of helix is chain-length dependent and the extent of beta sheet depends strongly on local conformation, estimates of secondary structure based on polypeptide models should not be taken as quantitative (103). Chen

et. al. (104) and Chen and Yang (105) have employed proteins of known structural composition (by X-ray diffraction) in order to calculate CD reference spectra. Although this is an improvement on the use of synthetic polypeptides the assumptions involved in assigning secondary structure to various peptide segments leads to spectra which are qualitatively the same but quantitatively different relative to other reference spectra. Until other proteins are included in statistically averaged spectra the most reliable conclusions which may be drawn are still qualitative (106).

Circular dichroism has been used by a number of laboratories to investigate the interaction between histones and DNA. Simpson and Sober (107) demonstrated that the positive DNA band near 275 nm is reduced and red-shifted when the DNA is complexed in nucleohistone. The binding of the polycationic histones neutralizes the DNA phosphates and condenses the DNA towards C form.

In a series of articles, Dr. G. Fasman and coworkers (108) have used CD to examine complexes of DNA and isolated histone fractions. When histone H 1 was annealed to DNA by gradient dialysis from 2.0 M NaF or KF to 0.14 M NaF, large B to C type transitions were observed (108a).

When the arginine-rich histone H 4 was reconstituted with DNA (108b) using a gradient from 5 M urea, 2 M NaCl to 0.15 M NaCl, large enhancements of the positive CD of DNA were found indicating a transition of B to A type spectrum. Above amino acid to nucleotide ( $aa/n = r$ ) values of 1.5 however, this A form spectrum decreased towards B form with increasing  $r$ . For complexes in which the gradient was continued to 0.15 M NaCl prior to urea removal, no changes in the B type CD were seen. Reconstitution of H 4 to DNA using a salt-urea gradient to low ionic

strength led Li et. al. (109) also to the conclusion that H 4 did not induce major conformational changes in the nucleic acid.

The reannealing of histone H 2 A to DNA (108c), using a 6 M to 0.15 M guanidinium hydrochloride (GuCl) gradient shifts the DNA spectrum from B to A form, similar to the response seen with the H 4 - DNA complexes reported earlier. With H 2 A, however, the reversal of the A type spectrum back to B type did not occur until  $r > 2.0$  aa/n. When reduced histone H 3 was complexed with DNA (108c) small B to A transitions were seen, however complexes of oxidized, dimer H 3 with DNA showed only B to C transitions. When the H 4 histone was reconstituted to DNA using 6 M GuCl (108d), large B to A transitions were seen which did not decrease as  $r$  exceeded 1.5 aa/n. On cleavage of H 4 to amino - (N) and carboxyl - terminus (C) fragments and reannealing of the purified fragments to DNA individually (108d) neither the N nor C fragment, or mixtures of N + C fragments, was able to induce DNA conformational changes. When H 4 was mixed with DNA in 2 M NaCl and diluted directly to 0.14 M NaCl, the complexes exhibited the red shifts and decreased positive band amplitude associated with the B to C transition. Using the GuCl gradient technique to associate histone H 2 B to DNA, Adler et al. (108e) showed B to A type CD transitions for these complexes as well. Leffak et al. (66), however, demonstrated that H 2 B - DNA complexes prepared by salt gradient dialysis in the presence of urea exhibited B to C type transitions.

The results of Dr. Fasman's group have been examined in detail because a unified picture begins to emerge to explain the effect of each histone as well as the effect of the reconstitution medium employed

on the DNA conformation. The effect of binding of H 1 on the DNA conformation is similar to that of polylysine. The ionic interactions between peptide and DNA cause a distortion of B form towards C and finally  $\Psi$  form. When histone H 2 B, H 2 A, H 4 or H 3 are reconstituted to DNA in the presence of GuCl, this salt may enhance the hydrophobic character of the binding of the histones to the DNA. As the apolar residues bind the nucleic acid, water is excluded to the medium and the bases find themselves in an increasingly apolar environment. The result is a distortion of the helix towards A form. As the GuCl concentration decreases to 0.15 M the more basic amino acids bind to the DNA, however the ionic strength of the environment helps maintain the A form. If a 0.15 M complex is placed in a low ionic strength medium the A form gradually disappears.

When H 4 is reconstituted to DNA in 5 M urea, 2 M NaCl the histone binds ionically as the salt is decreased to 0.15 M. Once the urea has been removed however, hydrophobic interactions between the H 4 and DNA again promote the A form. At ratios above  $r = 1.5$  however the A form returns towards B form. This may be due to histone-histone interaction through hydrophobic residues which reduces their effect on the DNA conformation. Empirically it is found that the tendency for histones to self-associate follows the sequence  $H 4 > H 2 A > H 2 B$ . It is interesting then that H 4 shows the A to B reversal at  $r = 1.5$  (108d), H 2 A shows this effect at  $r = 2.0$  (108c) and H 2 B does not demonstrate the reversal even at  $r = 3.0$  (108e).

Further support for this model of hydrophobic binding derives from H 3 dimer complexes. These complexes show only the B to C transition while monomer H 3 - DNA complexes show only the B to A transition.

The finding that H2B - DNA complexes (66) show only the B to C transition may then be due to the binding of histone H2B to DNA which has already been distorted towards the C form by the reannealing conditions of high salt and urea (96). Once the salt has decreased to ca. 1.0 M NaCl the histone binds. Further ionic strength reduction to low ionic strength (0.01 M tris) prior to urea removal allows only ionic contributions to the binding (110). Increasing histone content therefore yields increasing amounts of C form DNA.

In some complexes examined herein, the ratio  $A_{320}/A_{260}$ , an estimate of the light scattering of the complex, is high. That the results reported are not artifacts of light scattering is supported by the fact that both spectrophotometric and chemical determination of the concentration of the complexes agree closely. Particulate matter would be expected to give consistently higher values for the chemical determination than for the optical. Adler et al. (108c) have reported that measurements made in a UV cell designed to eliminate scattering artifacts agree with spectra made under ordinary circumstances. When measurements are made in CD cuvettes of varying pathlength and normalized to a 1 cm path, all results agree within experimental limits. As well, when artificial scattering media (colloidal sulfur, alumina) were added to complexes the DNA CD was unaffected (108b, 111, 112). To further obviate the artifactual contribution of light scattering to these results, those parameters of the CD spectra were used as monitors which are independent of concentration (68) namely:  $\Delta\epsilon_{278} / -\Delta\epsilon_{246}$ ;  $\lambda_{\max}$  - the wavelength of maximum peak amplitude; and  $\lambda_c$  - the wavelength of crossover.

## EXPERIMENTAL

When histone H2A is annealed to DNA by salt + urea gradient a progressive red shift of the peak and crossover wavelengths is observed (Figure 32). These changes are characteristic of the B to C change in DNA conformation. It is possible, using the equation of Li et al. (109) to subtract the free DNA spectrum ( $r=0$ ) from the spectrum of the complex and arrive at an estimation of the shape of the CD of bound histones in the complex (difference spectrum) :

$$\Delta \mathcal{E}_m = \Delta \mathcal{E}_{DNA} + r \Delta \mathcal{E}_{protein} \quad (13)$$

and

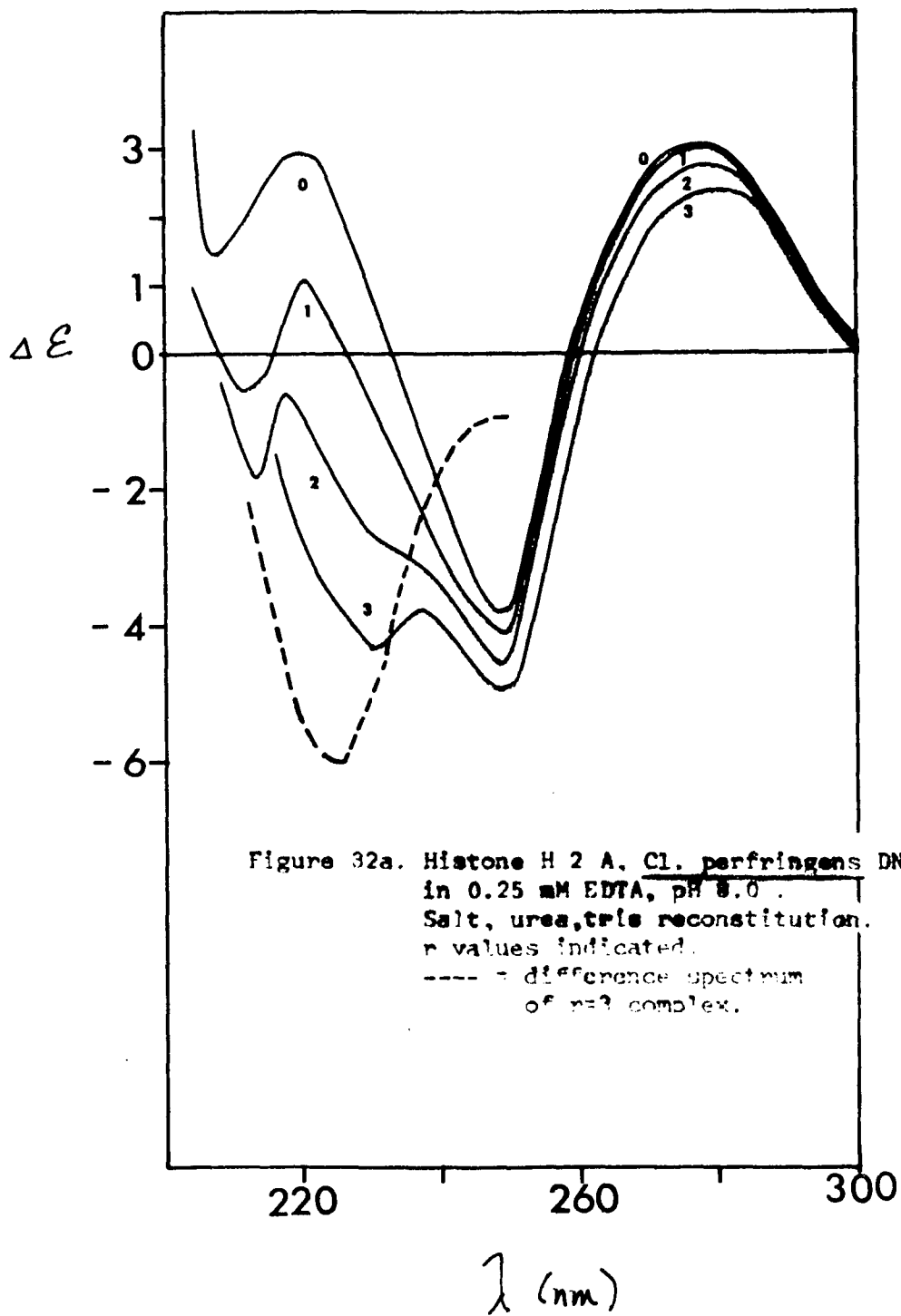
$$r \Delta \mathcal{E}_{protein} = \Delta \mathcal{E}_m - \Delta \mathcal{E}_{DNA} \quad (13a)$$

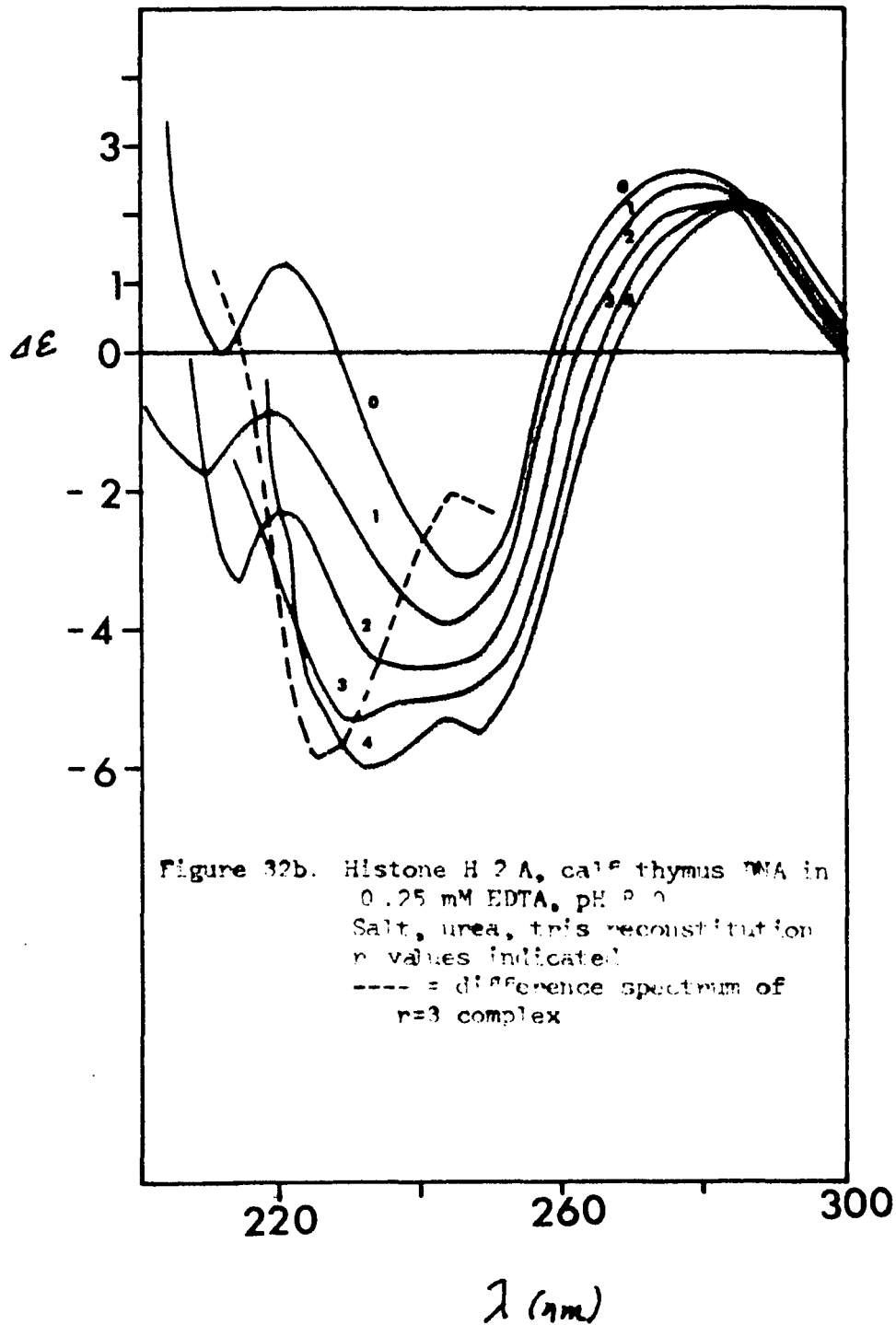
where  $\Delta \mathcal{E}_m$ ,  $\Delta \mathcal{E}_{DNA}$ , and  $\Delta \mathcal{E}_{protein}$  are the CD responses of the complex, free DNA and bound protein,  $r$  is the amino acid / nucleotide ratio and  $r \Delta \mathcal{E}_{protein}$  is the calculated CD of the bound histones (the difference spectrum). The assumptions involved in this estimation are that a) the  $r=0$  DNA spectrum does not vary greatly in the region 210 nm - 250 nm (98), the region of protein CD response; b) the contribution of light is small.

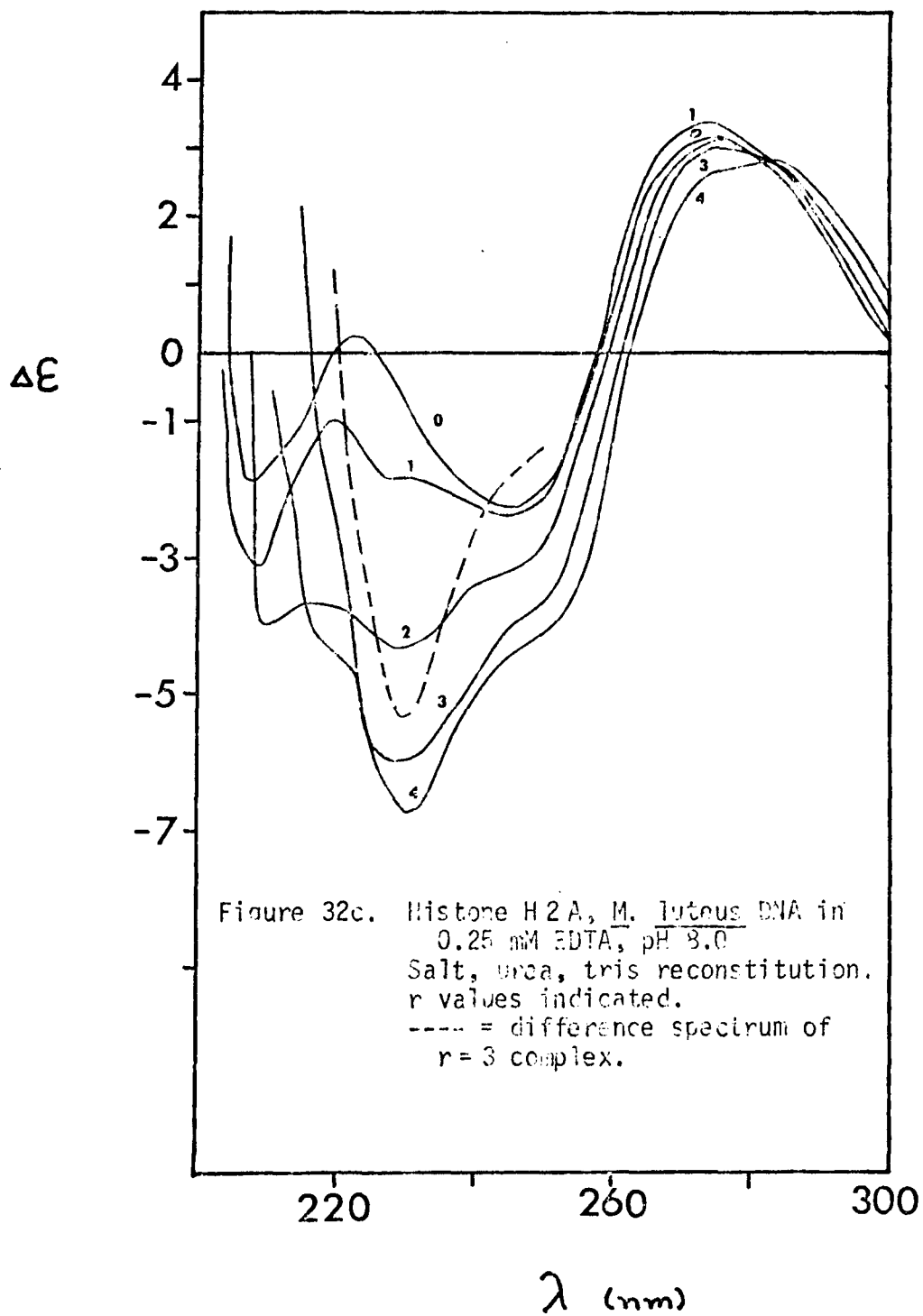
Disregarding the absolute amplitude of the difference spectra we may compare the shape of these curves to those of standard references.

Figure 33a presents the CD curves of poly - L - lysine in the alpha - helical ( $\alpha$ ), beta - sheet ( $\beta$ ) and random coil (rc) conformations (100). In Figure 33b the data of Figure 33a has been replotted to show the calculated CD spectra of poly - L - lysine under conditions of 50% $\alpha$  + 50% $\beta$ , 50% $\beta$  + 50% rc, and 50% $\alpha$  + 50% rc.

A comparison of the shape and wavelength of the most negative response of the difference spectra of Figure 32 with the spectra of Figure 33b demonstrates that the H2A histone is in a form resembling that of







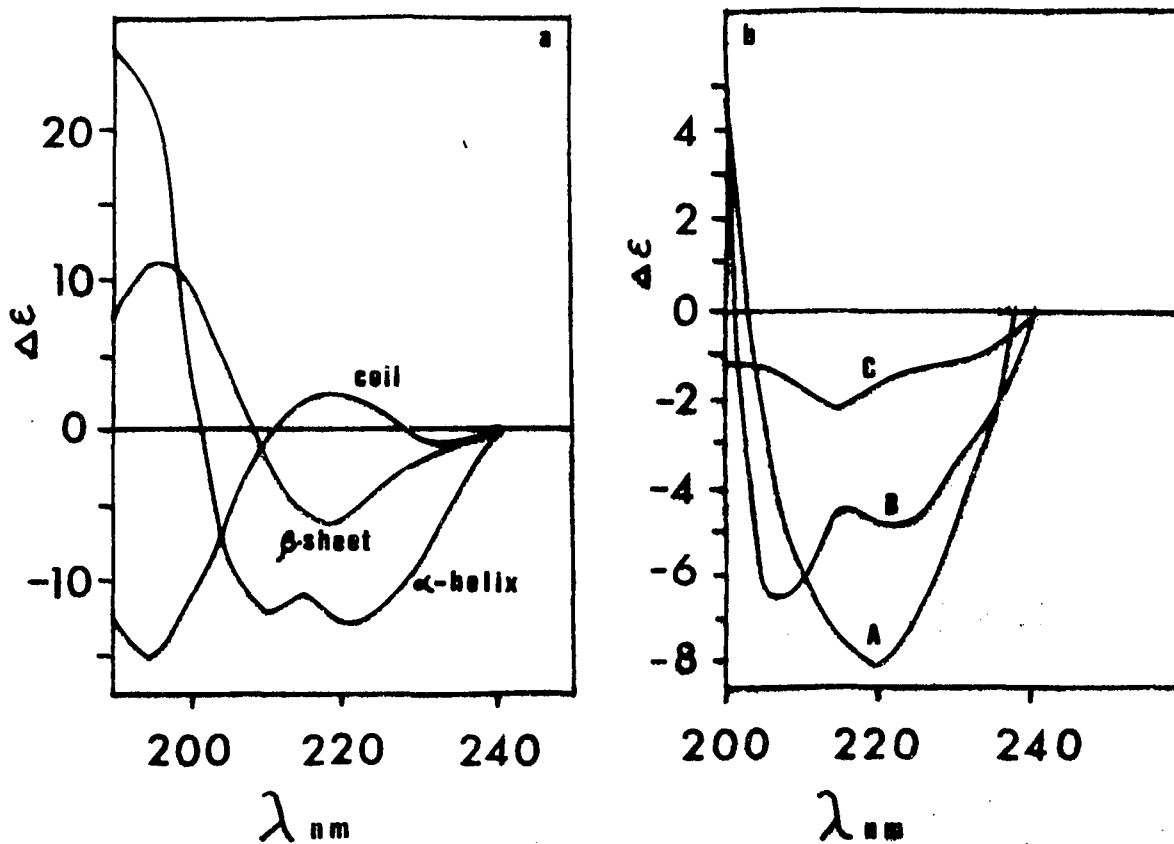


Figure 33.

- a. CD spectra of poly-L-lysine in 100%  $\alpha$ -helix  
 100%  $\beta$ -sheet  
 100% random coil conformations.
- b. Calculated CD spectra of poly-L-lysine in  
 (A) 50%  $\alpha$ -helix + 50%  $\beta$ -sheet  
 (B) 50%  $\alpha$ -helix + 50% random coil  
 (C) 50%  $\beta$ -sheet + 50% random coil conformations.

poly-L-lysine with 50%  $\alpha$  + 50%  $\beta$ . It should also be noted that the conformation of H2A is the same regardless of the DNA component of the complex.

From Figure 33a it is evident that only the  $\alpha$ -helix and beta-sheet conformations are negative at 220 nm. Therefore, by monitoring the change of ellipticity of each complex at 220 nm, we may estimate the relative amount of secondary structure in the complexes. In Figure 34a are plotted the change in  $\Delta\epsilon_{220}$  of the complex against the value  $\Delta\epsilon_{278} / -\Delta\epsilon_{246}$ . This latter value is a measure of the B to C transition. It is evident (Figure 34a) first that there is a linear relation between the amount of secondary structure in the bound histone and the extent of the B to C transition. Secondly, the slopes of these lines represent the amount to B to C transition per unit change in secondary structure. A plot of the slopes of these lines against the G+C content of the DNA component in each complex shows a linear relation between the G+C content and the deformability of the DNA due to the histone secondary structure. It is seen that increasing G+C content renders the DNA more susceptible to deformation. Since the number of phosphates per base pair is identical for each DNA the difference in deformability must be related either to the greater number of hydrogen bonds between G+C pairs relative to A+T pairs, or to the hydrophobicity of G+C pairs relative to A+T pairs. In DNA hydrogen-bonding interactions are weakened during the B to C transition (98). If hydrogen-bonding played a crucial role during the H2A-induced B to C transition then M. luteus DNA would be expected to be less deformable than calf DNA. It has been shown, however, that A+T pairs bind two additional molecules of hydrate water relative to G+C pairs (108a). This implies greater

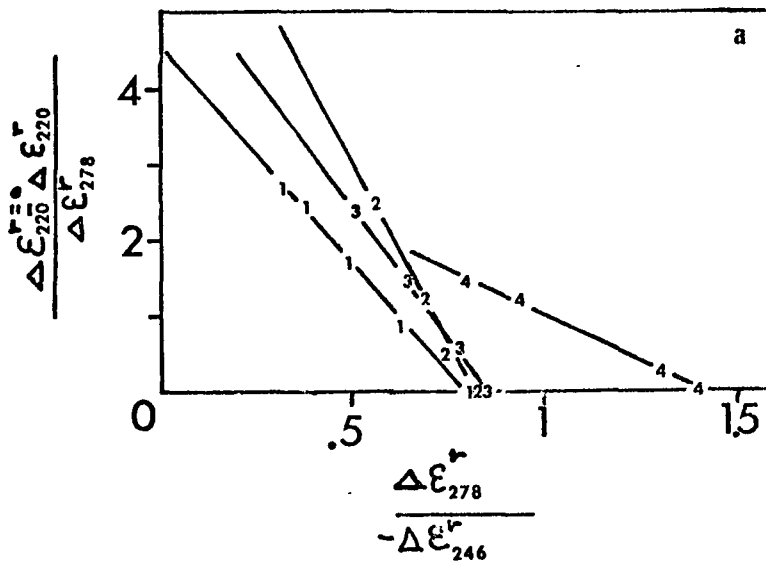


Figure 34. Deformability of histone H2A nucleohistones.

a.

1 = calf thymus DNA, salt, urea, tris reconstitution

2 = calf thymus DNA, salt, tris reconstitution

3 = Cl. perfringens DNA, salt, urea, tris reconstitution

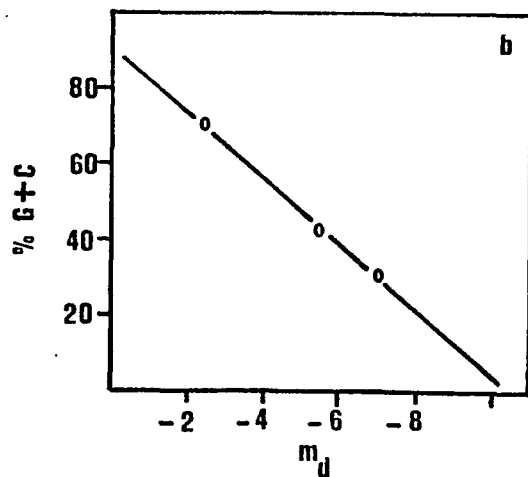
4 = M. luteus DNA, salt, urea, tris reconstitution

$$m_d = -5.5 \pm .5$$

$$-10 \pm 1.0$$

$$-7.1 \pm .7$$

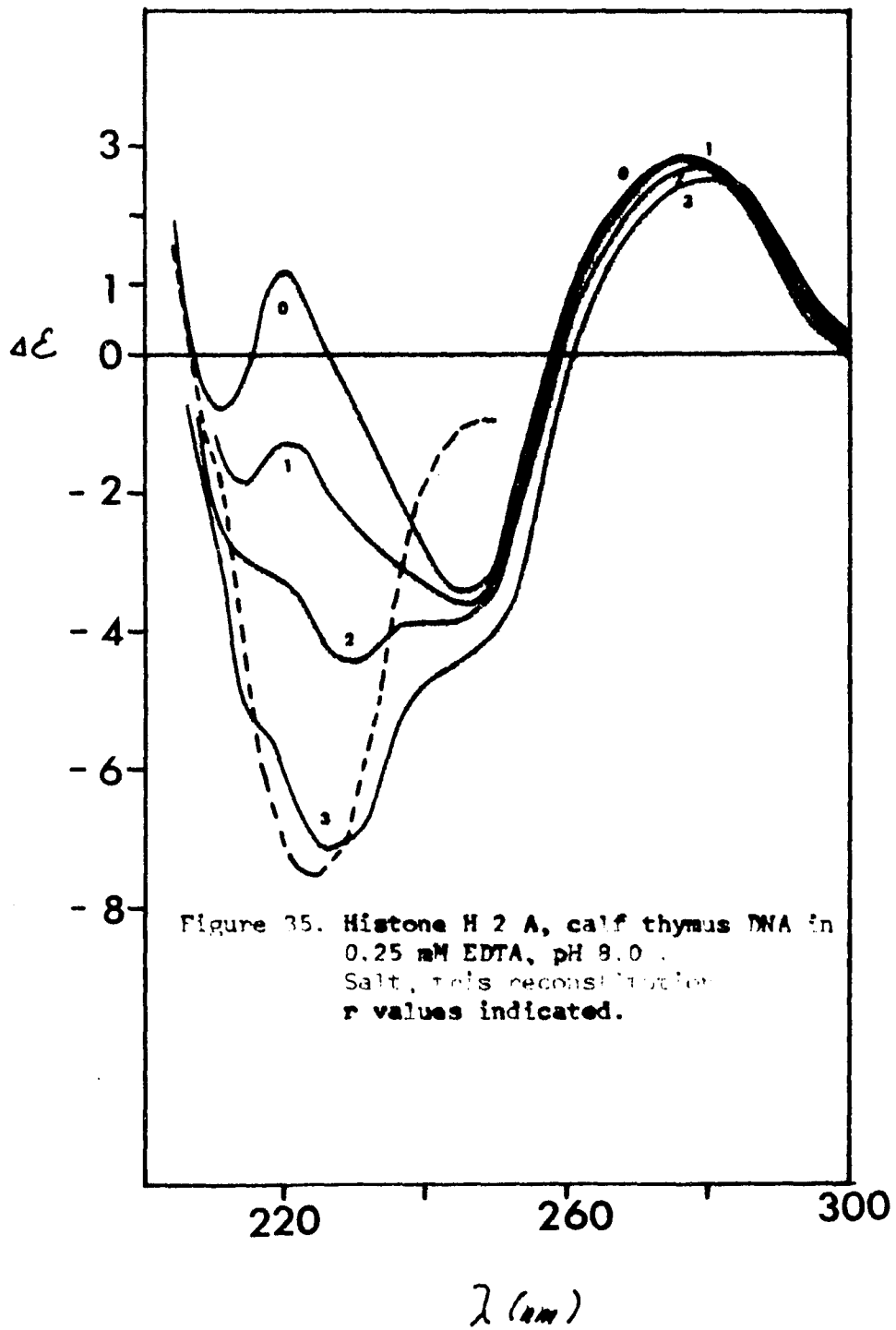
$$-2.4 \pm .2$$

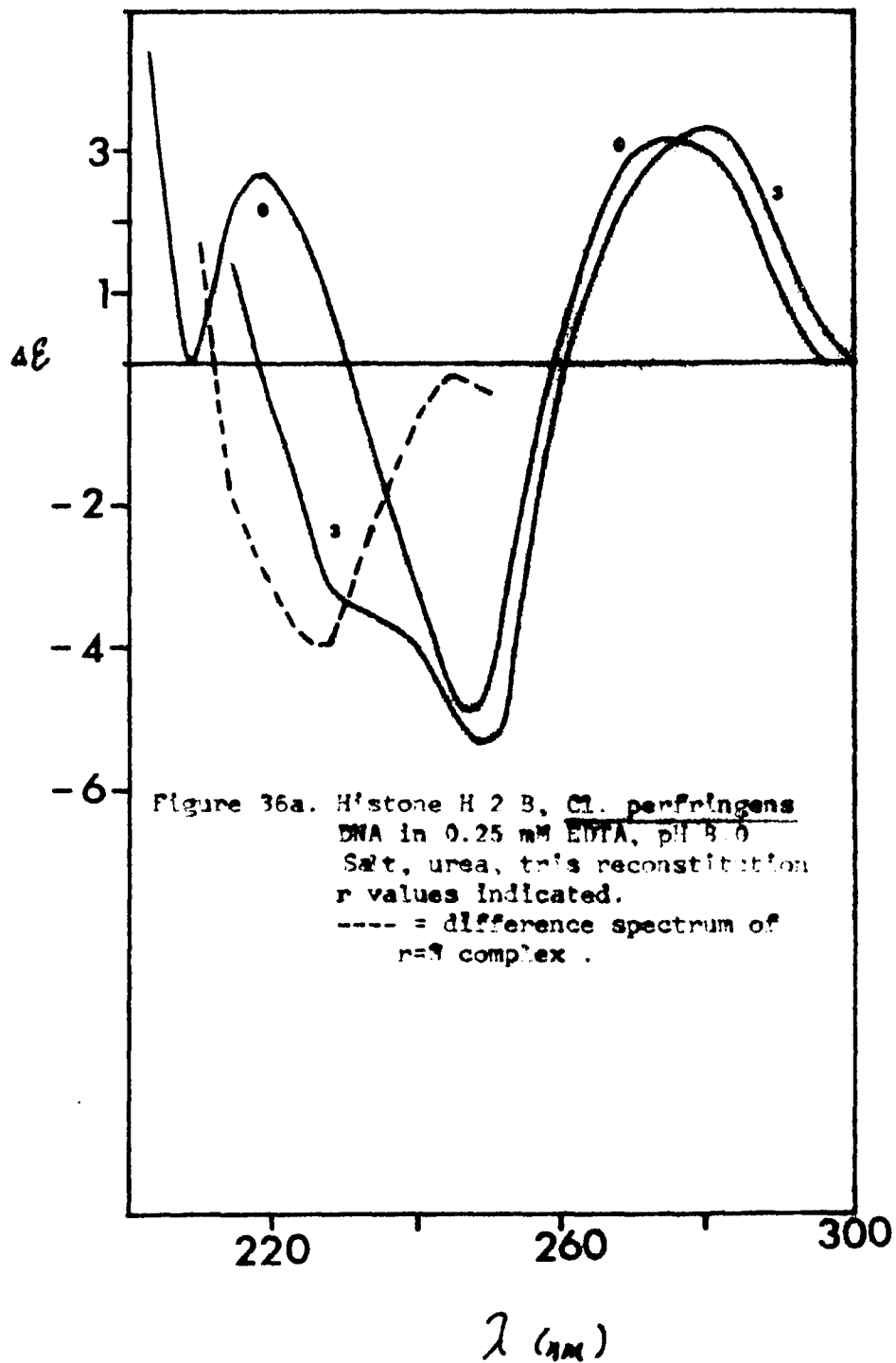


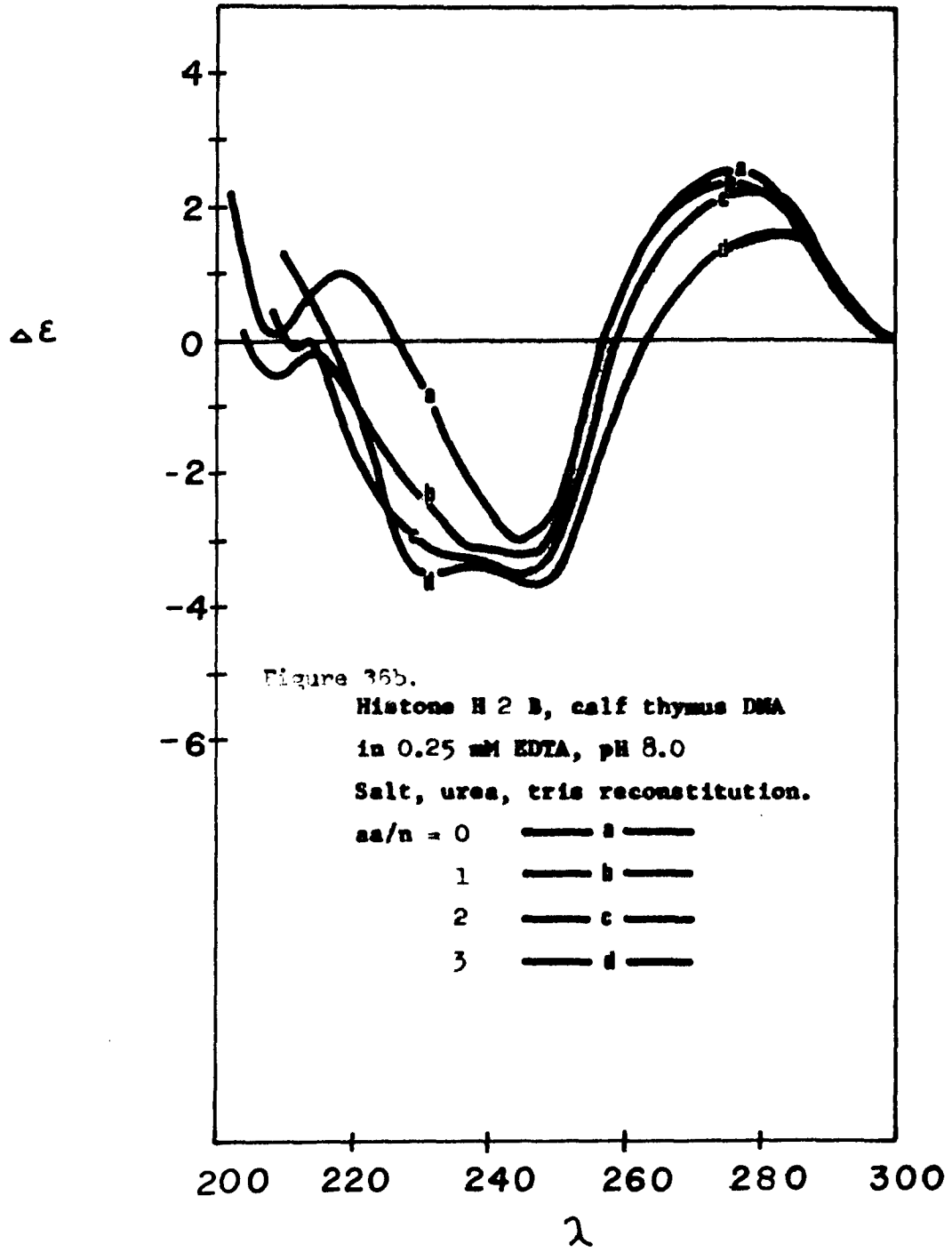
hydrophobicity for G+C pairs and stronger stacking interactions. A plausible conclusion then is that the ability of the DNA to interact with regions of secondary structure in the histones determines its deformability. It is known that the regions of ordered secondary structure in histones comprise the less basic, central hydrophobic portion of these proteins. Li et al. (95) have demonstrated that it is the less basic half of the histones responsible for both the major portion of the CD trough at 220 nm and reduction in the 275 nm peak seen in chromatin. These results support the interpretation that during reannealing the histones bind ionically upon lowering of the salt concentration and that once urea is removed the hydrophobic interactions between ordered histone and DNA lock the complex into its final conformation.

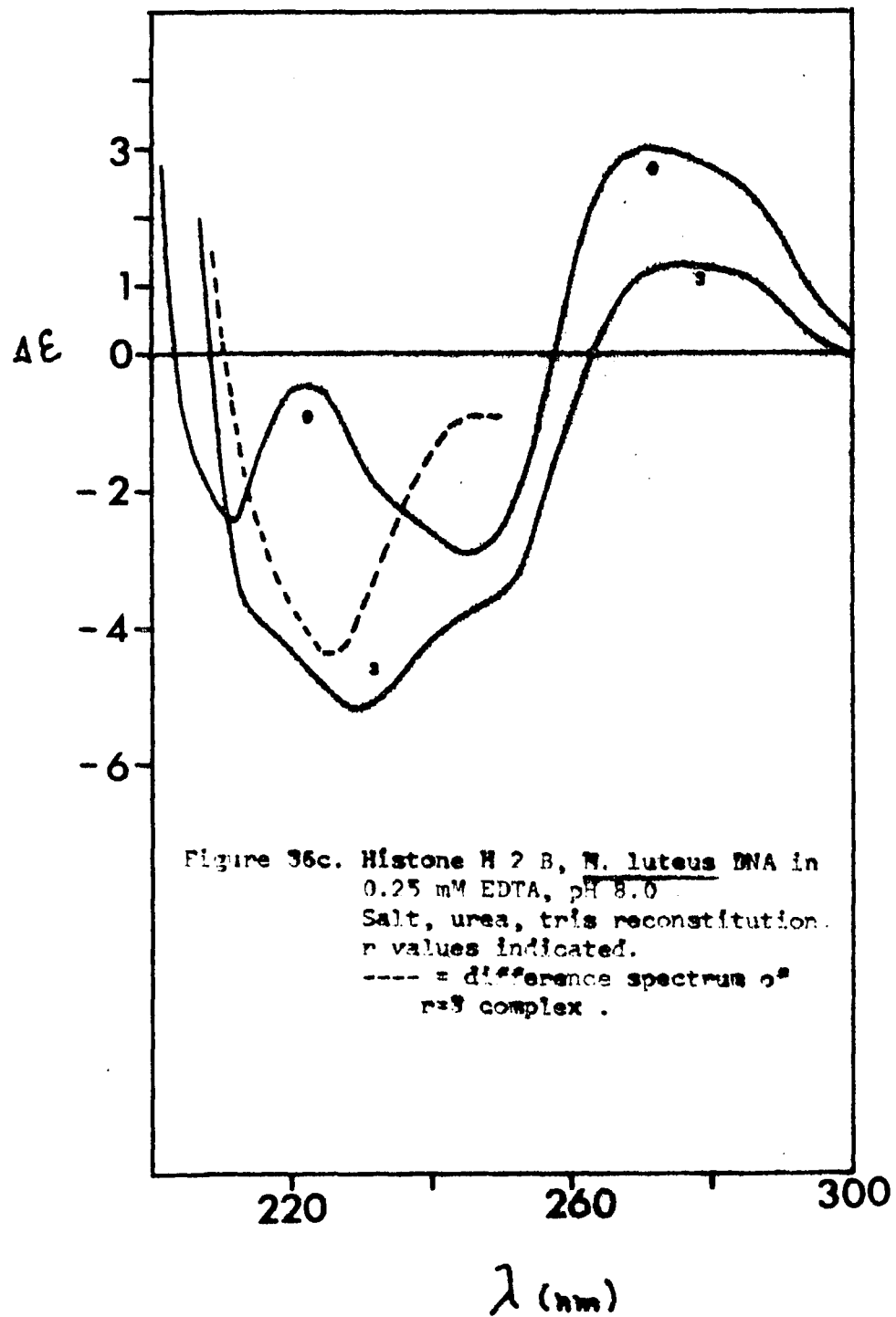
When H2A is complexed without urea to calf DNA (Figure 35) the slope of the line in Figure 34a becomes more negative, relative to the plus-urea calf DNA complex. In this reconstitution the histone H2A is in high salt prior to mixing with the DNA. This strengthens the hydrophobic histone-histone interaction so that these regions of secondary structure are less available for DNA binding and so cause less deformation per  $\Delta\epsilon_{220}$  unit. The difference spectrum of Figure 35 indicates that the type of secondary structure is the same as observed in Figure 32, however the relative amplitude is enhanced as would be anticipated if the histones are allowed to interact under conditions of high ionic strength while free in solution.

The CD spectra of histone H2B complexes are presented in Figure 36. The data of Figure 36b, when plotted as  $\Delta(\Delta\epsilon_{220})$  vs.  $(-\Delta\epsilon_{278}/\Delta\epsilon_{246})$  again reveal the linear relationship between secondary structure and the B to C transition (Figure 37). Also, the trend of increasing deform-









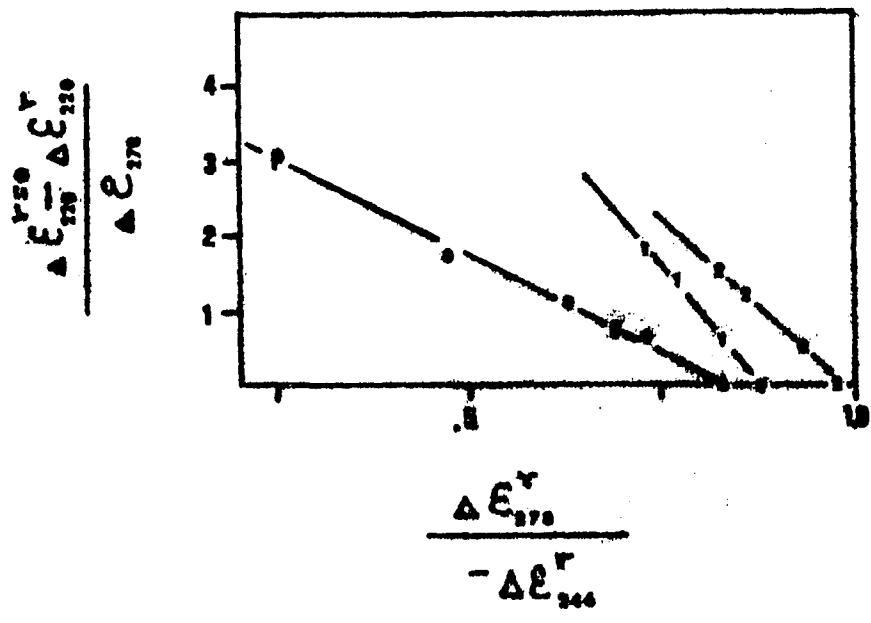
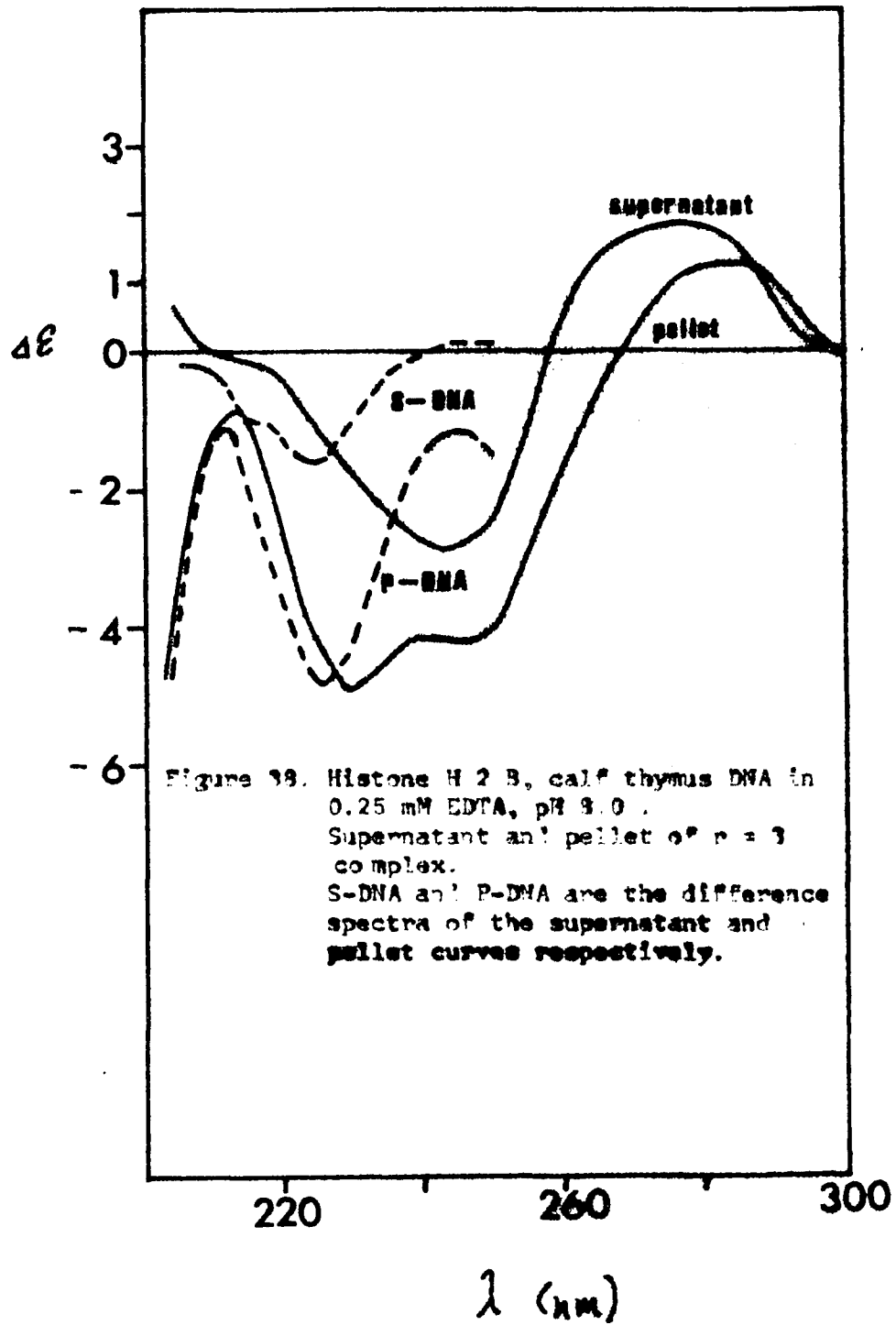


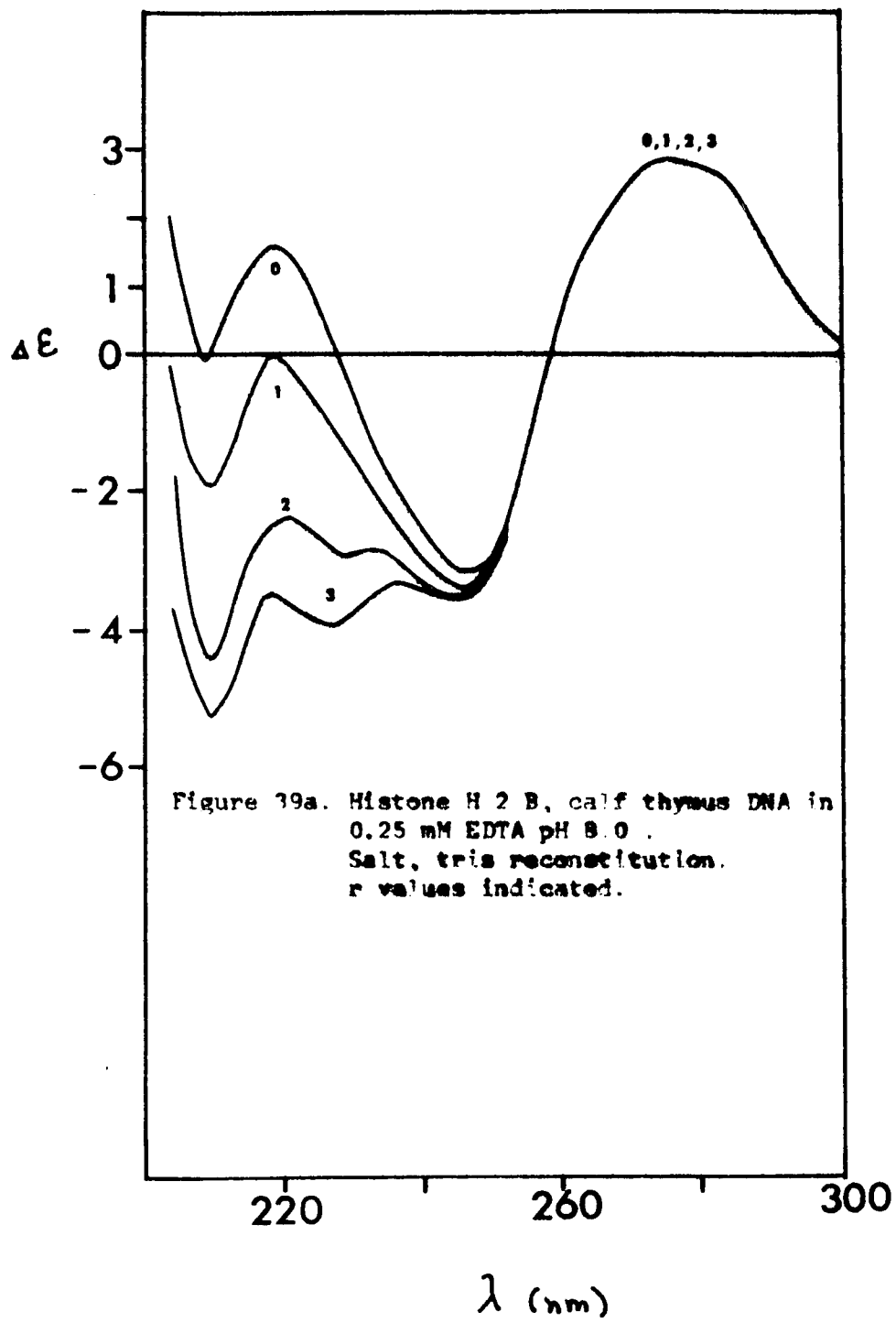
Figure 97. Deformability of histone H 2 B nucleohistones.

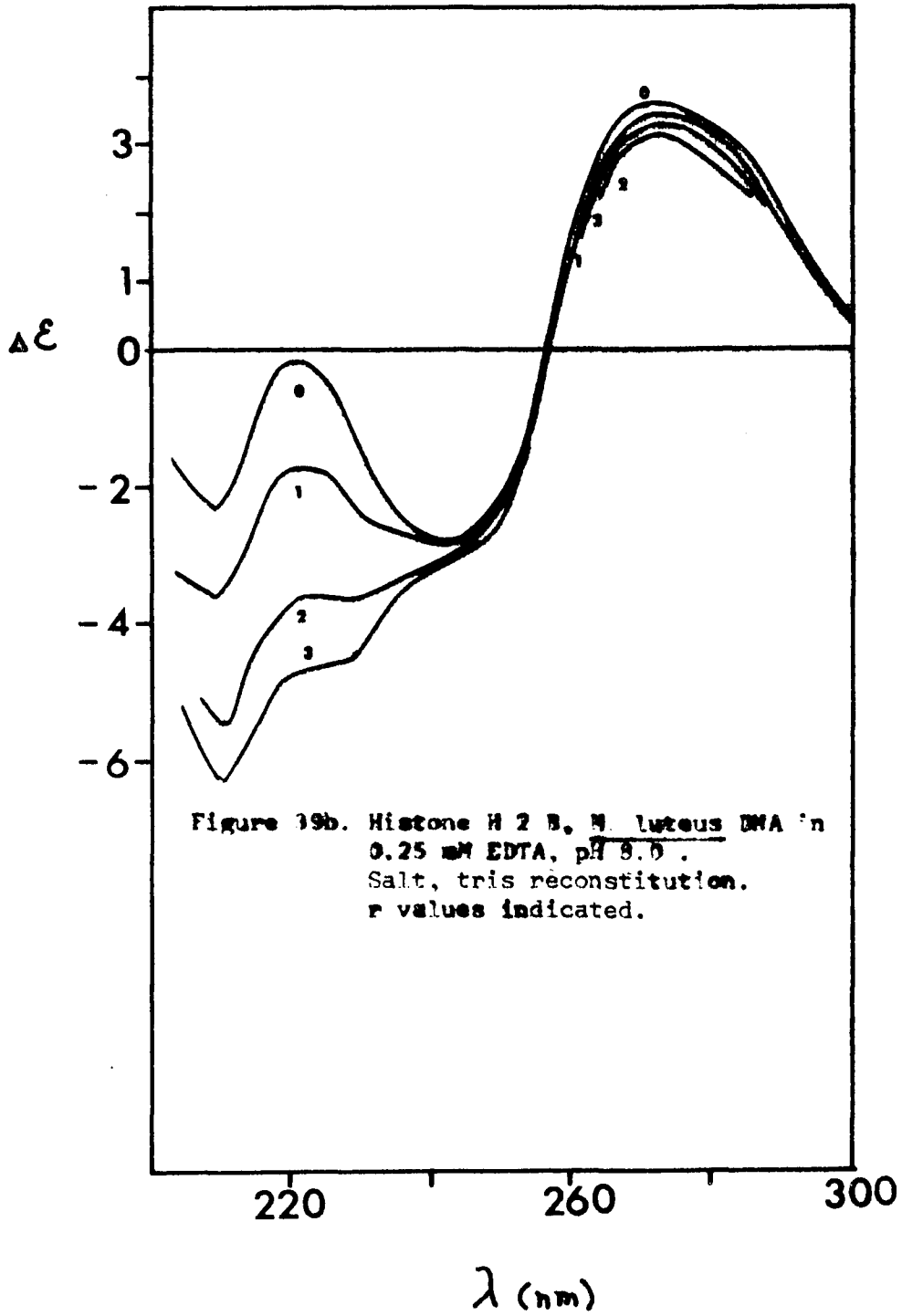
- $5.4 \pm .5$  ... curve 0 = calf thymus DNA, salt, urea, tris reconstitution.  
( s = supernatant, p = pellet )
- $13 \pm 1$  ... curve 1 = calf thymus DNA, salt, tris reconstitution.
- $11 \pm 1$  ... curve 2 = N. luteus DNA, salt, tris reconstitution.

ability with increasing G+C content is recognizable (Figure 36). Since full complexes of C<sub>l</sub>. perfringens and M. luteus DNAs (r=0, 1, 2, 3) were not analysed, a quantitative plot as in Figure 34b is not attempted. (The deformability data can be calculated, however. See Table 4 and the discussion of Figure 41.

If the H2B - calf DNA complex (r=3) is centrifuged (10,000 g, 30 min) the original complex may be separated into two fractions, supernatant and pellet. From thermal denaturation profiles (66) it has been shown that the pellet has more and the supernatant less histone bound. This is observable in the CD spectra as well (Figure 38). The supernatant curve resembles that of free DNA more closely than does the pellet spectrum, which shows decreased amplitude at 278 nm and red shifts of  $\lambda_{\max}$  and  $\lambda_c$ . As expected, the values of  $\Delta(\Delta\epsilon_{220})$  vs.  $(-\Delta\epsilon_{278} / \Delta\epsilon_{246})$  for both supernatant and pellet fall on the line for the original complex. The slope of this line is -5.5 for H2B, which compares well with the slope of -5.4 for H2A - calf DNA complexes. This result agrees with the reports of Li et. al. (95) and Wilhelm et. al. (81) that all histones except H1 are equivalent in their effect on DNA conformation. When H2B - DNA complexes are reconstituted in the absence of urea (Figure 39) the deformability ( $m_d$ ) of the DNA decreases (Figure 37), as with H2A - DNA complexes. The G+C - rich M. luteus DNA is still more susceptible to the B to C transition than the calf DNA. In these minus - urea complexes the slope of the deformability plot ( $m_d$ ) (Figure 37) for H2B - calf DNA is no longer equal to the slope for H2A - calf DNA complexes reconstituted without urea (Figure 34a). This apparently reflects the different tendencies of H2A and H2B to self - interact in the strongly polar reconstitution medium.

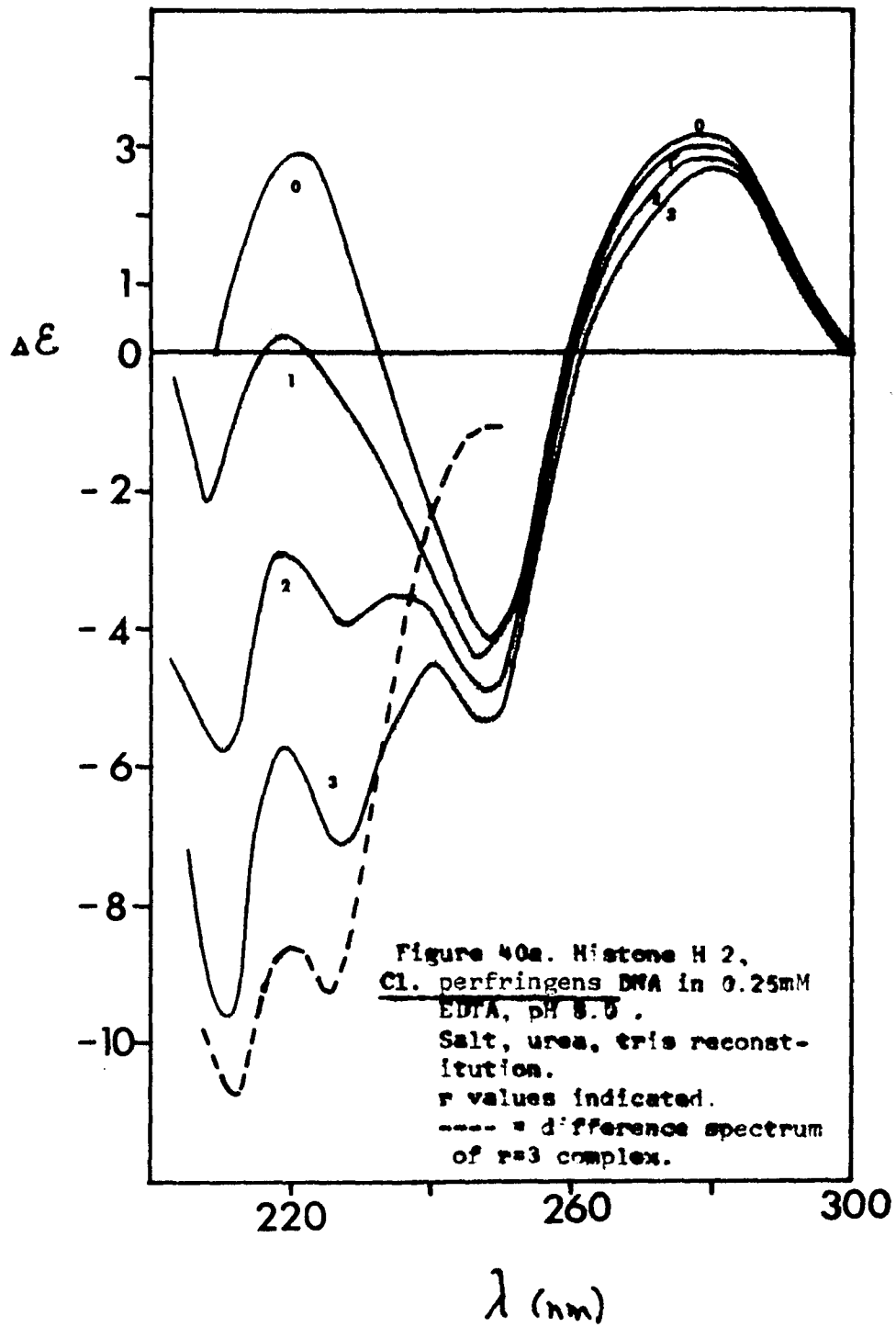


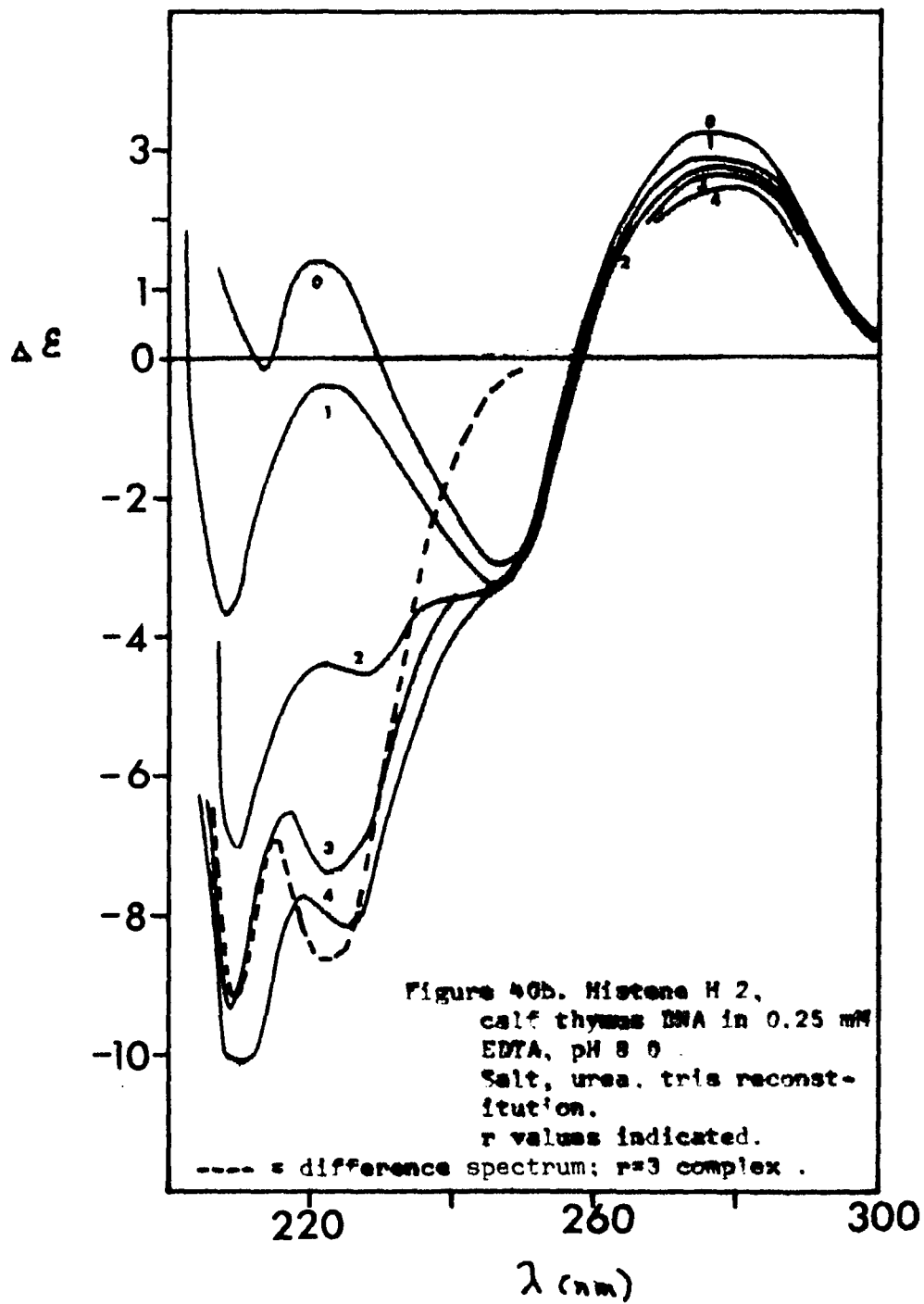


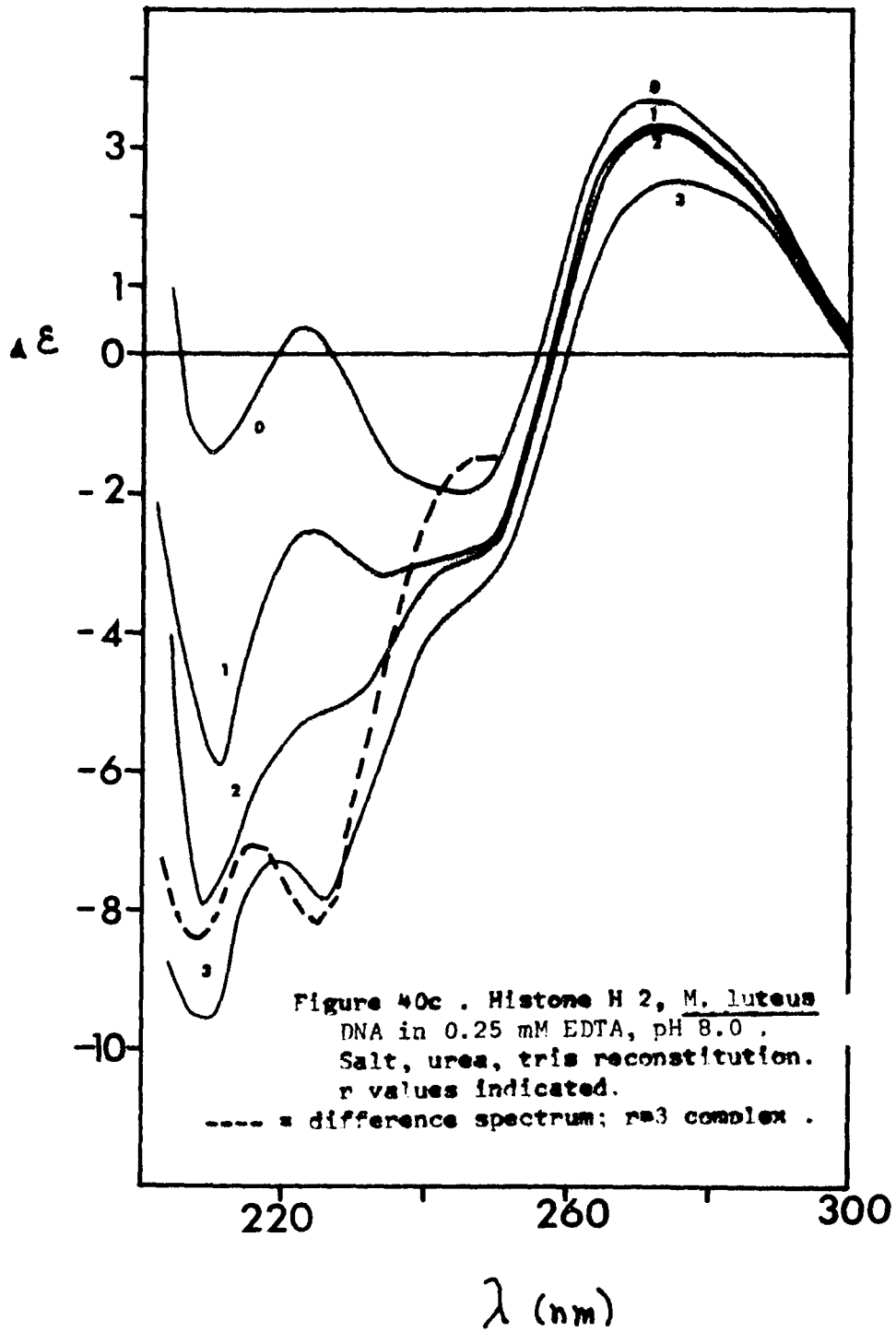


Histone H 2 , an equimolar mixture of H 2 A and H 2 B, yields the CD spectra of Figure 40 when reconstituted to DNA in the presence of salt and urea. The difference spectra of these complexes now appear to contain a substantial amount of random coil in addition to alpha helix (compare Figure 33). When  $\Delta(\Delta\epsilon_{220})$  is plotted vs.  $(-\Delta\epsilon_{278}/\Delta\epsilon_{246})$  (Figure 41) the slope ( $m_d$ ) of the calf DNA line is found to equal  $11.0 \pm 1$ . This is in excellent agreement with the sum of the slopes of the H 2 B - calf DNA plus H 2 A - calf complexes ( $-5.5 -5.4 = - 10.9$ ). Since the contribution of each histone to the DNA deformation is presumed to be equal, this result is not surprising. Although the deformability slopes ( $m_d$ ) of H 2 B - perfringens DNA and H 2 B - luteus DNA were not calculated, it is evident that the values for the H 2 complexes with these DNAs are twice the values for the H 2 B complexes. Therefore the histone effects on these DNAs are identical to their effects on calf DNA. Also, the linear relation between  $m_d$  and the G+C content is the same as with histone H 2 B. As observed previously, the minus - urea histone H 2 - calf DNA complex (Figure 42b) shows less deformability than the plus - urea complex (Figure 41).

When phosphate buffer (5 mM) is substituted for tris in the reconstitution medium (Figure 43) a change in the CD difference spectrum of the H 2 - calf DNA complex is observed. The negative peak above 220 nm is deepened while the companion peak between 210 nm - 215 nm shifts to more positive values. By comparison to Figure 33 this change appears to represent a slight enhancement of the amount of beta structure at the expense of the random coil of helical content. Figure 47 illustrates that the slope of the deformability plot for this complex has a value  $m_d = 8.9 \pm 0.3$ . This indicates that during salt - urea - phos-







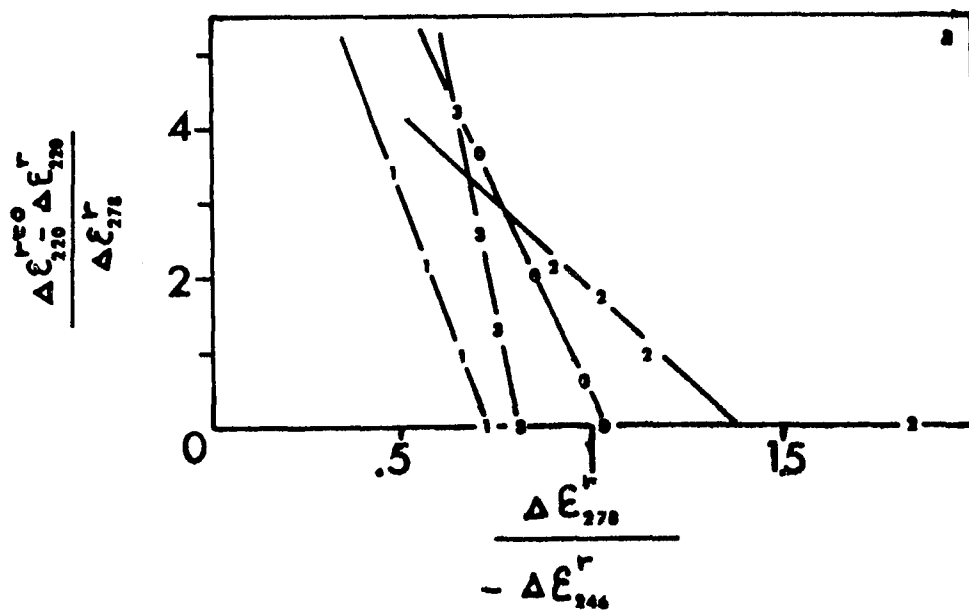


Figure 41. Deformability of histone H2 complexes.

a.

0 = calf thymus DNA; salt, urea, tris reconstitution

1 = *Cl. perfringens* DNA; salt, urea, tris reconstitution

2 = *M. luteus* DNA; salt, urea, tris reconstitution

3 = calf thymus DNA; salt, tris reconstitution

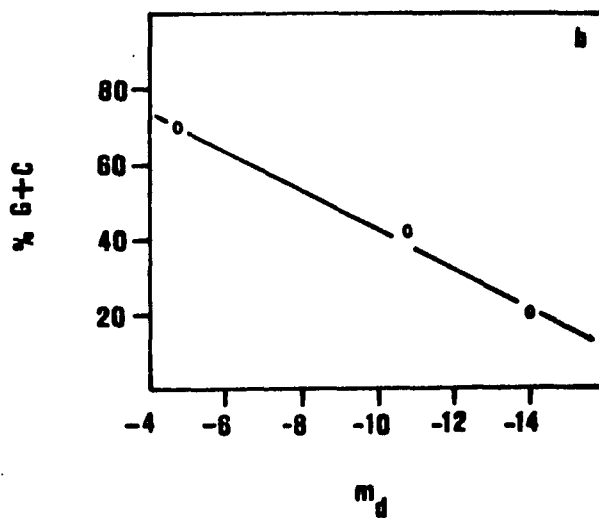
$m_d =$

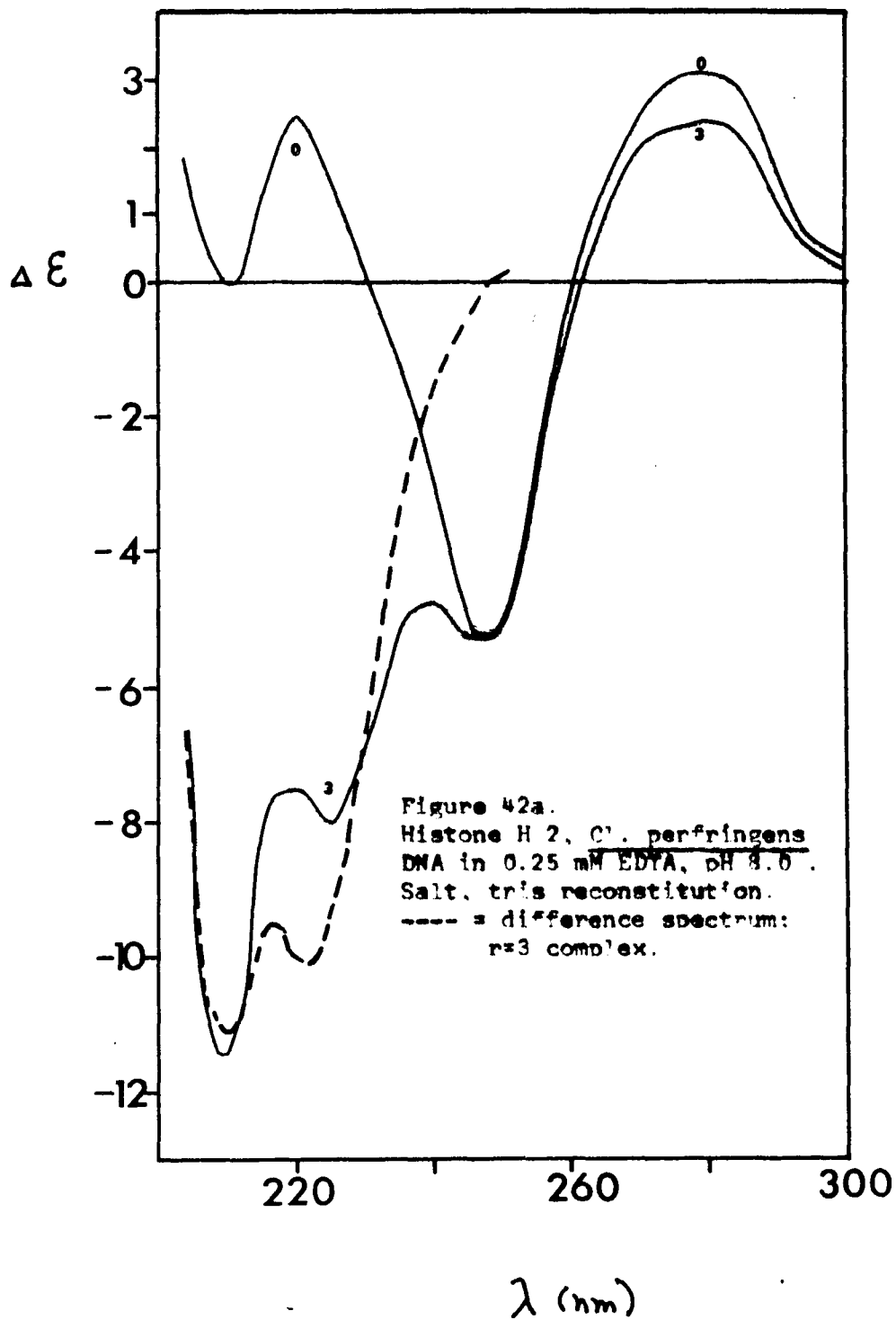
$-11 \pm 1$

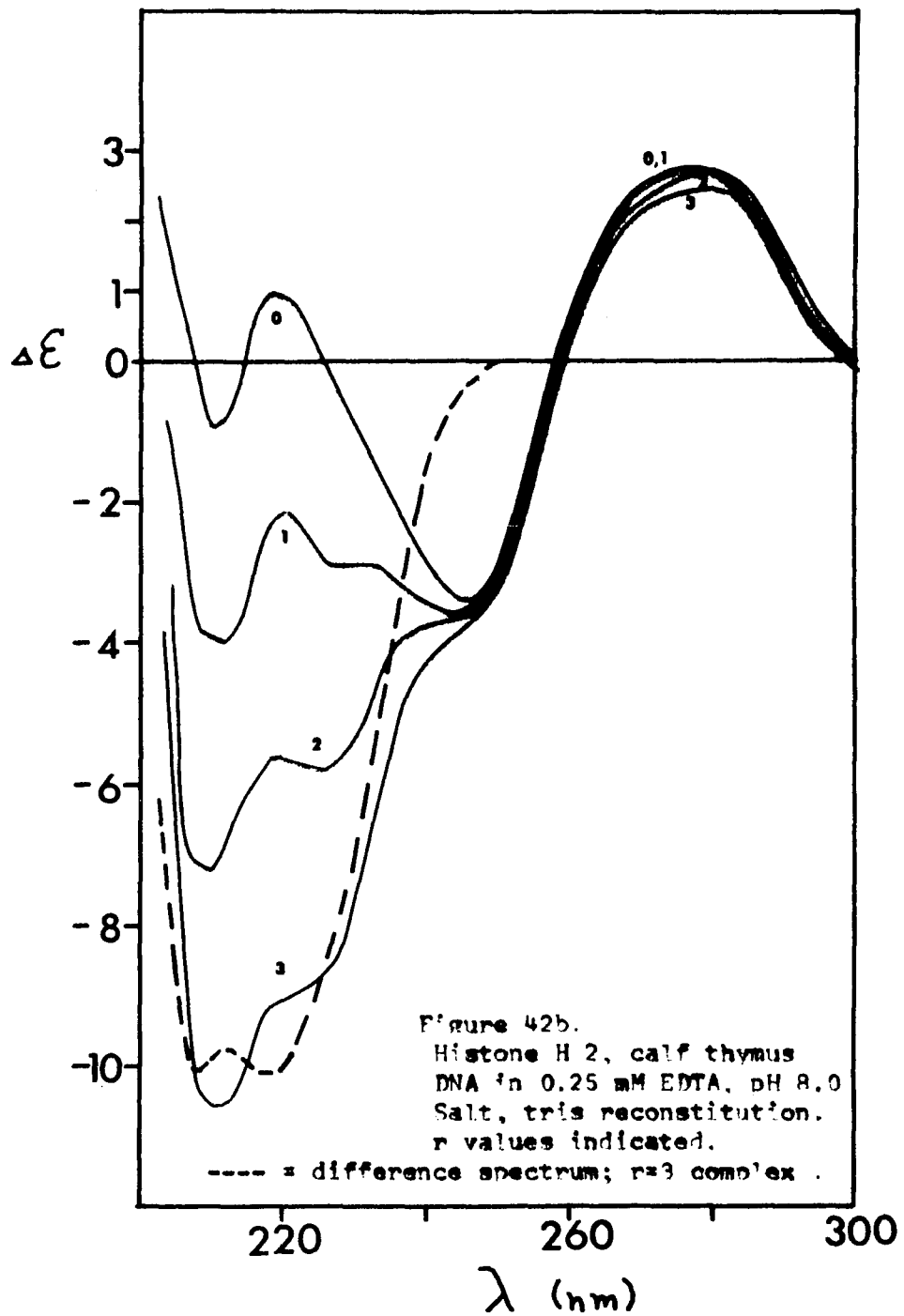
$-14 \pm 2$

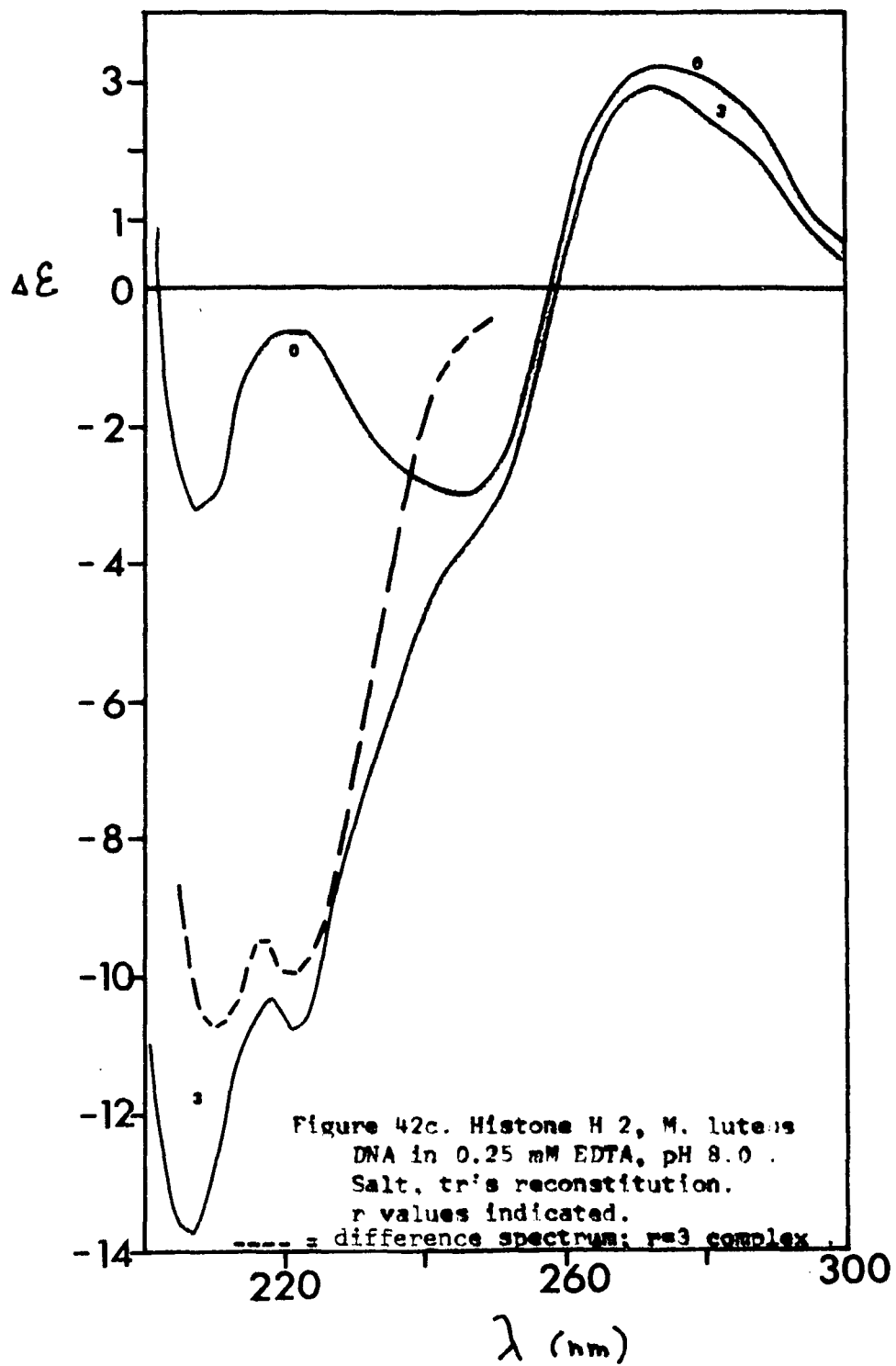
$-4.8 \pm .5$

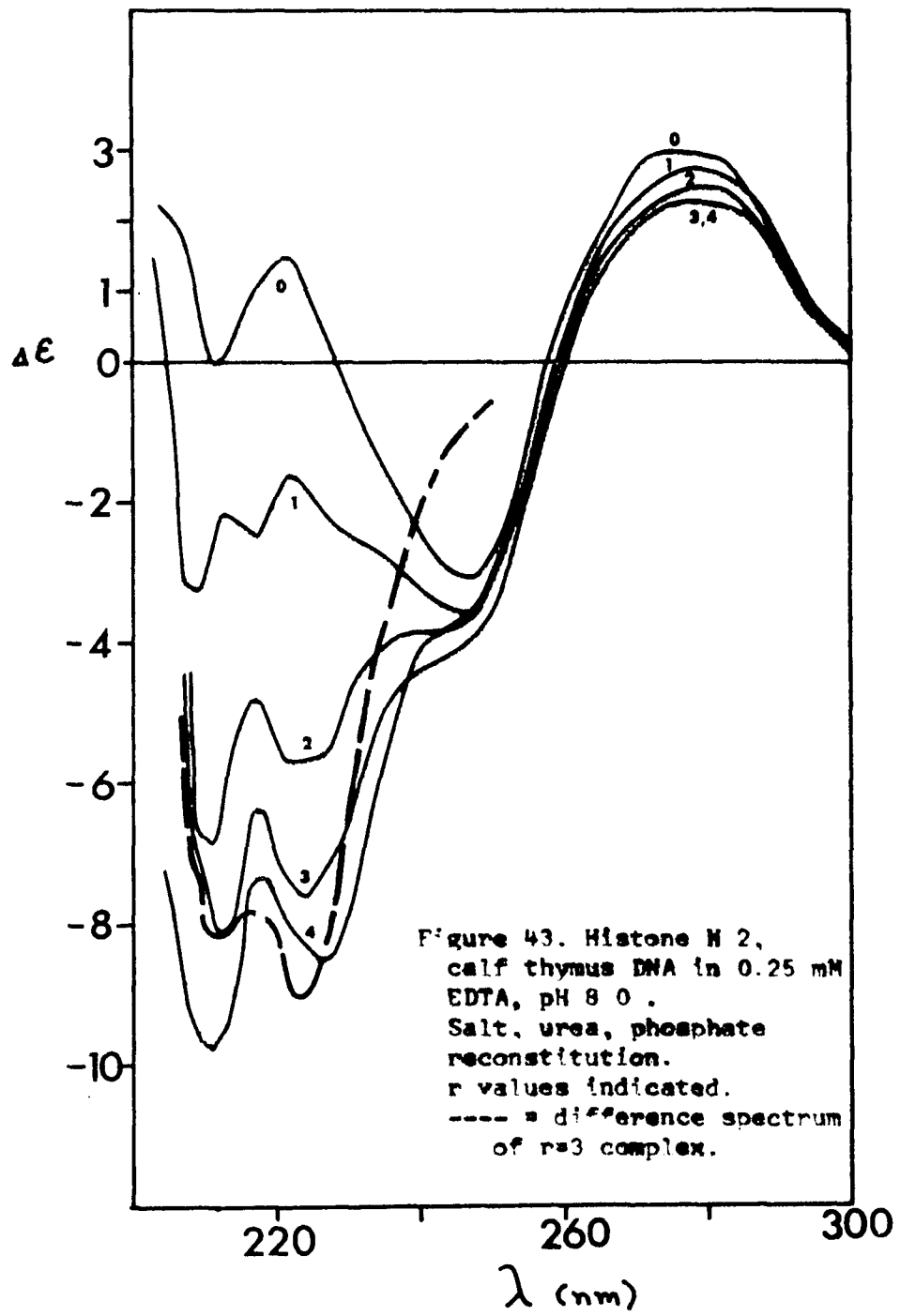
$-24 \pm 3$









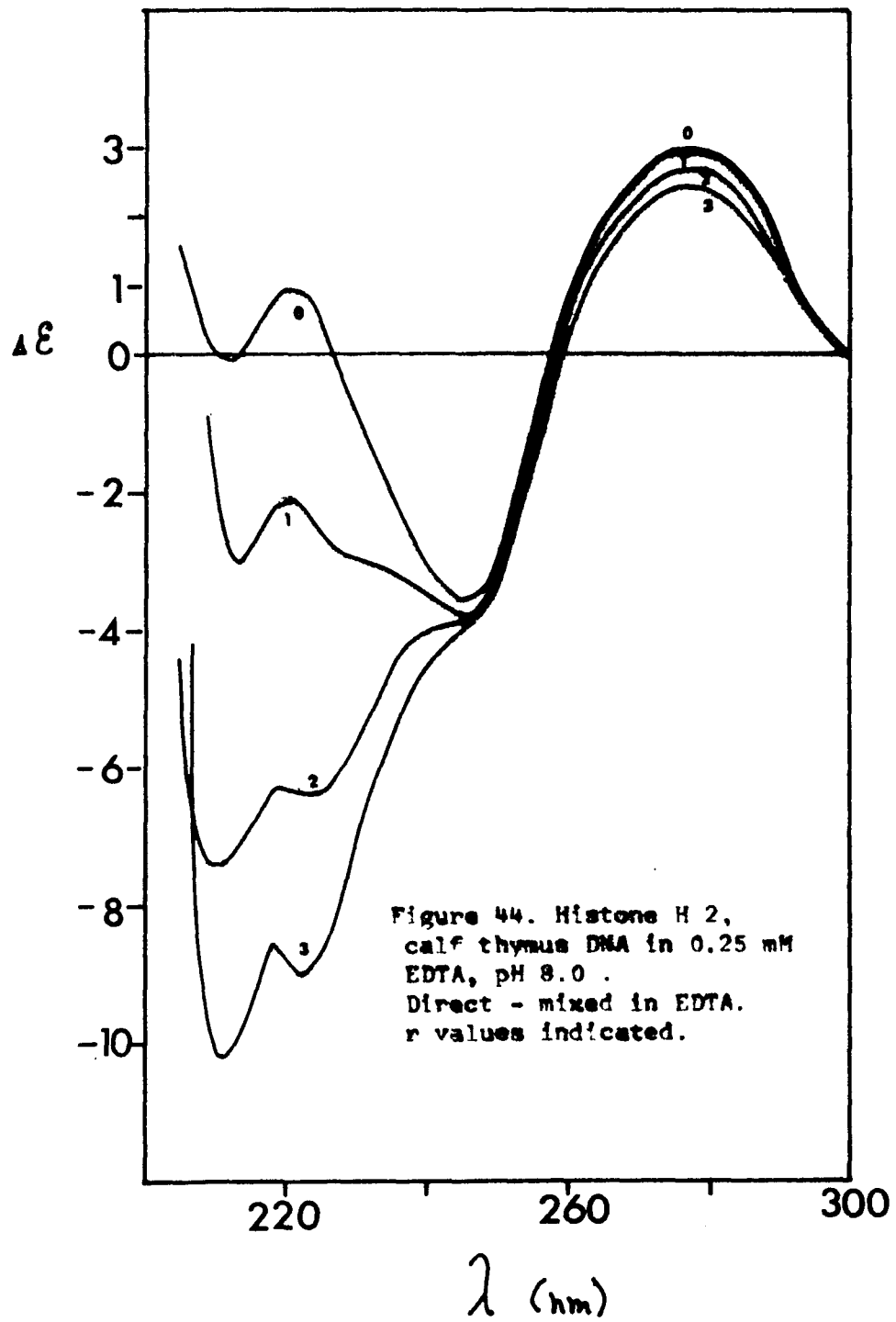


phate reconstitution the phosphate buffer enhances the secondary structure of the histone so as to increase its effect on the DNA conformation.

The spectra of H2 - calf DNA complexes ( $r=3$ ) presented in Figures 40b, 42b and 43 each closely resemble the CD spectrum of purified nucleohistone in shape,  $\lambda_{\max}$  and  $\lambda_c$  (95, 107). This similarity is quantitative in the protein conformation region (below 250 nm), however, the reduction of the DNA amplitude, which is greatest in the phosphate complexes (Figure 43) yields a value of  $\Delta\epsilon_{278} / -\Delta\epsilon_{246} = 0.54$  while  $\Delta\epsilon_{278} / -\Delta\epsilon_{246} = .33$  for chromatin (95). Therefore, while the slightly lysine - rich histone pair H2A+H2B is able to assume the general protein conformation seen in chromatin other agents must be responsible for the further distortion of the DNA structure.

When histone H2 and calf DNA are mixed directly at low ionic strength ( $2.5 \times 10^{-4}$  M EDTA) the CD spectra of the complex (Figure 44) show only small distortion of the B type CD. In this complex the interactions are expected to be primarily ionic in nature. The conformation of the histone immediately prior to complexing (Figure 45) is predominantly random coil. After complexing the difference spectrum of the  $r=3$  complex (Figure 46) appears to be a type of deformed alpha-helix, possibly due to the conformational constraints imposed on the histone by its binding along a particular path around the DNA helix. Figure 47 shows that this complex has a deformability slope  $m_d = -35 \pm 10$  indicating a very small effect of the hydrophobic residues on the DNA conformation.

When the same histone and DNA are each dissolved in 0.15 M NaCl - NaEDTA prior to complexing the resulting nucleoprotein complex has a



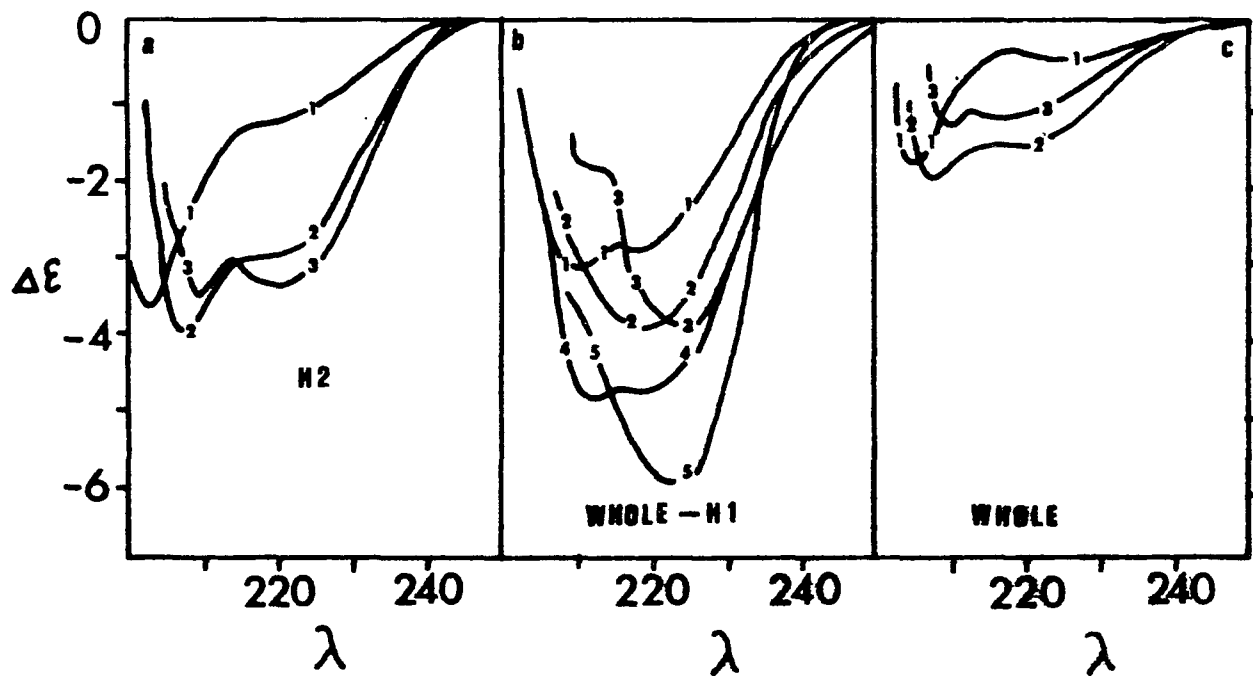


Figure 45. CD Spectra of histones in solution

Legend appears on page 128a.

Figure 45. CD spectra of histones in solution

H2

1 = in H<sub>2</sub>O

2 = in EDTA or .15 M NaCl, EDTA

3 = in 1 M or 2 M NaCl, .01 M tris, pH 8.0

Whole - H 1

1 = in EDTA, after dialysis from 5 mM phosphate

2 = in 0.15 M NaCl / EDTA

3 = in 0.15 M NaCl / EDTA, after 24 hr.

4 = in EDTA

5 = in .15 M NaCl / EDTA, after dialysis from 5 mM phosphate

Whole

1 = in EDTA, after dialysis from .15 M NaCl / EDTA

2 = in 0.15 M NaCl / EDTA

3 = in 0.15 M NaCl / 5 mM phosphate / EDTA

(in all cases EDTA refers to a solution of  
0.25 mM EDTA, pH 8.0)

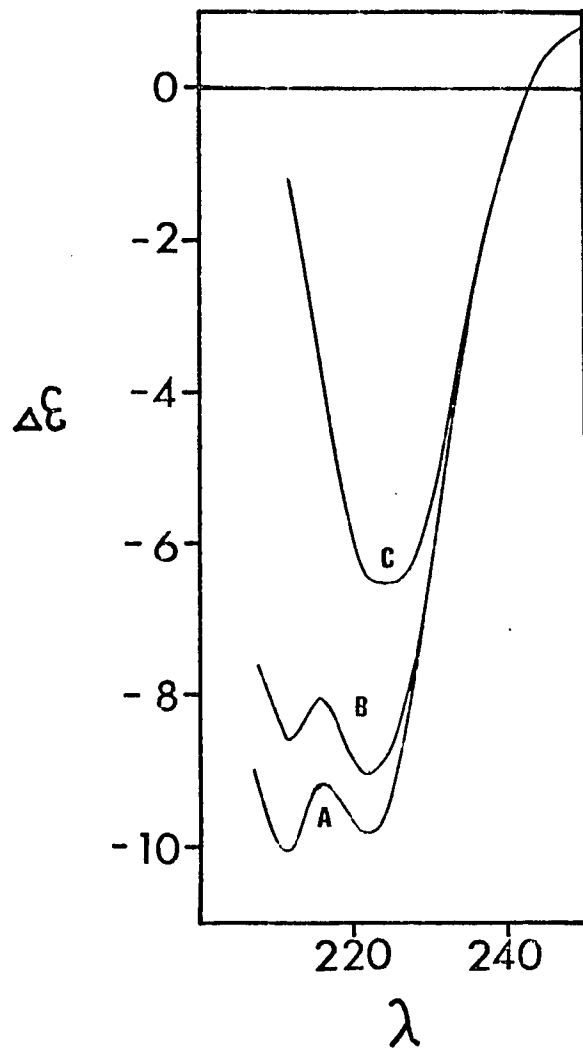


Figure 46. CD difference spectra of histone H2 - calf thymus nucleohistones.

A = direct - mixed in 0.25 mM EDTA

B = direct - mixed in 0.25 mM EDTA / .15 NaCl (postdialysis)

C = direct - mixed in 0.25 mM EDTA / .15 M NaCl (predialysis)

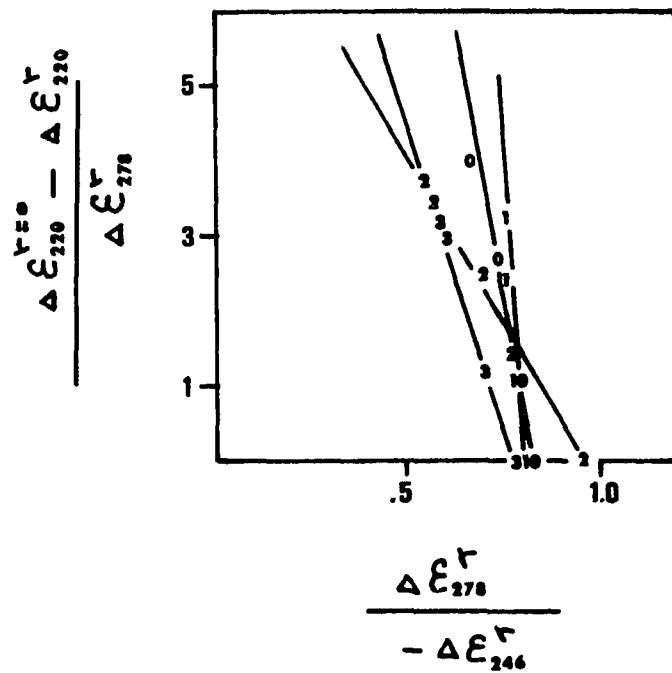


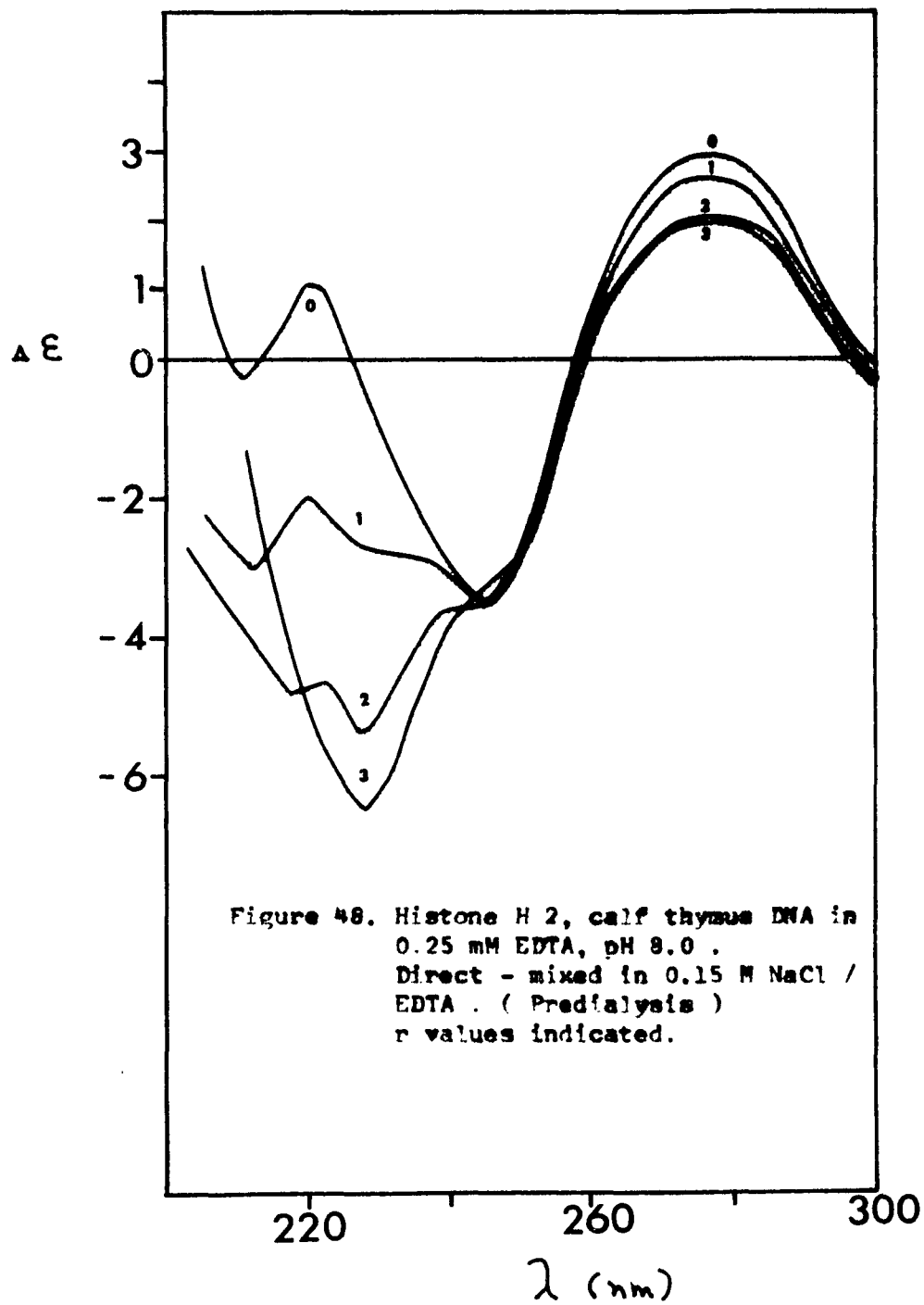
Figure 47. Deformability of histone H 2, calf thymus DNA nucleohistones.

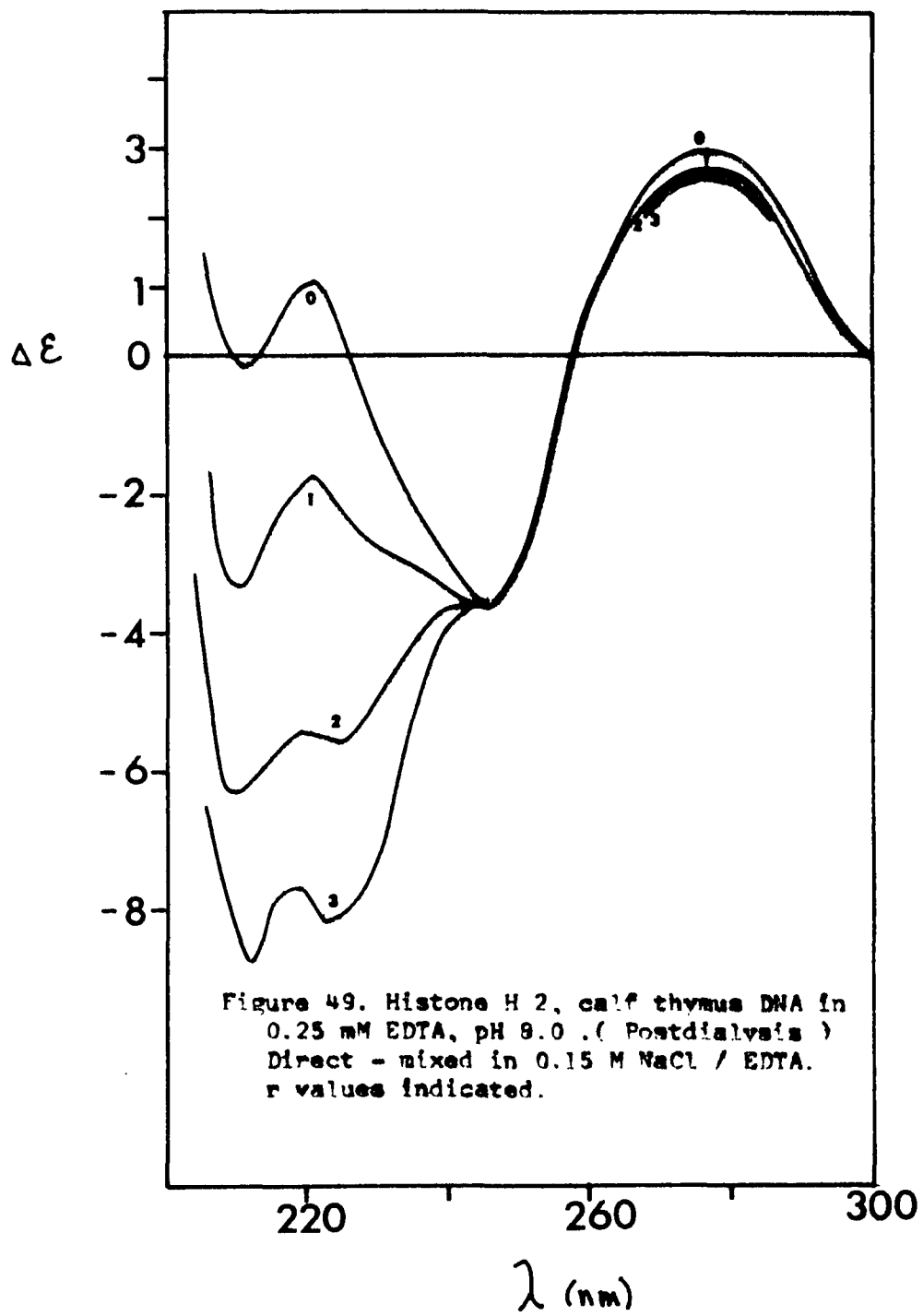
- curve 0 = direct - mixed in EDTA .....  $\frac{m_d}{-} = 35 \pm 10$
- curve 1 = direct - mixed in 0.15 M NaCl / EDTA...-  $83 \pm 20$   
( postdialysis )
- curve 2 = salt, urea, phosphate reconstitution...-  $9 \pm 1$
- curve 3 = direct - mixed in 0.15 M NaCl / EDTA ....-  $15 \pm 2$   
( predialysis )

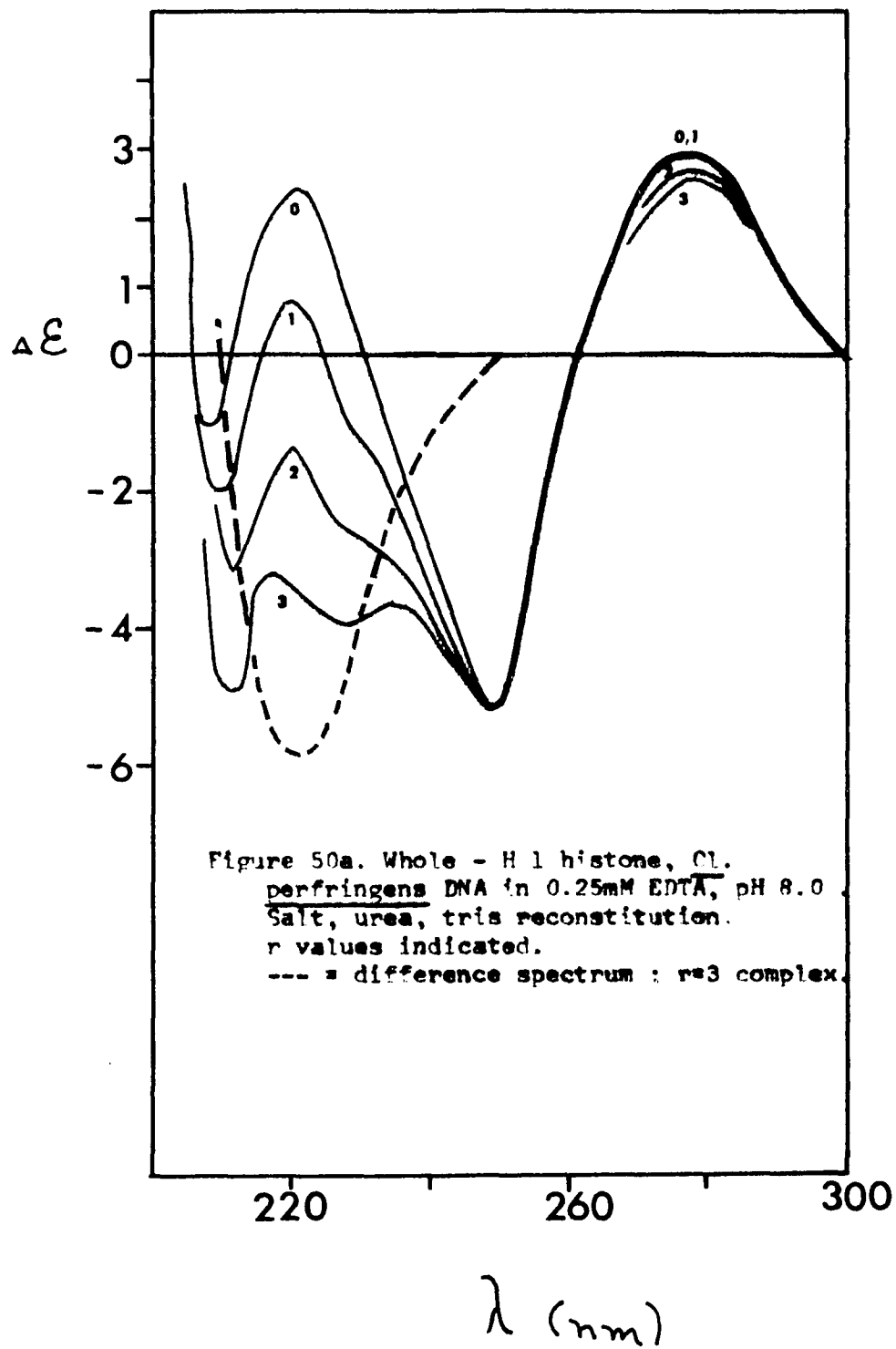
drastically different shape (Figure 48) compared to the direct - mixed complex without salt (Figure 44). Although the initial histone conformation is the same for both complexes (Figure 45) the effect of salt is to increase the hydrophobic nature of the histone - DNA interaction. The difference spectrum of this complex before the NaCl is dialysed away (Figure 46) demonstrates that the histone conformation contains mainly ordered secondary structure, i.e.,  $\alpha$ -helix and beta sheet (compare Figure 33). Once this complex is dialysed to  $2.5 \times 10^{-4}$  M EDTA, the structure of the complex changes back towards the B form, accompanied by a loss of beta conformation in the protein (Figure 49). This result agrees with the report of Shih and Fasman (108b) that complexes reconstituted to final ionic strength of 0.15 M NaCl reverted to a less distorted structure (towards B form) when dialysed against a low ionic strength buffer.

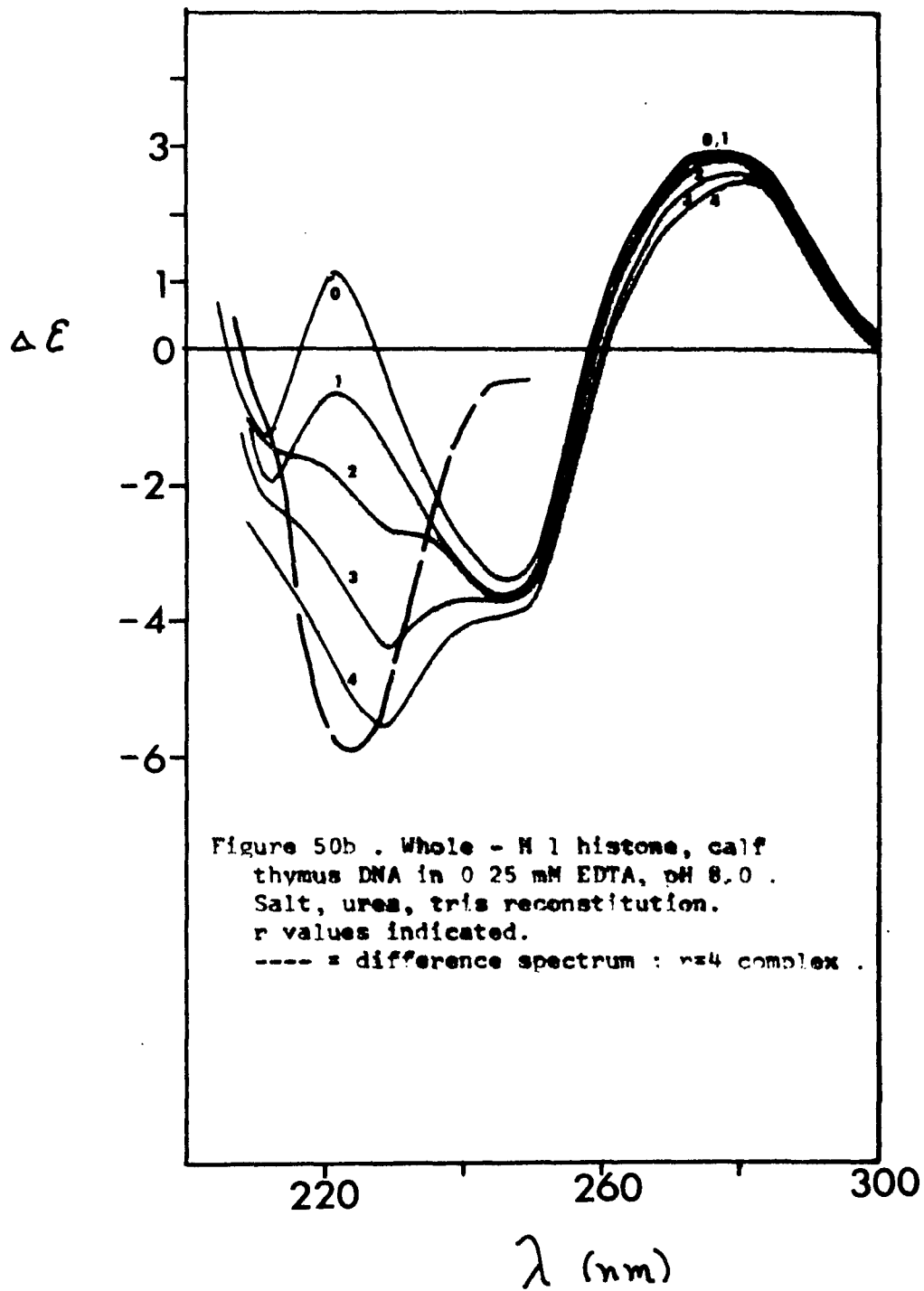
Figure 46 shows that the conformation of the protein in the salt - EDTA direct - mixed complex after dialysis to low ionic strength is similar to that of the protein when mixed with DNA at low ionic strength directly. The effect of these histones on the deformability of the DNA is comparable (Figure 47) while the histones in the salt - EDTA complex before dialysis have a higher deformability slope,  $m_d = -15 \pm 2$ .

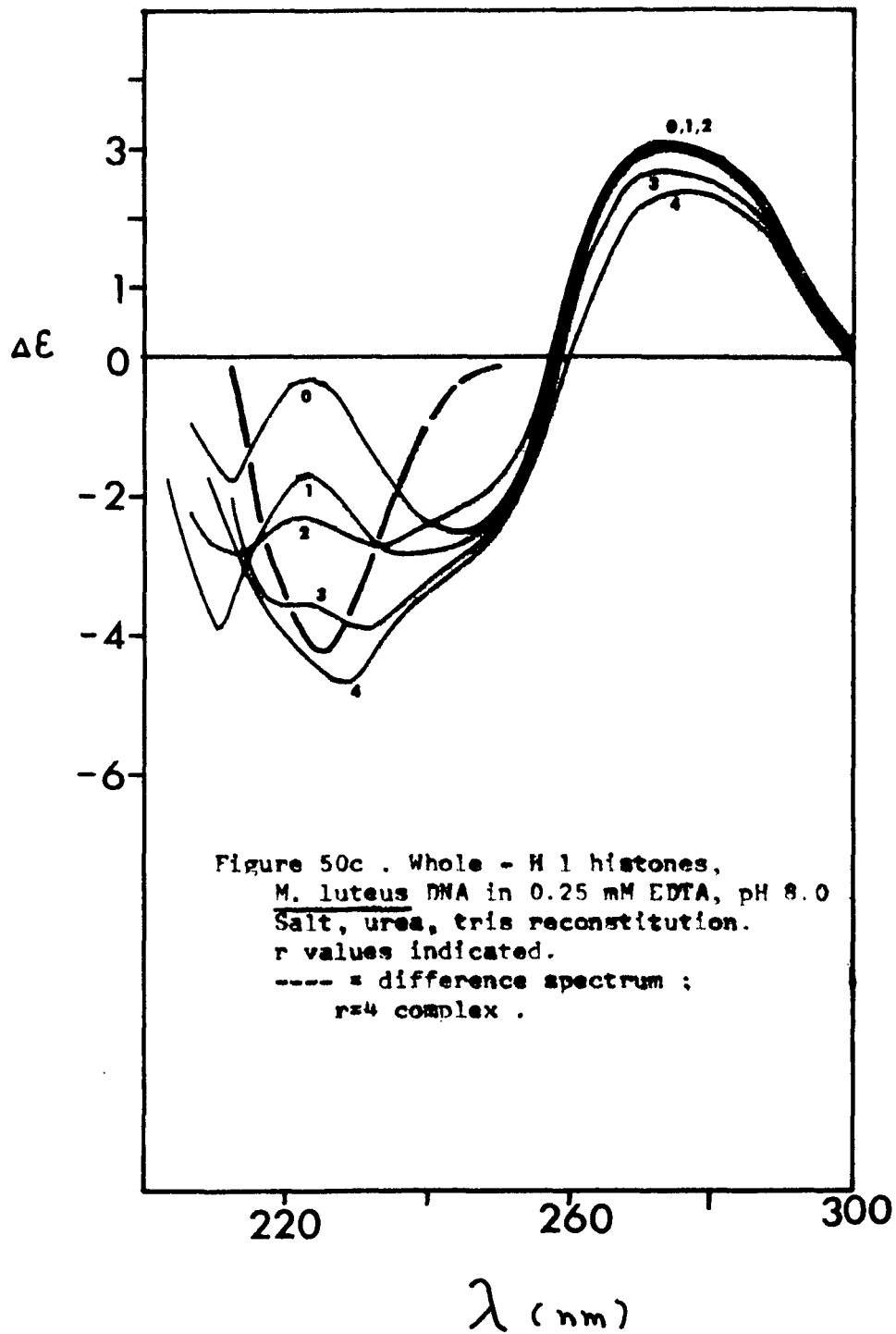
Figure 50 presents the CD spectra of complexes of whole histone depleted of histone H1 (whole - H1) with DNA. In contrast to the difference spectra of the histone H2 - DNA complexes (Figure 40) the histone conformation in these complexes shows relatively more beta structure. The deformability plots (Figure 51) show the same trend; with increasing G+C content, increased deformability. The values of











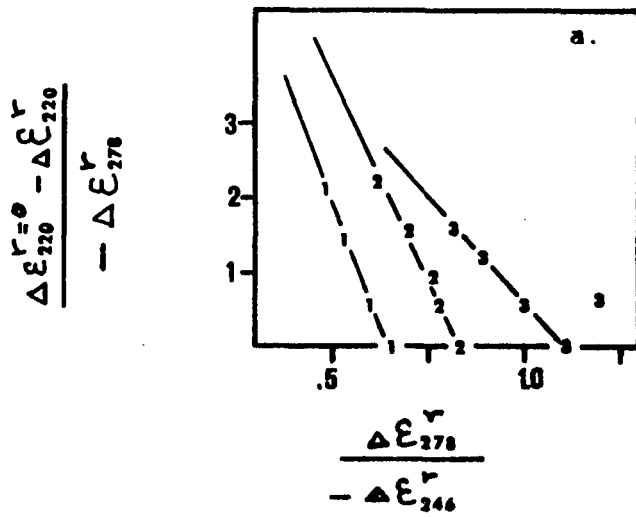
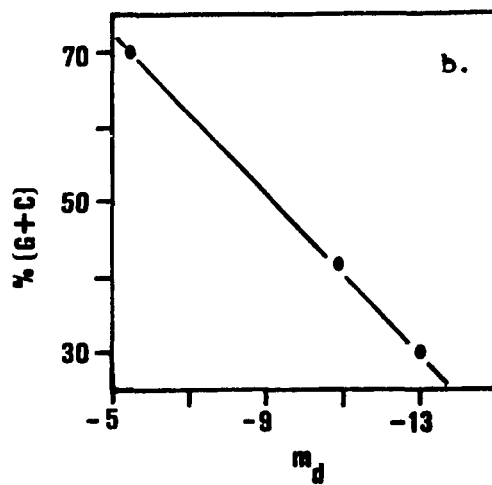


Figure 51.

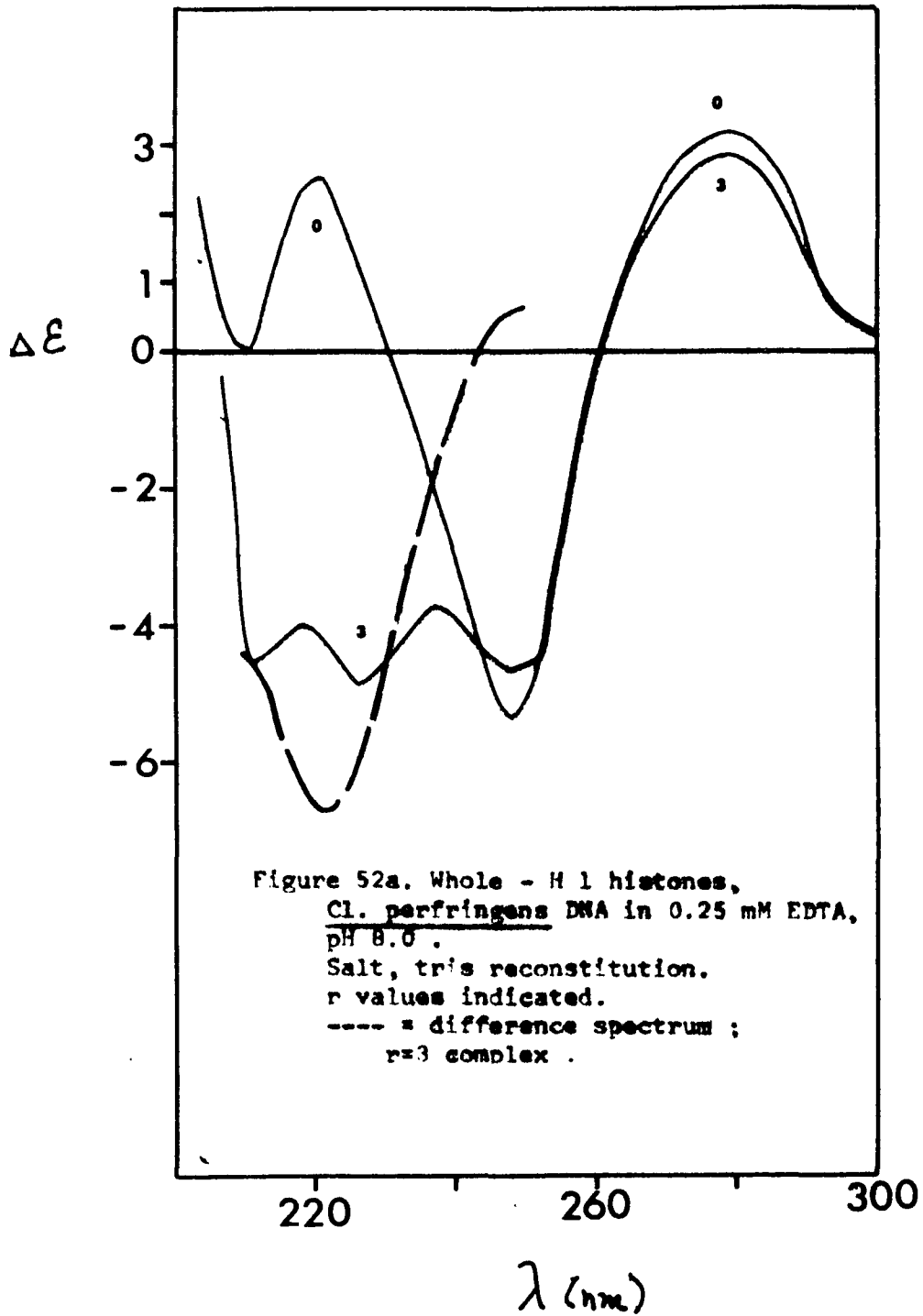
a. Deformability of whole - H 1 histone nucleohistones,  
Salt, urea, tris reconstitutions.

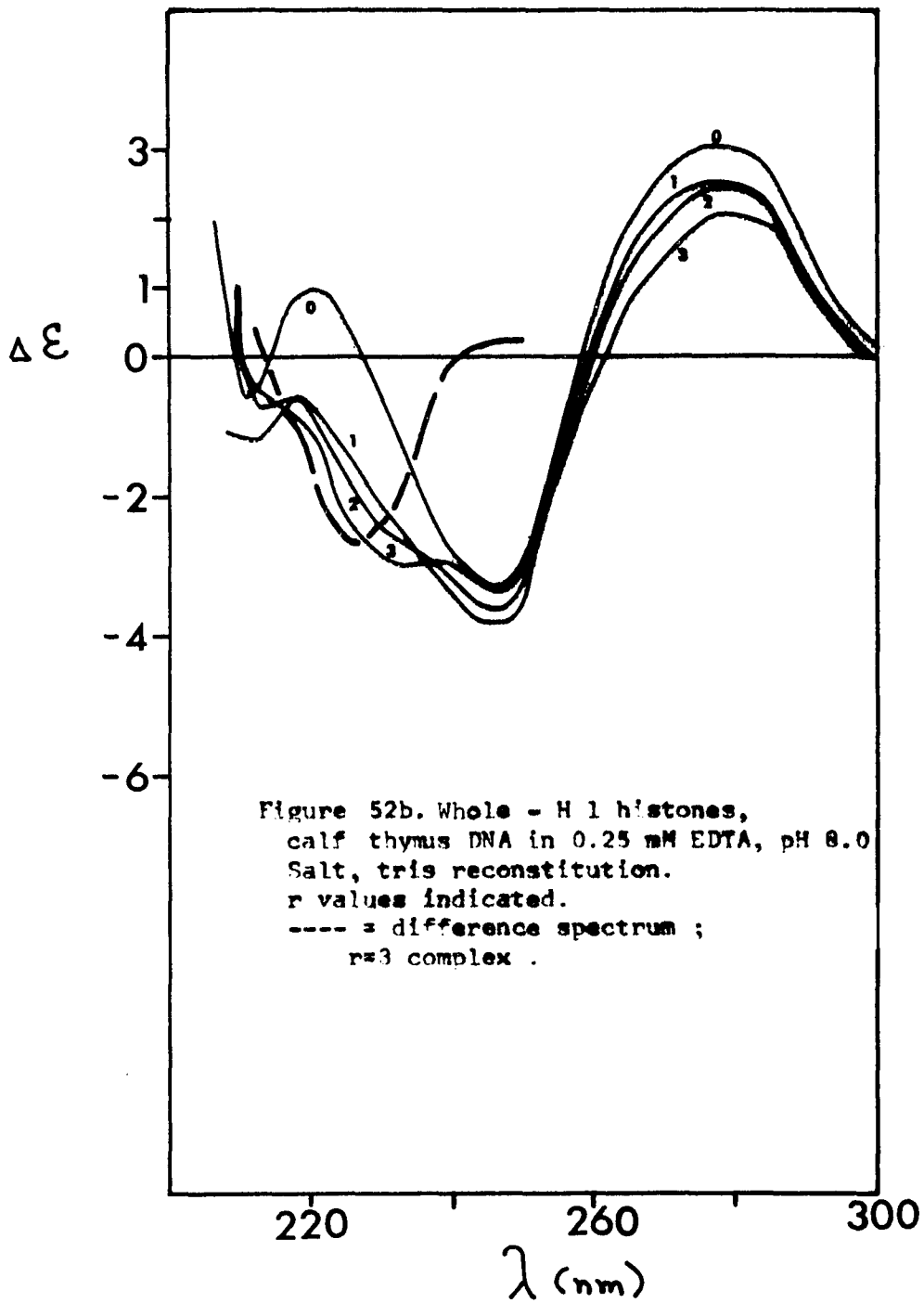
	$\underline{m_d}$
curve 1 = <u>Cl. perfringens</u> DNA .....	- 13 ± 1
curve 2 = <u>calf thymus</u> DNA .....	- 11 ± 1
curve 3 = <u>M. luteus</u> DNA .....	- 5.5 ± .5

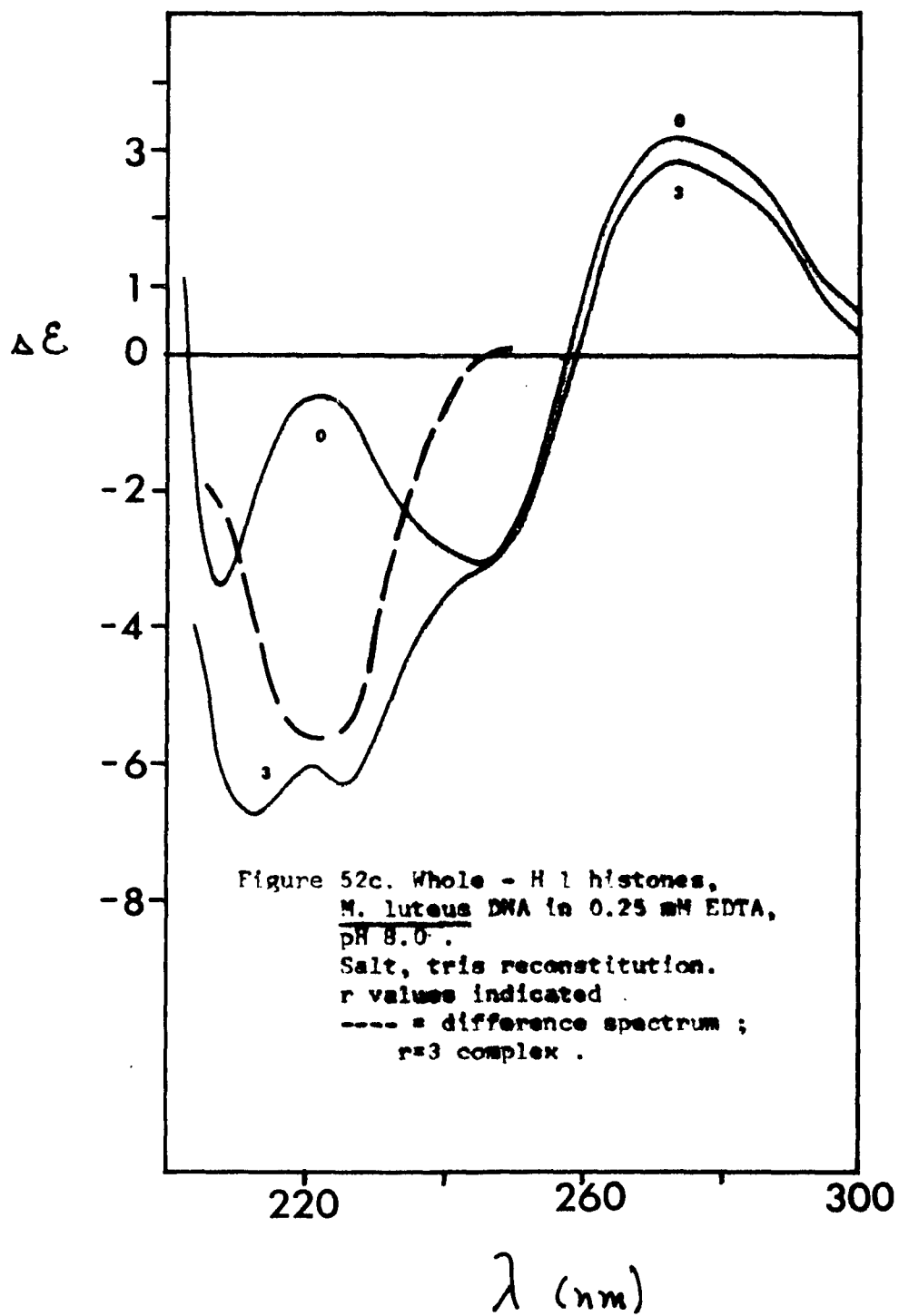


the slopes of these lines, however, are identical, within experimental error, with the comparable values for H2 complexes. Since the deformability slope ( $m_d$ ) was additive for the H2A+H2B pair, we would expect the  $m_d$  for whole-H1 to be twice as large as  $m_d$  of H2. Either the  $m_d$  values for the arginine-rich histones (H3 and H4) are zero so that  $m_{d(H2)} + m_{d(H3 + H4)} = m_{d(H2)}$  or some fraction of the hydrophobic residues in the whole-H1 unit are involved in histone-histone interaction and not in histone-DNA binding. The former alternative is dissonant with respect to the finding that each histone makes an equal contribution to the deformation of the DNA (95). This leaves us to postulate that, statistically, ca. 50% of the residues contributing to the  $\Delta\mathcal{E}_{220}$  are involved in histone-histone binding and ca. 50% in histone-DNA binding (or 50% of each hydrophobic residue interacts with other histones and 50% interacts with the DNA).

When whole histone-H1 is annealed to DNA in the absence of urea (Figure 52) the difference spectra again show beta sheet as the predominant form of secondary structure. The  $m_d$  for the calf DNA complex is  $-5.0 \pm 0.5$  (Figure 53). This represents a significant increase in the  $m_d$  value over the plus-urea complex (Figure 51,  $m_d = -11 \pm 1$ ). Whereas with H2A, H2B and H2: DNA complexes the omission of urea decreased the  $m_d$ , here the opposite effect is observed. The increase in the deformability of the DNA upon the inclusion of the arginine-rich histones in the minus-urea complex strongly points out the hydrophobic nature of the histone binding to DNA. The binding of the arginine-rich histones (H3 and H4) to DNA is known to have more hydrophobic character than the binding of the other histones (110) and the annealing of the whole-H1







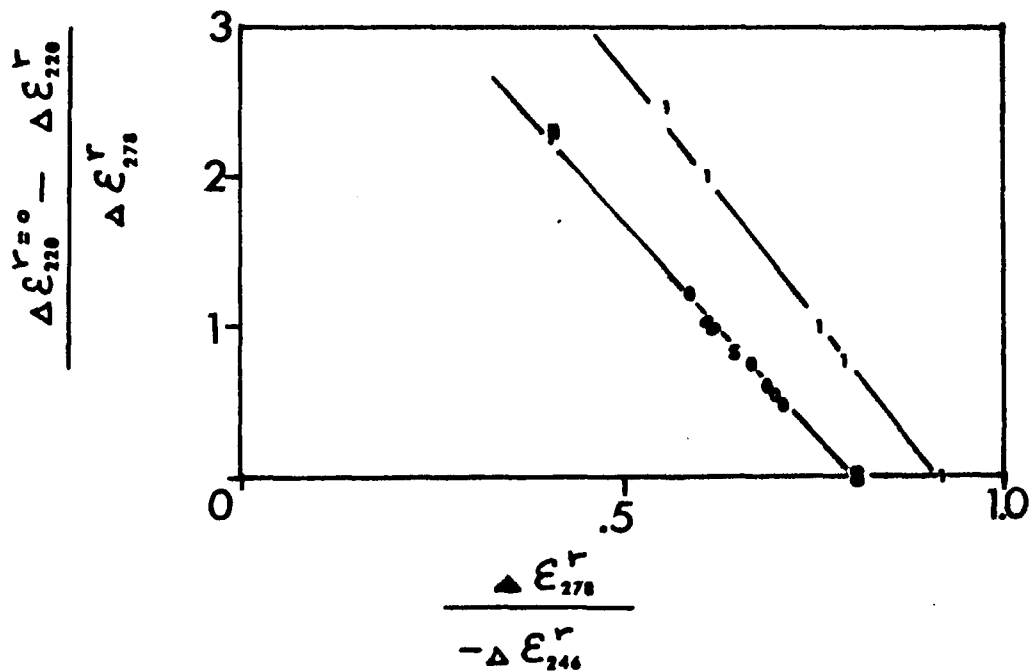


Figure 53. Deformability of whole - H 1 histone, calf thymus DNA nucleohistones.

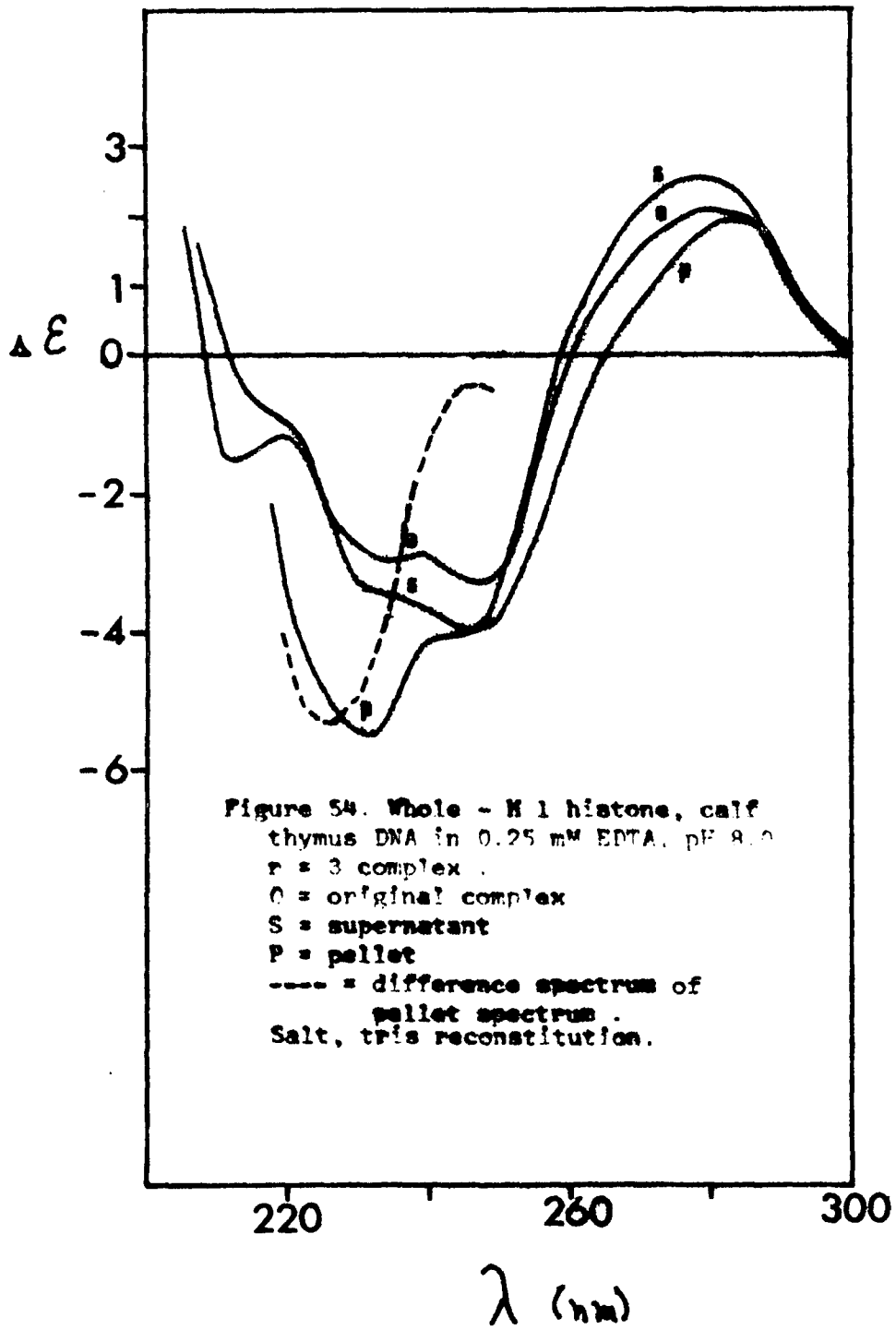
	$\frac{d}{d}$
curve 0 = salt, tris reconstitution .....	- 5 ± .5
( s = supernatant ; p = pellet )	
curve ● = salt, urea, tris reconstitution ;	
urea - out - first .....	- 5 ± .5
curve 1 = phosphate reconstitution.....	- 5.6 ± .5

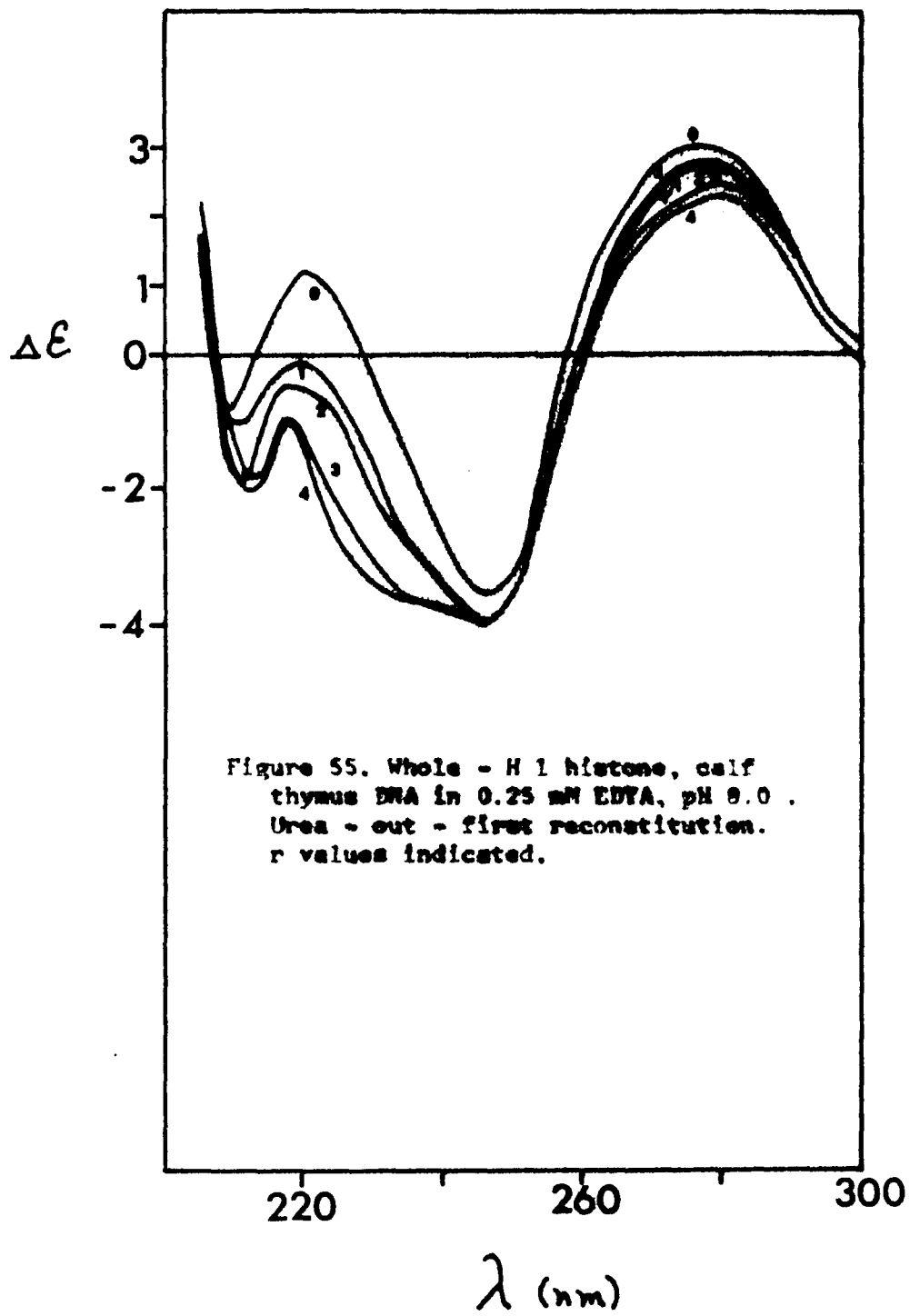
fraction in the high salt without urea enhances the interaction of the hydrophobic histone moieties with the nucleic acid.

As with histone H2B, the whole -H1 minus - urea complex was centrifuged to yield the supernatant and pellet fractions (Figure 54). Again, the supernatant and pellet  $m_d$  values fall on the same line as the original complex, although the pellet is seen to contain more histone - bound DNA and the supernatant less bound DNA.

The whole -H1 minus - urea complexes so far discussed were prepared by mixing the histone fraction (in 2 M NaCl) with the DNA fraction (also in 2 M NaCl) and dialysing the salt out by gradient. In another experiment histones and DNA were prepared in 2 M NaCl, 5 M urea to dissociate the proteins, followed by removal of the urea prior to the salt gradient. The rationale for this experiment is that if there exists a most stable complex for the histones, it should reform upon removal of urea and the salt gradient should then yield a complex equivalent to the complex prepared in the total absence of urea. The results are presented in Figure 55. This complex has a set of CD spectra virtually identical to the minus - urea complex (Figure 52b). Figure 53 illustrates that the  $m_d$  lines for the two complexes are also identical. Chang and Li (96) came to the same conclusion concerning the stability of the histone - histone interaction through experiments on the perturbation of nucleohistone structure, namely: there exists an aggregate conformation for the histones which is highly stable and reforms upon removal of the perturbant.

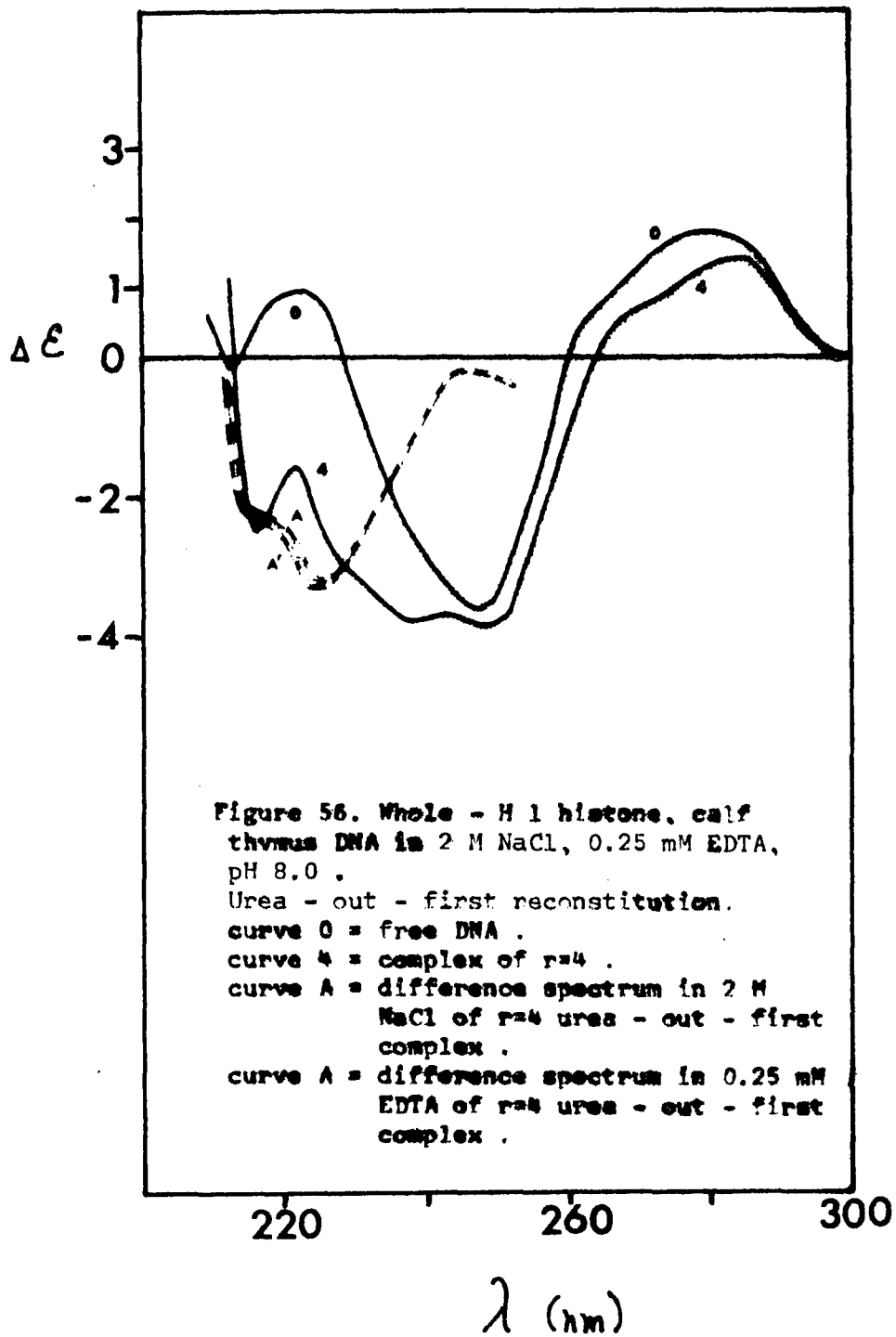
The conformation of the histone in 2 M NaCl / EDTA contains a significant amount of beta secondary structure (Figure 45b). The difference spectrum of the  $r = 4$  complex prepared without urea (Figure 54b)

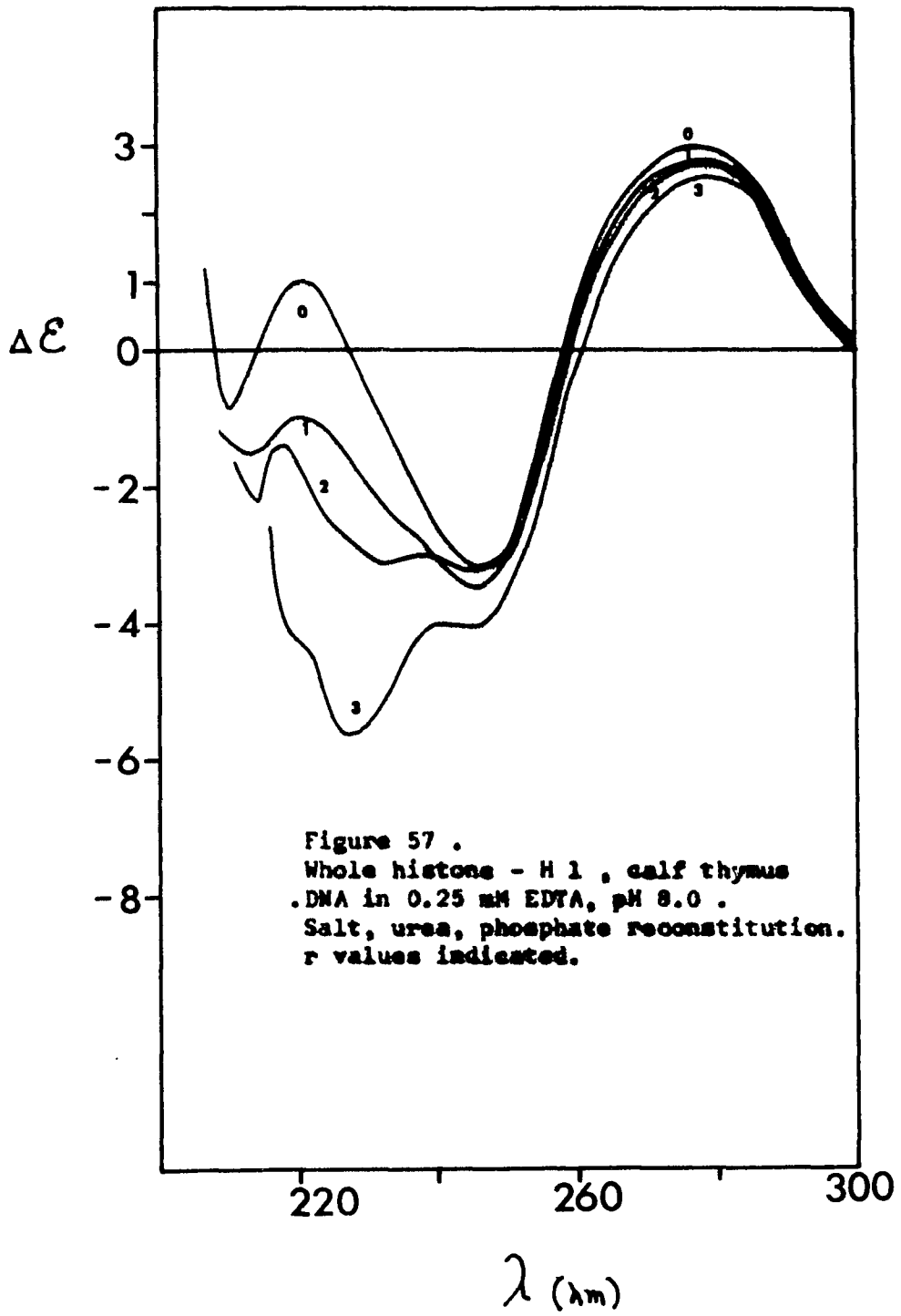


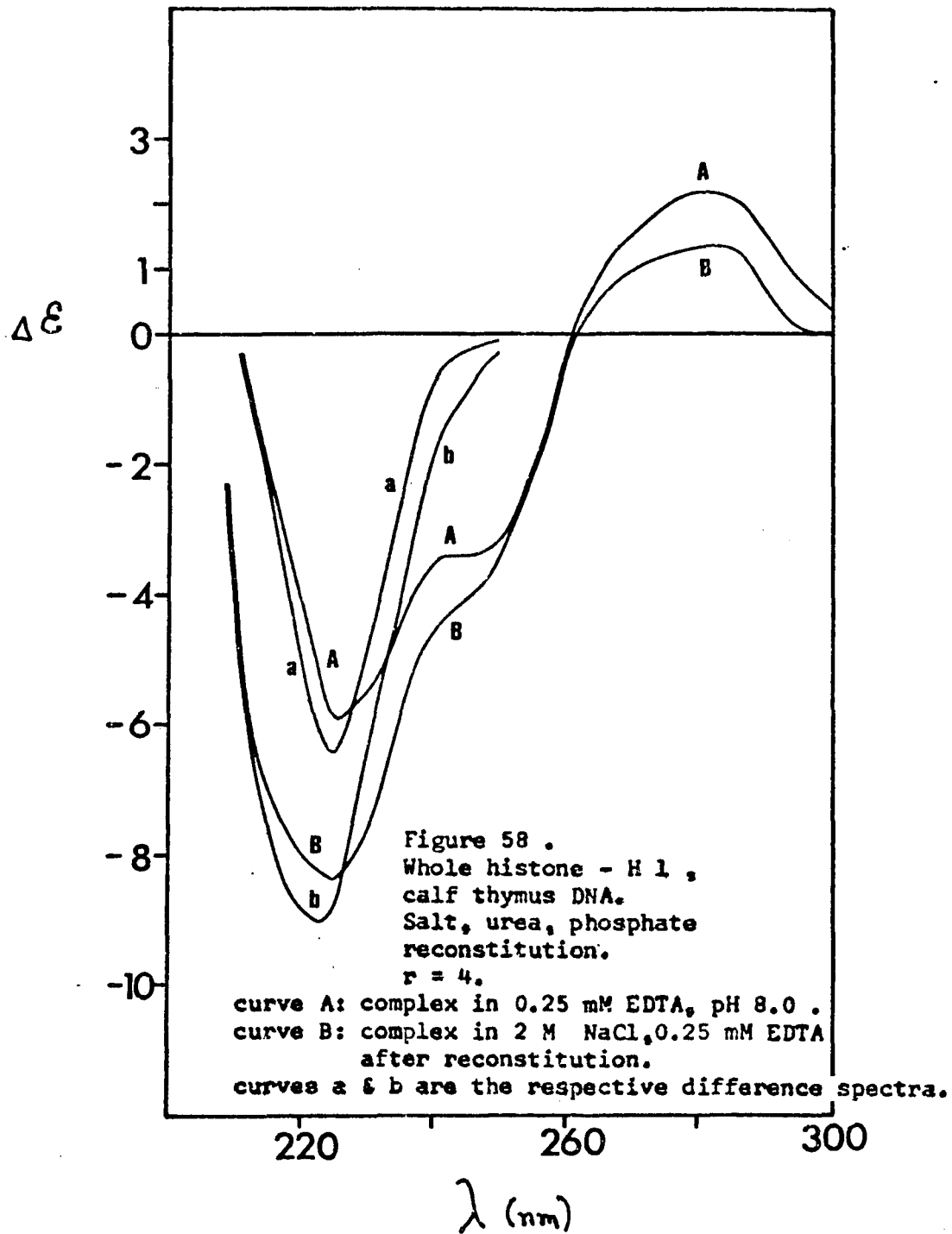


is the same as the  $r = 4$  complex prepared urea - out - first. Both of these are the same as the spectrum of unbound whole - H 1 in 2 M NaCl. If an equal volume of 4 M NaCl is added directly to the minus - urea complex the histones are dissociated and the CD spectrum becomes a composite of free DNA and whole - H 1 histone in salt (Figure 56). Subtracting the DNA spectrum from that of the complex yields a difference spectrum again identical to that of free whole - H 1 histone prior to annealing or whole - H 1 histone bound to the DNA after annealing. This provides physical supporting evidence for the observation by Weintraub et. al. (34) that a complex of whole - H 1 histone may be removed from chromatin by 2 M NaCl which retains the native histone conformations and histone - histone associations.

When whole - H 1 is reconstituted to DNA by salt, phosphate (Figure 57) the difference spectra (Figure 58) indicate a significant increase in the amount of beta structure in the complex. A comparison of the  $m_d$  for this complex (Figure 53) with that of the analogous complex reconstituted by salt - urea - tris (Figure 51) reveals a significant increase in the ability of the phosphate reconstituted histones to alter the conformation of the DNA. Presumably, this is due to the increase in beta structure observed in the phosphate reconstitutes. If the  $r = 4$  phosphate complex is removed from the DNA with 2 M NaCl the difference spectrum of the histone conformation is not the same as it is prior to salt addition, nor is it equivalent to whole - H 1 (non - phosphate treated) in salt. The phosphate buffer must exert effects on the histone which leaves the protein in a structural conformation different from that induced by NaCl. On the addition of NaCl the specific phosphate - induced associations are enhanced, as evidenced by the large depth of the 220 nm trough in the



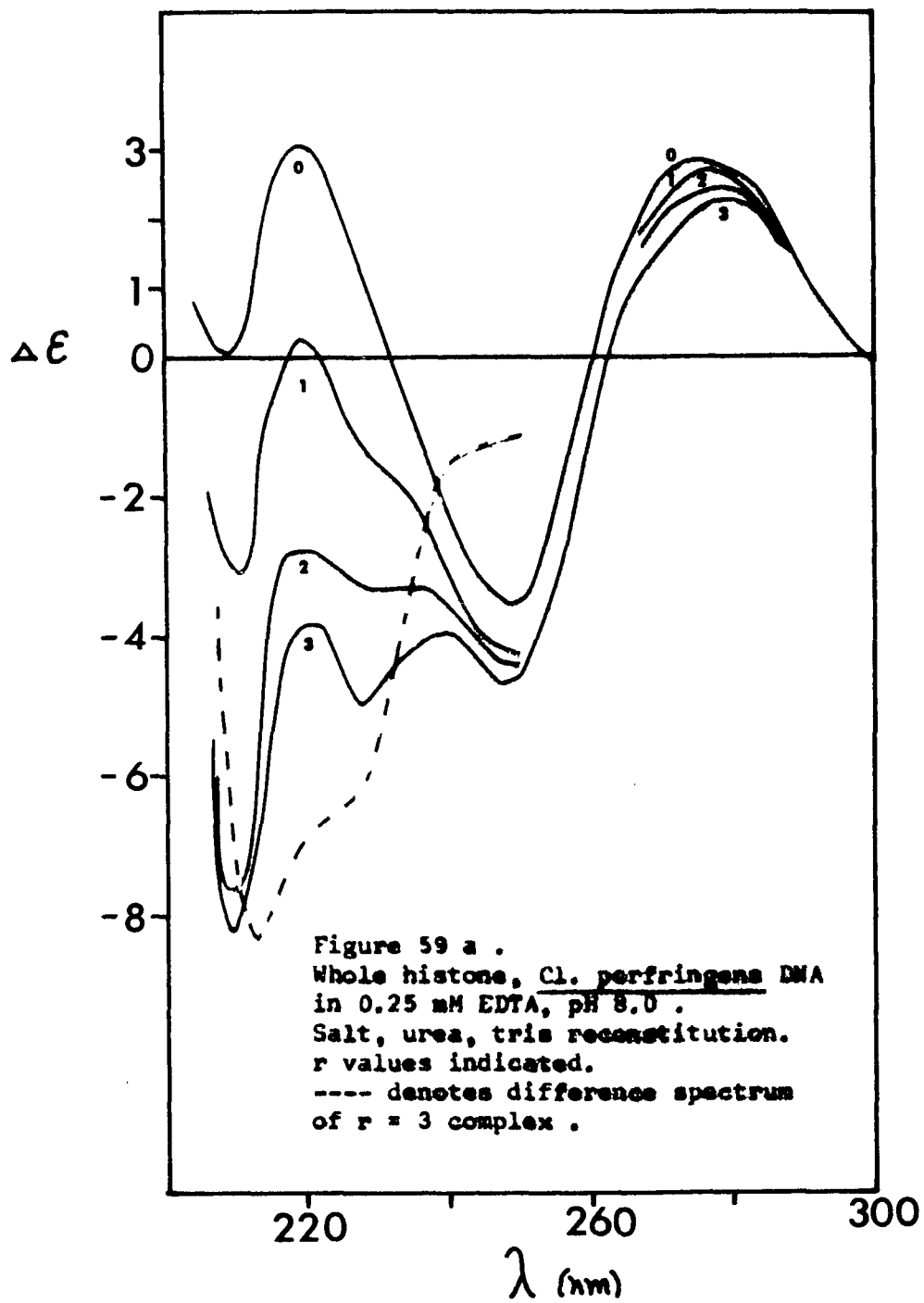


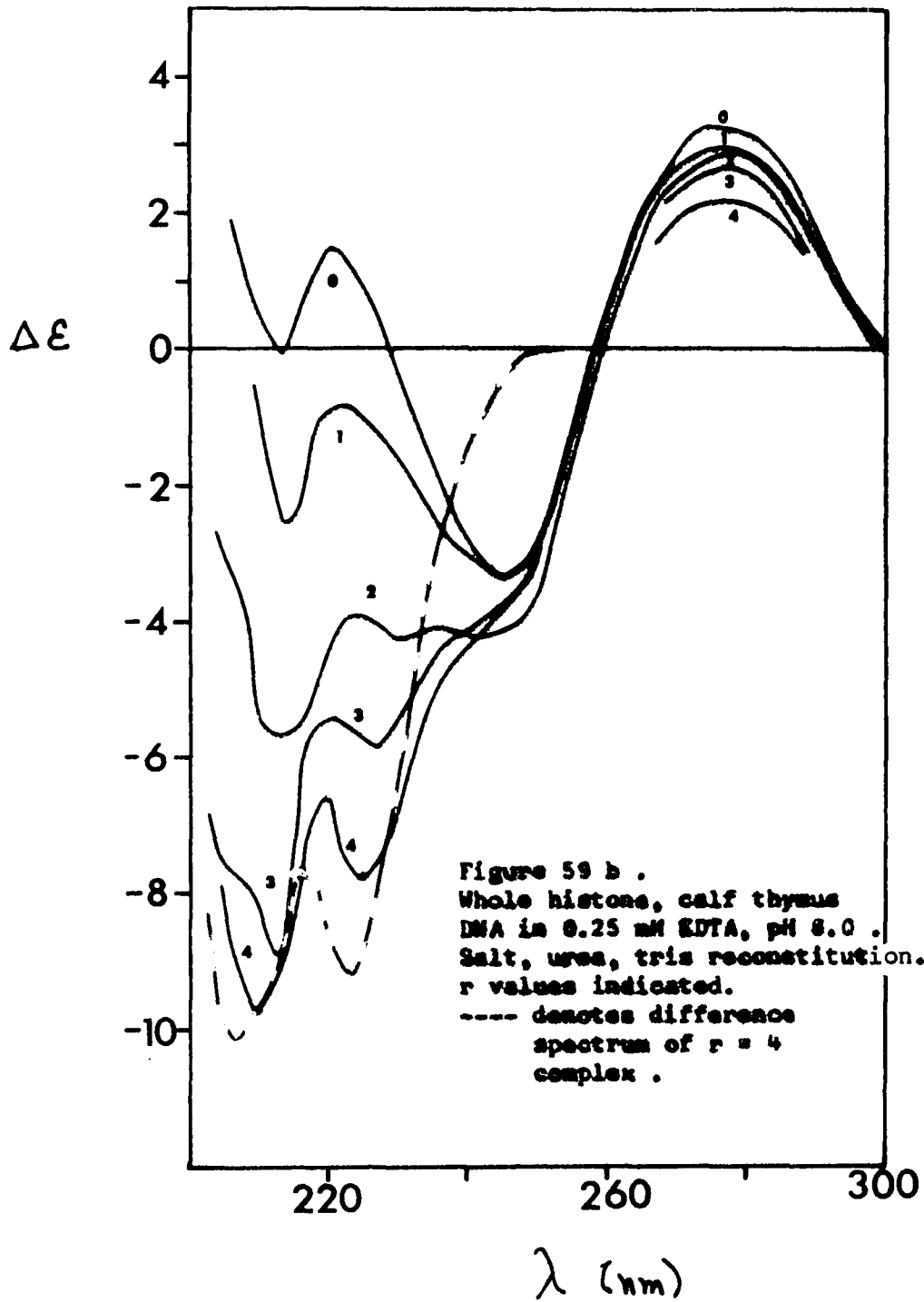


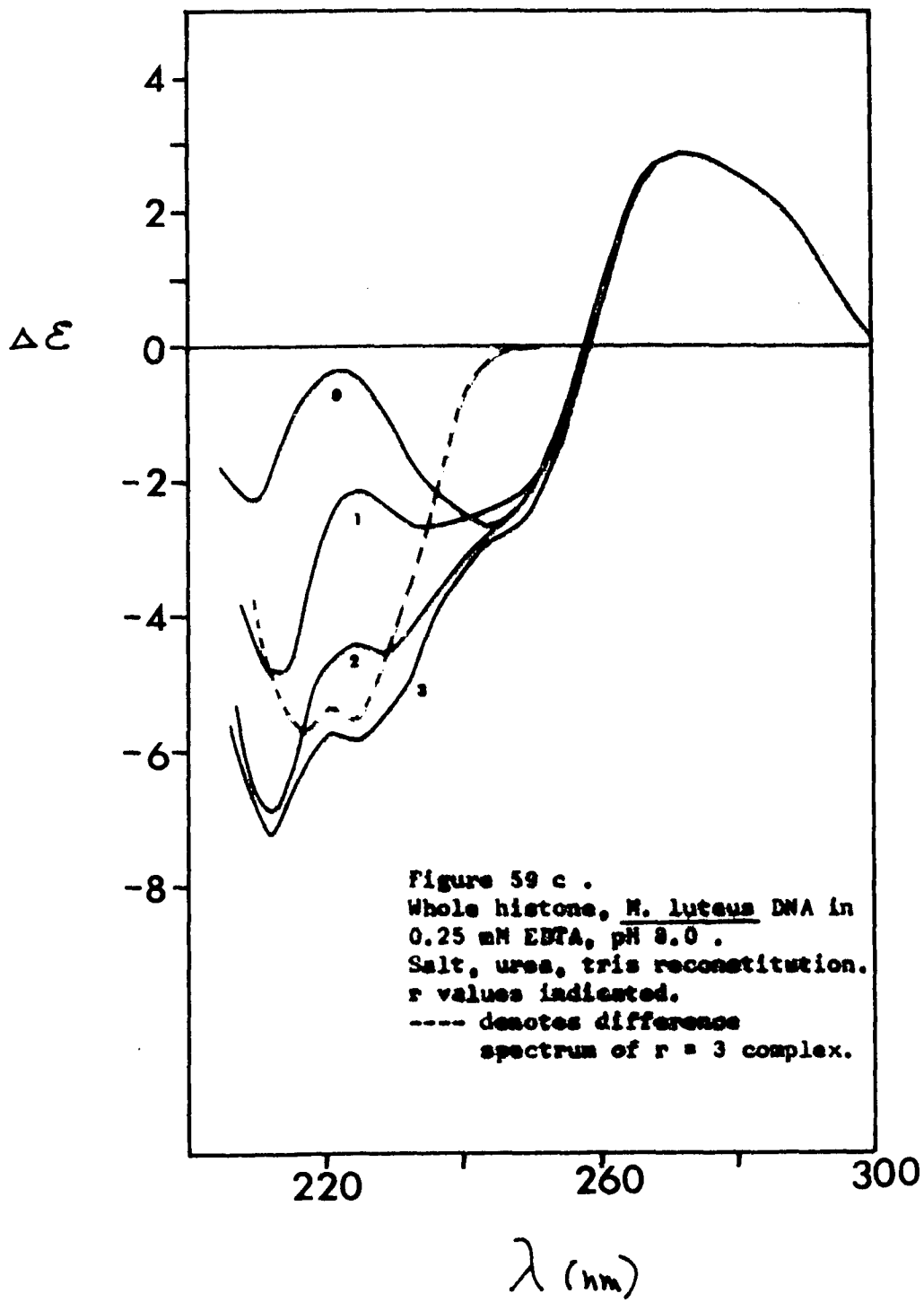
difference spectrum. It stands to reason then that since NaCl strengthens hydrophobic interactions and since phosphate is known to increase the ordered secondary structure of histones, the phosphate buffer has intensified the hydrophobic interaction between histones. That the phosphate buffer also heightens the hydrophobic histone - DNA interaction is supported by the data of Figure 53. The difference spectra of Figures 50, 52, 54, 56, 57 and 58 suggest that the beta sheet type of secondary structure is responsible for the observed B to C DNA transitions in whole - H 1 - DNA complexes.

The CD spectra of whole histone reannealed to DNA is shown in Figure 59. The inclusion of histone H 1 in the complex has caused a significant change in the shape of the difference spectra in this Figure. Whereas in whole - H 1 complexes the histones appeared to have a high degree of beta structure, whole histone - DNA complexes show increased amounts of random coil (compare Figure 33). In addition, it is now the Cl. perfringens - whole histone complex which is most deformable (Figure 60a). Figure 60b illustrates that the slopes of the deformability plots,  $m_d$ , are now inversely related to the G+C content whereas in histone.H 2 B, H 2 A and whole - H 1 complexes increasing G+C content was accompanied by increased deformability.

The CD spectra of Figure 61 show increased random coil content in those whole histone complexes reconstituted in the absence of urea as well. Figure 61a also indicates that the ability of whole histone to deform calf DNA is unchanged in the plus - urea and minus - urea complexes. Whole histone in EDTA contains significant amounts of random coil (Figure 45). This is presumably the contribution of histone H 1. When whole







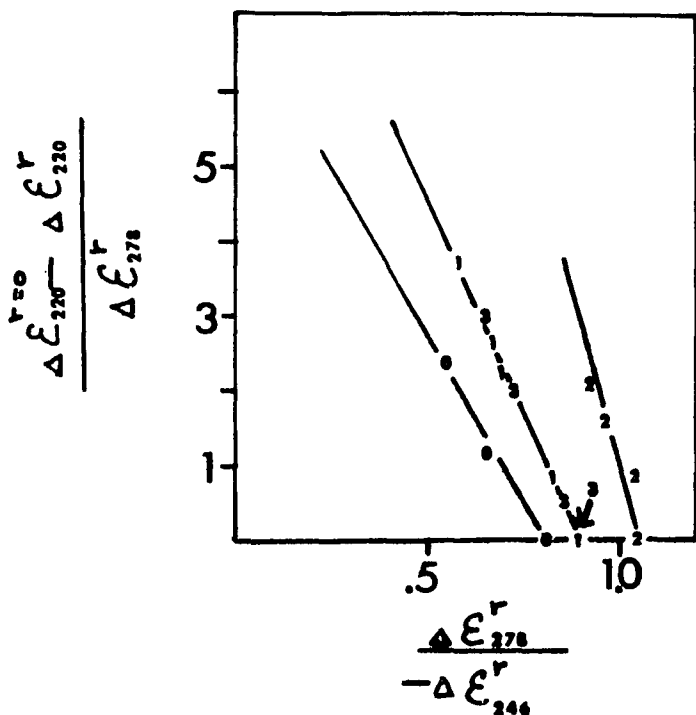


Figure 60 a . Deformability of whole histone nucleohistones.

$m_d =$	
$8.7 \pm .9$	0 = <u><i>Cl. perfringens</i> DNA</u> . Salt, urea, tris reconstitution.
$11 \pm 1$	1 = Calf thymus DNA . " " " "
$21 \pm 2$	2 = <u><i>M. luteus</i> DNA</u> . " " " "
$11 \pm 1$	3 = Calf thymus DNA. Salt, tris reconstitution.

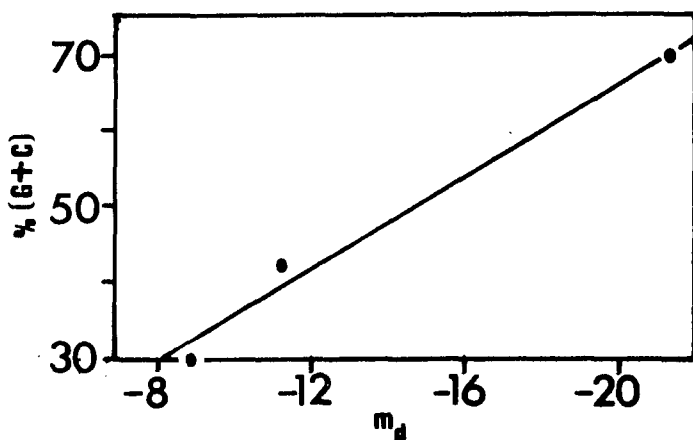
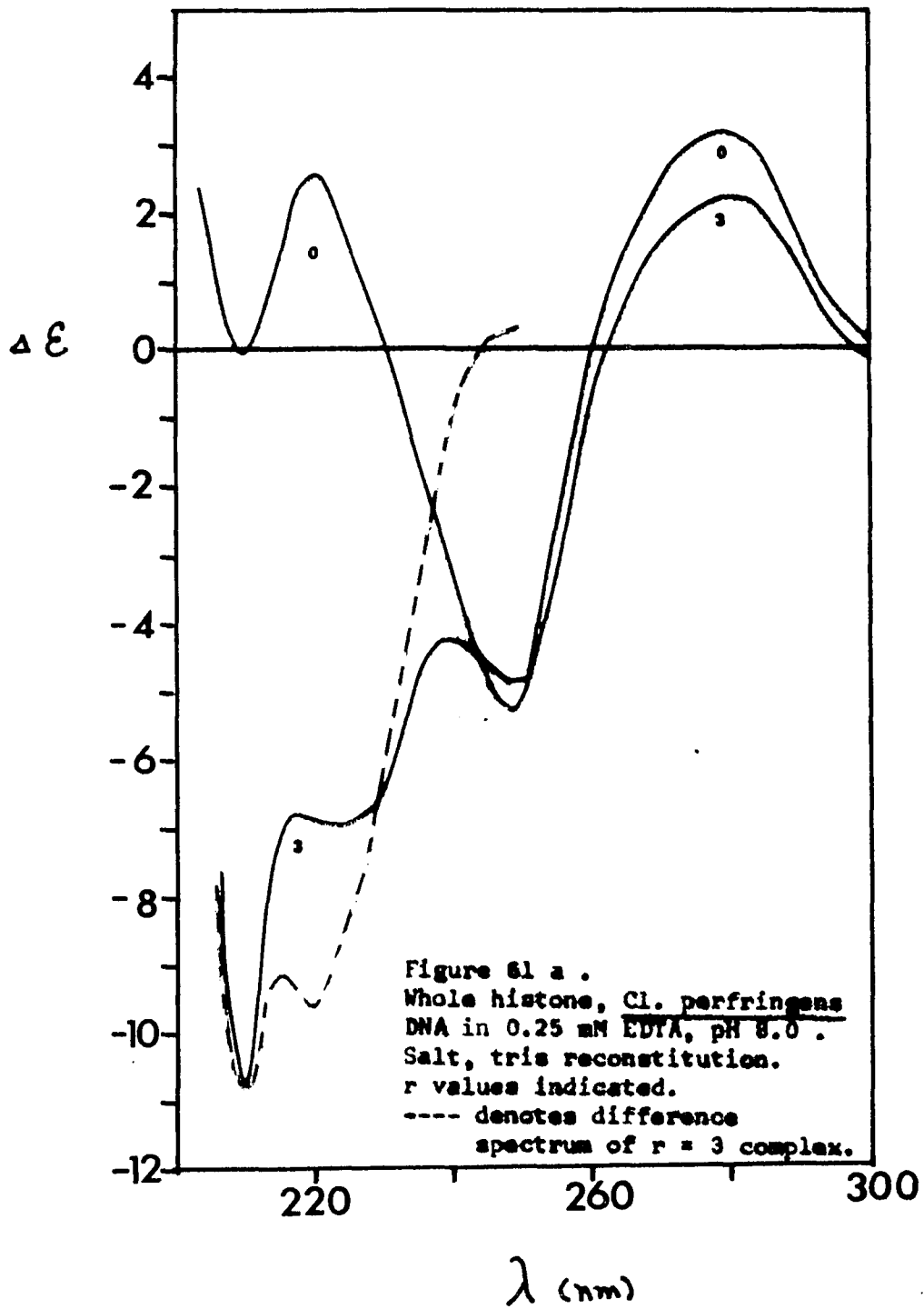
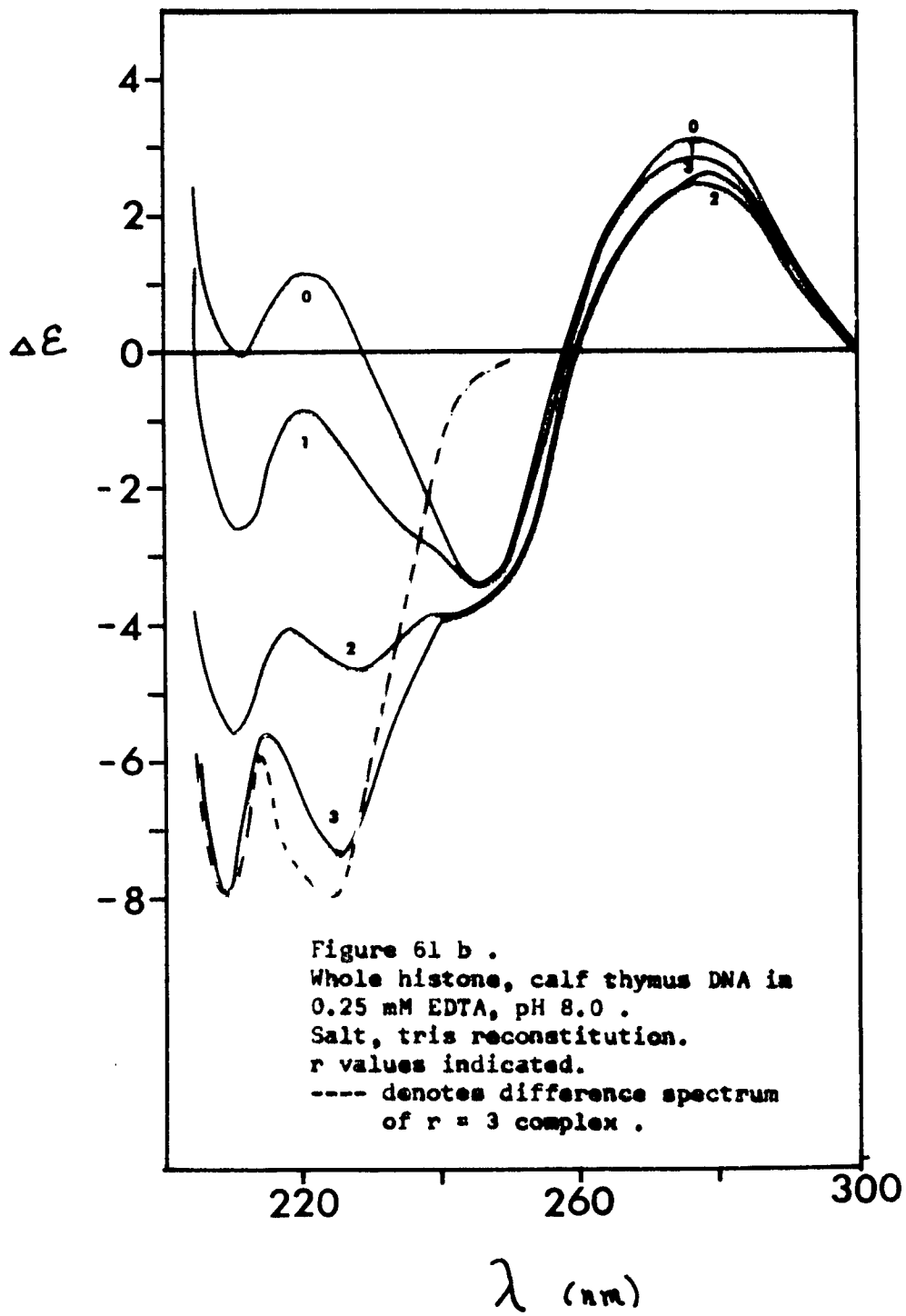
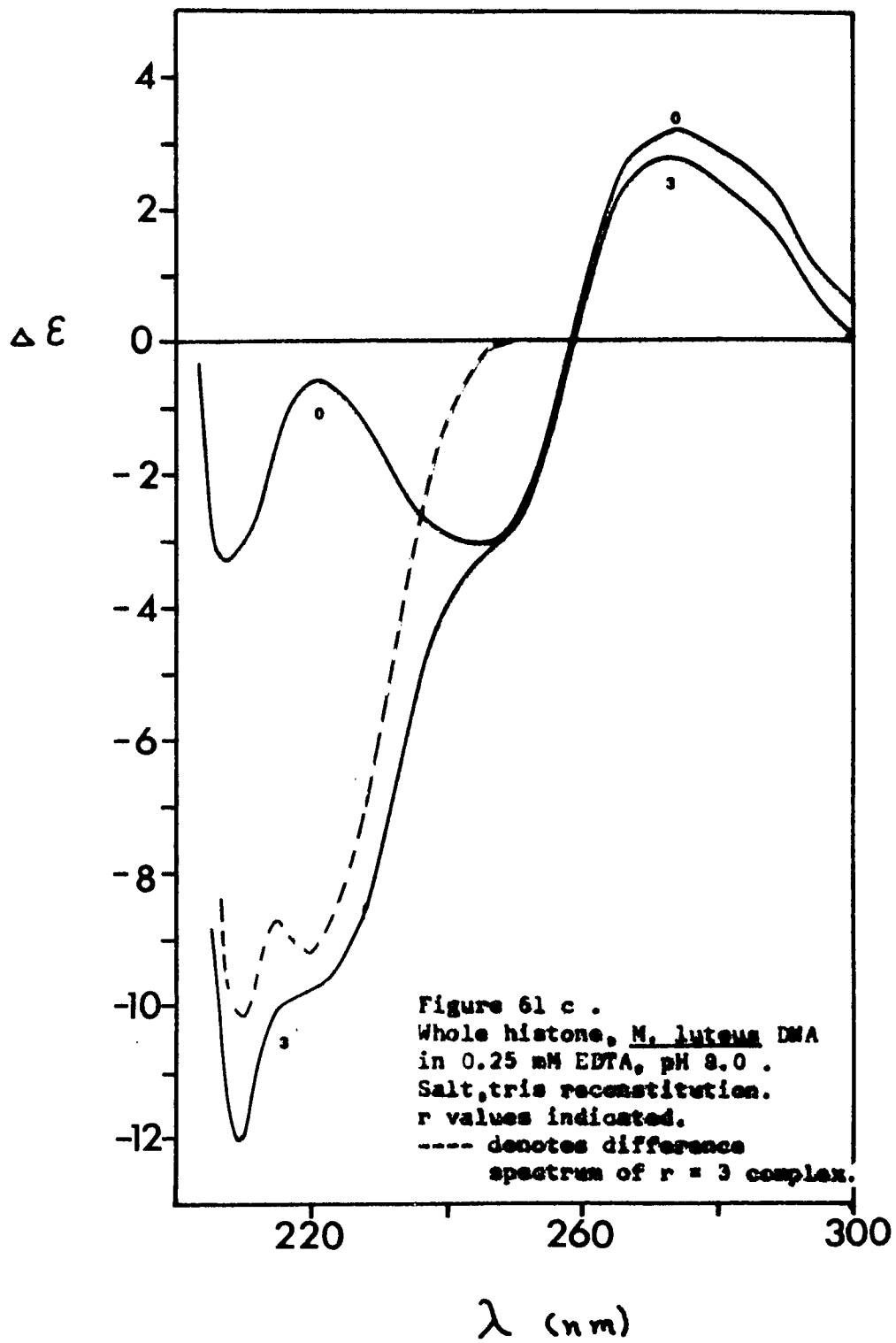


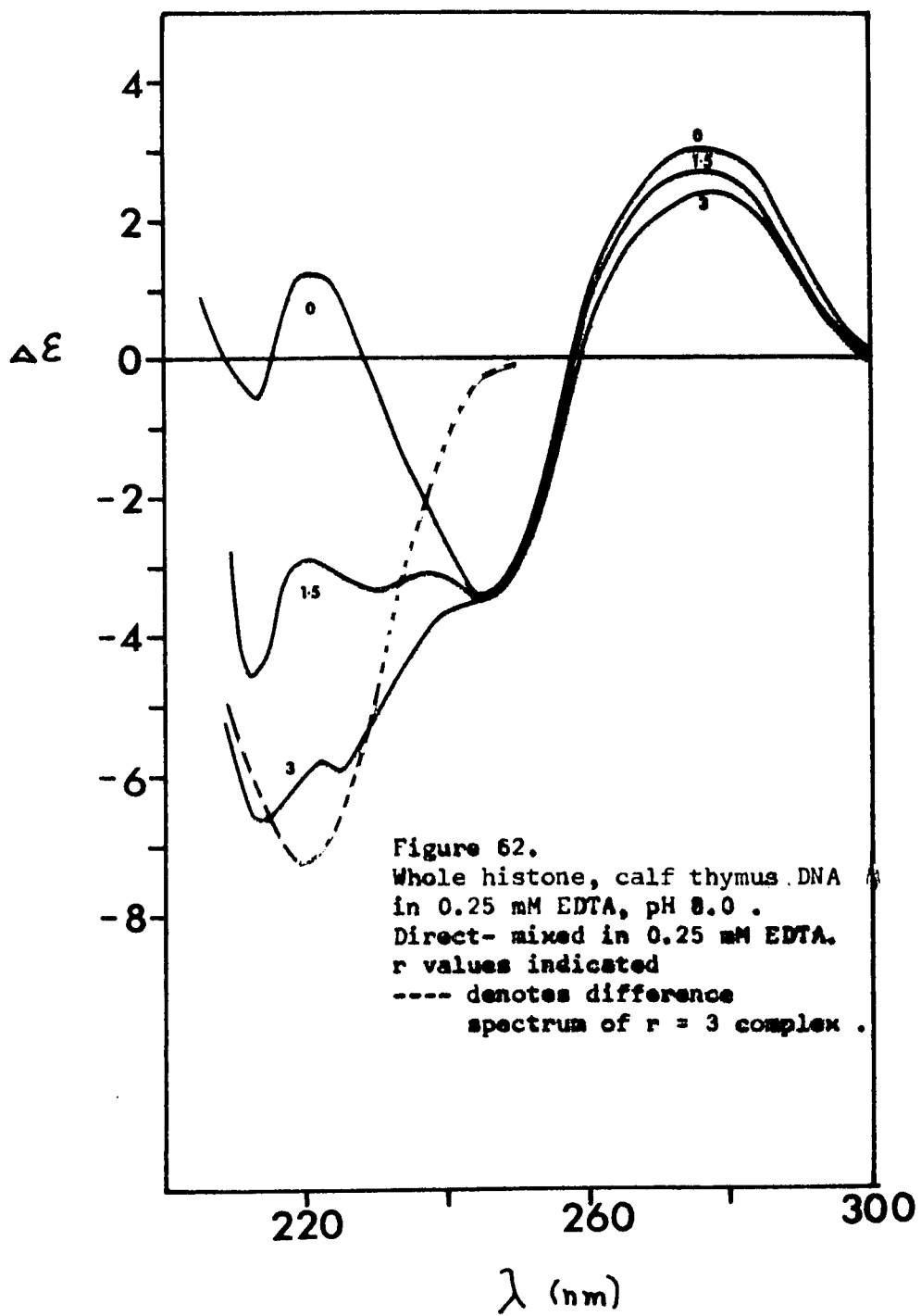
Figure 60 b .







histone is added to DNA at low ionic strength (Figure 62) the difference spectra do not show the doublet trough seen in gradient reconstituted complexes. In this complex, despite the apparent enhancement of beta structure, the  $m_D$  decreases to  $-15 \pm 2$  (Figure 63). When the protein and DNA components are mixed in 0.15 M NaCl / EDTA (Figure 64) the trough near 220 nm is further magnified. This increase in intensity of the 220 nm response is correlated with a strong red shift of the CD spectrum and the appearance of a small negative band near 295 nm, characteristic of the C type DNA spectrum. Since concentrations of NaCl in excess of 4 M are required to reduce the CD of DNA to  $\Delta \epsilon_{275} = 1$  and produce the negative peak at 295 nm (98), the 0.15 M NaCl present in the medium cannot be the cause of this drastic conformational alteration. The presence of histone H1 and its interaction with the other histones is apparently responsible for the B to C conversion seen in Figure 64. The ability of H1 to distort the B type DNA CD towards C type at H1  $r = 0.75$  aa/n in 0.14 M NaF has already been documented (108a). At a total  $r = 3$ , the H1 concentration in the complexes pictured here is ca. 0.6 aa/n. Furthermore, when the direct-mixed salt/EDTA complexes are dialysed to low ionic strength (Figure 65) the CD signal in the DNA region 260 nm returns to the B type spectrum. A similar response to decreased ionic strength was observed by Fasman et al. (108a) in histone H1 - DNA complexes. Although the extent of B to C conversion is the largest of any complex presented herein ( $\Delta \epsilon_{278} / -\Delta \epsilon_{246} = 0.23$ ), the reversal of the transition under dialysis to low ionic strength is not unique to histone H1 complexes (Figures 48, 49). However, the synergistic interaction of histone H1 with the other histones is



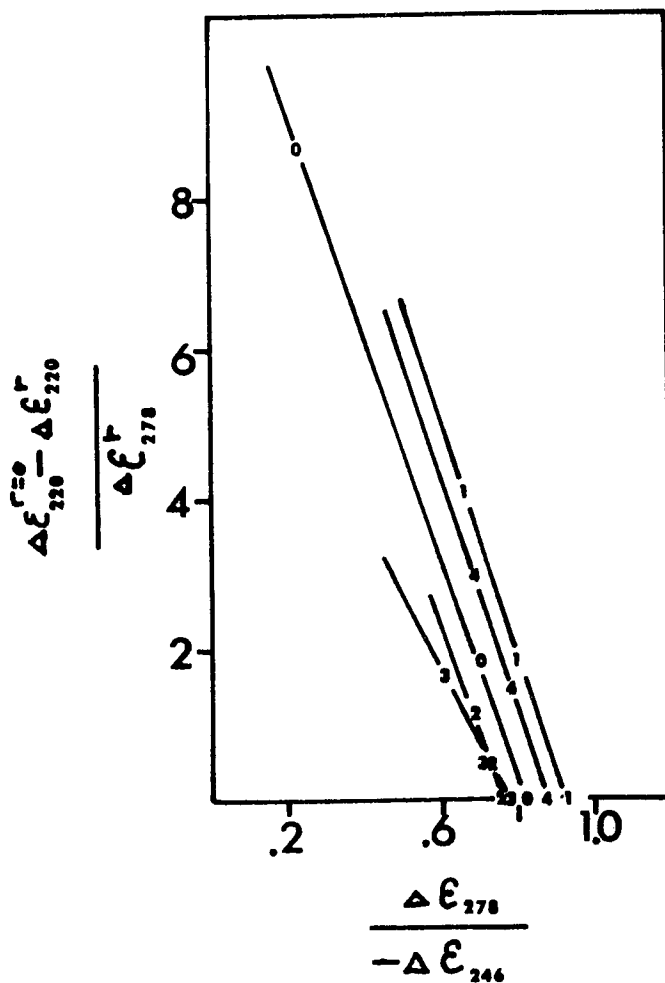
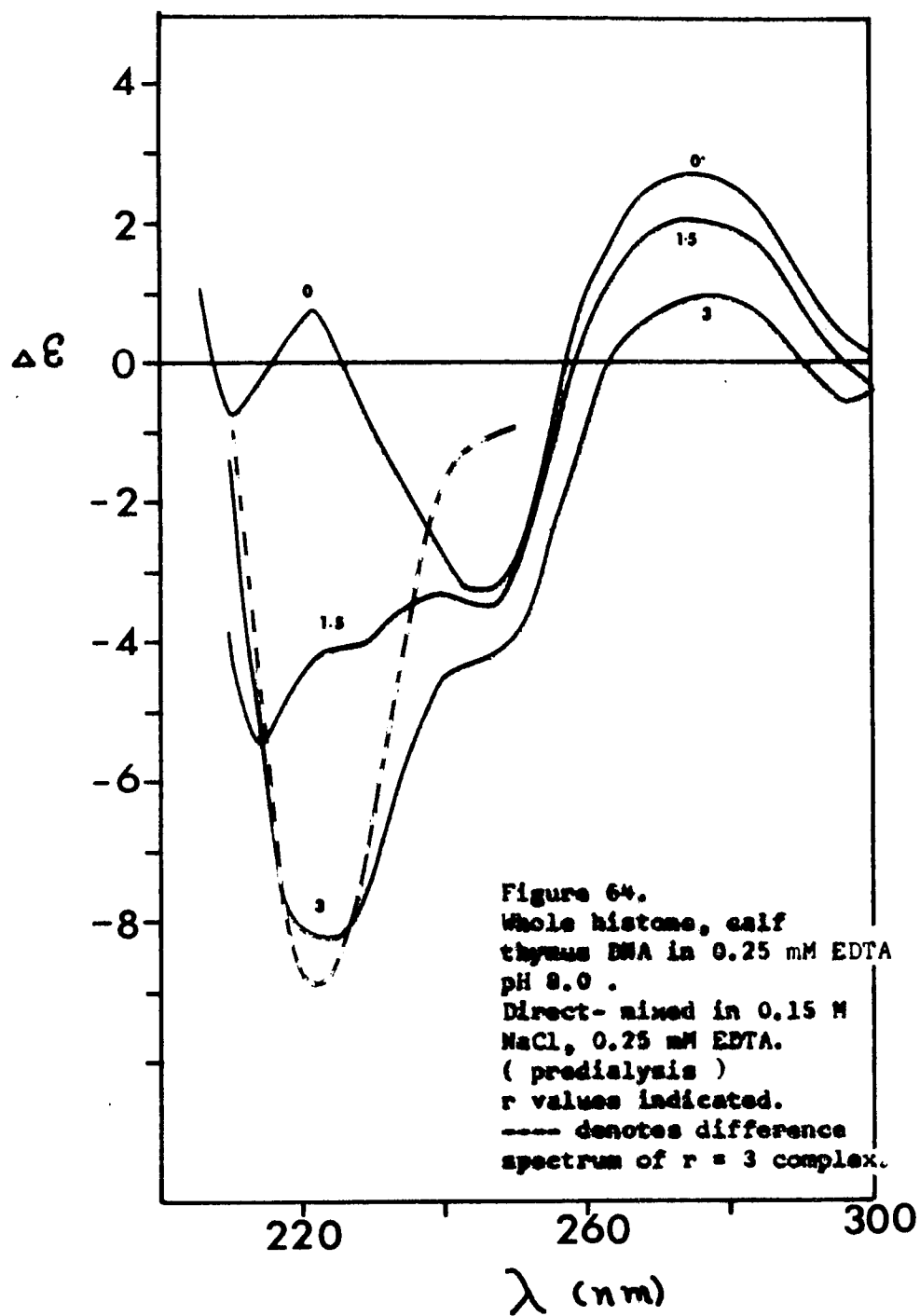


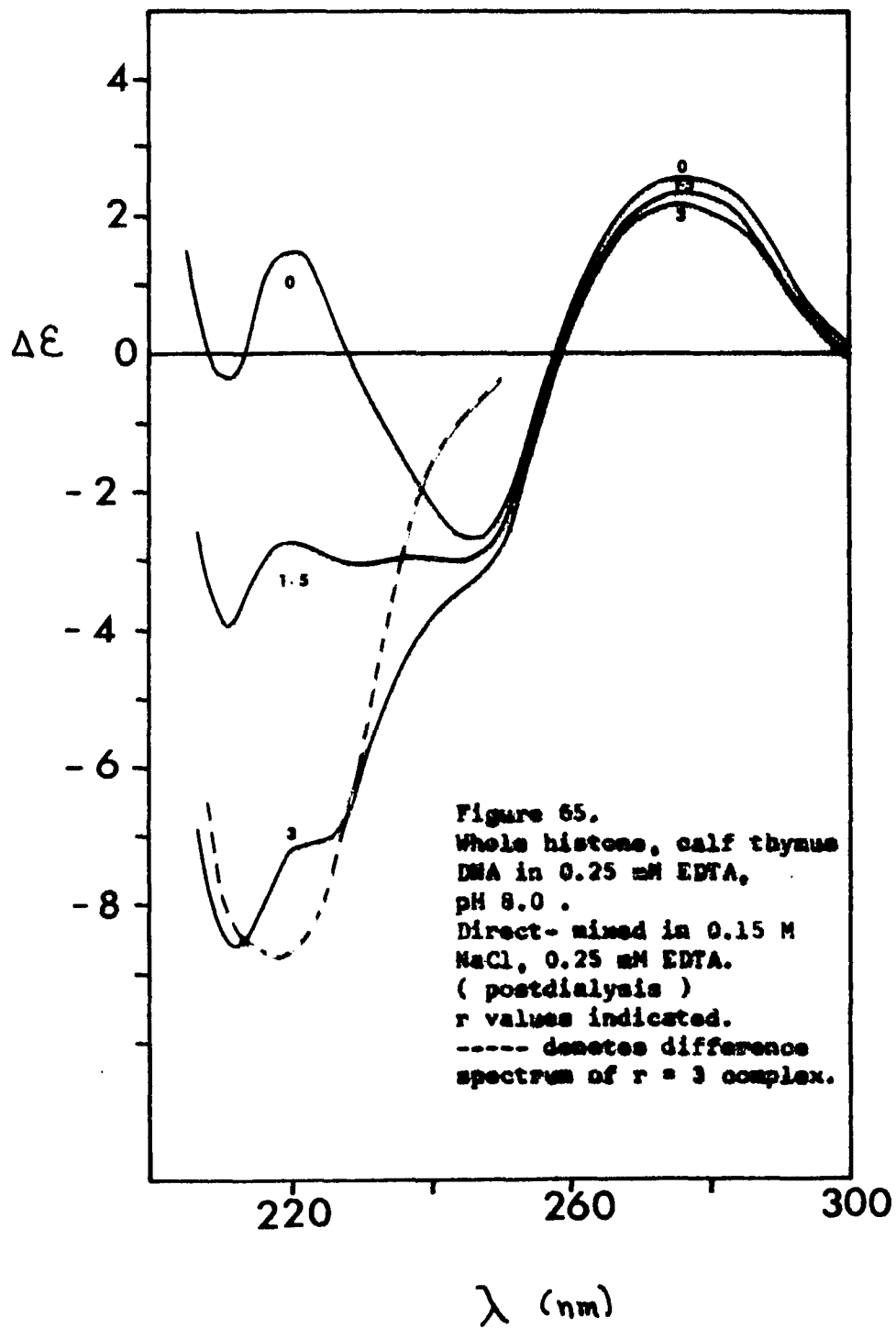
Figure 63. Deformability of whole histone nucleohistones, calf thymus DNA.

- 0 = direct- mixed, 0.15 M NaCl, EDTA ( predialysis )
- 1 = " " " " " ( postdialysis )
- 2 = direct- mixed, 0.15 M NaCl, 5 mM phosphate, EDTA ( postdialysis )
- 3 = " " " " " " " ( predialysis )
- 4 = direct- mixed, EDTA

( in all cases EDTA refers to a solution of 0.25 mM EDTA, pH 8.0 )

SAMPLE	$R_d$
0 . . . . .	$-15 \pm 2$
1 . . . . .	$-15 \pm 2$
2 . . . . .	$-15 \pm 2$
3 . . . . .	$-11 \pm 1$
4 . . . . .	$-15 \pm 2$



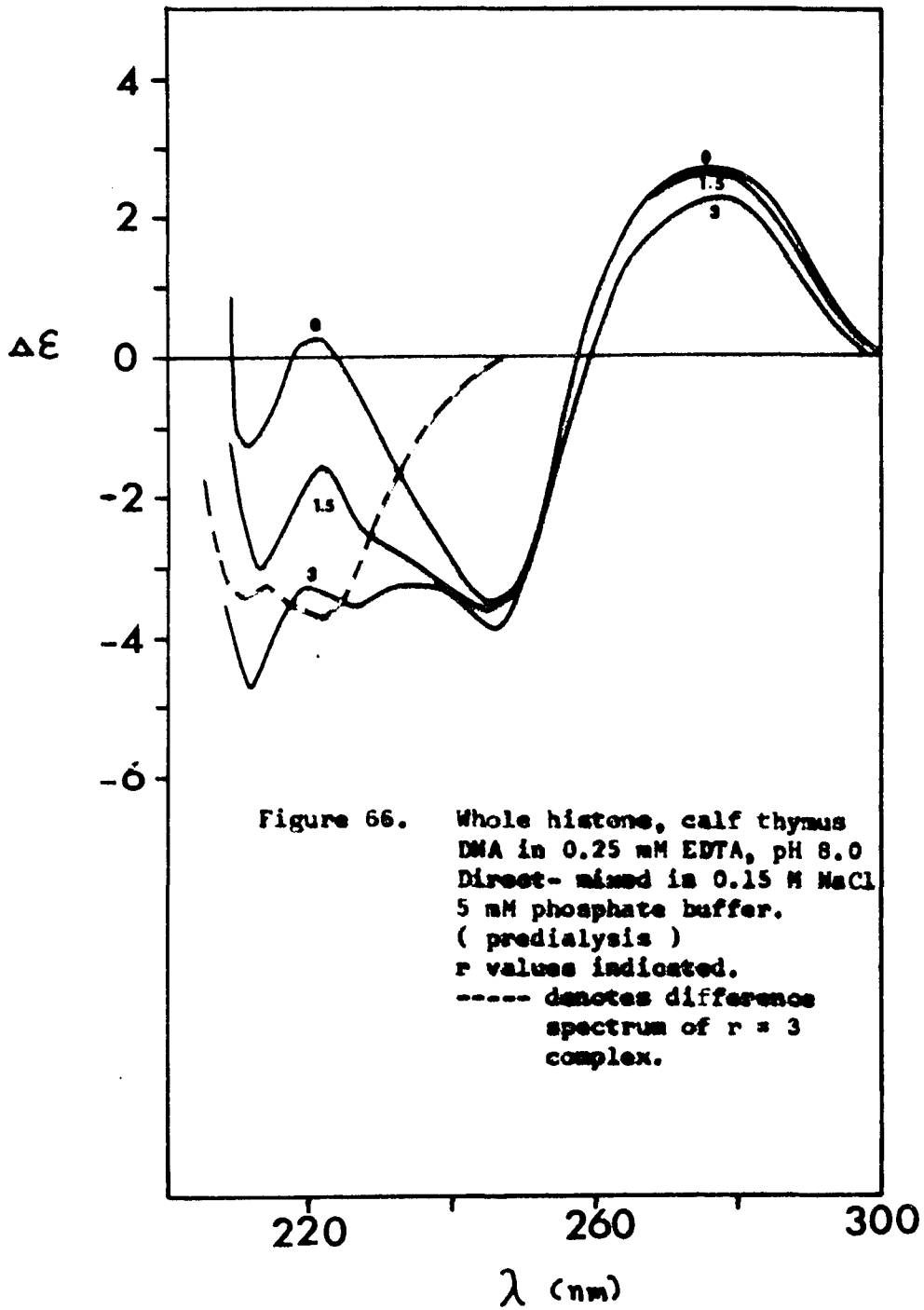


certainly implicated.

The  $m_d$  values for the complexes of Figures 64 and 65 are the same (Figure 63). The C to B transition may then be related to the shift in wavelength minimum of the 223 nm trough (Figure 64) to 217 nm (Figure 65). By comparison with Figure 33, this change may reflect a decrease in the amount of beta sheet conformation.

When whole histone is direct-mixed with DNA in 0.15 M NaCl / EDTA / phosphate buffer (Figure 66) and dialysed to EDTA (Figure 67) the ability of the histone to cause the B to C transition decreases (Figure 63). In phosphate buffer the 220 nm trough is deeper and broader than after the dialysis. This change in conformation after dialysis may be determined both by the DNA, as well as by the initial (pre-complexing) conformation of the histone. In direct-mixing experiments where the initial conditions favor a mixture of helix and random coil conformations (Figure 45) (e.g., EDTA, EDTA - .15 M NaCl) the difference spectrum of the final complex shows a large induction of beta structure (Figures 62, 64) which is retained even after dialysis to low ionic strength (Figure 65). In phosphate direct-mixed complexes, the free whole histone contains a mixture of  $\alpha$  and  $\beta$  structures (Figure 45). Upon complexing, the difference spectra again reveal an enhancement of the  $\beta$  structure (Figure 66), however, some of the helical conformation is retained. It appears then that the binding to DNA imposes some additional amount of beta structure on the histone. This finding tends to support the notion that hydrophobic forces are important in the binding of histone to DNA. The observation (Figure 63) that the  $m_d$  values for the complexes:

- a) direct-mixed in EDTA (Figure 62);
- b) direct-mixed in NaCl / EDTA, predialysis (Figure 64);
- c) direct-mixed in NaCl / EDTA, postdialysis



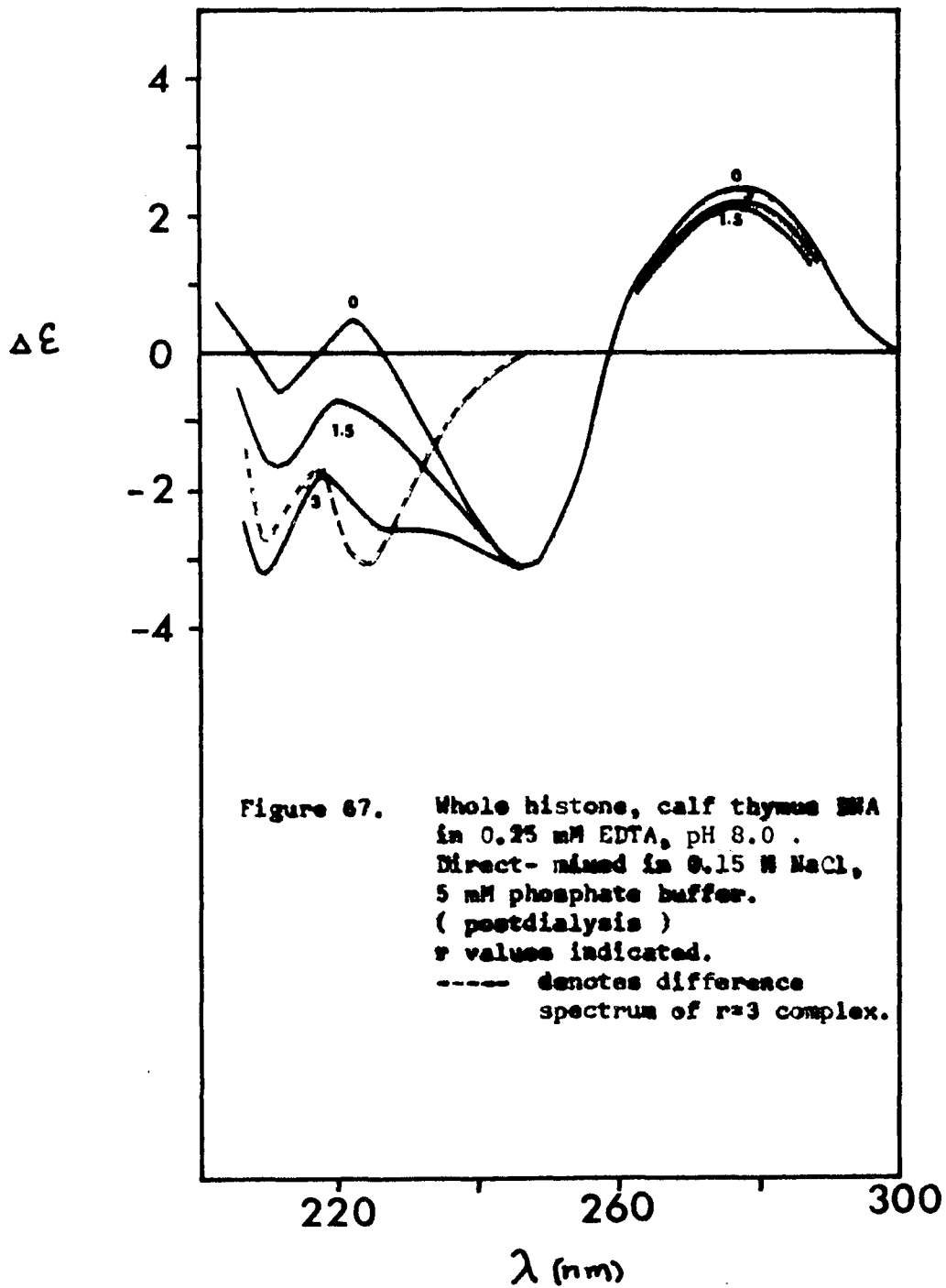


(Figure 65); and d) direct - mixed NaCl / EDTA phosphate, postdialysis (Figure 67) are the same indicates the existence of some common characteristic to histone binding, despite the different conformations of the histones prior to complexing and the variable conditions under which these complexes were formed. An observation which may be pertinent here is that whole histone complexes reconstituted with and without urea (Figures 59b, 61b) have identical deformability plots (Figure 60), while whole histone - H1 complexes (Figure 50b, 52b) are greatly affected by the omission of urea, which causes a 50% increase in  $m_d$  (Figure 51, 53). Apparently, the presence of H1 stabilizes the binding conformation of the remaining histones.

TABLE 4  
CD CHARACTERISTICS OF NUCLEOHISTONES

<u>HISTONE</u>	<u>DNA</u>	<u>CONDITIONS</u>	<u>aa / n</u>	<u><math>\lambda_m</math></u>	<u><math>\lambda_c</math></u>	<u><math>\frac{\Delta\epsilon_{278}}{-\Delta\epsilon_{246}}</math></u>	<u><math>m_d</math></u>
H 2 A	P	S - U - T <sup>(a)</sup>	0	276	258.5	.86	$-7 \pm .7$
			1	276	259.0	.79	
			2	279	261.0	.65	
			3	282	262.0	.51	
H 2 A	C	S - U - T	0	275	258.0	.81	$-5.5 \pm .5$
			1	276	259.5	.63	
			2	280	262.0	.49	
			3	283	265.5	.39	
			4	286	267.5	.31	
H 2 A	L	S - U - T	0	273	257.5	1.4	$-2.4 \pm .2$
			1	274	257.5	1.32	
			2	275	259.5	.94	
			3	277.5	262.5	.75	
			4	288.5	263.0	.61	
H 2 A	C	S - T <sup>(b)</sup>	0	277	258.0	.82	$-10 \pm 1$
			1	278	259.0	.75	
			2	280	259.5	.70	
			3	281	261.0	.57	
H 2 B	P	S - U - T	0	275	259.5	.66	$-7 \pm .7$ (calc)
			3	280	260.5	.60	

TABLE 4 CONTINUED

<u>HISTONE</u>	<u>DNA</u>	<u>CONDITIONS</u>	<u>aa / n</u>	<u><math>\lambda_m</math></u>	<u><math>\lambda_c</math></u>	<u><math>\frac{\Delta\epsilon_{278}}{-\Delta\epsilon_{246}}</math></u>	<u><math>m_d</math></u>
H 2 B	C	S - U - T	0	275	257	.9	$-5.4^{+.5}$
			1	175.5	257	.72	
			2	280	259	.62	
			3	285	263.5	.41	
H 2 B	L		0	274	258	1.0	$-2.4^{+.2}(\text{calc})$
			3	278	264	.34	
H 2 B	C	S - U - T supernatant	3	277	258	.68	$-5.4^{+.5}$
		S - U - T pellet	3	283	268.5	.26	$-5.4^{+.5}$
H 2 B	C	S - T	0	278	258.5	.88	$-13^{+1}$
			1	278	259	.82	
			2	278	259	.78	
			3	278	259.5	.74	
H 2 B	L	S - T	0	272.5	257.0	.97	$-11^{+1}$
			1	272.5	257.0	.94	
			2	272.5	257.5	.86	
			3	272.5	257.5	.84	
H 2	P	S - U - T	0	278	260	.73	$-14^{+2}$
			1	278	259.5	.66	
			2	279	260.5	.57	
			3	283	261.5	.48	

TABLE 4 CONTINUED

HISTONE	DNA	CONDITIONS	aa / n	$\lambda_m$	$\lambda_c$	$\frac{\Delta\epsilon_{278}}{-\Delta\epsilon_{246}}$	$m_d$
H 2	C	S - U - T	0	275	257.5	1.03	$-11 \pm 1$
			1	277	257.5	.97	
			2	278	258.5	.85	
			3	281	258	.79	
			4	281	258.5	.71	
H 2	L	S - U - T	0	272.5	256	1.70	$-4.8 \pm .5$
			1	273	258	1.14	
			2	275	258	1.03	
			3	277.5	260.5	.75	
H 2	P	S - T	0	280	260.5	.62	
			3	281.5	261.5	.43	
H 2	C	S - T	0	277	258	.82	$-12 \pm 1$
			1	278	258.5	.76	
			2	280	259.0	.74	
			3	281	259.5	.65	
H 2	L	S - T	0	272.5	258	1.03	
			3	274	259	.68	
H 2	C	S - U - p(c)	0	275	257.5	.97	$-8.9 \pm .5$
			1	276	259	.77	
			2	277	260	.71	
			3	277	260	.56	
			4	280	260.5	.56	

TABLE 4 CONTINUED

HISTONE	DNA	CONDITIONS	aa / n	$\lambda_m$	$\lambda_c$	$\frac{\Delta\epsilon_{278}}{-\Delta\epsilon_{246}}$	$m_d$
H 2	C	dm - EDTA <sup>(d)</sup>	0	277	258	.83	$-35 \pm 10$
			1	277	258	.78	
			2	277.5	258.5	.73	
			3	278	259.5	.66	
H 2	C	dm NaCl / EDTA (predialysis)	0	275	258	.83	$-15 \pm 2$
			1	275	259	.71	
			2	276	259.5	.61	
			3	276	259.5	.59	
H 2	C	dm NaCl / EDTA (postdialysis)	0	276	258	.81	$-83 \pm 20$
			1	277	258.5	.79	
			2	277.5	258.5	.76	
			3	277.5	258.5	.76	
W - H 1	P	S - U - T	0	277	260.5	.66	-13
			1	278	261	.59	
			2	280	262	.53	
			3	280	262	.49	
	C	S - U - T	0	275	258.5	.83	-11
			1	277	259.5	.78	
			2	280	259.5	.77	
			3	280	260.5	.70	
	L	S - U - T	0	273	258	1.12	-5.5

TABLE 4 CONTINUED

HISTONE	DNA	CONDITIONS	aa / n	$\lambda_m$	$\lambda_c$	$\frac{\Delta \epsilon_{278}}{-\Delta \epsilon_{246}}$	$m_d$
			1	273	258.5	1.0	
			2	274	258.5	1.27	
			3	273	259	.89	
			4	276	260	.82	
W - H 1	P	S - T	0	280	260.5	.66	
			3	280	260.5	.57	
	C	S - T	0	276	258	.83	$-5.0^{\pm 1}$
			1	279.5	259.5	.70	
			2	279.5	260	.67	
			3	281	261	.61	
	L	S - T	0	272	258	1.1	
			3	273	259	.86	
	C	urea - out - first	0	275	258	.83	
			1	279	259.5	.71	
			2	279	259.5	.68	
			3	280.5	260.5	.61	
			4	281	261	.59	
	C	S - U - P	0	277.5	258	.94	$-6^{\pm 1}$
			1	279	259.5	.79	
			2	279	259.5	.76	
			3	281	261	.61	
			4	282	262	.57	

TABLE 4 CONTINUED

HISTONE	DNA	CONDITIONS	aa / n	$\lambda_m$	$\lambda_c$	$\frac{\Delta \epsilon_{278}}{-\Delta \epsilon_{246}}$	$m_d$	
Whole	P	S - U - T	0	275	260	.82	$-9 \pm 1$	
			1	276.5	261	.66		
			2	279	261	.55		
			3	281	263	.47		
	C	S - U - T	0	275	258	.89	$-11 \pm 1$	
			1	276	258	.83		
			2	277	259	.69		
			3	277	259.5	.67		
			4	278	259.5	.50		
	L	S - U - T	0	273	258	1.04	$-21 \pm 2$	
			1	273	258	1.04		
			2	273	259	.96		
3			273	259	.93			
Whole	P	S - T	0	280	260.5	.62		
			3	281	263	.46		
	C	S - T	0	277	258	.88		$-11 \pm 1$
			1	278	258.5	.85		
			2	279	260	.72		
	L		0	273	258.5	1.03		
			3	273	258.5	.84		
Whole	C	dm - EDTA	0	275	258	.88	$-15 \pm 2$	
			1.5	276	258	.79		
			3	277	259.5	.69		

TABLE 4 CONTINUED

HISTONE	DNA	CONDITIONS	aa / n	$\lambda_m$	$\lambda_c$	$\frac{\Delta\epsilon_{278}}{-\Delta\epsilon_{246}}$	$m_d$
Whole	C	dm NaCl / EDTA (predialysis)	0	275	257	.82	$-15^{+2}$
			1.5	276	259	.71	
			3.0	277.5	263.5	.23	
Whole	C	dm NaCl / EDTA (postdialysis)	0	275	257.5	.93	$-15^{+2}$
			1.5	276	258.5	.79	
			3.0	277.5	259.0	.66	
Whole	C	.15 M NaCl / phosphate (predialysis)	0	275	258	.77	$-11^{+1}$
			1.5	275	258	.68	
			3.0	276	259.5	.61	
Whole	C	.15 M NaCl / phosphate (postdialysis)	0	275	258.5	.77	$-15^{+2}$
			1.5	277	258.5	.72	
			3.0	277	258.5	.69	

- (a) salt - urea - tris reconstitution
- (b) salt - tris reconstitution
- (c) salt - urea - phosphate reconstitution
- (d) direct - mixed complex

## APPENDIX

### CALCULATED CD PARAMETERS of CALF THYMUS NUCLEOHISTONES

Employing the equations formulated by Li et al. (109) and Chang and Li (96) the CD response of a nucleohistone complex may be separated into the CD of the protein component (Equation A-I) and the CD of the histone-bound DNA base pairs (Equation A-II):

$$\Delta \epsilon^P = \frac{\Delta \epsilon_m - \Delta \epsilon_{DNA}}{r} \quad (A-I)$$

$$b = \frac{\Delta \epsilon_m - (1-F) \Delta \epsilon^\circ}{F} \quad (A-II)$$

where:

$\Delta \epsilon^P$  = protein CD.

$\Delta \epsilon_m$  = measured CD.

$\Delta \epsilon_{DNA}$  = DNA CD.

and:

$\Delta \epsilon^b$  = CD of histone-bound base pairs.

$\Delta \epsilon^\circ$  = CD of free DNA.

F = fraction of DNA bound by histone.

1-F = fraction of histone-free DNA.

The values of  $\Delta \epsilon^P$  and  $\Delta \epsilon^b$  have been calculated for wavelengths at which the extent of protein secondary structure and the degree of B to C transition of the DNA can be evaluated, namely 220 nm and 278 nm, respectively. These values are presented in Table 1 and may be compared to the values obtained from the nucleohistone complex purified from calf thymus chromatin by Chang and Li (96).

Appendix Table 1 Calculated CD Parameters of Calf Thymus Nucleohistones

[All values refer to r=3 complexes unless noted]

	$\Delta \epsilon$ protein 220	$\Delta \epsilon$ bound DNA 278
H2A (+urea)	-1.3	1.6
H2A (-urea)	-2.3	2.3
H2B (+urea)	-0.5	1.3
H2B (-urea)	-1.7	2.8
H2 (+urea)	-1.8 r=1 -2.9 r=2 -2.8 r=3	2.3
H2 (-urea)	-3.3 r=1 -3.3 r=2 -3.3 r=3	2.3
H2 (phosphate)	-2.7	2.0
H2 (d.m. EDTA)	-3.2 r=1 -3.5 r=2 -3.2 r=3	2.1
H2 (d.m. NaCl/EDTA, predialysis)	-3.0 r=1 -2.9 r=2 -2.0 r=3	1.6
H2 (d.m. NaCl/EDTA, postdialysis)	-2.8 r=1 -3.0 r=2 -2.9 r=3	2.6
Whole - H1 (+urea)	-1.5 r=1 -1.3 r=2 -1.3 r=3 -1.3 r=4	2.6
Whole - H1 (-urea)	-1.5 r=1 -0.9 r=2 -0.7 r=3	1.5

Appendix Table 1 (continued)

	$\Delta\epsilon$ protein 220	$\Delta\epsilon$ bound DNA 273
Whole (+urea)	-2.5 r=1	2.3
	-2.5 r=2	
	-2.3 r=3	
	-2.2 r=4	
Whole (-urea)	-1.9 r=1	2.3
	-2.5 r=2	
	-2.5 r=3	
Whole d.m. EDTA	-2.7 r=1.5	
	-2.4 r=3	
Whole d.m. NaCl/ EDTA (predialysis)	-3.0 r=1.5	
	-2.8 r=3.0	
Whole d.m. NaCl/ EDTA (postdialysis)	-2.8 r=1.5	
	-2.9 r=3.0	
Whole d.m. NaCl/ Phos. (predialysis)	-1.4 r=1.5	
	-1.2 r=3.0	
Whole d.m. NaCl/ Phos. (postdialysis)	-0.7 r=1.5	
	-0.8 r=3.0	
Purified Calf thymus Nucleohistone (96)	-4.1	0.7

First, it is clear that the reconstitution procedures in general are only partially successful in duplicating the protein response found in purified nucleohistone. In addition, the histones in reconstituted complexes are not able to distort the DNA towards the C form characteristic of nucleohistone and chromatin. The explanation for this observation is unknown, however, other laboratories have reported that chromatin, dialysed against 2 M NaCl, 5 M urea to dissociate the nucleoprotein components and redialysed to low ionic strength to permit reannealing, showed only small distortions of the B type DNA CD (81).

Examination of Table 1 shows that minus-urea complexes of histone H2A (or H2B) exhibit more ordered secondary structure than do nucleohistones reconstituted in the presence of urea. The minus-urea nucleoproteins are less capable of distorting the B type DNA CD towards C form.

Histone H2 (H2A + H2B) also shows increased ordered secondary structure relative to plus-urea complexes. It may be noted that value of  $\Delta \epsilon_{220}^P$  is constant with increasing r value for minus-urea H2 nucleohistones suggesting that the interaction of H2A and H2B allows the formation of a stable unit which also has more secondary structure than would be seen in a mixture of noninteracting histones H2A and H2B. The greatest B to C transition caused by histone H2 is seen in nucleohistones prepared by mixing the protein and nucleic acid components at near-physiological ionic strength and measuring the CD under the same conditions. Once the sample is dialysed to low ionic strength the DNA partially reverts towards B form suggesting a synergistic action of the salt and histones on the DNA conformation since 0.15 M NaCl alone has a negligible effect on the CD of aqueous DNA solutions.

When whole-H1 histone is annealed to DNA in the presence of urea

the protein response is nearly constant with increasing  $r$  value. When the same mixture of histones is annealed to DNA in the absence of urea increasing amounts of histone cause progressive changes in the protein secondary structure. Figure 52b shows that this shift is towards increasing amounts of beta-sheet structure within the protein aggregate, probably due to the presence of the arginine-rich histones since the slightly lysine-rich histones H2A and H2B do not show this effect. Annealing of whole-H1 histone to DNA in a high ionic strength environment in the absence of urea is seen to cause a greater distortion of the DNA conformation than the reconstitution in the presence of urea. This implies that hydrophobic forces may be important in the correct binding of histones to DNA and the determination of the DNA conformation.

It is surprising then that the protein secondary structure and DNA conformation of whole histone nucleohistones are nearly insensitive to the presence or absence of urea in the gradient reconstitution medium. It may be that the full complement of histones is able to interact producing a stable aggregate unit the characteristics of whose binding to DNA during gradient reconstitution are determined more by the protein-protein interactions than by protein-solvent interactions.

CHAPTER V  
SELECTIVITY OF HISTONE BINDING

INTRODUCTION

Results from a number of laboratories have indicated that the affinity of various histones is not the same for different DNAs or for the entire base pair population of a single species of DNA (65, 113, 114, 115, 116). Under conditions which promote the reversible association of polypeptide and DNA, Leng and Felsenfeld (113) observed that polylysine preferentially interacts with A·T base pairs while polyarginine selectively binds G·C pairs. Li et al. (65) also observed the A·T selectivity of polylysine binding when this polypeptide was annealed to DNA by salt gradient dialysis. Recently, Hwan et al. (114) have demonstrated that the chicken red blood cell histone H5 preferentially binds to A+T - rich C1. perfringens DNA in a mixture of C1. perfringens and M. luteus DNAs (31% and 70% G+C, respectively). The H5 histone is found exclusively in erythrocytes but is similar to the lysine - rich H1 in size, structure and high positive charge density. Combard and Vendrely (115) have reported that the lysine - rich histone H1 tends to be associated with A+T - rich DNA in vivo while the arginine-rich histones are associated with G+C - rich DNA. Clark and Felsenfeld (116) have also found the arginine - rich histones bound to a fraction of DNA in calf thymus chromatin which has a higher G+C content (75% G+C) than the overall average % G+C of the DNA (42% G+C).

It appears then that the binding of polylysine to DNA may serve as a model for the binding of the lysine - rich histone H1. Both of these

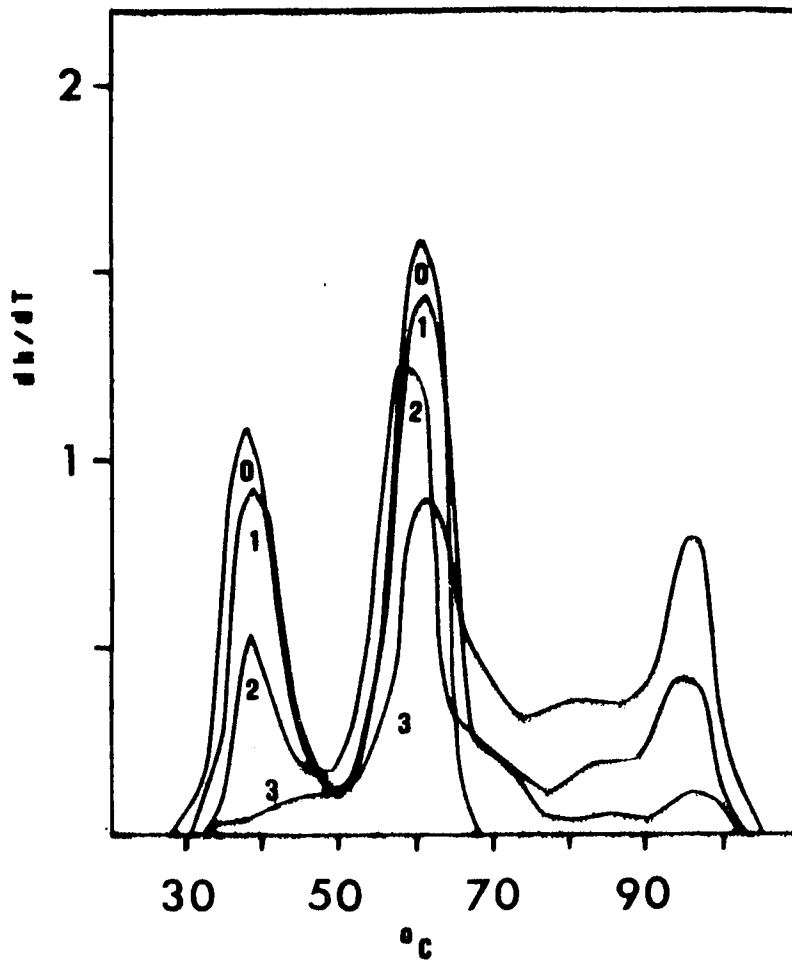
polycations have similar selectivities, solution conformations and interact primarily through ionic forces with the DNA. The arginine-rich histones and polyarginine select G+C-rich DNA under reversible binding conditions. Since the binding of the arginine-rich histones to DNA is believed to involve hydrophobic as well as ionic forces (110) it is possible to surmise that the hydrophobic residues of these histones are seeking out the more hydrophobic environment of the G·C pairs. Since polyarginine also preferentially binds G·C pairs, either hydrophobic binding is not of importance in the polyarginine-DNA interaction or the arginine residues are capable of hydrophobic interaction with the nucleic acid.

## EXPERIMENTAL

The experiments to be described below have been performed by mixing histones and two DNAs of different G+C content together in a medium of high salt or high salt plus urea. As the salt concentration is lowered by gradient dialysis, the histone interacts reversibly with the DNA and eventually binds. Since the G+C content of a DNA determines its melting temperature (65) the amount of each DNA remaining unbound in the mixture may be determined by thermal denaturation. In Figure 68 a mixture of C1. perfringens DNA and M. luteus DNA has been reconstituted with the slightly lysine-rich histone H2B. Free C1. perfringens DNA (31% G+C) and M. luteus DNA (70% G+C) have  $T_{ms}$  near  $37^{\circ}$  and  $61^{\circ}$  respectively. As each DNA is bound its free DNA peak decreases in amplitude and is replaced by a thermal transition at higher temperature. The area beneath each peak is equal to the integral of the  $dh/dt$  curve, the hyperchromicity between

Figure 58.

Histone H 2 B, *Cl. perfringens* and  
*M. luteus* DNAs in 0.25 mM EDTA, pH 8.0  
Salt, urea, tris reconstitution.  
 $r$  values indicated.



the high and low temperature boundaries of that transition.

It is possible then to quantitate the loss of DNA from each thermal transition by measuring the decrease in hyperchromicity between set temperatures. A natural trough is evident at 45°C - 50°C, between the Tms of the C1. perfringens and M. luteus DNAs. The interval selected to monitor the decrease in C1. perfringens melting is 30°C - 45°C, that for M. luteus DNA 50°C - 64°C. As the C1. perfringens DNA is bound, a small fraction of this DNA does melt in the 50°C - 64°C range. To correct for this effect the fraction of the C1. perfringens DNA melting between 50°C - 64°C relative to the fraction melting between 30°C - 45°C is estimated from the thermal denaturation profiles of histone - C1. perfringens DNA complexes. This factor is multiplied by the amount of C1. perfringens DNA melting between 30°C - 45°C in the mixed DNA complexes and is subtracted from the melting in the M. luteus range, 50°C - 64°C:

$$\Delta h_{(m, II)}^{calc} = \Delta h_{(m, II)}^{obs} - \left[ (\Delta h_{(P, II)} / \Delta h_{(P, I)}) \times (\Delta h_{(m, I)}^{obs}) \right] \quad (14)$$

Where:

$\Delta h_{(m, II)}^{calc}$  = calculated hyperchromicity in the mixture of DNAs (m) in the temperature interval II (50°C - 64°C).

$\Delta h_{(m, II)}^{obs}$  = observed hyperchromicity in the mixture in the temperature interval II.

$\Delta h_{(P, II)}$  = hyperchromicity in the second temperature interval in C1. perfringens DNA complexes.

$\Delta h_{(P, I)}$  = hyperchromicity in the first temperature interval in C1. perfringens DNA complexes.

$\Delta h_{(m, I)}^{obs}$  = hyperchromicity observed in the mixture of DNAs in Interval I, where none of the free or bound M. luteus DNA melts.

This correction is not perfect, since the amount of C1. perfringens DNA bound at a given histone / DNA ratio in a complex with C1. perfringens DNA alone is more than the amount of C1. perfringens DNA bound in the mixed DNA complexes. Since, however, at a ratio of  $r = 3 \text{ aa} / n$  less than 10% of the total hyperchromicity of the C1. perfringens complexes occurs in the  $50^{\circ}\text{C} - 64^{\circ}\text{C}$  range, the use of the correction of Equation 14 is warranted.

The effect of unequal amounts of each DNA in the competition mixture and the different hyperchromicities for the two DNAs can be mathematically compensated for by dividing the hyperchromicity observed or calculated for each temperature interval by the hyperchromicity within that interval in the free DNA mixture. A plot of  $\Delta h_{(r)} / \Delta h_{(r=0)}$  vs.  $r$  where:

$\Delta h_{(r)}$  = hyperchromicity difference of complex with input ratio  $r$  between defined temperature limits

$\Delta h_{(r=0)}$  = hyperchromicity difference of free DNA mixture ( $r=0$ ) in the same temperature interval

will quantitatively reflect the rate of decrease of each melting band with increasing amino acid per nucleotide coverage. Such a plot is shown in Figure 69. When histone H2B is reconstituted to C1. perfringens DNA

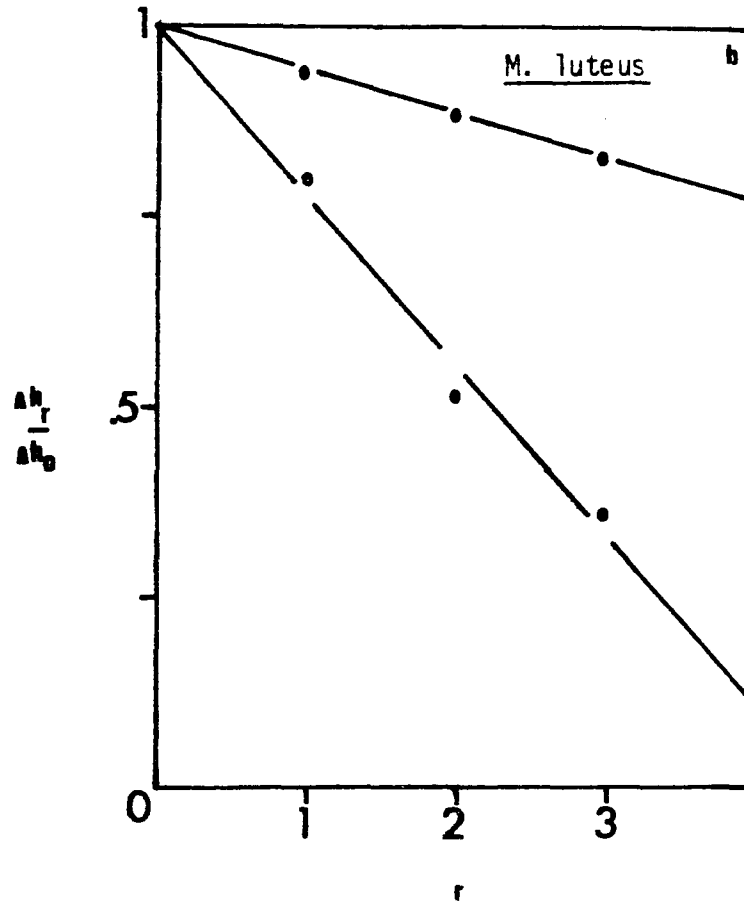
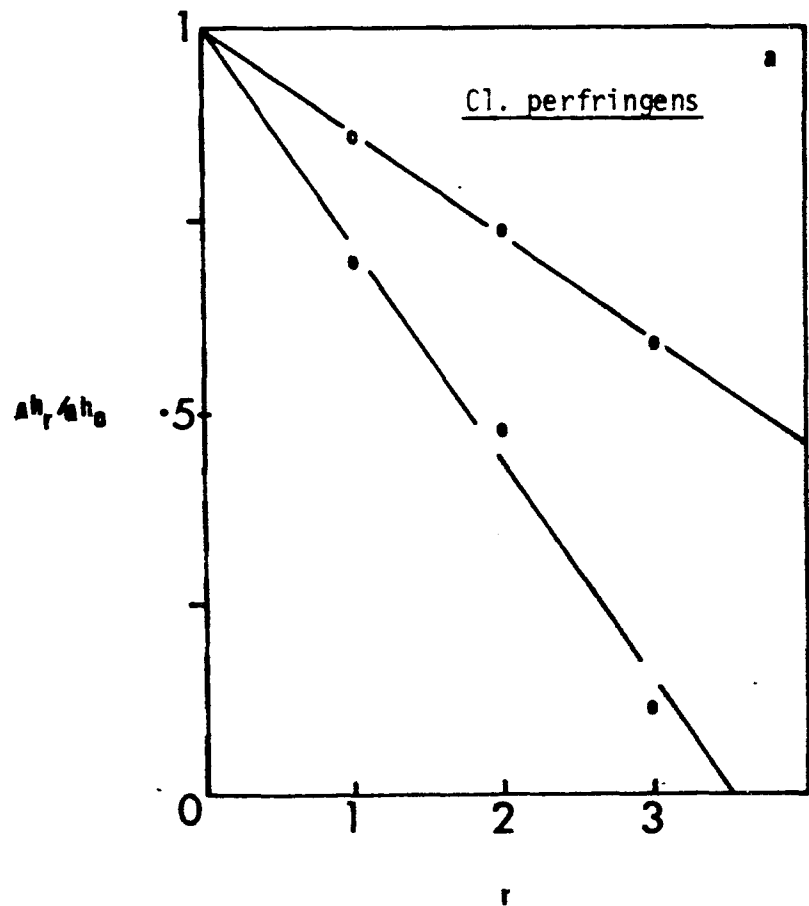


Figure 69. Selectivity of Histone H2 B binding to Cl. perfringens and M. luteus DNAs. Salt, urea, tris reconstitution.

$h_r/h_0$  = relative hyperchromicity  
 open circles = single DNA complexes  
 filled circles = mixed DNA complexes

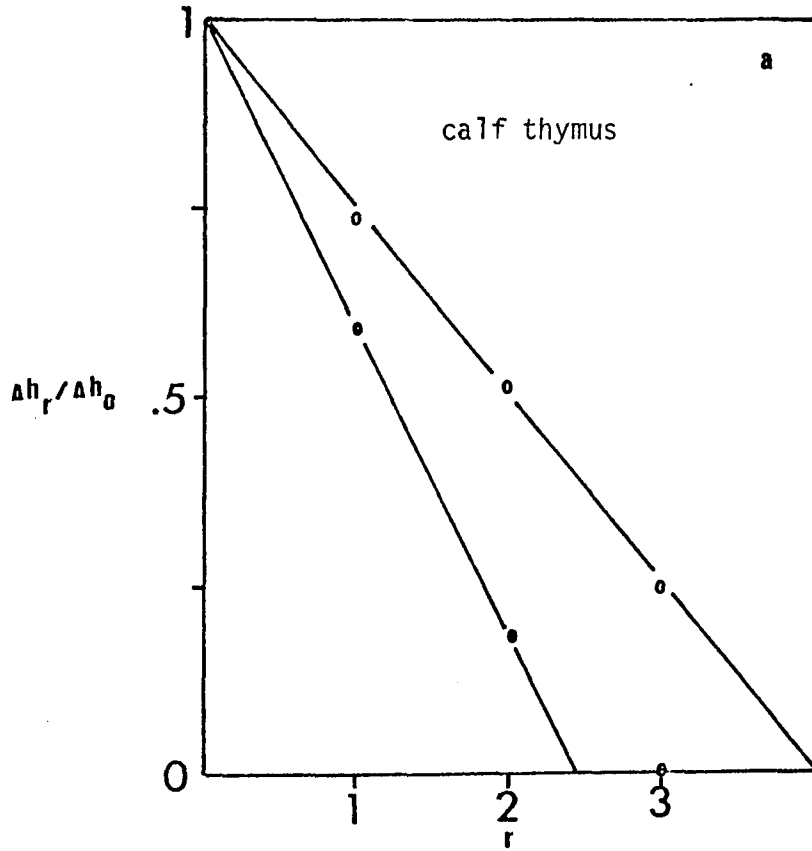
$P_{\bullet}$  slope =  $-.14$   
 $P_{\circ}$  slope =  $-.27$        $P_{\bullet} / P_{\circ} = 1.93$   
 $L_{\bullet}$  slope =  $-.21$   
 $L_{\circ}$  slope =  $-.06$        $L_{\bullet} / L_{\circ} = .29$

( all values  $\pm .02$  )

alone (Figure 69a, line  $P_0$ ) the rate of decrease, reflected in the selectivity slope,  $m_s$ , is  $-.14 \pm .02$ . When H2B is reconstituted to a mixture of Cl. perfringens and M. luteus DNAs, the Cl. perfringens  $m_s$  decreases to  $-.27 \pm .02$ . The ratio of the slopes of the lines  $P_\bullet$  and  $P_0$  is a measure of the preference of binding for the Cl. perfringens DNA. For H2B  $P_\bullet/P_0 = 1.93$ . A value of 2.00 would indicate perfect selectivity, while a value of 1.00 would result from binding with no A+T or G+C preference. Accordingly, the M. luteus DNA exhibits a ratio  $L_\bullet/L_0 = 1$ , i.e., it is selected against. Here,  $L_\bullet/L_0 = 0.29$  (Figure 69b). When calf DNA (42% G+C) and M. luteus DNA (70% G+C) compete for H2B (Figure 70a) the value  $C_\bullet/C_0 = 1.64$ . The decrease in the difference of G+C content between calf and M. luteus DNA (70% - 42% = 28%) relative to Cl. perfringens and M. luteus DNA (70% - 31% = 39%) results in a decrease in the selectivity for the A+T-rich DNA. That the difference in selectivity is due to the decrease in the difference in G+C content between the DNAs is illustrated by the graph of Figure 70b which shows that the ratio of the selectivity slopes for the DNA pairs Cl. perfringens + M. luteus and Cl. perfringens + calf thymus fall on a straight line which passes through the point of zero selectivity ( $P_\bullet/P_0 = 1$ ) at zero percent difference in G+C content. When calf + M. luteus DNAs compete for H2B in a reconstitution medium lacking urea, the selectivity of the histone for the A+T-rich calf DNA decreases to  $C/C_0 = 1.2$  (Figure 71). This indicates that in a reconstitution medium where hydrophobic self-interactions and intermolecular associations of histones are magnified the selectivity for A·T base pairs decreases.

When histone H2A is allowed to select between Cl. perfringens and

Figure 70.



a. Selectivity of histone H2B binding to calf thymus DNA and *M. luteus* DNA.

Salt, urea, tris reconstitution.

$h_r / h_0$  = relative hyperchromicity

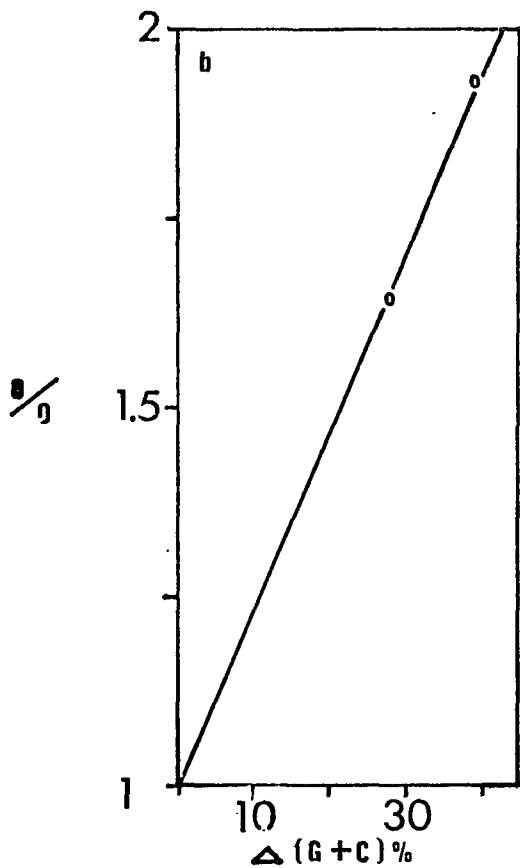
open circles = single DNA complexes

filled circles = mixed DNA complexes

$C_0$  slope = -0.25

$C_{\bullet}$  slope = -0.41

$C_{\bullet} / C_0 = 1.64$



b. Relation between selectivity [ $(\bullet/o)$ ] and difference in G+C content [ $\Delta(G+C)\%$ ]

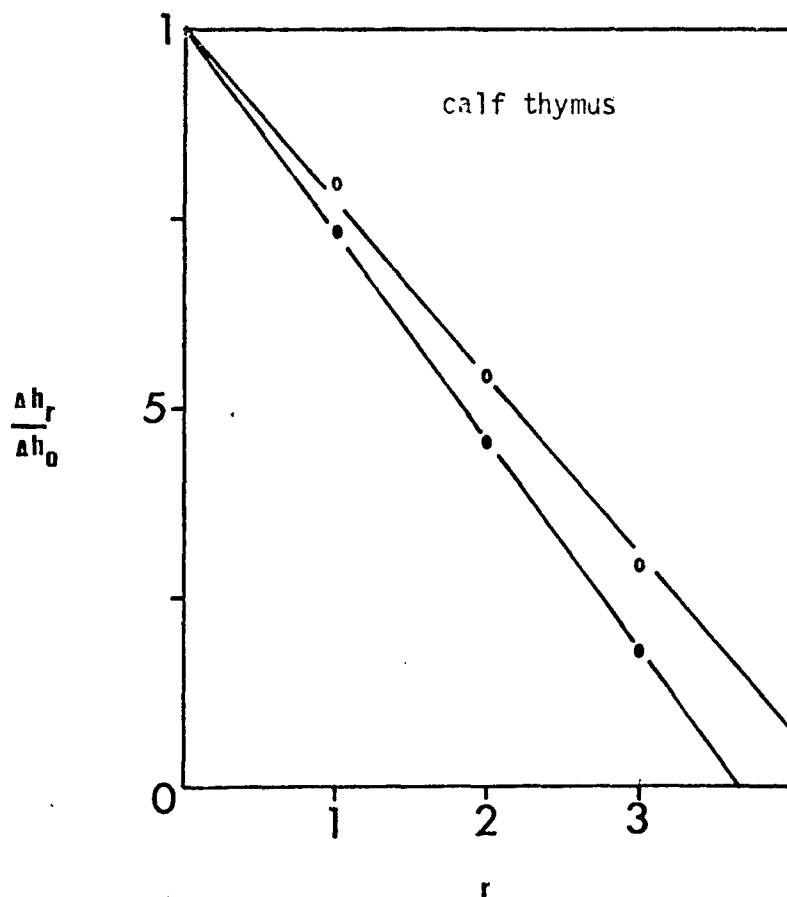


Figure 71. Selectivity of histone H2B binding to calf thymus and M. luteus DNAs.

Salt, tris reconstitution.

$h_r/h_0$  = relative hyperchromicity

open circles = single DNA complex

filled circles = mixed DNA complex

$C_o$  slope =  $-.23$

$C_{\bullet}$  slope =  $-.27$

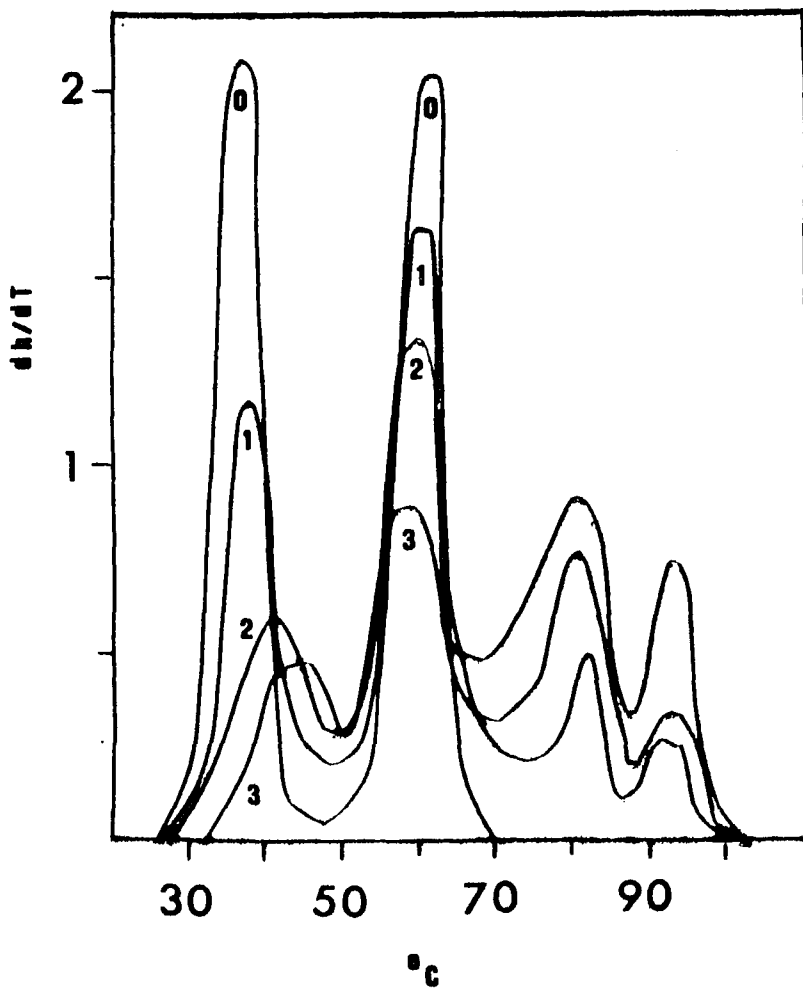
$C_{\bullet}/C_o = 1.2$

(all values  $\pm .02$ )

M. luteus DNAs in the presence of urea (Figure 72), the preference for Cl. perfringens DNA is not as great (Figure 73) as when histone H2B was the protein component of the mixture. The value  $P_{\bullet} / P_0$  for these complexes is 1.5, compared to 1.93 for H2B reconstitutions. It may be that the greater percentage of secondary structure inducing residues in H2A decreases its selectivity for the Cl. perfringens DNA. The hypothesis that the number of residues in ordered forms of secondary structure relates to the selectivity of histone binding is supported by the selectivity of complexes of histone H2 (H2A+H2B) with various DNAs (Figure 74). H2 chooses between Cl. perfringens and M. luteus DNA with a selectivity value  $P_{\bullet} / P_0 = 1.32$  (Figure 75). This is smaller than the selectivity value of either H2B ( $P_{\bullet} / P_0 = 1.93$ ) or H2A ( $P_{\bullet} / P_0 = 1.5$ ) for Cl. perfringens DNA over M. luteus DNA. D'Anna and Isenberg (32) have observed that the complexing and interaction of the histone fractions H2A and H2B with each other induces additional secondary structure in one or both partners of the aggregate. They find 15 residues of alpha-helix beyond that found in isolated, noninteracting histone H2A and H2B solutions. The additional secondary structure induced in the slightly lysine-rich histone pair may be responsible for the measured decrease in selectivity. When H2 selects between the synthetic double-stranded polymer poly dAT · poly dAT and calf DNA the selectivity value  $dAT_{\bullet} / dAT_0 = 1.35$  (Figure 76). The difference in G+C content for these DNAs is 42%. When Cl. perfringens and calf DNA (G+C = 11%) compete for histone H2 the selectivity value  $P_{\bullet} / P_0$  decreases to 1.15 (Figure 77). The results of the three selectivity complexes are summarized in Figure 78 which shows that, as with histone H2B, there is a linear dependence of the extent of

Figure 72.

Histone H 2 A, *Cl. perfringens* and  
*M. luteus* DNAs in 0.25 mM EDTA, pH 8.0  
Salt, urea, tris reconstitution.  
r values indicated.



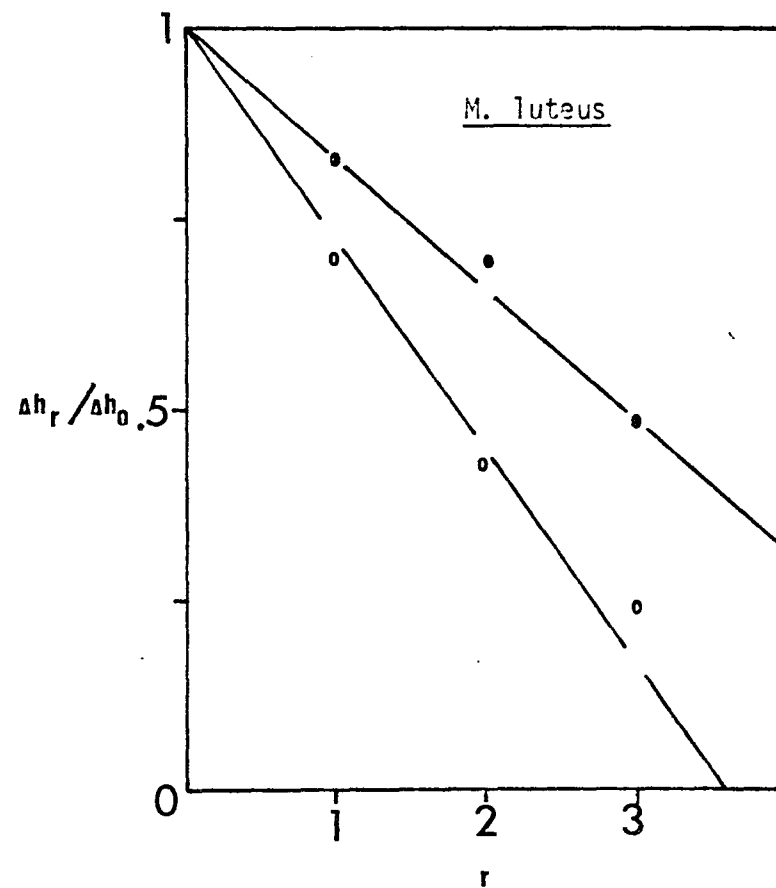
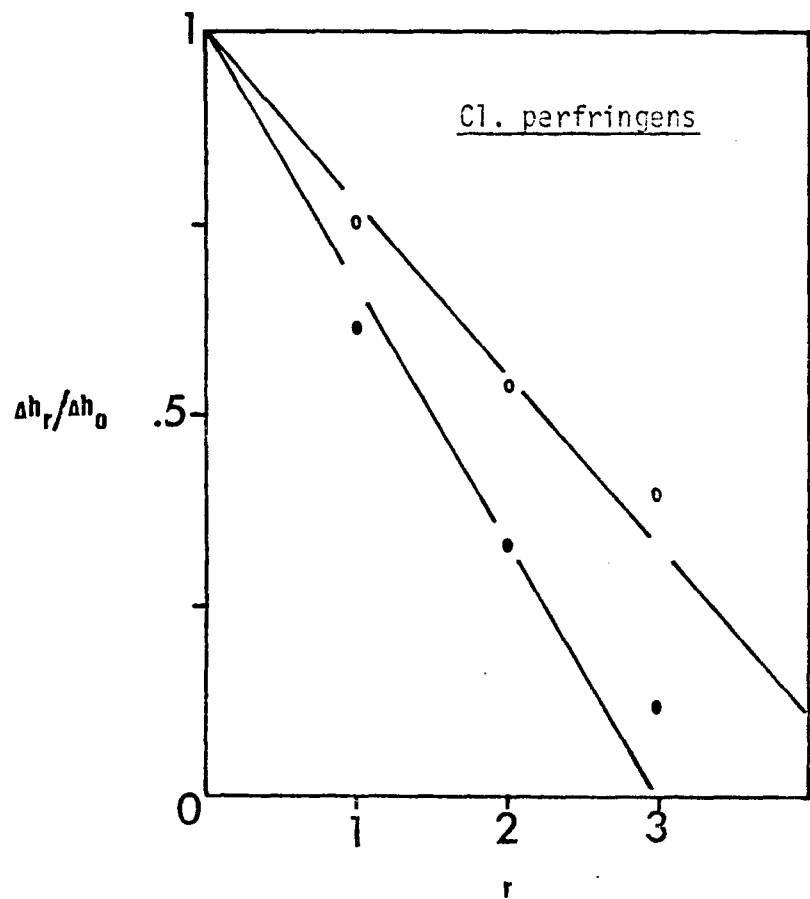


Figure 73. Selectivity of histone H2A binding to Cl. perfringens and M. luteus DNAs.

Salt, urea, tris treconstitutions.

$h_r / h_0$  = relative hyperchromicity

open circles = single DNA complex

filled circles = mixed DNA complex

$P_C$  slope =  $-.22$

$P_{\bullet}$  slope =  $-.33$

$L_C$  slope =  $-.28$

$L_{\bullet}$  slope =  $-.17$

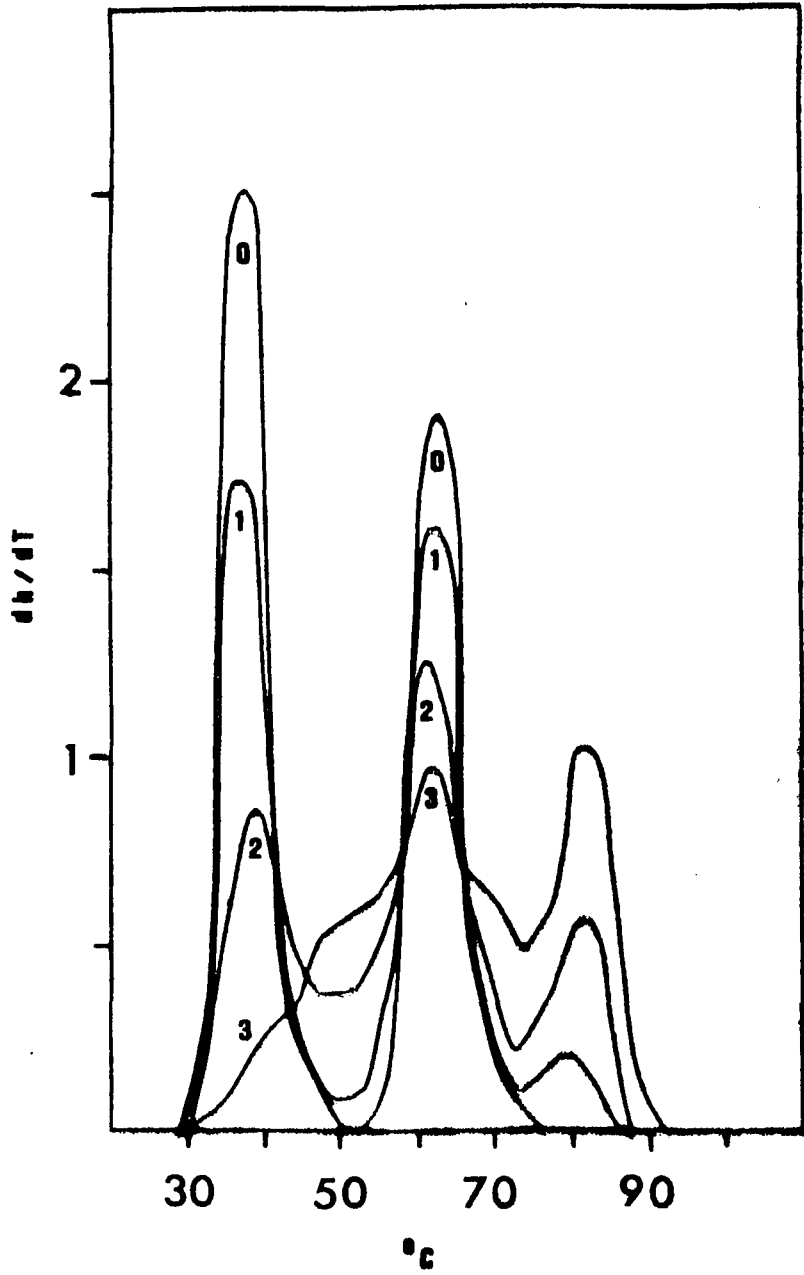
(all values  $\pm .2$ )

$P_{\bullet} / P_C = 1.5$

$L_{\bullet} / L_C = .61$

Figure 74.

Histone H 2, *Cl. perfringens* and  
*M. luteus* DNAs in 0.25 mM EDTA, pH 8.0  
Salt, urea, tris reconstitution.  
r values indicated.



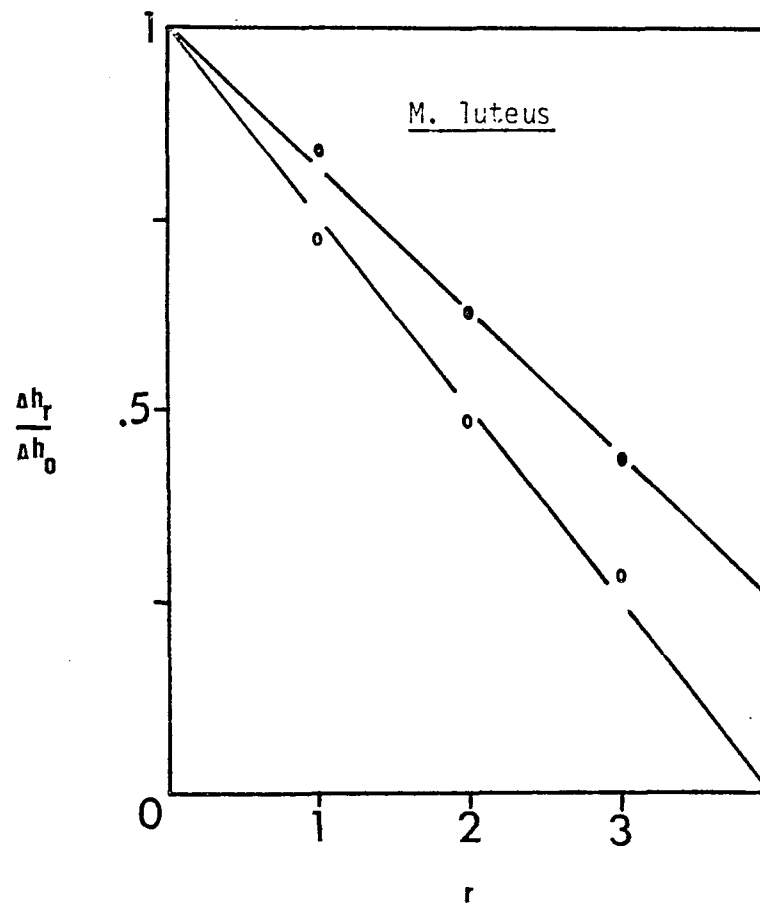
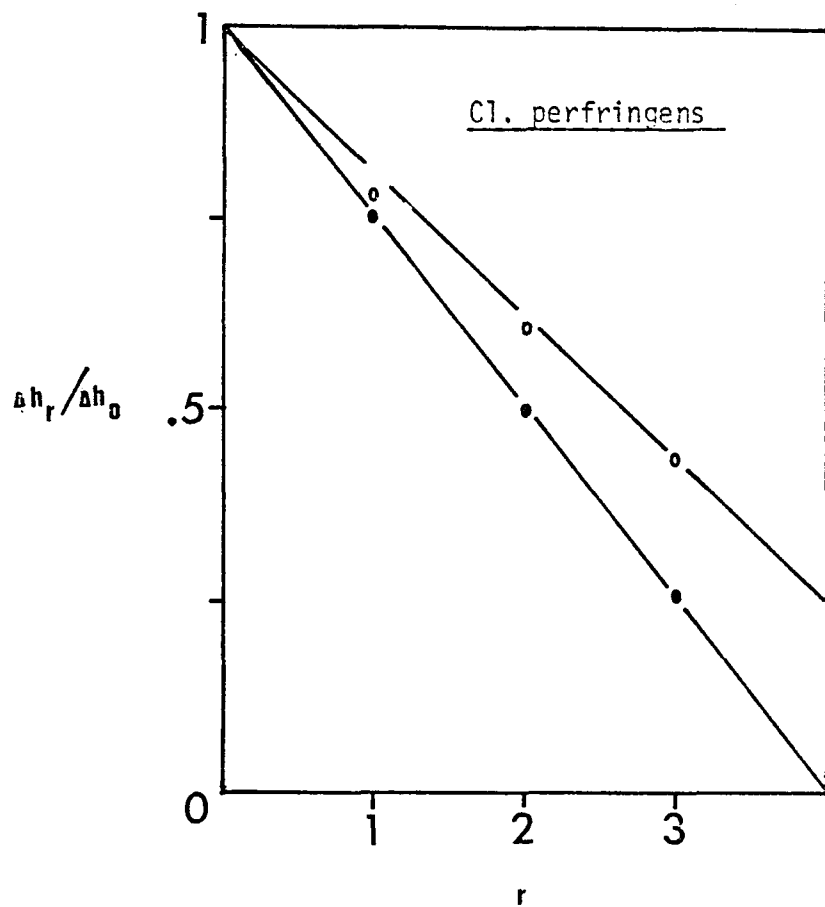


Figure 75. Selectivity of histone H2 binding to Cl. perfringens and M. luteus DNAs.  
Salt, urea, tris reconstitution.

$h_r/h_0$  = relative hyperchromicity  
 open circles = single DNA complex  
 filled circles = mixed DNA complex

$P_0$  slope =  $-.19$   
 $P_\bullet$  slope =  $-.25$        $P_\bullet / P_0 = 1.32$   
 $L_0$  slope =  $-.25$   
 $L_\bullet$  slope =  $-.19$        $L_\bullet / L_0 = .80$   
 (all values  $\pm .02$ )

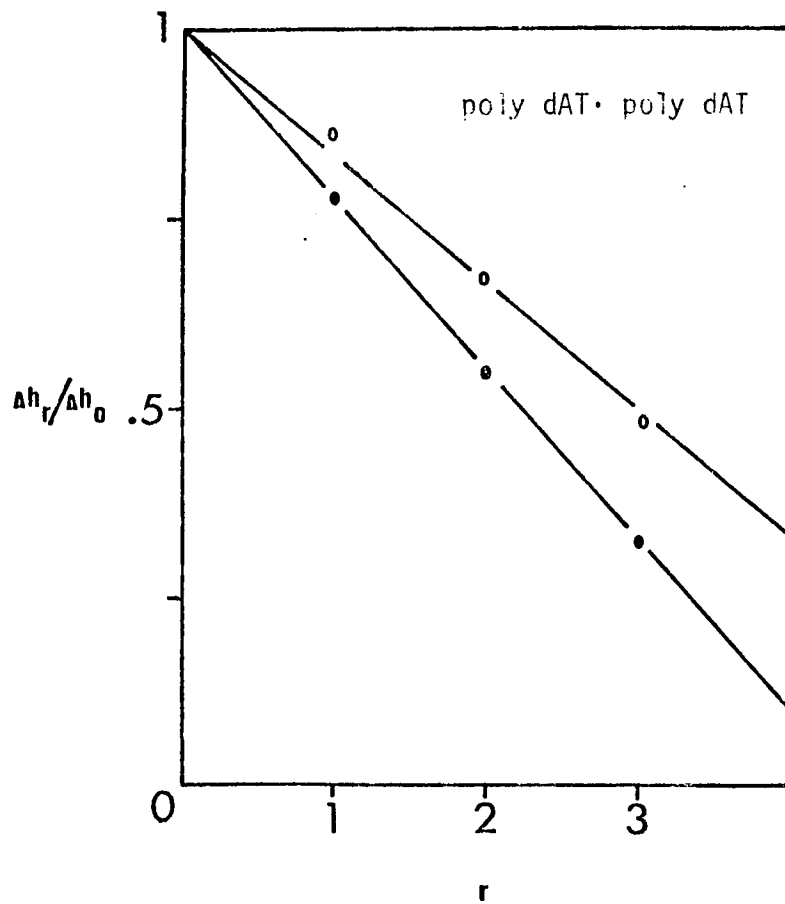


Figure 76. Selectivity of histone H2 binding to poly dAT · poly dAT and calf thymus DNA. Salt, urea, tris reconstitution.

$h_r/h_0$  = relative hyperchromicity

open circles = single DNA complex

filled circles = mixed DNA complex

poly dAT · poly dAT ○ slope = -0.17

poly dAT · poly dAT ● slope = -0.23

poly dAT · poly dAT ● / poly dAT · poly dAT ○ = 1.35

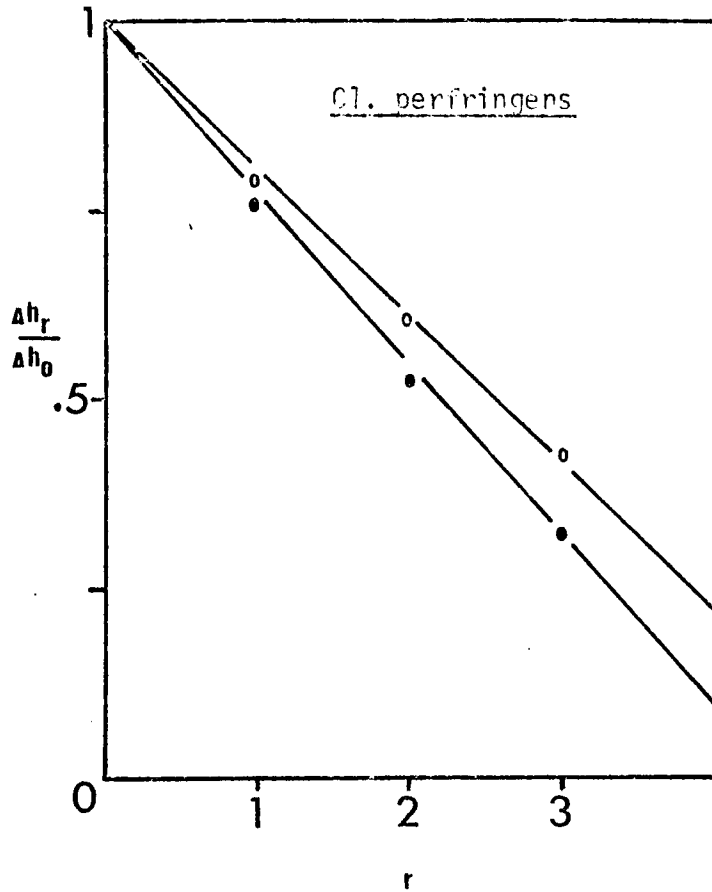


Figure 77. Selectivity of histone H2 binding to Cl. perfringens and calf thymus DNA.

salt, urea, tris reconstitution.

$h_r / h_0$  = relative hyperchromicity

open circles = single DNA complex

filled circles = mixed DNA complex

$P_0$  slope =  $-.2$

$P_{\bullet}$  slope =  $-.23$   $\frac{P_{\bullet}}{P_0} = 1.15$

( all values  $\pm .02$  )

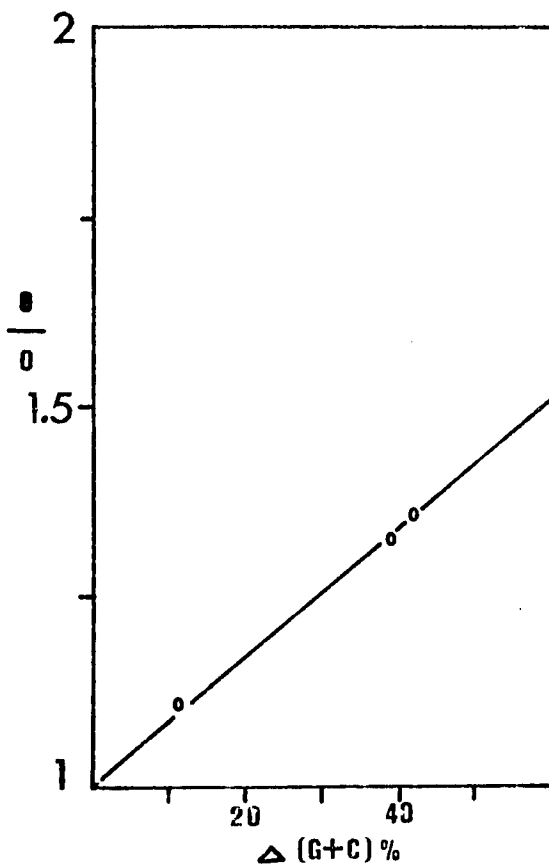


Figure 78. Relation between selectivity and difference of G+C %.

selectivity on the difference in G+C content,  $\Delta(G+C)\%$ , between the competing DNAs. The selectivity values each fall on a straight line which intersects zero selectivity,  $\Delta h_{(r)} / \Delta h_{(0)} = 1.0$ , at 0%  $\Delta(G+C)$ . As with H2B complexes, when urea is omitted from the reconstitution mixture the selectivity of the histone decreases (Figure 79) relative to the plus-urea competition.

The selectivity of whole-H1 histone is seen to be even less than that of the histone H2 pair (Figure 80). In *Cl. perfringens* vs. *M. luteus* complexes the value  $P_{\bullet} / P_0 = 1.24$  (Figure 81). When urea is excluded from the reconstitution medium the value  $P_{\bullet} / P_0 = 1.19$  (Figure 82). This represents a decrease of ca. 4% due to the omission of urea. In H2B competitions the decrease in the selectivity value upon deletion of urea is ca. 37% while in H2 complexes the omission of urea leads to a decrease of ca. 14%. This trend suggests that in the series H2B > H2 > whole-H1 the hydrophobic interactions between histones are progressively more stable so that the inclusion or deletion of urea has a reduced effect.

When whole histone is reconstituted to a mixture of *Cl. perfringens* and *M. luteus* DNA (Figures 83, 84), or *Cl. perfringens* and calf thymus DNA (Figure 85), or *Cl. perfringens* and *E. coli* DNA (Figure 86) the value of the selectivity quotient  $P_{\bullet} / P_0$  remains constant at ca. 1.15. Evidently the preference of A+T-rich DNA is so small that differences between these various competing sets are obliterated. When urea is excluded from the reconstitution protocol (Figure 87) the selectivity value still remains at 1.15. The lack of any observable difference in the preference of whole histone for DNAs of different G+C content with and without urea further supports the contention that the interactions of the histones increase the amount of ordered secondary structure within the histone

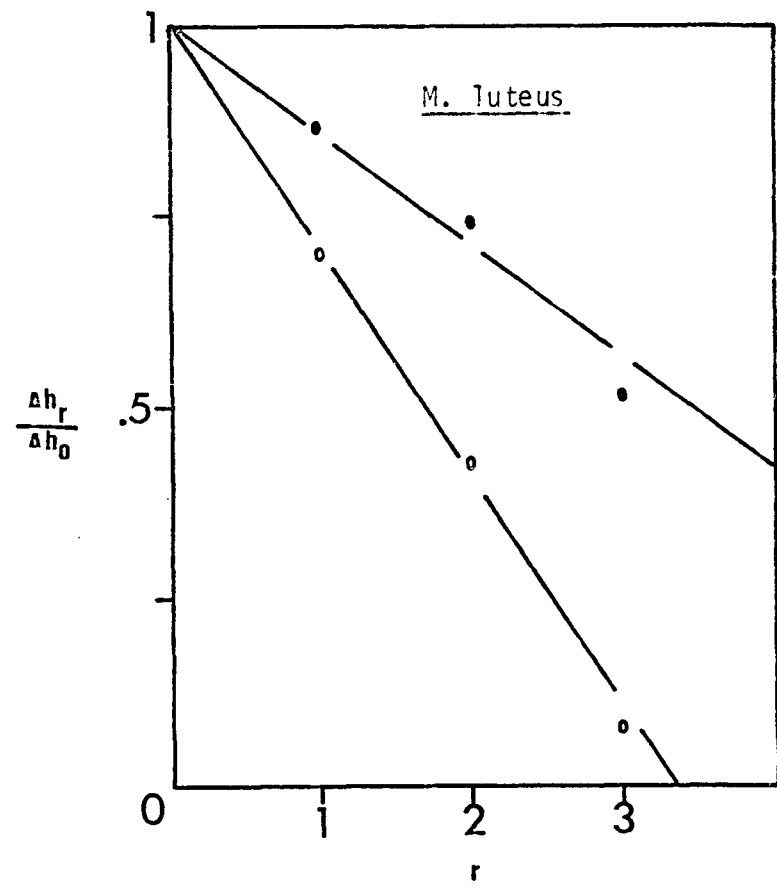
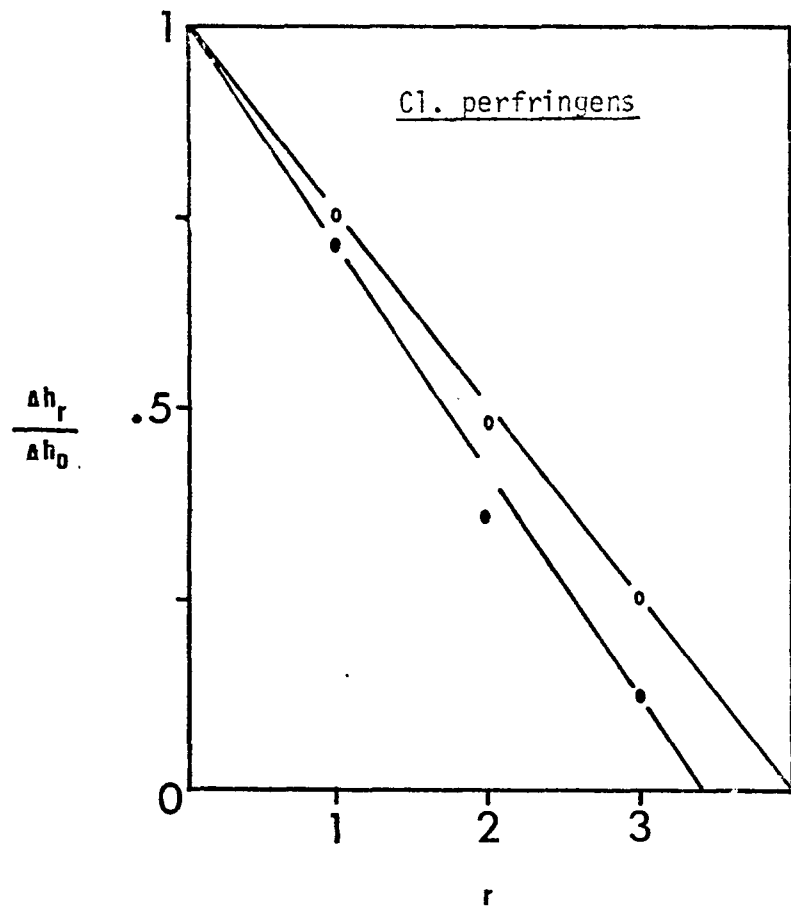


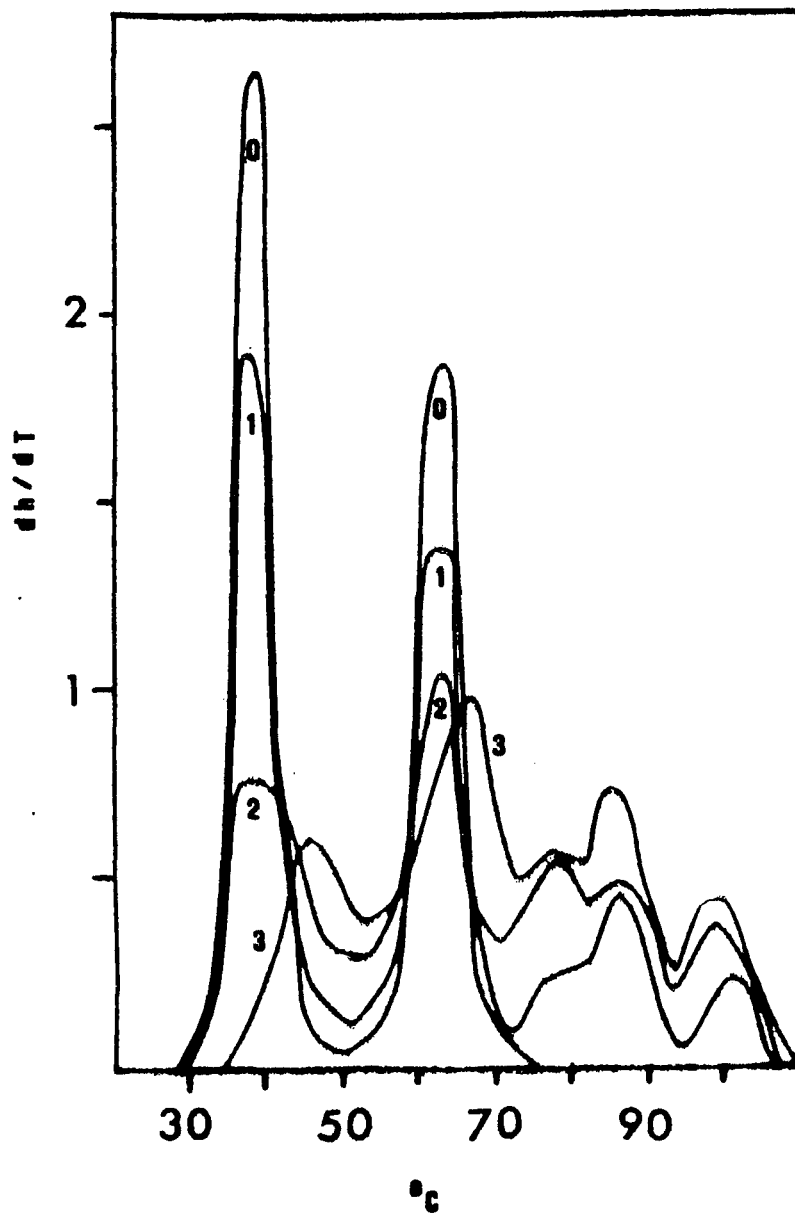
Figure 79. Selectivity of histone H2 binding to Cl. perfringens and M. luteus DNAs. Salt, tris reconstitution.

$h_r/h_0$  relative hyperchromicity  
 open circles = single DNA complex  
 filled circles = mixed DNA complex

P ● slope = -.25  
 P ● slope = -.29      P ● / P ● = 1.16  
 L ● slope = -.3  
 L ● slope = -.15      L ● / L ● = .50  
 (all values  $\pm .02$ )

Figure 80.

Whole histone - H 1, *Cl. perfringens* and  
*N. luteus* DNAs in 0.25 mM EDTA, pH 8.0  
Salt, urea, tris reconstitution.  
r values indicated.



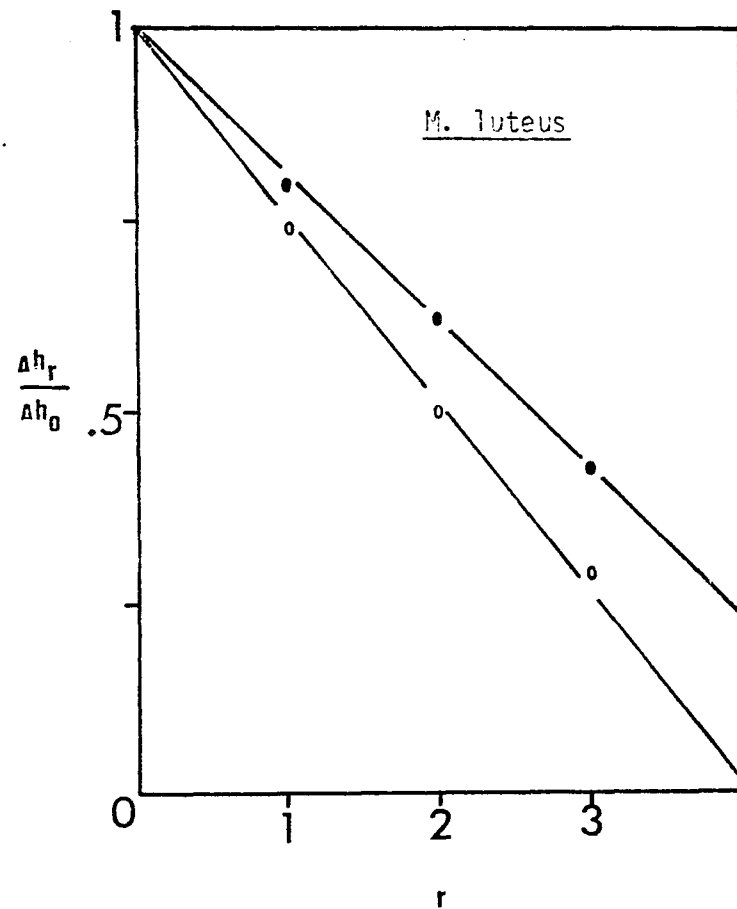
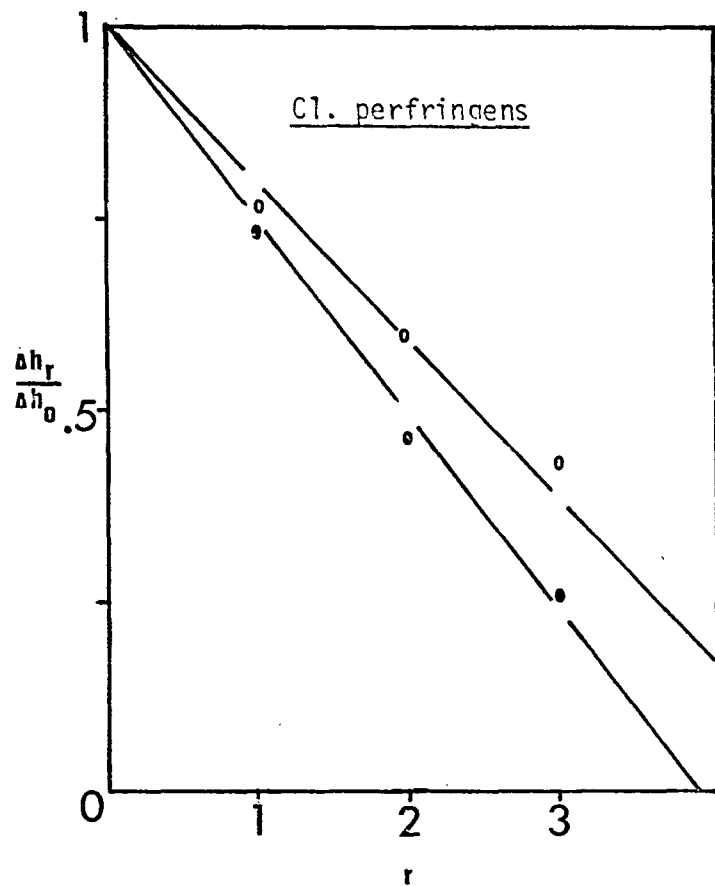


Figure 81. Selectivity of Whole - H1 histone binding to Cl. perfringens and M. luteus DNAs.

Salt, urea, tris reconstitution.  
 $h_r / h_0$  = relative hyperchromicity  
 open circles = single DNA complex  
 filled circles = mixed DNA complex

$P_{\bullet}$  slope =  $-.21$   
 $P_{\circ}$  slope =  $-.26$        $P_{\bullet} / P_{\circ} = 1.24$   
 $L_{\circ}$  slope =  $-.19$   
 $L_{\bullet}$  slope =  $-.25$        $L_{\bullet} / L_{\circ} = .76$   
 (all values  $\pm .02$ )

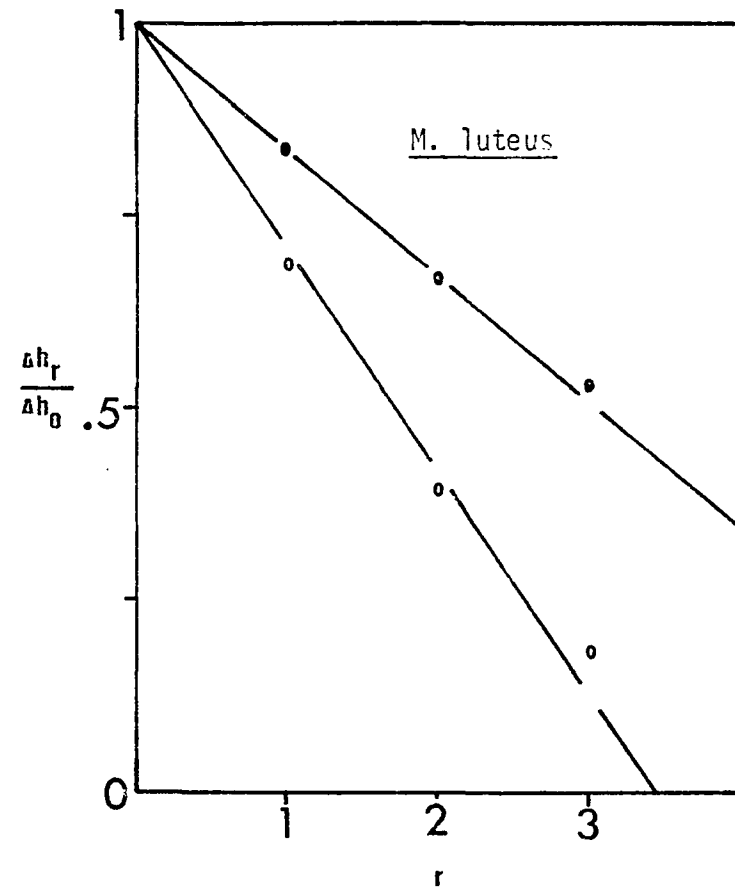
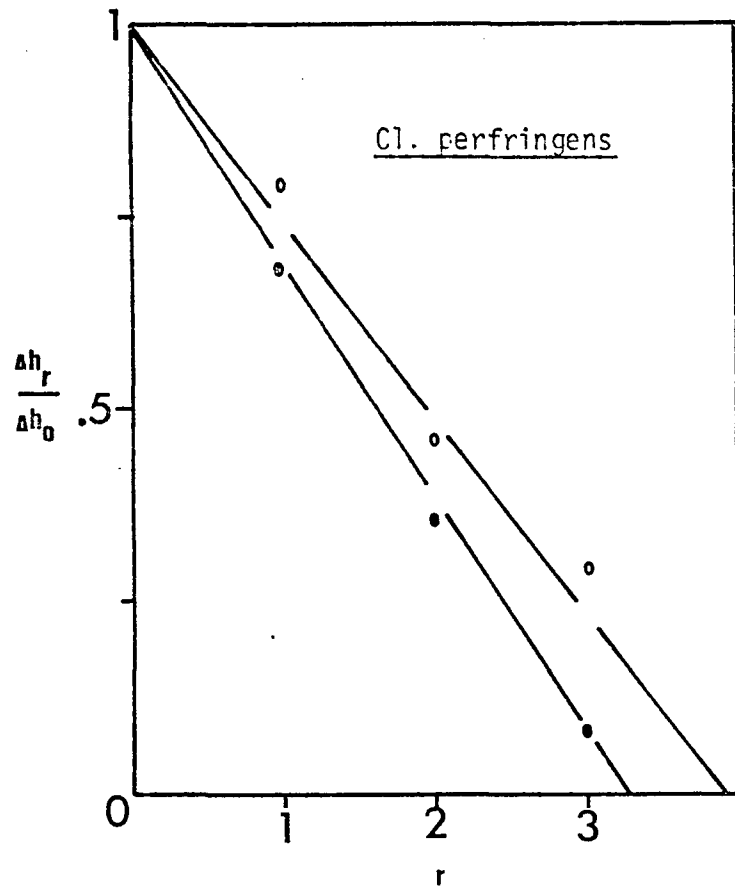


Figure 82. Selectivity of Whole - H1 histone binding to Cl. perfringens and M. luteus DNAs.

Salt, tris reconstitution.

$h_r / h_0$  = relative hyperchromicity

open circles = single DNA complex

filled circles = mixed DNA complex

$P_{\bullet}$  slope =  $-.26$

$P_{\circ}$  slope =  $-.31$

$L_{\bullet}$  slope =  $-.29$

$L_{\circ}$  slope =  $-.17$

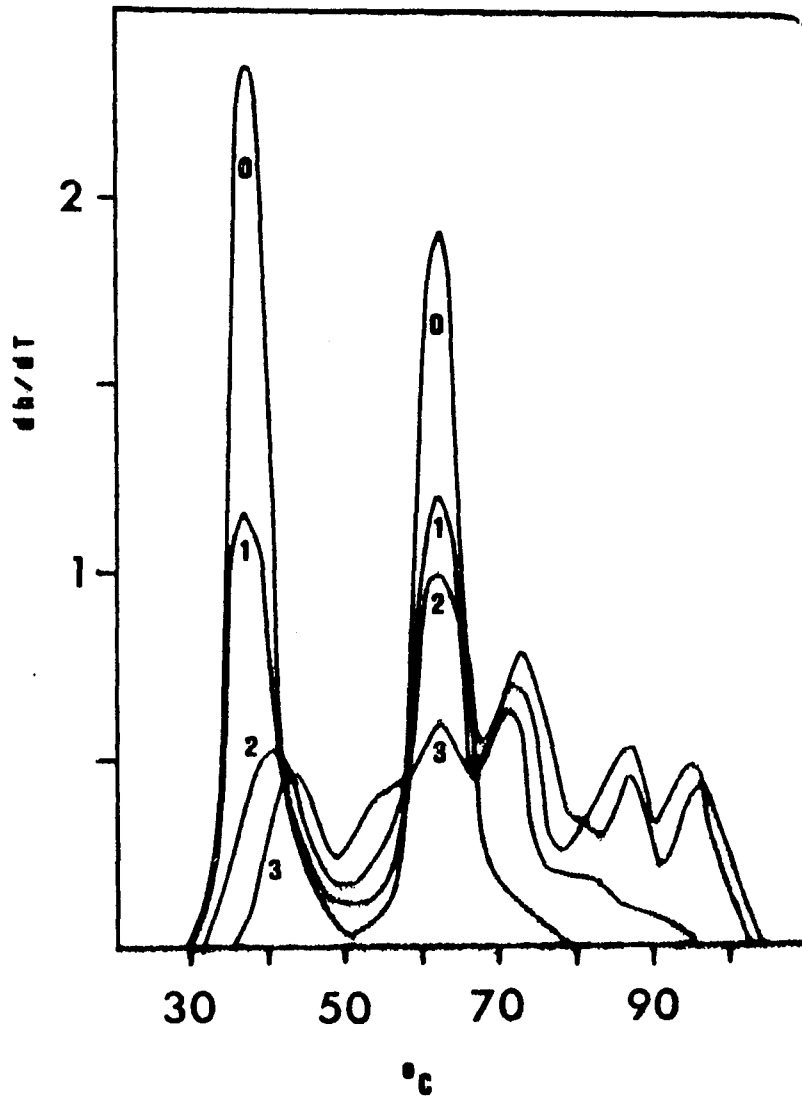
( all values  $\pm .02$  )

$P_{\bullet} / P_{\circ} = 1.19$

$L_{\bullet} / L_{\circ} = .59$

Figure 83.

Whole histone, *Cl. perfringens* and  
*M. luteus* DNAs in 0.25 mM EDTA, pH 8.0  
Salt, urea, tris reconstitution.  
r values indicated.



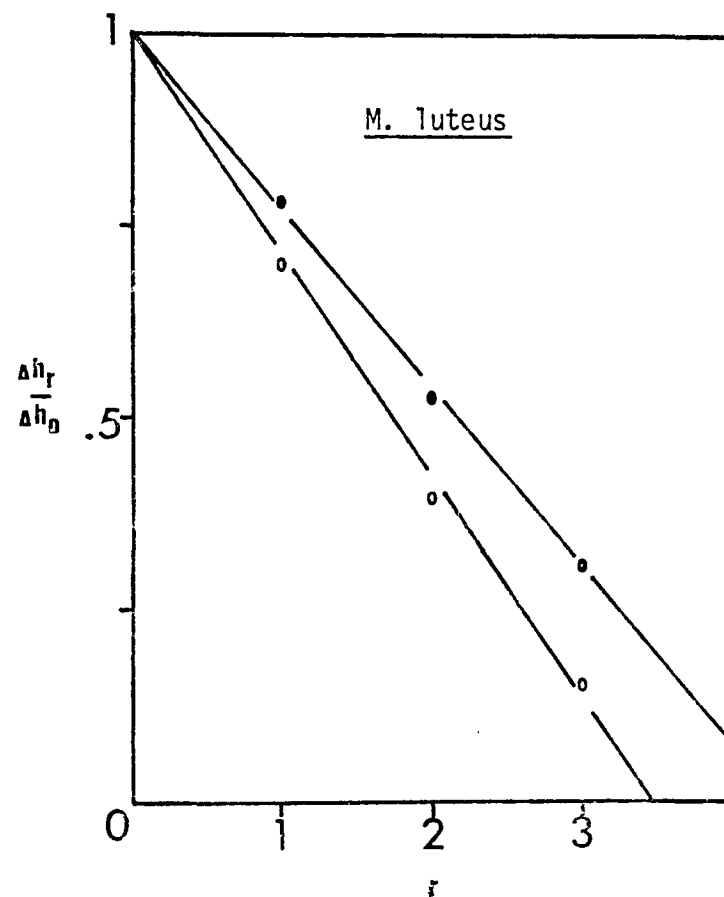
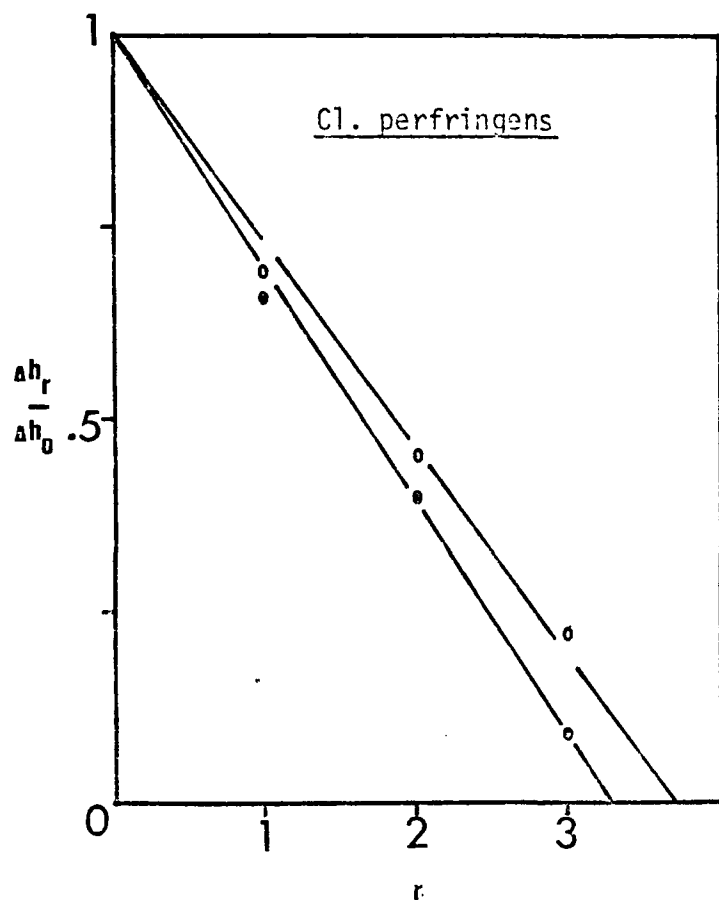


Figure 84. Selectivity of whole histone binding to Cl. perfringens and M. luteus DNAs.  
 Salt, urea, tris reconstitution.  
 $h_r / h_0$  = relative hyperchromicity  
 open circles = single DNA complexes.  
 filled circles = mixed DNA complexes.

$P_{\bullet}$ slope = $-.27$	$P_{\bullet} / P_{\circ} = 1.15$
$P_{\circ}$ slope = $-.31$	
$L_{\bullet}$ slope = $-.29$	$L_{\bullet} / L_{\circ} = .79$
$L_{\circ}$ slope = $-.23$	
( all values $\pm .02$ )	

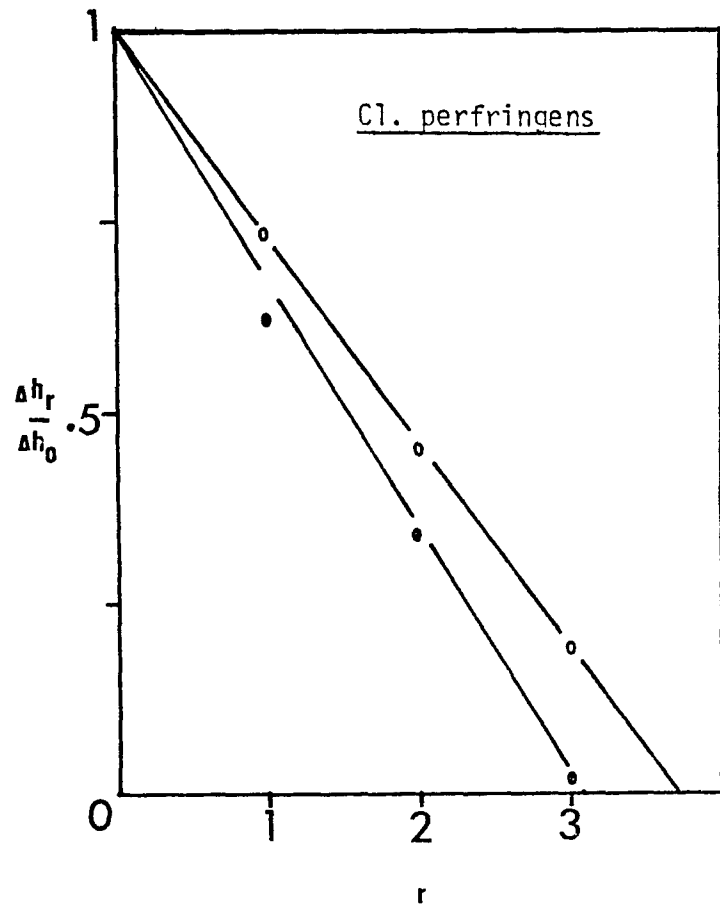


Figure 85. Selectivity of Whole histone binding to Cl. perfringens and calf thymus DNAs.

$h_r / h_0$  = relative hyperchromicity  
 open circles = single DNA complex  
 filled circles = mixed DNA complex  
 $P_{\bullet}$  slope =  $-.27$   
 $P_{\circ}$  slope =  $-.32$   
 $P_{\bullet} / P_{\circ} = 1.17$

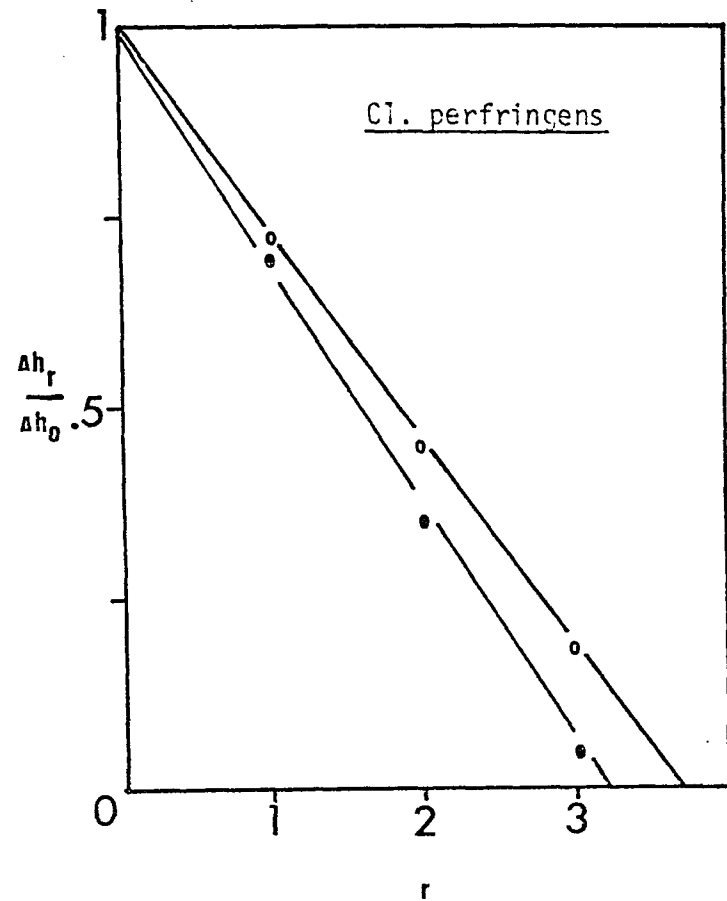


Figure 86. Selectivity of whole histone binding to Cl. perfringens and E. coli DNAs.

$P_{\bullet}$  slope =  $-.27$   
 $P_{\circ}$  slope =  $-.31$   
 $P_{\bullet} / P_{\circ} = 1.15$

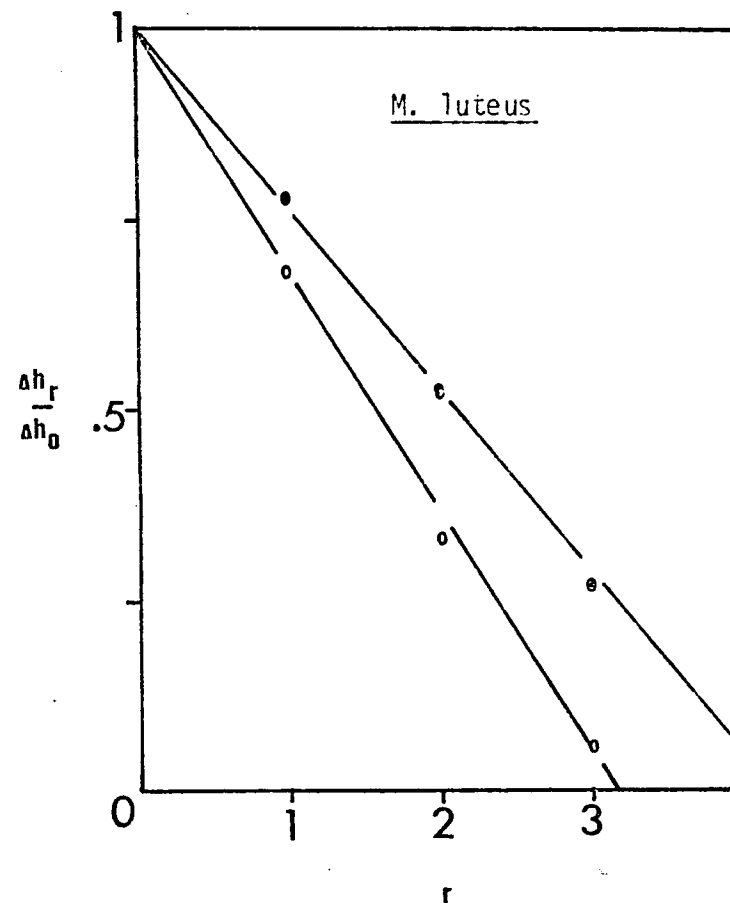
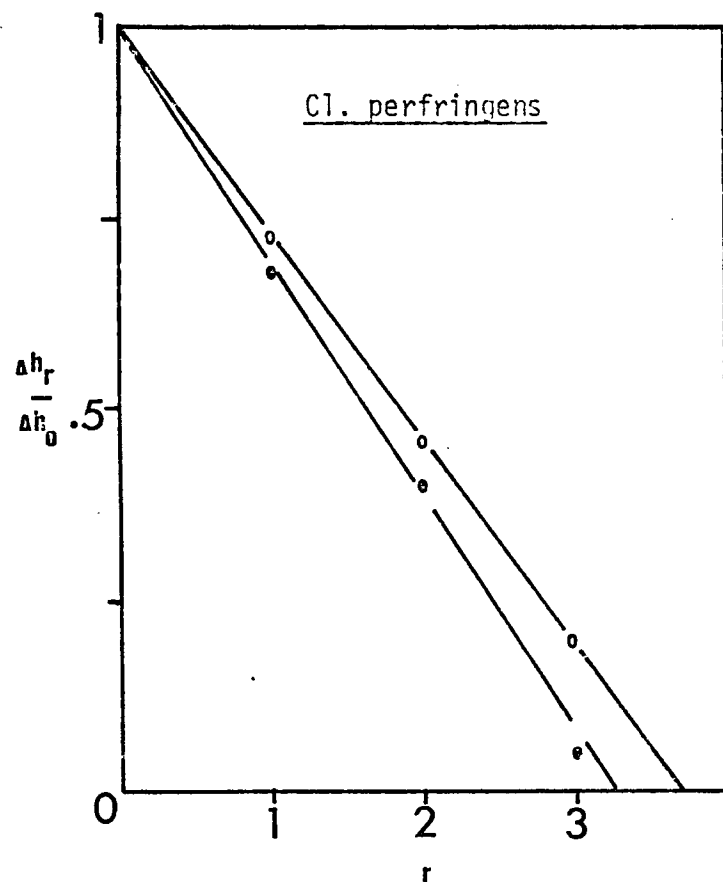


Figure 87. Selectivity of whole histone binding to Cl. perfringens and M. luteus DNAs.

Salt, tris reconstitution.

$h_r/h_0$  = relative hyperchromicity

open circles = single DNA complex

filled circles = mixed DNA complex

P<sub>o</sub> slope = -.27

P<sub>•</sub> slope = -.31

L<sub>o</sub> slope = -.32

L<sub>•</sub> slope = -.24

P<sub>•</sub> / P<sub>o</sub> = 1.15

L<sub>•</sub> / L<sub>o</sub> = .75

(all values  $\pm$  .02)

unit which in turn stabilizes the histone - histone and histone - DNA hydrophobic associations and leads to decreased selectivity for the relatively more hydrophilic A • T pairs.

## CHAPTER VI

### DISCUSSION

The basic assumption underlying the work described herein is that in vitro experiments may reproduce some features of the in vivo chromatin system despite major differences in the packing and concentration of the genetic material. Evidence that this assumption is nonetheless valid comes from experiments with in situ chromatin or whole cells or nuclei which compare favorably with in vitro results. For example, nuclei may be digested with endogenous or exogenous nucleases and the DNA product found to contain fragments of discrete size classes (45). The same result is observed when isolated chromatin is digested in vitro (46). When histone crosslinking agents are administered to whole cells or isolated chromatin, the histone dimers produced are identical in each case (38, 39). In addition, histone-histone interactions in solution have been shown to favor complexes of the identical histones obtained in crosslinked form from nuclei (28-32). These results suggest that the histone-DNA and histone-histone interactions occurring in chromatin in vivo can be reproduced in vitro. The experiments described in this dissertation represent an attempt to investigate some of the dominant forces involved in the maintenance of chromatin structure by reconstituting various species of histones to DNA.

Reconstituted nucleohistones exhibit thermal profiles which are quite similar despite the origin of the DNA component. Each melting spectrum shows a low temperature melting band associated with the helix-coil transition of free DNA, two melting bands at higher temperature

representing the melting of histone-bound DNA, and a region of intermediate melting of variable extent (63). The retention of this general pattern in all the nucleohistone complexes implies a similarity in the histone-DNA interactions of each complex. In concert with the changes observed in the conformations of the histones and DNA by circular dichroism, modifications of the melting pattern of the nucleohistone complex have been used to investigate the characteristics of the histone-histone and histone-DNA interaction. When histones H2A, H2B or H2 (H2A + H2B) are reconstituted to DNA the thermal denaturation profile of each complex shows the four main thermal transitions described above. The H2A nucleohistones have relatively more intermediate melting than the H2B or H2 nucleohistones. Of these three species of histone, H2A has the greatest tendency to self-interact and aggregate. Accordingly, the  $A_{320}/A_{260}$  values for nucleohistone H2A complexes prepared with or without urea is greater than for any other nucleohistone complex described here (Table 3). Due to the extensive self-interaction it is not possible to derive a  $\beta$  value for the H2A nucleohistones. The cause of the large amount of melting observed between  $T_m$  and  $T_{mII}$  probably arises from some aspect of this histone-histone interaction. When histone H2B binds DNA, less of the nucleohistone is denatured in the intermediate temperature range. The  $\beta$  value for nucleohistone H2B is ca. 4.2 aa/n. It should be noted that nucleohistones constructed with different DNAs have  $r$  vs.  $F$  (fraction of DNA bound) values which are colinear, indicating a similarity in the way the histone binds to the mammalian and bacterial nucleic acids. When histone H2B is reannealed to DNA in the absence of urea the  $\beta$  value of the nucleohistone increases, indicating an inter-

action between histone molecules which allows a greater amount of protein bound to a given segment of DNA. At the same time, the melting temperature of melting band III decreases. This may be due to the repulsion between like - charged amino acid residues leading to a decrease in the extent of neutralization of the DNA phosphates. Prior to annealing, the DNA and histone are in a high salt environment which precludes binding and reduces the effect of like - charge repulsion on the histone. The high ionic strength of the medium also intensifies hydrophobic intramolecular and intermolecular interactions. A decreasing salt gradient allows histone - DNA binding, however, the protein has bound the DNA in a more compacted state. Further decreases in the ionic strength of the medium coupled with the hydrophobic microenvironment of histones within the DNA helix serve to magnify the repulsion of those charged residues not fully neutralized by complexing. Thus the histone is not able to stabilize the DNA to as high a temperature as if it had bound the DNA while in a urea - induced, relaxed random coil conformation. Examination of the  $m_d$  values of the minus - urea complexes shows a reduction in the ability of those residues in ordered secondary structures to deform the DNA relative to plus - urea complexes. Evidently they are more involved in histone - histone rather than histone - DNA interaction. The CD spectra of the H2B nucleohistone support this conclusion. In the minus - urea complexes, there is more secondary structure observable in the region of protein response (200 nm - 250 nm) but less reduction of the 275 nm peak amplitude which would indicate a B form to C form transition.

Similar effects are observed in H2 nucleohistones. When reconstituted in 5 M urea, 2 M NaCl, NaEDTA, nucleohistone H2 exhibits a thermal denaturation profile whose shape is qualitatively similar to that of chromatin,

although the melting temperatures in nucleohistone H2 are elevated. The CD spectrum of the H2 nucleohistone also displays features similar to the CD of chromatin, namely a large negative trough near 220 nm and a reduced 275 nm positive peak. When histone H2 is reconstituted to DNA from 2 M NaCl, NaEDTA, however, the TmIII thermal transition is severely reduced, and, while more secondary structure is evident in the CD spectrum, less of a B to C deformation is observed in the long wavelength region. As with nucleohistone H2B the  $\beta$  value of the minus-urea complex is increased relative to the plus-urea reconstitute. This may be due to the tendency of the slightly lysine-rich histone pair to form oligomers,  $(H2A - H2B)_n$ , in solution (42).

The  $m_d$  values of H2B, H2A and H2 all decrease in minus-urea complexes relative to plus-urea complexes. The amount of reduction in the  $\Delta\epsilon_{278} / -\Delta\epsilon_{246}$  response to increases in secondary structure (monitored at 220 nm) decreases in the order H2B (140% decrease) > H2A (80% decrease) > H2 (14% decrease). This indicates that the binding to H2B to DNA in high salt is more different from its binding in salt-urea than the binding of H2A or H2 which characteristically have more hydrophobic nature. This interpretation is supported by the finding that the formation of a complex of the slightly lysine-rich histones induces additional secondary structure in one or both members of the complex (32). Furthermore, the reconstitution of nucleohistone H2 in salt-urea-phosphate results in a 22% increase in the ability of those hydrophobic residues involved in regions of ordered secondary structure to induce the B to C transition in DNA. Presumably, in the salt-urea-phosphate medium the histones are disordered. Lowering of the salt concentration allows binding but in an extended form due to the presence of urea. When

the urea is dialysed away the hydrophobic residues respond to the effect of phosphate buffer which induces regions of ordered secondary structure. These localized hydrophobic regions may now interact but in doing so they deform the DNA to which they are anchored. Evidently, the hydrophobic interactions which occur after the histone has bound the DNA contribute more to the distortion of the B form structure while those hydrophobic interactions which take place prior to binding have a greater effect on the conformation of the histone. When the H2 histone pair is complexed with DNA by direct mixing in low ionic strength buffer the histone and DNA interact irreversibly and ionically. The result is that although large amounts of helix or beta type structures are evident in the CD spectra, little change in the DNA conformation is observed. If the histones and DNA are dissolved in a buffer of physiological ionic strength (0.15 M NaCl) prior to complexing significant conformational distortion of the DNA occurs although the amount of protein secondary structure in the complex is much less than in the complexes made by direct mixing at low ionic strength. Once the 0.15 M NaCl is dialysed away, however, the effect of the histone on the DNA conformation decreases severely while the conformation of the histone is altered from one containing significant amounts of beta structure to a conformation similar to that found in complexes prepared by low ionic strength direct mixing, i.e., alpha helix and random coil. These results illustrate the dynamic nature of the conformation of the histone. Further evidence for this conclusion comes from nucleohistone H2 complexes prepared in the absence of urea but mixed with urea after annealing. Although urea causes no net shift of protein from one bound DNA region to another, the conformation of the bound histone is altered so that on

removal of the urea and thermal denaturation of the complex the decreased stability of the histone-bound DNA regions is apparent. Evidently the histone interactions which occur during the original minus-urea reconstitution are of a stable nature. Disruption of these interactions while the histones are bound may allow some freedom of motion in the DNA helix. On urea removal the histones are no longer able to reestablish those associations which promote the stability of DNA binding.

As the decrease in  $m_d$  values and the ionic nature of the histone-DNA binding follows the series  $H2B > H2A > H2$ , so does the selectivity of each histone species for A+T-rich DNA. The selectivity values are  $H2B = 1.93$ ,  $H2A = 1.5$ ,  $H2 = 1.32$ . This suggests that an A+T pair, which binds two additional moles of water relative to a G+C pair, might represent a less hydrophobic environment than a G+C pair and so is preferentially bound by the H2B histone. As the ionic nature of the binding decreases, so does the A+T selectivity. As expected, the selectivity of slightly lysine-rich histone binding decreases when the reconstitution is performed without urea. The increased ionic nature of the medium magnifies hydrophobic interactions and decreases the ionic interactions leading to selectivity. The decrease in the H2B selectivity is ca. 40% while the decrease in H2 selectivity is ca. 12%, presumably reflecting the difference in the inherent hydrophobic character of their DNA binding.

When the arginine-rich histones H3 and H4 are added to the slightly lysine-rich histones to form the whole-H1 histone fraction, the characteristics of the nucleohistone formed between DNA and these histones are significantly different from H2 nucleohistones. The most notable result may be that the thermal denaturation profiles and CD

spectra of the whole -H 1 nucleohistones do not reproduce those of chromatin. The  $\beta$  value for complexes prepared in urea is ca. 6 aa/n. This indicates significant histone-histone associations in the bound DNA regions. When whole -H 1 is reconstituted to DNA in the absence of urea or in a salt-urea-phosphate reconstitution the  $\beta$  value of the complex decreases. This behavior is exactly opposite to that of the H 2 B or H 2 nucleohistones. A plausible explanation may be that during a salt-urea-tris reconstitution the histones bind the DNA cooperatively and during removal of the urea nonspecific histone-histone aggregations occur as evidenced by the greater amount of protein secondary structure observed in plus-urea relative to minus-urea whole -H 1 nucleohistones. Thus, the binding of the histones in the form of a dissociated complex results more in their distortion than in the distortion of the DNA. When whole -H 1 histones are dissolved in salt without urea the histones aggregate, but only to a finite limit, a tetramer (34). This stable structure now deforms the DNA as it binds rather than being deformed itself. Consonant with the results of Weintraub et al. (34) it is found that the whole -H 1 histone complex is in the same conformation free in 2 M NaCl solution or bound to DNA after minus-urea reconstitution. Further evidence for the stability of the whole -H 1 tetramer is presented by experiments in which the whole -H 1 histone fraction is subjected to dissociation in 5 M urea, 2 M NaCl followed by removal of the urea prior to the salt gradient. The whole -H 1 histone complex reforms and binds to DNA to yield nucleohistones with physical properties virtually identical to the minus-urea reconstitute. The explanation for the decrease in the  $\beta$  value of whole -H 1 nucleohistones reconstituted without urea or with urea in the presence of phosphate buffer is that a limit is placed on the extent of aggregation of the histones in the

latter complexes. This differs from the response of the slightly lysine-rich histones to reconstitution without urea since these histones are believed to form oligomers in solution (42). When whole-H1 histone is reconstituted to calf DNA in the presence of urea two thermal transitions are evident between  $T_m$  and  $T_{mII}$ , at  $70^{\circ}\text{C}$  and  $79^{\circ}\text{C}$ . In minus-urea reconstitutions the  $70^{\circ}\text{C}$  peak disappears while the  $79^{\circ}\text{C}$  peak is enhanced. If these transitions may be attributed to DNA conformational changes then the binding of whole-H1 to DNA in the absence of urea must allow a deformation of the DNA by the histone which is more stable to heat disruption than those conformational changes induced in urea. When whole-H1 is reconstituted to DNA in the presence of phosphate buffer both the  $T_{mII}$  transition associated with the binding of the hydrophobic half-molecule and the  $79^{\circ}\text{C}$  intermediate melting transition are intensified as well. This explanation is supported by the observation from CD spectra that the  $m_d$  values of minus-urea and salt-urea-phosphate complexes are significantly increased over the  $m_d$  value of the plus-urea complex.

The deviation in selectivity values between plus-urea and minus-urea whole-H1 nucleohistones (4%) is even smaller than for histone H2 nucleohistones (12%). This implies that the difference in the extent of hydrophobic histone-DNA binding in whole-H1 complexes is similar with or without urea. Since urea destabilizes hydrophobic bonds but has little apparent effect on the selectivity of the whole-H1 fraction it may be that in the presence of urea we see the sum of the selectivities of the slightly lysine-rich and arginine-rich histones which tend to neutralize each other, although other explanations are possible.

The fact that the whole-H 1 nucleohistones do not show the same melting profiles and CD spectra as chromatin deserves mention. Weintraub et. al. (34) have reconstituted whole-H 1 histone to DNA by salt dialysis and found that the pattern of nuclease-resistant DNA fragments in the complex is the same as derived from the nuclease digestion of chromatin. This result suggests that although the whole-H 1 complex may be annealed to DNA in such a way as to allow the correct spacing between whole-H 1 units and the correct exposure of the DNA to exogenous nucleases, other agents are required to achieve the proper distortion of the histone and DNA conformations observed in chromatin. One of these agents may be the lysine-rich histone H 1.

The urea reconstituted complexes of calf DNA with whole histone (H 1, H 2 A, H 2 B, H 3, H 4) show thermal denaturation profiles and CD spectra which are similar to those of calf thymus chromatin. In addition, the  $\beta$  value of these complexes, 3.7 aa/n, is the same as the value of chromatin (76). The temperature of the thermal transitions of the whole histone nucleohistones are still higher than those observed in chromatin, however. Some insight into the forces responsible for this effect is gained when nucleohistone purified from chromatin and reconstituted whole histone nucleohistone are melted in 5 M urea. Under these conditions the melting profiles of both samples are virtually identical both in shape and in the temperatures of each melting band. It is implied, therefore, that under conditions where the hydrophobic forces of each nucleohistone are broken, both samples behave identically. It appears likely then that the basis for the elevated melting temperatures observed in whole histone nucleohistone and possibly histone H 2 nucleohistone is the absence of those hydrophobic forces which, in chromatin,

destabilize the DNA relative to reconstituted nucleohistone. It should be recalled that in whole histone nucleohistones as well as H2A, H2B, H2 and whole-H1 complexes, exclusion of urea from the reconstitution mixture and the concomitant enhancement of hydrophobic forces lowers the temperature of the highest melting transition. Further evidence for the role of hydrophobic forces in the maintenance of chromatin structure comes from direct-mixing reconstitution in 0.15 M NaCl. Large reductions in the positive CD peak near 275 nm are observed in these complexes. Equivalent reductions in the value  $\Delta\epsilon_{278} / -\Delta\epsilon_{246}$  were observed by Ivanov et al. (98) in 80% MeOH/H<sub>2</sub>O in 0.1 M NaCl. The requirement for a solvent of such low polarity and the induction of similar changes by histones in aqueous solutions of similar salt concentration suggests that the microenvironment of the histone-DNA aggregate is considerably less polar than that of the medium at large. When the 0.15 M NaCl is dialysed out of the medium, the DNA of the whole nucleohistone reverts towards the normal B form. This implies that hydrophobic forces in addition to those supplied by the histones are required to achieve the distortion of the DNA observed in chromatin.

The reconstitution of whole histone to DNA in the absence or presence of urea does not alter the ability of the hydrophobic histone residues to effect changes in the DNA conformation. This is probably a reflection of the stability of the whole histone complex and implies that the individual histone constituents may still interact with each other as they bind the DNA, even in the presence of urea. Also it is noted that the presence or absence of urea has no effect on the selectivity of whole histone binding.

Although the results of many experiments on the physical properties

of histone:DNA complexes suggest the involvement of hydrophobic forces in the determination of the characteristics of the nucleohistone complex. The view that hydrophobic forces play a role comparable in magnitude to that of the ionic forces within the protein:nucleic acid unit is still highly speculative. The prime conclusion to be drawn from this work is that the balance of ionic and hydrophobic forces within the histone subunit and within the histone:DNA complex determines the histone and DNA conformations as well as the stability of the protein:protein and protein:DNA interactions. Alterations of these forces due to changing environmental conditions (pH, salt, dielectric constant) or covalent modification of the histones will necessarily change the properties of the nucleohistone.

## LITERATURE CITED

1. Shih, T.Y., Bonner, J. 1970. J. Mol. Biol. 48 : 469
2. Smart, J.E., Bonner, J. 1971. J. Mol. Biol. 58 : 661
3. Smart, J.E., Bonner, J. 1971. J. Mol. Biol. 58 : 675
4. Kossel, A. 1884. Z. Physiol. Chem. 8 : 511
5. Stedman, E., Stedman, E. 1950. Nature 166 : 780
6. Elgin, S.C.R., Weintraub, H. 1975. Ann. Rev. Biochem. 44 : 725
7. Gilbert, W., Maizels, N., Maxam, A. 1973. Cold Spring Harbor Symp. Quant. Biol. 38 : 845
8. Maniatis, T., Ptashne, M., Maurer, R. 1973. Cold Spring Harbor Symp. Quant. Biol. 38 : 857
9. Lyon, M. F. 1961. Nature 190 : 372
10. Berendes, H.D. 1971. Symp. Soc. Exp. Biol. 25 : 145
11. Berendes, H.D. 1973. Int. Rev. Cyto. 35 : 61
12. Paul, J., Gilmour, R.S. 1968 J. Mol Biol. 34 : 305
13. Bekhor, I., Kung, G.M., Bonner, J. 1969. J. Mol. Biol. 39 : 351
14. Smith, K.D., Church, R.B., McCarthy, B.J. 1969 Biochemistry 8 : 4271
15. Garrard, W.T., Pearson, W.R., Wake, S.K., Bonner, J. 1974. Biochem. Biophys. Res. Commun. 58 : 50
16. Elgin, S.C.R., Bonner, J. 1972. Biochemistry 11 : 772
17. Teng, C.S., Teng, C.T., Allfrey, V.G. 1971. J. Biol. Chem. 246 : 3597
18. Kleinsmith, L.J., Heidema, J., Carroll, A. 1970. Nature 226 : 1025
19. Kleinsmith, L.J. 1973. J. Biol. Chem. 248 : 5648
20. Axel, R., Cedar, H., Felsenfeld, G. 1973. Cold Spring Harbor Symp. Quant. Biol. 38 : 773

- 21a. DeLange, R.J., Smith, E.L. 1975 Ciba Found. Symp. 28 : 59
- 21b. DeLange, R.J., Smith, E.L. 1974. Proteins 4: Chap. 2, 3rd Ed.
22. Lake, R.S., Goidl, J.A., Salzman, N.P. 1972. Exp. Cell Res. 73 : 113
23. Gurley, L.R., Walters, R.A., Tobey, R.A. 1973. Biochem. Biophys. Res. Commun. 50 : 744.
24. Bradbury, E.M., Inglis, R.J., Matthews, H.R., Sarner, N. 1973. Eur. J. Biochem. 33 : 131
25. Bradbury, E.M., Inglis, R.J., Matthews, H.R. 1974. Nature 247 : 257
26. Bradbury, E.M., Inglis, R.J., Matthews, H.R., Langan, T.A. 1974. Nature 249 : 553
27. Byvoet, P. 1966. J. Mol. Biol. 17 : 311
28. Hancock, R. 1969. J. Mol. Biol. 40 : 457
29. D'Anna, J.A.Jr., Isenberg, I. 1972. Biochemistry 11 : 4017
30. Smerdon, M.J., Isenberg, I. 1974. Biochemistry 13 : 4046
31. D'Anna, J.A.Jr., Isenberg, I. 1973. Biochemistry 12 : 1035
32. D'Anna, J.A.Jr., Isenberg, I. 1974. Biochemistry 13 : 2098
33. Van Holde, K.E., Isenberg, I. 1975. Chem. Res. 8 : 327
34. Weintraub, H., Palter, K., Van Lente, F. 1975. Cell 6 : 85
35. Kelley, R.I. 1973. Biochem. Biophys. Res. Commun. 54 : 1588
36. Roark, D.E., Geoghegan, T.E., Keller, G.H. 1974. Biochem. Biophys. Res. Commun. 59 : 542
37. Skandriani, E., Mizon, J., Sautiere, P., Biserte, G. 1972. Biochimie 54 : 1267
38. Martinson, H.G., McCarthy, B.J. 1975. Biochemistry 14 : 1073
39. Martinson, H.G., Shetlar, M.D., McCarthy, B.J. In press
40. Van Lente, F., Jackson, J.F., Weintraub, H. 1975. Cell 5 : 45
41. Kornberg, R.D. 1974. Science 184 : 868
42. Kornberg, R.D., Thomas, J.O. 1974. Science 184 : 865
43. Weintraub, H., Van Lente, F. 1974. Proc. Nat. Acad. Sci. USA 71 : 4249

44. Hewisch, D., Burgoyne, L. 1973. Biochem. Biophys. Res. Commun. 52 : 504
45. Noll, M. 1974. Nature 251 : 249
46. Axel, R. Melshior, W., Sollner - Webb, B., Felsenfeld, G. 1974. Proc. Nat. Acad. Sci. USA 71 : 4101
47. Weintraub, H., Van Lente, F. 1975. Ciba Found. Symp. 28 : 291
48. Olins, A.L., Olins, D.E. 1974. Science 183 : 330
49. Olins, A.L., Carlson, R.D., Olins, D.E. 1975. J. Cell. Biol. 64 : 528
50. Oudet, P., Gross - Bellard, M., Chambon, S. 1975. Cell 4 : 281
51. Bradbury, E.M., Molgaard, H.V., Stephens, R.M. 1972. Eur. J. Biochem. 31 : 474
52. Richards, B.M., Pardon, J.F. 1970. Exp. Cell. Res. 62 : 184
53. Baldwin, J.P., Boseley, P.G., Bradbury, E.M. Ibel, K. 1975. Nature 253 : 245
54. Senior, M.B., Olins, A.L., Olins, D.E. 1975. Science 187 : 173
55. Finch, J.T., Klug, A. 1976. Proc. Nat. Acad. Sci. USA 73 : 1897
56. Van Holde, K.E., Sahasrabudde, C.G., Shaw, B.R. 1974. Nucleic Acids Res. 1 : 1579
57. Li, H.J. 1975. Nucleic Acids Res. 2 : 1275
58. Marmur, J. 1961. J. Mol. Biol. 3 : 208
59. Bonner, J., Chalkley, G.R., Dahmus, M., Fambrough, D., Fujimura, F., Huang, R.C.C., Huberman, J., Jensen, R., Marushige, K., Ohlensubch, H., Olivera, B., Widholm, J. 1968. Methods Enzymol. Vol. 12, Nucleic Acids, part B (L. Grossman and K. Mořdave, eds.) p.3. Academic Press, Inc., New York and London.
60. Sanders, L.A., McCarty, K.S. 1972. Biochemistry 11 : 4218
61. Panyim, S., Chalkley, R. 1969. Arch. Biochem. Biophys. 130 : 337
62. Oliver, D., Chalkley, R. 1972. Biochem. J. 129 : 349
63. Li, H.J., Bonner, J. 1971. Biochemistry 10 : 1461
64. Phillips, D.M.P. 1971. Histones and Nucleohistones, Chapter 2 Plenum Press, New York (D.M.P. Phillips, ed.)
65. Li, H.J., Brand, B., Rotter, A. 1974. Nuc. Acids Res. 1 : 257

66. Leffak, I.M., Hwan, J.C., Li, H.J., Shih, T.Y. 1974. Biochemistry 13 : 1116
67. Burton, K. 1956. Biochem. J. 62 : 315
68. Adler, A., Moran, E., Fasman, G.D. 1975. Biochemistry 14 : 4179
69. Leach, S.J., Scheraga, H.A. 1960. J. Amer. Chem. Soc. 82 : 4790
70. Ohlenbusch, H.H., Olivera, B.M., Tuan, D., Davidson, N. 1967. J. Mol. Biol. 25 : 229
71. Ansevin, A.T., Hnilica, L.S., Spelsberg, T.C., Kehm, S.L. 1971. Biochemistry 10 : 4793
72. Tsuboi, M., Matsuo, K., Ts'ao, P.O.P. 1966. J. Mol. Biol. 15 : 256
73. Olins, A.L., Olins, D.E., Von Hippel, P.H. 1968. J. Mol. Biol. 33 : 265
74. Li, H.J. 1973. Biopolymers 12 : 287
75. Johns, E.W. in Histones and Nucleohistones, Chapter 1, Plenum Press, New York, 1971. (D.M.P. Phillips, ed.)
76. Li, H.J., Chang, C., Weiskopf, M. 1973 Biochemistry 12 : 1763
77. Clark, R.J., Felsenfeld, G. 1971. Nature New Biol. 229 : 101
78. Shih, T.Y., Lake, R.S. 1972. Biochemistry 11 : 4811
79. Yu, S.S., Li, H.J. 1973. Biopolymers 12 : 2777
80. Inoue, S., Ando, T. 1970. Biochemistry 9 : 388
81. Wilhelm, F.X., DeMurcia, G.M., Champagne, M.H., Daune, M.P. 1974. Eur. J. Biochemistry 45 : 431
82. Ivanov, V.I., Minchenkova, L.E., Schyolkina, A.K., Poletayev, A.I. 1973. Biopolymers 12 : 89
83. Bradbury, E.M., Crane - Robinson, C. 1971. Histones and Nucleohistones Plenum Press, New York (D.M.P. Phillips, ed.)
84. Hnilica, L.S. 1973 in The Structure and Biological Function of the Histones. CRC Press, Cleveland
85. Subirana, J.A. 1973. J. Mol. Biol. 74 : 363
86. Chou, P.Y., Fasman, G.B. 1974. Biochemistry 13 : 211
87. Ansevin, A.T., Brown, B.W. 1971. Biochemistry 10 : 1133

88. Yu, S.S. 1976 Ph.D. Dissertation, City University of New York
89. Bartley, J.A., Chalkley, R.G. 1972. J. Biol. Chem. 247 : 3647
90. Kinkade, J.M.Jr., Cole, R.D. 1966 J. Biol. Chem. 241 : 5790
91. Sherod, D., Jackson, G., Chalkley, R. 1974. J. Biol. Chem. 249 : 3923
92. Varshavsky, A.J., Bakayev, V.V., Georgiev, G.P. 1976. Nucleic Acids Res. 3 : 477
93. Bustin, M. 1973. Nature New Biol. 245 : 207
94. D'Anna, J.A.Jr., Isenberg, I. 1974. Biochemistry 13 : 4992
95. Li, H.J., Chang, C., Evagelinou, Z., Weiskopf, M. 1975. Biopolymers 14 : 1211
96. Chang, C., Li, H.J. 1974. Nucleic Acids Res. 1 : 945
97. Tunis - Schneider, M.J.B., Maestre, M.F. 1970. J. Mol. Biol. 52 : 521
98. Ivanov, V.I., Minchenkova, L.E., Schyolkina, A.K., Poletayev, A.I. 1973. Biopolymers 12 : 89
99. Davis, D.R. 1967. Ann. Rev. Biochemistry 36 : 321
100. Greenfield, N., Fasman, G.S. 1969. Biochemistry 8 : 4108
101. Beychok, S. 1966. Science 154 : 1288
102. Holzwarth, G., Doty, P. 1965. J. Amer. Chem. Soc. 87 : 218
103. Madison, V., Schellman, J. 1972. Biopolymers 11 : 1041
104. Chen, Y.H., Yang, J.T., Martinez, H.M. 1972. Biochemistry 11 : 4120
105. Chen, Y.H., Yang, J.T. 1971. Biochem. Biophys. Res. Commun. 44 : 1285
106. Bannister, W.H., Bannister, J.V. 1974 Int. J. Biochem. 5 : 673
107. Simpson, R.T., Sober, H.A. 1970. Biochemistry 9 : 3103
- 108a. Fasman, G.D., Schaffhausen, B., Goldsmith, L., Adler, A. 1970. Biochemistry 9 : 2814
- 108b. Shih, T.Y., Fasman, G.D. 1971. Biochemistry 10 : 1675
- 108c. Adler, A., Moran, E., Fasman, G.D. 1975. Biochemistry 14 : 4179
- 108d. Adler, A., Fulmer, A.W., Fasman, G.D. 1975. Biochemistry 14 : 1445

- 108e. Adler, A.J., Ross, D.G., Chen, K., Stafford, P.A., Woiszwillo, M.J., Fasman, G.D. 1974. Biochemistry 13 : 616
109. Li, H.J., Isenberg, I., Johnson, W.C.Jr. 1971. Biochemistry 10 : 2587
110. Cohen, P., Kidson, C. 1968. J. Mol. Biol. 35 : 241
111. Gratzer, W.B., McPhie, P. 1966. Biopolymers 4 : 601
112. Leng, M., Felsenfeld, G. 1966. Proc. Nat. Acad. Sci. USA 56 : 1325
113. Hwan, J.C., Leffak, I.M., Li, H.J., Huang, P.C., Mura, C. 1975. Biochemistry 14 : 1390
114. Combard, H., Vendrely, R. 1970. Biochem. J. 118 : 875
115. Clark, R.J., Felsenfeld, G. 1972. Nature New Biol. 240 : 226